# MEG, myself, and I: Understanding inter-individual diversity of neurophysiological brain activity

Jason da Silva Castanheira

Integrated Program in Neuroscience McGill University

Montreal, Quebec, Canada

December 2023

*A thesis submitted to McGill University in partial fulfillment of the requirements of the degree of Doctor of Philosophy (Ph.D)*

# Abstract / Résumé

Neuroscientific research aims to understand the biological nature of individual traits and behaviours. The field has made great strides toward this goal with the advancement of openly available, large neuroimaging datasets and computational tools. However, as sample sizes in neuroscience grow towards the population scale, it becomes increasingly difficult to reconcile group-level effects with inter-individual variability. Recent studies in functional magnetic resonance imaging (fMRI) argue that resting-state functional connectivity can both successfully distinguish individuals and predict individual traits. From these approaches emerged the notion of a brain-fingerprint, a set of functional neuroimaging features that distinguish between individuals within a cohort. The neurophysiological foundations and clinical relevance of such brain-fingerprints remain uncharted and are at the core of my thesis. I have therefore contributed to the clarification of neurophysiological inter-individual differences, in both health and disease, present in the rich and complex dynamics of task-free magnetoencephalography (MEG). In the first experiment (Chapter 2), I demonstrate that individuals can be robustly differentiated from one another using brief neurophysiological recordings. This work extends the derivation of brain-fingerprints to direct measures of polyrhythmic brain activity across the cortex. In the second experiment (Chapter 3), I explore how inter-individual differences in task-free neurophysiology change across the adult lifespan. I report that while older adults can be differentiated from one another, the most salient features of participant differentiation diverge between younger and older ages along anatomical and neurochemical axes. In the third experiment (Chapter 4), I demonstrate the clinical relevance of brain-fingerprinting. I show that in Parkinson's disease, rhythmic brain-fingerprints enable further insight into the pathophysiology of the disease while arrhythmic brain-fingerprints show greater within-individual variability and challenge research on inter-individual differences. In the last chapter (Chapter 5), I elaborate on the possible genetic origins of brain-fingerprints by leveraging a twin-study approach. The findings corroborate that monozygotic twins have strikingly similar neurophysiological brain-fingerprints compared to dizygotic twins. In addition, the most salient

neurophysiological features for differentiating between individuals covary with a ventromedial–dorsolateral gradient of gene expression. This gene signature is enriched for biological processes related to ion transport, preferentially expressed in neurons, and becomes more pronounced throughout development. My findings demonstrate that inter-individual differences in brain activity, as measured by neurophysiological brain-fingerprints, are robust across the adult lifespan, relate to gene expression, and capture meaningful variations across population sub-groups. I emphasize the significance of considering how inter-individual differences in brain activity diverge across populations. This dissertation informs future work on the biological origins of the self.

## MEG et moi-même: Comprendre la diversité interindividuelle de l'activité cérébrale neurophysiologique

La recherche neuroscientifique vise à comprendre la nature biologique des traits et des comportements individuels. Le domaine a fait de grands progrès vers cet objectif grâce à l'avancée des grands ensembles de données de neuro-imagerie et des nouveaux outils informatiques librement accessibles. Toutefois, à mesure que la taille des échantillons en neurosciences augmente pour atteindre l'échelle de la population, il devient de plus en plus difficile de concilier les effets au niveau du groupe avec la variabilité interindividuelle. Des études récentes sur l'imagerie par résonance magnétique fonctionnelle (IRMf) montrent que la connectivité fonctionnelle à l'état de repos permet à la fois de distinguer les individus et de prédire les traits individuels. Ces approches ont donné naissance à la notion d'empreinte cérébrale, un ensemble de caractéristiques fonctionnelles de neuro-imagerie qui permettent de distinguer les individus au sein d'une cohorte. Les fondements neurophysiologiques et la pertinence clinique de ces empreintes cérébrales demeurent inexplorés et sont au cœur de ma thèse. J'ai donc contribué à la clarification des différences neurophysiologiques interindividuelles, tant dans la santé que dans la maladie, présentes dans la dynamique riche et complexe de la magnétoencéphalographie sans tâche (MEG). Dans une première étude (chapitre 2), je démontre

que les individus peuvent être solidement différenciés les uns des autres à l'aide de brefs enregistrements neurophysiologiques. Ce travail étend la dérivation des empreintes cérébrales à des mesures directes de l'activité cérébrale polyrythmique dans le cortex. Dans la deuxième expérience (chapitre 3), j'étudie comment les différences interindividuelles dans la neurophysiologie sans tâche évoluent au cours de la vie adulte. J'ai constaté que les adultes plus âgés peuvent être différenciés les uns des autres, mais les caractéristiques les plus marquantes de la différenciation des participants divergent entre les jeunes et les plus âgés au long des axes anatomiques et neurochimiques. Dans la troisième étude (chapitre 4), je démontre la pertinence clinique des empreintes cérébrales. Je montre que dans le cas de la maladie de Parkinson, les empreintes cérébrales rythmiques permettent de mieux comprendre la physiopathologie de la maladie, tandis que les empreintes cérébrales arythmiques présentent une plus grande variabilité intra-individuelle et remettent en question les recherches sur les différences interindividuelles. Dans le dernier chapitre (chapitre 5), je développe les origines génétiques possibles des empreintes cérébrales en m'appuyant sur une étude de jumeaux. Les résultats corroborent le fait que les jumeaux monozygotes ont des empreintes cérébrales neurophysiologiques étonnamment similaires à celles des jumeaux dizygotes. En outre, les caractéristiques neurophysiologiques les plus marquantes pour différencier les individus covarient avec un gradient ventromédial-dorsolatéral d'expression génique. Cette signature génétique est enrichie pour les processus biologiques liés au transport des ions, s'exprime préférentiellement dans les neurones et s'accentue tout au long du développement. Les résultats de ma thèse démontrent que les différences interindividuelles dans l'activité cérébrale, mesurées par les empreintes cérébrales neurophysiologiques, sont robustes tout au long de la vie adulte, qu'elles sont liées à l'expression des gènes et qu'elles reflètent des variations significatives entre les sous-groupes de la population. J'insiste sur l'importance d'examiner comment les différences interindividuelles dans l'activité cérébrale divergent d'une population à l'autre. Cette thèse inspirera les travaux futurs explorant les origines biologiques de la diversité comportementale entre les individus.

# Acknowledgements

I acknowledge the funding I received throughout my degree from the following sources: Fonds de recherche du Québec Nature et Technologie scholarship (Masters and Doctoral), Natural Sciences Engineering Research Council of Canada scholarships (Masters and Alexander Graham Bell Doctoral award), Integrated Program in Neuroscience (IPN) travel award, Post-Graduate Student Society travel award, Centre for Research on Brain Language and Music Travel award, and Montreal Neurological Institute/ Hospital Student Travel award. Thank you for supporting me in the pursuit of my goals.

I would like to thank my supervisor Porf. Sylvain Baillet for his continued support throughout my degree. We made it!

To my advisory committee members Prof. Bratislav Misic and Prof. Anna Weinberg, thank you for being so welcoming and receptive to my ideas. Your support means the world to me.

To the collaborators on these projects, Alex Wiesman, Justine Hansen, Jonathan Poli and Hector Perez, thank you for listening to me ramble.

To the members of the lab, thank you for your continued support along this long journey: Mathieu Landry, Luc Wilson, Eleanor Hill, Jonathan Rudolf Gallego, Olivia Bizimundu, Zaida Martínez Moreno, Max Levinson, Niloofar Gharesi, Marc Lalancette, Raymundo Cassani, Santiago Flores and many many more.

To my family, I am beyond grateful for your unwavering support. Para os meus pais e avos que sonharam que eu acabasse os meus estudos, Obrigado! Dedico-vos este doutorado. Vocês passaram muitas noites de saudade nenhum país estrangeiro para que eu pudesse ter uma vida melhor.

# Funding

The research projects completed for this thesis received funding support from the Fonds de recherche du Québec- Santé (FRQS), the National Institute of Health NIH (R01-EB026299), a Discovery grant from the Natural Science and Engineering Research Council of Canada (436355-13), the CIHR Canada Research Chair in Neural Dynamics of Brain Systems, the Brain Canada Foundation with support from Health Canada, and the Innovative Ideas program from the Canada First Research Excellence Fund, awarded to McGill University for the HBHL initiative. In addition, this work was supported by a master and Doctoral fellowship from the Fonds de recherche du Québec – Nature et technologie (FRQNT) and

Natural Science and Engineering Research Council of Canada (NSERC).

# Author contribution

Chapter 2. All authors contributed to the conceptualization of the study. J.d.S.C performed the analyses presented in Figures 2-5 and the supplemental Figures. H.D.O.P. contributed to the analyses presented in Figure 2. S.B. and B.M. provided guidance with methods and data interpretation. J.d.S.C. wrote the first draft of the manuscript. All authors contributed to the writing and editing of the manuscript.

Chapter 3. All authors contributed to the conceptualization of the study. J.d.S.C performed the analyses. S.B.and A.W. provided guidance with methods and data interpretation. J.d.S.C. wrote the first draft of the manuscript. All authors contributed to the writing and editing of the manuscript.

Chapter 4. All authors contributed to the conceptualization of the study. J.d.S.C performed the analyses presented in Figures 1-6 and the supplemental Figures. J.Y.H. contributed to the analyses presented in Figure 5. S.B., B.M., and A.W. provided guidance with methods and data interpretation. J.d.S.C. wrote the first draft of the manuscript. All authors contributed to the writing and editing of the manuscript.

Chapter 5. J.d.S.C conceptualized the study. J.d.S.C performed the analyses presented in Figures 2-7 and the supplemental Figures. J.P. contributed to the analyses presented in Figure 2. J.Y.H. provided guidance with the analyses presented in Figure 4-6. S.B.and B.M. provided guidance with methods and data interpretation. J.d.S.C. wrote the first draft of the manuscript. All authors contributed to the writing and editing of the manuscript.

# Abbreviations

| | |
|---|---|
| AD | Alzheimer's Disease |
| AHBA | Allan Human Brain Atlas |
| BOLD | blood oxygen level dependent |
| BWAS | brain-wide association study |
| CI | confidence interval |
| DZ | dizygotic |
| ECG | electrocardiography |
| EEG | electroencephalography |
| EOG | electrooculogram |
| FC | functional connectivity |
| fMRI | functional magnetic resonance imaging |
| fNIRS | functional near-infrared spectroscopy |
| ICC | intra-class correlation |
| MCI | mild cognitive impairment |
| MEG | magnetoencephalography |
| MRI | magnetic resonance imaging |
| MZ | monozygotic |
| OMEGA | Open MEG Archive |
| PCA | principal component analysis |
| PD | Parkinson's disease |
| PLS | Partial Least Squares |
| PSD | power spectral density |
| P-AD | Prevent Alzheimer's Disease |
| SSP | signal source projection |

# Table of Contents

# Figure List

## Chapter 2



## Chapter 3



## Chapter 4



## Chapter 5



## Chapter 6

# Chapter 1

# Introduction

Every day, we are confronted with the diversity of human behaviour. The uniqueness of our personalities, cognitive abilities, values, and beliefs are at the forefront of neuroscientific research exploring the biological nature of individual traits and behaviours (Costa et al., 2019; Dubois & Adolphs, 2016; Finn et al., 2015; *APA Handbook of Personality and Social Psychology, Volume 4*, 2015; Van Horn et al., 2008). With the increasing availability of large openly available neuroimaging datasets that approach the realm of population-science (Niso et al., 2016a; Sudlow et al., 2015; Taylor et al., 2017; Van Essen et al., 2012), neuroscientists grapple with the considerable inter-individual variation of the brain. No two brains look alike—this diversity among individual brains has prompted neuroscientists to investigate how variability in brain activity reflects the uniqueness of individuals.

## Brain-behaviour relationships

Historically, human neuroimaging and neurophysiology research has quantified group average differences in brain activity, such as contrasting patients and healthy controls. While this group-level inference has advanced our understanding of how brain activity relates to behaviours and diseases, it neglects inter-individual variation.

More recently, researchers have utilized correlational analyses to discover the neurological biomarkers of personality traits (Kennis et al., 2013; Lai et al., 2019), working memory (Richard Clark et al., 2004; Rosenberg, Martinez, et al., 2020), and attention (Rosenberg et al., 2017a; Rosenberg, Scheinost, et al., 2020). This approach referred to as brain-wide

association studies (BWAS) (Button et al., 2013; Marek et al., 2022; Spisak et al., 2023), allowed scientists to explore brain-behaviour relationships, generate novel hypotheses, and predict individual differences out of sample.

The BWAS method links inter-individual variability of brain activity with variation in behavioural measures like cognitive performance and traits. This is typically done either through linear correlations or machine learning models. However, this method has recently faced criticism, particularly regarding its application in small sample sizes. Concerns about BWAS methods are heightened by the seemingly modest effect sizes of brain-behavior relationships, resulting in limited reproducibility across studies and poor generalization across populations (Button et al., 2013; Greene et al., 2022; J. Li et al., 2022; Marek et al., 2022; Spisak et al., 2023).

An example critic of the BWAS approach reports that brain-behaviour relationships do not generalize across populations, bringing into question whether these neural correlates truly reflect inter-individual variability in behaviour, or other covariates not accounted for in the BWAS method (Greene et al., 2022). Such covariates include clinical measures and sociodemographic factors, like the native language of participants. Brain-behaviour model failure is observed within a subset of individuals and may reflect different cognitive processes and strategies participants take to perform a behavioural task (Greene et al., 2022). In a verbal memory task, native English speakers' performance may relate to articulation rates while native Mandarin speakers' performance relates to their increased phonological store (Greene et al., 2022; Mattys et al., 2018). Different performance strategies on cognitive tasks, like chunking in a working memory task—i.e., grouping stimuli into a single unit for ease of memorization—may explain participant behavioural variance, and therefore contribute to the failure of brain-behaviour model generalization across populations (Thalmann et al., 2019).

The biases observed in brain-behavior relationships, as discussed above, are not unique to neuroscience and extend to various scientific fields (Buolamwini & Gebru, 2018; Obermeyer et al., 2019). As such, researchers emphasize caution in interpreting brain-behavior prediction models, as these models may not generalize to different populations and may even exhibit systematic biases against certain individuals (Greene et al., 2022; J. Li et al., 2022).

These findings underscore the complexities inherent in studying brain-behavior relationships and emphasize the need for researchers to carefully consider population and clinical heterogeneity. Focusing on a single population, like healthy young adults, does not necessarily provide researchers with a comprehensive model that may generalize to other populations, e.g., older adults. Model failure across populations challenges the interpretation of identified brain-behaviour relationships. This is particularly relevant as data volumes increase in size and capture more diverse groups of individuals. To progress the field of brain-behaviour relationships forward, researchers need to consider data from diverse populations, with individuals of various ages and clinical challenges (e.g., different cognitive deficits) (Ricard et al., 2023).

### The brain-fingerprinting method: a novel approach to study inter-individual differences

Recent advancements in neuroscience highlighted the challenges and promises associated with inter-individual variability in brain function. These findings demonstrate that individuals can be differentiated from a large cohort using their unique '*brain-fingerprint*'—a profile of brain activity that is characteristic of a given individual (Finn et al., 2015a). The brain-fingerprinting method proposes that an individual's brain phenotype is more similar (i.e., correlated) to themselves across multiple instances of data collection than to any other unrelated individual (Amico & Goñi, 2018a; Bari et al., 2019). Unlike BWAS methods which exclusively examine between-participant variance, brain-fingerprinting contrasts within- and between- participant variability.

Notably, the brain-fingerprinting approach reported that brain activity characteristic of individuals relates to individual differences in intelligence test performance (Finn et al., 2015a), working memory (Rosenberg, Martinez, et al., 2020), and attention (Rosenberg et al., 2017a; Rosenberg, Scheinost, et al., 2020).

Convenience sampling and sampling bias, however, limit the generalization of brain-fingerprints to other populations. This research has exclusively examined inter-individual differences in healthy young adults (Finn et al., 2015a). While differentiating individuals from a homogenous population is more challenging, the results obtained from a healthy young adult sample may not generalize to other populations. Both the accuracy of individual differentiation and the most salient features for participant differentiation may depend on the population

studied. Take for example healthy aging: Older adults show robust neurophysiological group-level differences in alpha oscillations (8-12 Hz) as well as arrhythmic brain activity (Andrews-Hanna et al., 2007; Damoiseaux et al., 2008; Scally et al., 2018; Voytek et al., 2015a; L. E. Wilson et al., 2022). These population-level differences in brain activity may impact which brain activity features are characteristic of individuals—i.e., features that were useful for differentiating young adults may become less efficacious at distinguishing older adults from one another. If this is the case, these findings would challenge the idea of a singular set of brain activity features that differentiate individuals across all populations, and would instead corroborate that individual differences in brain activity vary across populations complicating the interpretation of brain-behaviour relationships.

Another instance which may challenge individual differentiation is the robust neurophysiological alterations observed in neurological diseases. Various studies report several significant group-level differences in the brain activity of patient populations (Boon et al., 2019; D. T. Jones et al., 2011; Stoffers et al., 2008a; Tinkhauser et al., 2017; Wiesman, Castanheira, et al., 2022; Wiesman, Donhauser, et al., 2023). Yet little is known about how disease may affect the so-called brain-fingerprint. Whether disease impacts the performance of brain-fingerprinting methods and the most differentiable brain activity features remains an active topic of research. The question of inter-individual differences is of particular importance for research on personalized medicine.

### The electrophysiological basis of brain-fingerprints remains unclear

Beyond questions concerning how inter-individual differences generalize across populations, the electrophysiological and biological origins of brain-fingerprints remain unclear. Most published work on brain-fingerprints to date has focused on hemodynamic signals (Amico & Goñi, 2018a; Bari et al., 2019; Finn et al., 2015a; Miranda-Dominguez et al., 2014). Given the indirect relationship between the hemodynamic signal and neural brain signals (Brookes, Hale, et al., 2011; Haufe et al., 2018; Logothetis et al., 2001), the electrophysiological origins of brain-fingerprints remain to be explored.

Brain activity as measured by electrophysiology is composed of rich and complex signals. Spontaneous brain dynamics were long considered a nuisance and a by-product of neural noise (Başar, 1990; Donoghue et al., 2020a; Stein et al., 2005; Uddin, 2020). Recent experimental evidence, however, suggests that spontaneous electrophysiological brain signals measured during task-free conditions express similar resting-state brain networks as fMRI (Florin & Baillet, 2015) and relate to conscious perception, sensory processing, and working memory (Bagherzadeh et al., 2020; Balestrieri & Busch, 2022; Iemi et al., 2019; Richard Clark et al., 2004; Samaha et al., 2020).

Beyond the different origins of hemodynamic and electrophysiological signals, brain-fingerprinting has exclusively focused on measuring how brain-network derivatives measured as the statistical associations between signals from two brain regions are characteristic of individuals—i.e., functional connectomes (Amico & Goñi, 2018a; Bari et al., 2019; Finn et al., 2015a; Miranda-Dominguez et al., 2014). Yet, there are several processing decisions and different derivatives of the neurophysiological time series that yield a functional connectome matrix (Cole et al., 2010; J. D. Power et al., 2014; Sadaghiani et al., 2022). This is particularly true in electrophysiology, where there is great variability in methods to derive functional connectomes from EEG and MEG (Sadaghiani et al., 2022). Therefore, it is unclear whether simpler measures of local brain activity may equally differentiate individuals.

Electromagnetic brain activity is complex, characterized by slow and fast rhythms, and arrhythmic fluctuations (Baillet, 2017; Donoghue et al., 2020b; L. E. Wilson et al., 2022). Recent evidence proposes diverging interpretations of the rhythmic and arrhythmic components of brain activity, with the latter reflecting the local balance of excitatory/ inhibitory currents (Donoghue et al., 2020b; R. Gao et al., 2017). Further research is therefore needed to determine whether the entire frequency spectrum of electrophysiological activity is characteristic of individuals, or if unique brain activity is confined to specific rhythmic or arrhythmic components (Donoghue et al., 2020b; R. Gao et al., 2017). Given the richness of the local electromagnetic brain signals, I anticipate that individuals can be equally differentiated from simpler measures of the spatial distribution of spectral power.

The scant research that has explored the electrophysiological origins of brain-fingerprints to date exclusively relied on electroencephalography (EEG) (*EEG Fingerprints: Phase Synchronization of EEG Signals as Biomarker for Subject Identification | IEEE Journals & Magazine | IEEE Xplore*, n.d.; Fraschini et al., 2015; Rocca et al., 2014). This research was restricted to scalp recordings and therefore provides little neuroanatomical insight. Moreover, electroencephalography recordings are often contaminated by artifacts of different natures including instrument noise, muscle contractions, and eye and head movements. These artifacts may be idiosyncratic of individuals and bias brain-fingerprinting. Together, this suggests that unique inter-individual differences in the fast dynamics of neurophysiology remain to be thoroughly explored.

### Research objectives & original contributions of this dissertation

In this thesis, I investigated inter-individual differences in fast neurophysiological brain activity using magnetoencephalography (MEG) and brain-fingerprinting methodology. In this effort, I conducted several experiments and defined brain-fingerprints of individuals from diverse populations including healthy young adults, healthy older adults, and patients with idiopathic Parkinson's disease. I further explore the biological origins of electrophysiological brain-fingerprints, using normative atlases of cortical neurochemical systems and genetic expression patterns. These findings are presented in the following four chapters:

#### Chapter 2: Brief segments of neurophysiological activity enable individual differentiation

Research on inter-individual differences in brain activity has largely focused on hemodynamic measures of functional connectomes. It remains unclear how such variations between individuals translate to the rich and complex dynamics of resting-state electrophysiology. Which neurophysiological features are characteristic of individuals? In my first experiment (Chapter 2), I explore whether simpler measures of the spatial distribution of neurophysiological spectral signal power can differentiate individuals using brain activity recorded from magnetoencephalography (MEG). I demonstrate, leveraging the high temporal resolution of MEG signals, that brief 30-second segments of brain activity can differentiate individuals with high accuracy. These inter-individual differences in fast neurophysiological brain activity are robust to environmental and

physiological artifacts, and can differentiate individuals with recordings taken weeks apart. Altogether, this study establishes the robustness of so-called electrophysiological brain-fingerprints and elaborates on the relationship between inter-individual differences in electrophysiological brain activity and their relationship to demographics in healthy adults.

### Chapter 3: Neurophysiological brain-fingerprints evolve across the lifespan

There are robust structural and functional differences between the brains of young and older adults. Despite these differences, can we differentiate older adults from their brain-fingerprints, for example, with the same accuracy as young adults? In this chapter, I explore the stability of neurophysiological brain-fingerprints across the adult lifespan cross-sectionally. I demonstrate that electrophysiological brain-fingerprints relate to inter-individual differences in fluid intelligence across ages. In addition, I elaborate that while differentiation accuracy remains robust regardless of age, the most salient features to differentiate individuals differ between younger and older adults. The brains of older adults are best characterized by brain activity in regions that show the greatest age-related cortical thinning. Together, these findings showcase that differentiable brain activity evolves throughout the adult lifespan and suggest the importance of considering divergence in differentiable brain activity when studying populations with varying ages and cognitive abilities.

### Chapter 4: The neurophysiological brain-fingerprint of Parkinson's disease

Neurological diseases, like Parkinson's disease (PD), are known to alter large-scale multi-frequency brain signalling. While these group-level differences between patients and controls help neuroscientists understand the neural correlates of disease, little is known about how the disease may alter the uniqueness of neurophysiological activity. In my third experiment (Chapter 4), I explore how PD alters the robustness of neurophysiological brain-fingerprints. I demonstrate that rhythmic brain-fingerprints differentiate between patients and patients from age-matched healthy with the same performance as between healthy controls. The Parkinson's brain-fingerprint maps onto polyrhythmic activity in unimodal sensori-motor regions, decode disease staging, and coincides with brain regions rich in neurotransmitter systems that are affected by

the disease pathophysiology. In contrast, arrhythmic brain activity is remarkably variable within PD patients. Together, these findings corroborate the clinical utility of brain-fingerprinting by delineating stable polyrhythmic features that features are both patient-specific and relate to disease staging. We discuss how these rhythms may aid in the identification and testing of therapeutic neurostimulation targets.

### Chapter 5: Neurophysiological brain-fingerprints are heritable

Little is known about the microscale origins of inter-individual differences in electrophysiology. Prior research has suggested that brain-phenotypes are, in part, heritable and influenced by genetics. Researchers, however, have yet to determine the heritability of brain-fingerprints themselves. In my last experiment (Chapter 5), I clarified the heritability of inter-individual variability of resting-state neurophysiology. Leveraging twin-study methodology, I demonstrate that monozygotic twin pairs (MZ) —who share ~100% of their genetics—can be matched based on their sibling's neurophysiological brain-phenotype. In line with the construal that brain-fingerprints are heritable, we fail to match dizygotic twins (DZ) who share only 50% of their genome. Salient features for participant differentiation covary with a ventromedial–dorsolateral gradient of gene expression. This transcriptomic gradient is enriched for genes related to the neurochemical communication between cells and is preferentially expressed in neurons. The identified genetic signature, similarly, covaries with brain activations related to cognitive task performance and becomes more pronounced across development. These findings, taken together, corroborate the genetic origins of neurophysiological brain-fingerprints and pave the way for future research on the micro-scale origins of inter-individual differences in electrophysiology.

Altogether, this dissertation will elucidate how fast neurophysiological brain activity differentiates individuals across several demographic, clinical, and genetic landscapes. The results from these four experiments will clarify the biological origins of inter-individual differences and open new avenues for future research on brain-behaviour relationships using advanced machine learning techniques.

# Chapter 2

# Brief segments of neurophysiological activity enable individual differentiation

## Preface

The manuscript in this chapter demonstrates for the first time how measures of the spatial distribution of neurophysiological spectral signal power differentiate individuals. I showcase that electrophysiological brain-fingerprints are robust to environmental and physiological artifacts. This manuscript establishes the robustness of spectral brain-fingerprints for future investigations.

The manuscript was published as:

da Silva Castanheira, J. *, Orozco Perez, H.D. *, Misic, B. et al. Brief segments of neurophysiological activity enable individual differentiation. Nat Commun 12, 5713 (2021). https://doi.org/10.1038/s41467-021-25895-8

*These authors contributed equally: Jason da Silva Castanheira, Hector Domingo Orozco Perez

## Abstract

Large, openly available datasets and current analytic tools promise the emergence of population neuroscience. The considerable diversity in personality traits and behaviour between individuals is reflected in the statistical variability of neural data collected in such repositories. Recent studies with functional magnetic resonance imaging (fMRI) have concluded that patterns of

resting-state functional connectivity can both successfully distinguish individual participants within a cohort and predict some individual traits, yielding the notion of an individual's neural fingerprint. Here, we aim to clarify the neurophysiological foundations of individual differentiation from features of the rich and complex dynamics of resting-state brain activity using magnetoencephalography (MEG) in 158 participants. We show that akin to fMRI approaches, neurophysiological functional connectomes enable the differentiation of individuals, with rates similar to those seen with fMRI. We also show that individual differentiation is equally successful from simpler measures of the spatial distribution of neuro- physiological spectral signal power. Our data further indicate that differentiation can be achieved from brain recordings as short as 30 seconds, and that it is robust over time: the neural fingerprint is present in recordings performed weeks after their baseline reference data was collected. This work, thus, extends the notion of a neural or brain fingerprint to fast and large-scale resting-state electrophysiological dynamics.

## Introduction

Understanding the biological nature of individual traits and behavior is an overarching objective of neuroscience research(Dubois & Adolphs, 2016; M. B. Miller & Van Horn, 2007; Van Horn et al., 2008; Yarkoni, 2015). The increasing availability of large, openly available datasets and advanced computational tools propels the field toward this aim(Marcus et al., 2011; Niso et al., 2016a; Poldrack & Gorgolewski, 2014). Yet, with bigger and deeper data volumes, neuroscientists are confronted with a paradox: while big-data neuroscience approaches the realm of population neuroscience, we remain challenged by understanding how interindividual data variability echoes the singularity of the self(Dubois & Adolphs, 2016; Mars et al., 2018; Mišić & Sporns, 2016; Van Horn et al., 2008).

This epistemological question has become particularly vivid with recent research showing that individuals can be differentiated from a cohort via their respective neural fingerprints derived from structural magnetic resonance imaging (MRI)(Valizadeh et al., 2018; Wachinger et al., 2015), functional MRI (fMRI)(Amico & Goñi, 2018a; Bari et al., 2019; Finn et al., 2015a; Kaufmann et al., 2017a; Miranda-Dominguez et al., 2014), electroencephalography (EEG)(Fraschini et al., 2015; Kong et al., 2023; Rocca et al., 2014), or functional near-infrared

spectroscopy (fNIRS)(de Souza Rodrigues et al., 2019). Neural fingerprints are associated with individual differences in intelligence test performance, working memory, and attention(Greene et al., 2018a; Rosenberg, Scheinost, et al., 2020; Yamashita et al., 2018; Yoo et al., 2018). Most published work so far is methodologically based on inter-individual similarity measures of functional connectivity—understood as statistical dependencies between ongoing signals across brain regions in task-free awake conditions(Bullmore & Sporns, 2012; Smith et al., 2013)—as defining features of neural fingerprints. Yet, the indirect coupling between hemodynamic and neural brain signaling interrogates the neurophysiological nature of brain fingerprints.

In electrophysiology, ongoing brain dynamics at rest are rich and complex (Smith et al., 2013) and have long been considered a nuisance, a by-product of neural noise(Başar, 1990; Stein et al., 2005; Uddin, 2020). Recent experimental evidence, spurred by systems neuroscience models, indicates that spontaneous brain activity captured using electrophysiological techniques expresses similar resting-state connectomes as fMRI and influences conscious, sensory processes(Florin & Baillet, 2015; Iemi et al., 2019; Samaha et al., 2020). Ongoing neurophysiological activity varies considerably between individuals and across the lifespan. One instance is the inter-individual variability of prominent features of human brain neurophysiological activity, such as the alpha rhythm (8–12 Hz) peak frequency(Bodenmann et al., 2009; Haegens et al., 2014). Previous EEG fingerprinting work was restricted to scalp data, and therefore, provided limited neuroanatomical insight(Fraschini et al., 2015; Kong et al., 2023; Rocca et al., 2014). Another distinctive aspect of electrophysiology is the contamination of recordings by artifacts of different natures including environment and instrument noise, muscle contractions, eye and head movements, which can be distinctive of individuals and can bias fingerprinting with non-neural signal features. Overall, the unique signature components of fast neurophysiological brain dynamics across individuals remain unchartered.

In this work, we use resting-state recordings of magnetoencephalography MEG (Baillet, 2017) from a cohort of participants to identify neurophysiological features of individual differentiation. We both derive measures of functional organization (i.e., functional connectivity) inspired by fMRI neural fingerprinting approaches, and spectral signal markers that are proper to the wider frequency spectrum of brain signaling accessible to neurophysiological data. Our data

exemplify that individual differentiation based on connectome features is akin to previous fMRI reports, and further demonstrate that we can equally differentiate individuals with simpler measures of the spatial distribution of neurophysiological spectral signal power. In addition, individual differentiation is achieved with recordings as short as 30seconds and is robust across recordings preformed weeks after their baseline reference data was collected. Together, our work extends the notion of a neural fingerprint to the fast and large-scale resting-state dynamics of electrophysiology.

## Results

We used MEG data from 158 participants available from the Open MEG Archives OMEGA6. Data collected on multiple days were available for a subset of these participants (N=47; mean duration between consecutive sessions: 201.7 days; Fig. 1). The participants were both healthy and patient volunteers (ADHD and chronic pain) spanning in age from 18–73-years old (see Supplemental Information). T1-weighted structural MRI volumes were available from OMEGA for all participants and were used to produce source maps of resting-state brain activity(Baillet et al., 2001). We derived several neurophysiological signal features from MEG brain source time series summarized within the Desikan-Killiany atlas—68 regions of interest (ROIs) parcellating the entire cortical surface37. The MEG features comprised power-spectral-density estimates (PSD) within each of the 68 ROIs37, and 68×68 functional connectomes (FC) between these ROIs. The approach is illustrated in Fig. 1 and the FC and PSD methodological details are provided in "Methods".

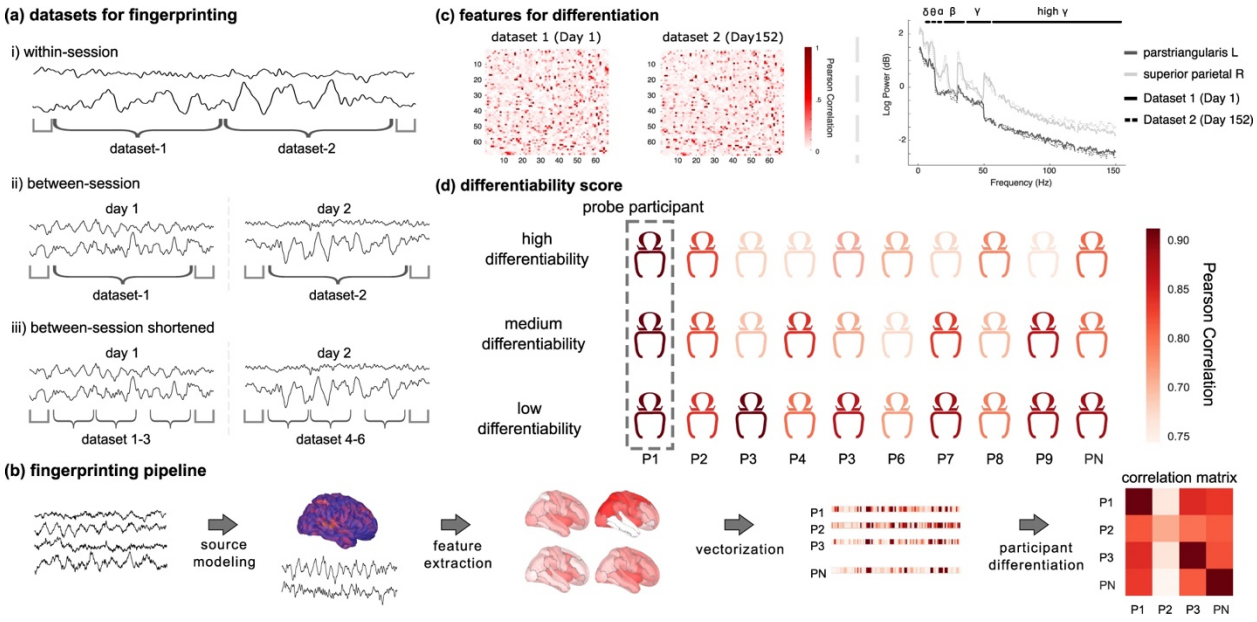


Chapter 2 Figure 1 Neural fingerprinting analysis pipeline and definition of differentiability.

**a** Schematic of exemplar MEG data divided into datasets used in each of the specified differentiation challenges. (i) Within-session challenge: the session data was split in half to generate segments of equal duration; (ii) Between-sessions challenge: differentiation was performed using data recorded on two separate days; (iii) Between-session shortened challenge: data recorded on two different days were split into three 30 s segments. **b** Schematic of the data analysis pipeline: source modeling was first performed before extracting features from each region of the Desikan-Killiany atlas(Desikan et al., 2006a). These features were vectorized and subsequently used to fingerprint individuals, yielding a participant correlation matrix. **c** Features for the between-session challenge from an exemplar subject. Left panel depicts amplitude envelope correlation (AEC) functional connectivity matrices across two datasets; both matrices feature the Pearson correlation coefficients between all 68 regions of the Desikan-Killiany atlas(Desikan et al., 2006a). Right panel plots the power spectrum density estimates from two regions of the atlas, across two datasets. **d** Differentiability was derived for each participant as the z-score of their correlation to themselves, relative to the correlation between themselves and the rest of the cohort. A participant with a high correlation to themselves and low correlations to others was qualified as highly differentiable. An individual highly correlated to both themselves and many others in the cohort was qualified as less differentiable.

Participant differentiation was performed across pairs of MEG data segments taken from either the same (within-session differentiation) or a repeated session (between-session differentiation) using two distinct datasets (Fig. 1a) and based either on FC or PSD features (referred as connectome and spectral fingerprinting, respectively). The within-session challenge with longer data segments was considered to assess the baseline performances of the MEG fingerprinting approaches proposed. The more challenging situations developed in the present report concern individual differentiation from shorter 30 s time segments within or between recording sessions. For each pair of participants, the Pearson's correlation coefficient between their respective features (i.e., FC or PSD) was the corresponding entry in the group correlation matrix (see Supplemental Information). The fingerprinting procedure for each individual proceeded via a lookup operation through the corresponding row of the correlation matrix; the index of the column featuring the largest correlation coefficient determined the predicted (anonymous) identity of the individual in the cohort. Thus, if a given individual's data features from the first dataset were most correlated to the data features from their second dataset, the individual would be correctly differentiated. Note that taking the maximum along the rows or columns simply switches which dataset is used for deriving the differentiation features (e.g., differentiating individuals using dataset 1 from features derived from dataset 2; results for all possible combinations of datasets are reported in Supplemental Information). The overall accuracy of the neural fingerprinting procedure was computed as the proportion of participants correctly differentiated. We ran three types of differentiation challenges: within-session fingerprinting consisted of the differentiation between 158 participants (i.e., the datasets were from same-day recordings split in half); a between-session differentiation challenge for a subset of 47 participants for whom the datasets were from two separate days; and a between-session differentiation using considerably shorter data segments (30s) (Fig. 1a). We conducted the differentiation challenges using either broadband MEG data or band-limited versions within the typical frequency bands used in neurophysiology. We also derived a differentiability score for every participant, which indicates the saliency of the differentiation of any given individual in the tested cohort (see "Methods").

### Within-session connectome and spectral data differentiate individuals

Within-session MEG connectome and spectral fingerprinting achieved 94.9% and 96.2% participant differentiation accuracy, respectively (Fig. 2). This outcome was robust to switching datasets (Supplemental Information). While previous work(Amico & Goñi, 2018a) reported that data reduction strategies improved fingerprinting performances, this was not the case with our data. Data reduction strategies only marginally improved individual differentiation, as explained in Supplemental Information.

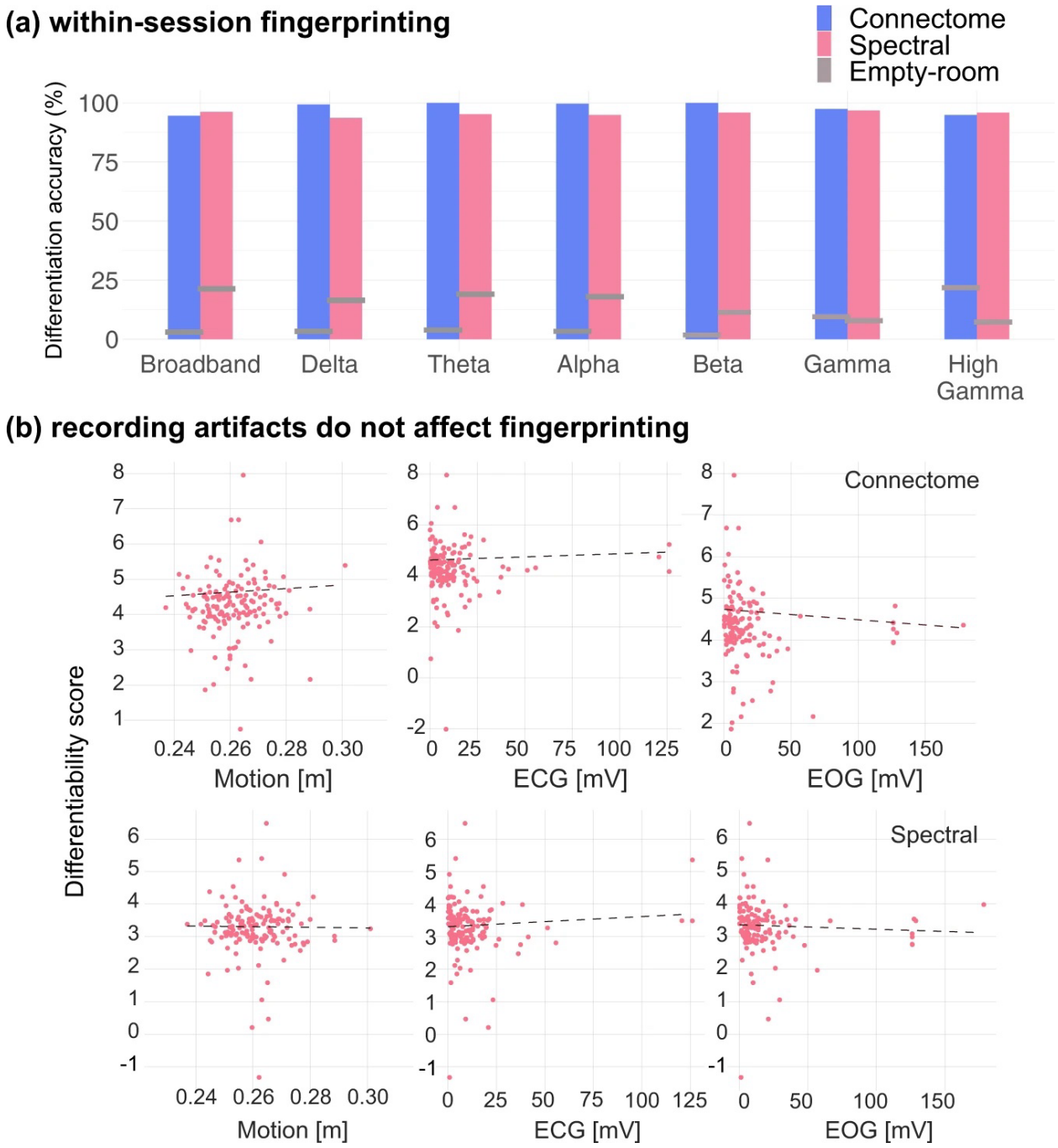


Chapter 2 Figure 2 Within-session differentiation is not related to recording artifacts.

**a** Differentiation accuracy of connectome and spectral fingerprinting based on broadband and narrowband brain signals. Horizontal gray bars indicate reference differentiation levels obtained from empty-room data recorded on the same days as participants (see “Methods”). **b** Differentiability scores were not related to typical confounds such as head motion, eye

movements, and heartbeats. Top row: using connectome fingerprinting; bottom row: spectral fingerprinting. Source data are provided as a Source Data file.

## MEG fingerprinting is robust over time

We tested whether participants who underwent MEG sessions on separate days were differentiable from datasets collected weeks to months apart (with a range of 1–1029 days apart and an average of 201.7 days, SD=210.1). We applied the above fingerprinting procedures towards this between-session challenge on the subset of participants concerned (N=47). Connectome fingerprinting decreased in performance compared to the differentiation accuracy scores obtained from the within-session challenge (89.4%). Performance of connectome fingerprinting from narrowband signals also decreased, with the greatest robustness obtained from using signals in the beta and theta bands (Fig. 3 and Supplemental Information). In contrast, spectral fingerprinting was robust longitudinally, with differentiation accuracy scores of 97.9% (broadband) and >90% (narrowband) that were similar to those obtained in the within-session challenge (Fig. 3 and Supplemental Information). Differentiability scores were not correlated with the number of days between MEG sessions (connectome: $r=0.09$, $p=0.5$; spectral: $r=0.08$, $p=0.65$).

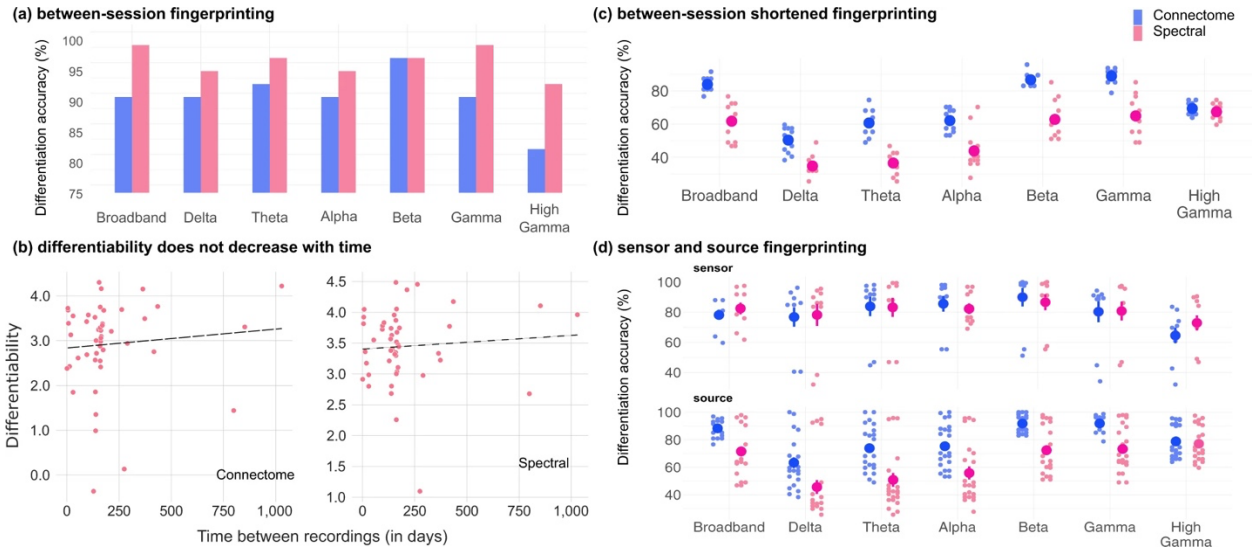


Chapter 2 Figure 3 Characteristic features of connectome and spectral fingerprinting.

**a** Differentiation accuracy for connectome and spectral between-session fingerprinting. Fingerprinting performances are similar to those from the within-session challenge. **b** Pearson correlation analyses did not reveal an association between differentiability and the delay between session recordings (connectome fingerprinting: $r = 0.09$, $p = 0.5$; spectral fingerprinting: $r = 0.08$, $p = 0.60$). **c** Between-session-shortened differentiation accuracy using shorter 30 s data segments collected days apart (average: 201.7 days). Each data point represents one combination of datasets used for fingerprinting (see "Methods" for details). **d** Scatter plots of all fingerprinting challenges across frequency bands for source (brain) and sensor (scalp) level fingerprinting (Supplemental Information details the results obtained for all sensor data fingerprinting challenges). Source data are provided as a Source Data file.

We further challenged MEG individual differentiation between sessions days apart using shorter data segments. We extracted three 30 s segments from the between-session data on each day (Fig. 1a) and ran the same fingerprinting procedures as above. Differentiation performances from connectome fingerprinting remained high across all 30 s segments tested (Fig. 3c) using broadband MEG signals (differentiation accuracy 83.8%). Performance of spectral fingerprinting was decreased (differentiation accuracy: 61.6% Fig. 3c). We observed similar discrepancies in performance robustness between connectome and spectral fingerprinting using narrowband signals (Fig. 3), especially in the delta, theta, and alpha bands. We report results

obtained from using sensor data only and for the within-session shortened challenge in Supplemental Information.

## Salient neurophysiological features for fingerprinting

We identified the features which were the most characteristic of individuals for MEG fingerprinting. We derived measures of intraclass correlation (ICC)(Amico & Goñi, 2018a) to quantify how much each feature, such as an edge of the FC connectome or the signal power in a frequency band from an anatomical parcel, contributed to fingerprinting (see "Methods"). This metric was reported in previous brain fingerprinting studies and captures the inter-rater reliability of each participant as their own rater, to identify the neurophysiological signal features that are the most consistent across individuals(Amico & Goñi, 2018a; Shrout & Fleiss, 1979a). We performed this analysis for both the broadband connectome and the band-specific spectral fingerprinting within-session challenges. The data show that the dorsal attention and visual networks were the most specific across individuals for connectome fingerprinting, in all frequency bands (Fig. 4). Beta-band connectivity of the limbic network was particularly distinctive of individuals. For spectral fingerprinting, theta, alpha, beta, and gamma bands discriminated individuals along midline, parietal, lateral temporal, and visual areas (Fig. 4b). These results are consistent with our narrowband analysis (see Fig. 2a), which highlights beta activity as the most informative in differentiating individuals.

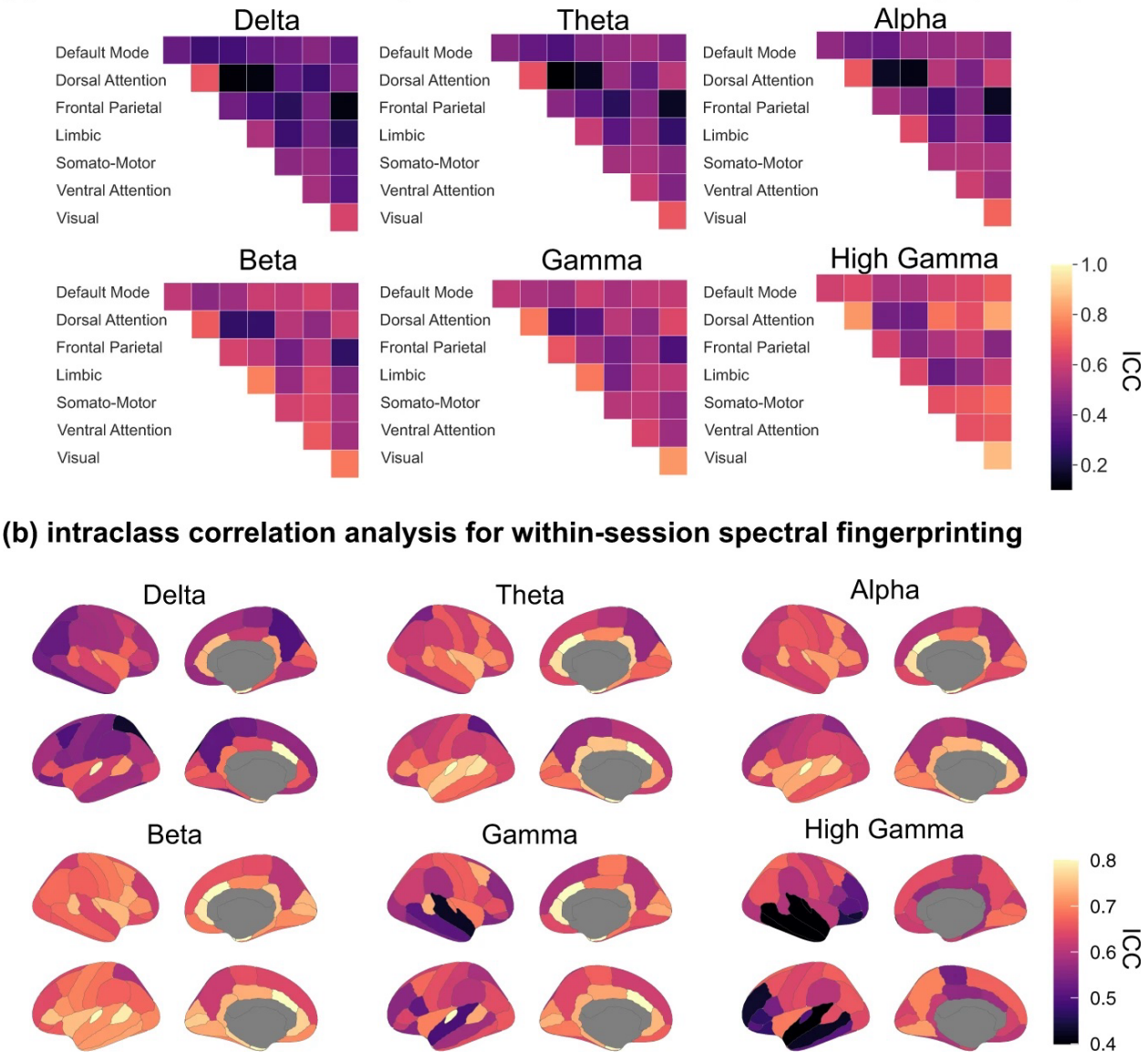


Chapter 2 Figure 4 Characteristic features of connectome and spectral fingerprinting.

Intraclass correlation (ICC) for connectome and spectral within-session fingerprinting. **a** ICC for connectome fingerprinting plotted for each tested frequency band, using network labels from Yeo et al.[81]. The most prominent networks for connectome fingerprinting were the Visual, Dorsal Attention, and Limbic networks. **b** ICC for spectral fingerprinting plotted for each tested frequency band and mapped using the Desikan-Killiany cortical parcellation(Desikan et al., 2006a). The most salient features were the theta, alpha, and gamma band signals expressed in midline structures and the beta band across the cortex.

## Neurophysiological fingerprinting features are associated with demographics

Beyond differentiating individuals in a cohort, we tested whether resting-state neurophysiological features could also predict meaningful participant traits, using an exploratory partial-least-squares (PLS) analysis (see "Methods"(McIntosh & Mišić, 2013)). Briefly, PLS explains the structure of the covariance between two observation matrices—here a demographic matrix and a neurophysiological signal matrix composed of ROI-specific connectome of spectral measures—with latent components. PLS analysis of our data revealed three significant latent components, which were distinct for connectome and spectral fingerprinting (Supplemental Information). The first latent component in connectome fingerprinting was related to clinical population ($r=0.2$, 95% CI [0.160, 0.3]) and handedness ($r=0.2$, 95% CI [0.1, 0.3]). This demographic profile was associated with reduced beta-band functional connectivity over the frontal-parietal network (Fig. 5). For spectral fingerprinting, the first salient latent component was related to a younger age ($r=-0.3$, 95% CI [−0.1, −0.5]), female ($r=0.4$, 95% CI [0.2, 0.5]) and clinical population ($r=0.5$, 95% CI [0.2, 0.5]). This demographic profile was associated with stronger expressions of broadband neurophysiological signal power in superior parietal regions and the pericalcarine gyrus bilaterally, and reduced neurophysiological signals in the isthmus cingulate (Fig. 5).

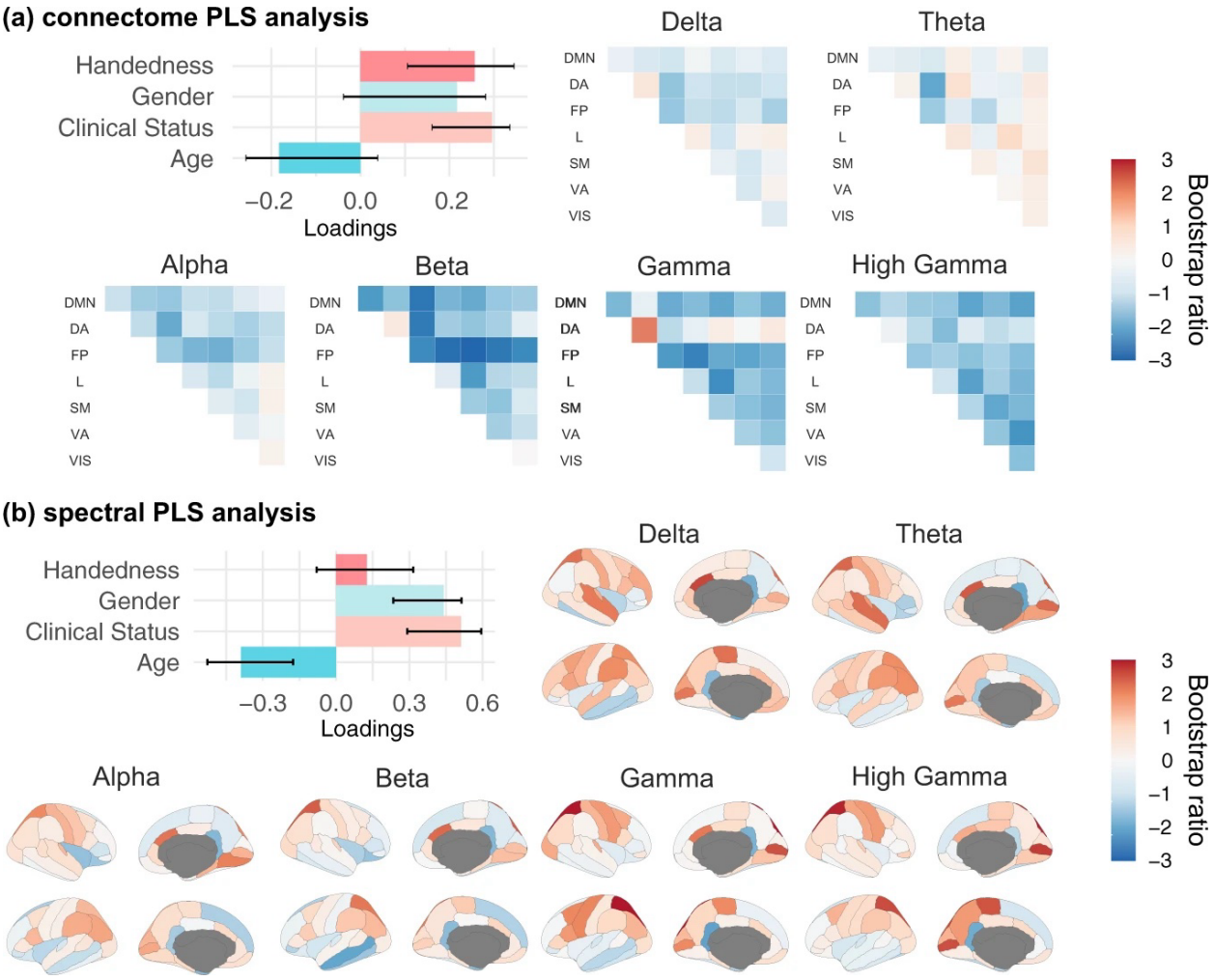


Chapter 2 Figure 5 Partial Least-Squares analysis relates demographics to connectome and spectral features.

(**a**) and (**b**) from left to right, depicts the design saliency patterns for the first latent variables and their associated neural-data bootstrap ratios. Confidence Intervals (95% CI) were calculated through a bootstrapping procedure (n = 10,000), and as such may not necessarily be symmetric. Bootstrap ratios computed for (**a**) connectome and (**b**) spectral features are plotted according to the resting-state networks labeled according to Yeo et al.81 and the Desikan-Killiany parcellation(Desikan et al., 2006a), respectively: Default Mode Network (DMN), dorsal attention (DA), frontal-parietal (FP), limbic (L), somato-motor (SM), ventral attention (VA), and visual (VIS). Source data are provided as a Source Data file.

# Discussion

The recent leveraging of large, open fMRI datasets has brought empirical evidence that individuals may be differentiated within a cohort from their brain imaging functional connectivity, inspiring the metaphor of a neural fingerprint. Unlike hand fingerprints, their cerebral counterpart predicts task performance and a variety of traits(Finn et al., 2015a; Greene et al., 2018a; Rosenberg, Scheinost, et al., 2020; Yamashita et al., 2018; Yoo et al., 2018). These intriguing findings require a better understanding of their neurophysiological foundations, which we sought to characterize from direct neural signals captured at a large scale with MEG.

Our data show that individuals can be differentiated in a cohort of 158 unrelated participants from their respective resting-state connectomes and spectral profiles in a range of fast brain signals. MEG fingerprinting was successful using data lengths (30s) much shorter than those reported for fMRI fingerprinting(Finn et al., 2015a; Noble et al., 2017). Brain electrophysiological signals are rich, complex, and convey expressions of large-scale neural dynamics channeled by individual structural anatomy and physiology(Cabral et al., 2017). Indeed, we also showed that MEG fingerprinting is robust across time, making individuals potentially differentiable from data collected days, months, or years apart. Lastly, we characterized whether individual differences in resting-state neural dynamics are demographically meaningful through an exploratory PLS analysis. We showed that both resting-state connectomes and spectra predict latent demographic components. Recent findings corroborate our results, demonstrating individual differences between functional connectivity derived from resting-state electrophysiology(Nentwich et al., 2020). Future work will be required to replicate and expand these findings in more samples of individuals.

## Connectome and spectral neurophysiological fingerprints

Our results highlight two sets of brain-wide electrophysiological features that contributed to successful fingerprinting: connectome and spectral measures across the neurophysiological frequency spectrum. Overall, connectome and spectral fingerprinting with MEG performed equivalently to fMRI approaches, achieving overall differentiation rates above 90%, with robust

individual differentiation over time and against noise(Amico & Goñi, 2018a; Finn et al., 2015a; Horien et al., 2019).

We found that for connectome fingerprinting, the anatomical regions the most characteristic of individuals differed between MEG and fMRI. While fMRI highlighted the default-mode network and the fronto-parietal resting-state networks, MEG connectome fingerprinting emphasized functional connectivity within limbic and visual networks as contributing to individual specific neurophysiological signatures. In contrast, both MEG and fMRI fingerprinting emphasize the importance of the dorsal attention network(Finn et al., 2015a). These observations are not mutually exclusive, considering the different nature of brain signals captured by the respective modalities. One possible interpretation—requiring further investigation—is that the fast neurophysiological signals that contribute to differentiation with MEG have hemodynamic counterparts that are not as salient in fMRI as the fingerprinting networks reported so far. Nevertheless, our data indicate that neurophysiological signals in the beta band contribute to the highest differentiation accuracy amongst all other typical bands. This finding is compatible with previous work reporting that correlated amplitude changes of MEG brain signals are related to the microstructure of white matter tracts and reveal, with the same amplitude envelope correlation method as used here, MEG resting-state brain networks that align with fMRI's(Brookes, Woolrich, et al., 2011; Hunt et al., 2016). Beta-band activity also emerges from recent literature as a signalling vehicle of re-afferent "top-down" communications in brain circuits(Michalareas et al., 2016; Morillon & Baillet, 2017). One can therefore speculate that beta-band signals would convey electrophysiological representations of internal cognitive models that are by essence intimately specific of each individual(Baillet, 2017).

Such brain signal amplitude signatures are further emphasized by the ability of simple spectral brain maps to enable MEG fingerprinting. Within- and between-session spectral fingerprinting were achieved with remarkable accuracy (>90%) with broadband MEG brain signals or restricted to the typical bands of electrophysiology. Spectral differentiation based on signals from the faster bands (gamma and high-gamma) was overall the most robust longitudinally and against using shorter data segments. This observation is consistent with the width of (high) gamma frequency bands spanning broader ranges (here between 30–50 Hz and

50–150 Hz) than slower bands such as delta (1–4 Hz), theta (4–8 Hz) and alpha (8–12 Hz). The spectral estimates averaged across the broader (high) gamma bands were, therefore, the most robust against using shorter data segments. The reduced number of sliding time windows available over shorter data durations increased the variance of the summary statistics extracted to derive the spectral fingerprints from the signals defined over narrower bands. The higher frequency bands were less affected because the larger number of frequency bins involved in the extraction of their summary power statistics tended to compensate the higher empirical variance of spectral estimates from a lesser number of observations over time. Connectome fingerprinting was more immune against using shorter data durations. The underlying approach indeed did not require spectral transformations but resorted to a bank of narrowband filters applied over the original duration of MEG recordings before the resulting filtered signals were segmented in shorter epochs for the fingerprinting challenges. The consequence is that the number of data points used for all narrowband signals was identical across all frequency bands, yielding moderate variability in differentiation performances compared to those obtained with the spectral approach. Another point of robustness for connectome fingerprinting is that connectivity weights between network nodes may fluctuate very slowly over time in task-free brain activity: Florin and Baillet(Florin & Baillet, 2015) reported fluctuation rates of 0.01 Hz in MEG, indicating typical time cycles of 100 s—a duration substantially longer than the 30 s shortest time window used here. Over longer periods of time though, such as in the between-session challenge, spectral fingerprinting outperformed its connectome counterpart. We note a slight increase of spectral differentiation accuracy in the between-session challenge (e.g., +1.6% for broadband fingerprinting) compared to within-session, which was a statistical fluctuation due to using a smaller sample of participants.

On average across all source fingerprinting challenges reported herein, and despite successful fingerprinting across lower frequency bands (delta 54.4%, theta 62,3%, alpha 65.5%), performances were markedly better using high-frequency signal components (beta 82.0%; gamma 82.5%; high gamma 77.9%). Gamma and faster activity have long been associated with concurrent and colocalized hemodynamic fluctuations(Haufe et al., 2018; Logothetis et al., 2001). Because they may be seen as dual manifestations of BOLD signaling used in fMRI fingerprinting,

this may explain why these signals contributed robustly to MEG brain fingerprinting in our data. However, gamma-band and faster brain signals are on average weaker in amplitude and therefore may be masked by contamination from artifacts and noise(Nottage & Horder, 2015; Whitham et al., 2007; Yuval-Greenberg et al., 2008). The preprocessing applied to our data attenuated such nuisance to a point where individuals were not differentiable from typical sources of signal contamination such as individual head motion behavior.

Although a rhythm of prominent amplitude in humans during rest, alpha-band activity (8–12 Hz) was not particularly specific to differentiate individuals in the cohort. In that respect, our data is aligned with previous MEG works on resting-state connectomes extracted from neurophysiological MEG signals, which did not report on a salient role of alpha activity in driving inter-regional connectivity(Brookes, Woolrich, et al., 2011; Florin & Baillet, 2015). We argue that the spatial topography of alpha resting activity may be relatively stereotypical across individuals, involving thalamo-cortical loops that project focally to the parieto-occipital junction, with limited variability across individuals(Niso et al., 2016a). In task, alpha activity has been related to attention orienting, alertness and anticipation, and the registration of (multimodal) sensory information, thereby reflecting transient mental states(Bagherzadeh et al., 2020; Clayton et al., 2018; Foster & Awh, 2019; Lennert et al., 2021; Samaha et al., 2020) rather than individual traits.

The data also indicates that MEG fingerprinting is robust against typical recording artifacts that may be idiosyncratic of individuals and therefore, could have confounded fingerprinting. Session environmental conditions captured by empty-room MEG recordings were not sufficient to differentiate individuals within or between sessions. The participant's anatomical and head-position information embedded in their respective MEG source imaging kernels were also not sufficient to differentiate individuals. Note that head position changed between sessions. Further studies are required to clarify how these results may vary depending on the type of MEG source modeling adopted. We anticipate little influence of the type of source model used though, based on evidence that beamforming kernels are mathematically equivalently to other major classes of linear source estimation kernels, such as weighted minimum-norm estimators(Mosher et al., 2003). Future work should corroborate these results with regards to fingerprinting. The choice of connectivity measure to derive electrophysiological connectomes may also influence

fingerprinting(Sareen et al., 2021a). We look forward to current progress in electrophysiological brain connectomics to put forward measures of network connectivity informed by mechanistic principles and emerging as a standard metrics in the field to confirm and expand present fingerprinting results(Sadaghiani et al., 2022).

While our present data show robust longitudinal fingerprinting performances, future work involving more participants with multiple MEG visits is required to both replicate these observations and investigate whether individual deviations from baseline fingerprints could be early signals of asymptomatic neuropathophysiology(Baillet, 2017). We hope the remarkable ability to fingerprint individuals from the present electrophysiological features serves as a stepping stone for future investigation, which may include multimodal noninvasive assessments based on MEG, combined with, e.g., fMRI and/or EEG.

### Neural fingerprints of individual traits

Our data suggest that individual differences in resting-state neurophysiological functional connectivity and spectral power relate to latent demographic clusters. These observations are in line with previous fMRI work that showed that connectomes are predictive of individual differences in attention, working memory, and intelligence test performance. For instance, connectivity patterns between the default mode and the dorsal attention networks predict attentional behavior during the task and self-reported mind wandering(Rosenberg et al., 2016; Rosenberg, Scheinost, et al., 2020)(see(Rosenberg et al., 2017a) for review). Overall, a possible conceptual framework is that task-free neural dynamics are the signatures of an individual scaffold of brain functions that is predictive of task behavior. This view is also that of the spontaneous trait reactivation hypothesis wherein the organization of the human cortex at rest (manifested e.g., by functional connectivity) is a window into the self's unique traits and abilities(Harmelech & Malach, 2013). Early evidence indeed suggests that functional connectivity and brain activity are associated with personality traits and even inter-personal closeness in social networks(Cai et al., 2020; Parkinson et al., 2018).

Yet, the mechanistic implementation of these intriguing observations remains elusive. Inter-individual variability in the distribution of synaptic weights across the cerebrum, shaped through lifetime experiences according to Hebbian principles, may account—at least in part—for connectome fingerprinting(Harmelech & Malach, 2013). The heritability of functional connectivity has also been discussed, especially for a variety of brain networks (e.g., dorsal and ventral attention network and the default mode network)(Glahn et al., 2010; Korgaonkar et al., 2014; Miranda-Dominguez et al., 2018). Heritability of brain spectral characteristics is also actively discussed(Hodgkinson et al., 2010; Leppäaho et al., 2019; Salmela et al., 2016). This emerging literature and the empirical evidence of brain fingerprinting certainly motivate more research on new, fascinating questions about the biological nature of the self.

### Sampling population diversity for personalized interventions

Robust individual signatures of brain activity may be transformative to neurophysiological phenotyping and population neuroscience. With the increasing availability of multi-omic data repositories, there is a research opportunity to span the diversity of statistical normative characteristics of brain fingerprints across the population in relation to behavior, environmental, and clinical variables(Baillet, 2017; Dubois & Adolphs, 2016; Van Horn et al., 2008). Our study highlights the utility of datasets of individuals who have been scanned on multiple occasions to capture and characterize interindividual variability as meaningful information. Ideally, large databanks of individual variants sampled across multiple dimensions of socio-economic, age, and geographic factors enable normative modeling approaches to establish the risk traits of developing syndromes of, e.g., early cognitive decline, neurodegeneration, or mental illness. Previous work has shown that mental disorders may affect the stability of individual fingerprints over time and therefore points at possible translational applications of the approach(Kaufmann et al., 2017a, 2018a). We also foresee that changes over time or lack thereof of a person's brain fingerprint may also constitute a new class of non-invasive markers of responses to neurological and other treatment in a variety of chronic, neurodegenerative, or acute (e.g., stroke) conditions. Brain fingerprints derived from short, task-free sessions may play a leading role to realize this vision in practice.

Brain fingerprinting may also contribute to future endeavors in establishing how oscillatory dynamics at rest support cognitive functions across the lifespan. MEG brain fingerprinting presents several potential advantages in terms of safety, shorter scan duration, and the immediate proximity of a care person during data collection, especially for special populations.

The methodological approaches proposed herein can, in principle, transfer to EEG fingerprinting(Fraschini et al., 2015; Kong et al., 2023; Rocca et al., 2014) which would be more readily available in clinics. Whether results would be as robust with EEG as MEG remains to be demonstrated. Indeed, EEG source mapping is more prone to contamination from muscle artifacts and is more sensitive to approximations in the biophysical modeling of head tissues, which may compromise further fingerprinting capabilities(Baillet, 2017).

In sum, our study extends the concept of neural or brain fingerprint to fast and large-scale resting-state electrophysiological dynamics, which encapsulate meaningful individual differences in both functional connectivity and neuroanatomical maps of power spectrum characteristics. We are hopeful that the present contribution paves the way to replication and extension using larger open datasets. Many fascinating outstanding questions remain about the biological nature of inter-individual variability expressed via neural oscillations and brain network dynamics, and more specifically how these differences associate with behavior and diseases natural history. The research ahead is for future population neuroscience studies.

# Methods

**The Open MEG Archives (OMEGA).** We used data from the Open MEG Archives (OMEGA(Niso et al., 2016a)) consisting of resting-state MEG recordings acquired using the same MEG system (275 channels whole-head CTF; Port Coquitlam, British Columbia, Canada). The sampling rate was 2400 Hz, with an antialiasing filter applied at 600 Hz cut-off, and built-in third-order spatial gradient noise cancellation (see ref.(Niso et al., 2016a) for details on data acquisition).

We analyzed MEG resting-state data from 158 unrelated OMEG participants (77 females, 31.9±14.7 years old). Recordings were ~5-min long. Supplementary Table 1 provides details on

scanning procedures and Supplementary Table 2 on demographics. A subset of these individuals (N=47) had recordings over multiple visits (different days) and were used in the between-session fingerprinting challenge. The OMEGA data management protocol was approved by the research ethics board of the Montreal Neurological Institute. We followed the ethical procedure of our local ethics board (the Montreal Neurological Institute).

MEG data preprocessing and feature extraction.MEG data were preprocessed using Brainstorm(Tadel et al., 2011); version Oct-12-2018 in MATLAB 2017b (Mathworks, Inc., Massachusetts, USA) following good-practice guidelines(Gross et al., 2013). Unless specified, all steps below were performed using the Brainstorm toolkit, with default parameters. Line noise artifact (60 Hz) along with 10 of its harmonics were removed using a notch filter bank. Slow-wave and DC-offset artifacts were removed using a high-pass FIR filter with a 0.3-Hz cut-off. We derived Signal-Space Projections (SSPs) to remove cardiac and ocular artifacts. We used electro-cardiogram and-oculogram recordings to define signal projectors around identified artifact occurrences. We also applied SSPs to attenuate low-frequency (1–7 Hz) and high-frequency noisy components (40–400 Hz) due to saccades and muscle activity, respectively. Bandpass filtered duplicates of the cleaned data were produced for each frequency band of interest (delta: 1–4 Hz, theta: 4–8 Hz, alpha: 8–13 Hz, beta: 13–30 Hz, gamma: 30–50 Hz, and high gamma: 50–150 Hz). Distinct brain source models were then derived for all narrowband versions of the MEG sensor data.

Each individual T1-weighted MRI data were automatically segmented and labeled with Freesurfer(Fischl, 2012). Coregistration with MEG sensor locations was derived using dozens of digitized head points collected at each MEG session. We produced MEG forward head models for each participant using the overlapping spheres approach, and cortical source models with linearly-constrained minimum-variance (LCMV) beamforming, all using Brainstorm with default parameters (2016 version for source estimation processes). We performed data covariance regularization. To reduce the effect of variable source depth, the estimated source variance was normalized by the noise covariance matrix. Elementary MEG source orientations were constrained normal to the surface at 15,000 locations of the cortex. Noise statistics for source

modeling were estimated from two-minute empty-room recordings collected as close as possible in time to each participant's MEG session. Source timeseries were clustered into 68 cortical ROIs defined from the Desikan-Killiany atlas(Desikan et al., 2006a) and dimension-reduced via the first principal component of all signals within each ROI.

Connectome and spectral fingerprinting features were computed from ROI source timeseries. Individual connectomes were derived in all frequency bands from the amplitude envelope correlation (AEC) approach(Bruns et al., 2000). ROI timeseries were Hilbert transformed and all possible pairs of resulting amplitude envelopes were used to derive the corresponding Pearson correlation coefficients, yielding a 68×68 symmetric connectome array. We used Welch's method to derive power spectrum density (PSD) estimates for each ROI(Welch, 1967), using time windows of 2 s with 50% overlap sled over all ROI timeseries and averaged across all PSDs within each ROI. The resulting frequency range of PSDs was 0–150 Hz, with a frequency resolution of 0.5 Hz. The connectome and spectral features were then exported to Python (3.7.6) for subsequent fingerprinting analyses.

**Fingerprinting and differentiability.** We used a fingerprinting approach directly adapted from fMRI connectome fingerprinting methods(Amico & Goñi, 2018a; Finn et al., 2015a) which relies on correlational scoring of individuals between datasets. A given probe participant is differentiated from a cohort by computing all Pearson correlation coefficients between the spectral or connectome features of said probe at one timepoint (e.g., dataset 1) and the entire cohort at a different timepoint (e.g., dataset 2). The entry presenting the highest correlation to the probe determined the probe's estimated identity, i.e., identified entry in the cohort. This approach was applied between all pairs of participants in the cohort, yielding an asymmetric correlation matrix spanning the cohort. We report scores of differentiation accuracy as the ratio between the number individuals correctly differentiated with the described procedure and the total number of individuals in the cohort. Differentiation accuracy scores are obtained from fingerprinting challenges from dataset 1 to dataset 2 and vice-versa, within- and between-sessions. Figure 1 details the definition of the dataset labels used, and Supplemental Information contains the results from across all combinations of datasets/sessions.

Amico and Goñi(Amico & Goñi, 2018a) proposed an identifiability score to quantify, for a given participant, the reliability of its differentiation from others in the cohort. Here, we extend this notion with the introduction of a differentiability measure, $D_{self}$. Let A be the correlation matrix spanning the cohort (square, asymmetric) between dataset 1 and dataset 2, and N be the number of participants to differentiate. We define $D_{self}$ as the z-score of participant $P_i$'s correlation to themselves between dataset 1 and dataset 2, with respect to $P_i$'s correlation to all other individuals in the cohort, noted: $D_{self\ (i)} = (Corr_{ii} - \mu_{ij})/\sigma_{ij}$, where $Corr_{ii}$ is the $P_i$'s correlation between dataset 1 and dataset 2, $\mu_{ij}$ is the mean correlation between participant $P_i$ in dataset 1 and all other individuals in dataset 2 (i.e., the mean along the $i^{th}$ row of matrix A), and $\sigma_i$ is the empirical standard deviation of inter-individual features correlations. Thus, if a participant is easily differentiable, its differentiability increases; whereas small differentiability scores indicate a participant that is particularly difficult to differentiate from the rest of the cohort.

**Recording artifacts and differentiability.** To investigate the effects of recording parameters and artifacts on fingerprinting, we related each individual's differentiability to several possible confounds. The duration of each scan was compared to differentiability to verify that longer recordings available from a subset of individuals did not make them easier to differentiate. We also correlated the root mean square (RMS) of signals that measured ocular, cardiac, and head movement artifacts over the duration of the entire recording to participants' differentiability score. For cardiac artifacts for instance, we derived the RMS of ECG recordings; for ocular artifacts we used the HEOG and VEOG electrode recordings; and for motion artifacts we extracted the RMS of all three head coil signals that measured 3-D head movements during MEG recordings. These derivations were conducted for both the connectome and spectral broadband within-session fingerprinting challenge.

**Fingerprinting across frequency bands.** We replicated the above fingerprinting approach using data restricted to each frequency band of interest (delta 1–4 Hz, theta 4–8 Hz, alpha 8–13 Hz, beta 13–30 Hz, gamma 30–50 Hz, and high gamma 50–150 Hz). We report the differentiation accuracy obtained from each narrowband signal in both the spectral and connectome fingerprinting

challenges in Figs. 2 and 3, for the within- and between-session fingerprinting challenges respectively.

We also performed fingerprinting tests based on sensor data only. We used the same connectome and spectral approaches as the MEG source maps, considering the time series of each of the 275 MEG channels instead of the 68 ROI time series derived from the brain map parcels. We report the differentiation performances from both the sensor and source analyses in Fig. 3 and in Supplemental Information.

**Between-session and shortened fingerprinting challenges.** We verified the robustness of MEG fingerprinting with respect to (1) the ability to differentiate participants over time and (2) reduced data durations. We subdivided participants into three additional challenges: the within-session-shortened, between-session, and between-session-shortened challenge. First, we used the participant data described in the within-session analysis and extracted connectome and spectral fingerprinting features over three 30-second non-overlapping time segments. This duration was based on the length of the shortest recording in the data sample (Fig. 1aii). We applied the same fingerprinting procedure as described in Fingerprinting and Differentiability across all possible combinations of the three 30 s datasets. Second, we assessed the stability of the fingerprinting outcomes using a subset of participants with consecutive MEG sessions separated by several days (N=47; separated on average by 201.7 days, see Supplemental Information for details). Again, we applied the same fingerprinting procedure as described in Fingerprinting and Differentiability for this between-session challenge. Lastly, we applied the same shortened analysis—described above—to the subset of individuals with multiple scans (i.e., the between-sessions data). We report all possible combinations of datasets (i.e., three 30s segments from day 1 and three 30s segments from day 2; see Fig. 1a for example) in Fig. 3.

**Empty-room fingerprinting.** We tested whether environment and instrument noise daily conditions would bias individual differentiation using empty-room recordings collected from each MEG session. The empty-room data was processed identically to the participants data, using the same individual imaging kernels, and were used to differentiate participants. We ran all possible

combinations of empty-room vs. participants datasets (e.g., empty-room 1 vs. participant dataset 1, empty-room 2 vs. participant dataset 1, etc.) and computed the sample mean of the differentiation accuracies across all dataset combinations. The differentiation accuracies obtained represent estimates of baseline reference performances that can be compared to each form of fingerprinting based on actual participant data (i.e., connectome or spectral, broadband or band-specific; see Fig. 2 and Supplemental Information). In a similar fashion, we also used sensor-level empty-room recordings of each participant for fingerprinting—attempting to differentiate individuals' recordings from their empty-room features. The results of this analysis are reported in the Supplemental Information.

**Most characteristic features for fingerprinting.** We quantified the contribution of each feature (i.e., edges in the connectivity matrix or a frequency band in an anatomical parcel) towards differentiating individuals using intraclass correlations (ICC). ICC is commonly used to measure the agreement between two observers (e.g., ratings vs. scores). The stronger the agreement, the higher the ICC(Amico & Goñi, 2018a; Shrout & Fleiss, 1979a). ICC derives a random effects model whereby each item is rated by different raters from a pool of potential raters. We selected this measure to capture the inter-rater reliability of each participant as their own rater to identify which edges (e.g., connections in FC) are the most consistent (i.e., which features of a participant Pi in dataset 1 are most like dataset 2). Here, the higher the ICC, the more consistent a given feature was within individuals. In addition, we computed two other measures of edgewise contribution proposed by Finn and colleagues14: group consistency and differential power (Supplemental Information). We applied all measures (i.e., ICC, group consistency, and differential power) in the context of the broadband within-session fingerprinting challenge. The source maps shown in Figs. 4, 5 and Supplemental Information were generated using R (V 3.6.3(R Core Team, 2022); with the ggseg package(Mowinckel & Vidal-Piñeiro, 2022)).

**Partial Least-Squares: MEG features of participant demographics.** We conducted a Partial Least-Squares (PLS) analysis with the Rotman-Baycrest PLS toolbox(McIntosh & Lobaugh, 2004) in MATLAB 2017b (Mathworks, Inc., Massachusetts, USA). PLS is a multivariate statistical method

that relates two matrices of variables (e.g., neural activity and participant demographics) by estimating a weighted linear combination of variables from both data matrices to maximize their covariance. The associated weights can be interpreted neural patterns (e.g., functional connections) and their associated demographic profiles. PLS used singular value decompositions of the z-scored neural activity-demographics covariance matrix. This decomposition yielded orthogonal latent variables (LV) associated to a pattern of neural activity (i.e., functional connectivity or spectral power) and demographics. To assess the significance of these multivariate patterns, we computed permutation tests (10,000 permutations). Each permutation shuffled the order of the observations (i.e., the rows) of the demographic data matrix before running PLS on the resulting surrogate data under the null hypothesis that there was no relationship between the demographic and neural data. A p-value for the LVs was computed as the proportion of times the permuted singular values exceeded that of the original data. We explored the first significant LV from the broadband connectome and spectral fingerprinting features. We also assessed the contribution of each variable in the demographics and neural activity matrices by bootstrapping observations with replacement (10,000 bootstraps). We computed 95% confidence intervals for the demographic weights and bootstrap ratios for the neural weights. The bootstrap ratio was computed as the ratio between each variable's weight and the bootstrap-estimated standard error.

## Acknowledgements

S.B. is grateful for the support received from the NIH (R01 EB026299), a Discovery Grant from the Natural Science and Engineering Research Council of Canada (436355-13), the CIHR Canada Research Chair in Neural Dynamics of Brain Systems, the Brain Canada Foundation with support from Health Canada, and the Innovative Ideas program from the Canada First Research Excellence Fund, awarded to McGill University for the Healthy Brains for Healthy Lives initiative. This research was undertaken thanks in part to funding from the Canada First Research Excellence Fund, awarded to McGill University for the Healthy Brains for Healthy Lives initiative. BM acknowledges support from the Natural Sciences and Engineering Research Council of Canada (NSERC Discovery Grant RGPIN \#017-04265) and from the Canada Research Chairs

Program. J.D.S.C. acknowledges the support of the Alexander Graham-Bell Doctoral NSERC fellowship.

## Reporting summary

Further information on research design is available in the Nature Research Reporting Summary linked to this article.

## Data availability

Resting-state data were obtained from the OMEGA repository6. Raw MEG recordings can be accessed by requesting the data (https://www.mcgill.ca/bic/omega-registration). The power spectra and connectomes derived from the preprocessed OMEGA samples and used to differentiate individuals in the present study can be reproduced using the code that has been made available and are available from the corresponding author upon reasonable request. Source data are provided with this paper.

## Code availability

All codes for preprocessing and data analysis can be found on the project's GitHub (https://github.com/neurohazardous/megFingerprinting and at Zenodo (https://zenodo.org/record/5181836)(*MEG, Myself, and I: Individual Identification from Neurophysiological Brain Activity*, n.d.).

## Additional information

Supplementary information The online version contains supplementary material available at https://doi.org/10.1038/s41467-021-25895-8.

Correspondence and requests for materials should be addressed to Bratislav Misic or Sylvain Baillet.

Peer review information Nature Communications thanks Matthew Brookes, Matteo Fraschini and the other, anonymous, reviewer(s) for their contribution to the peer review of this work. Peer reviewer reports are available.

## References

Amico, E., & Goñi, J. (2018). The quest for identifiability in human functional connectomes. Scientific Reports, 8(1), Article 1. https://doi.org/10.1038/s41598-018-25089-1

Bagherzadeh, Y., Baldauf, D., Pantazis, D., & Desimone, R. (2020). Alpha Synchrony and the Neurofeedback Control of Spatial Attention. Neuron, 105(3), 577-587.e5. https://doi.org/10.1016/j.neuron.2019.11.001

Baillet, S. (2017). Magnetoencephalography for brain electrophysiology and imaging. Nature Neuroscience, 20(3), Article 3. https://doi.org/10.1038/nn.4504

Baillet, S., Mosher, J. C., & Leahy, R. M. (2001). Electromagnetic brain mapping. IEEE Signal Processing Magazine, 18(6), 14–30. https://doi.org/10.1109/79.962275

Bari, S., Amico, E., Vike, N., Talavage, T. M., & Goñi, J. (2019). Uncovering multi-site identifiability based on resting-state functional connectomes. NeuroImage, 202, 115967. https://doi.org/10.1016/j.neuroimage.2019.06.045

Başar, E. (1990). Chaos in Brain Function: Containing Original Chapters by E. Basar and T. H. Bullock and Topical Articles Reprinted from the Springer Series in Brain Dynamics. Springer Berlin Heidelberg.

Bodenmann, S., Rusterholz, T., Dürr, R., Stoll, C., Bachmann, V., Geissler, E., Jaggi-Schwarz, K., & Landolt, H.-P. (2009). The Functional Val158Met Polymorphism of COMT Predicts Interindividual Differences in Brain α Oscillations in Young Men. Journal of Neuroscience, 29(35), 10855–10862. https://doi.org/10.1523/JNEUROSCI.1427-09.2009

Brookes, M. J., Woolrich, M., Luckhoo, H., Price, D., Hale, J. R., Stephenson, M. C., Barnes, G. R., Smith, S. M., & Morris, P. G. (2011). Investigating the electrophysiological basis of resting state networks using magnetoencephalography. Proceedings of the National Academy of Sciences, 108(40), 16783–16788. https://doi.org/10.1073/pnas.1112685108

Bruns, A., Eckhorn, R., Jokeit, H., & Ebner, A. (2000). Amplitude envelope correlation detects coupling among incoherent brain signals. Neuroreport, 11(7), 1509–1514.

Bullmore, E., & Sporns, O. (2012). The economy of brain network organization. Nature Reviews Neuroscience, 13(5), Article 5. https://doi.org/10.1038/nrn3214

Cabral, J., Kringelbach, M. L., & Deco, G. (2017). Functional connectivity dynamically evolves on multiple time-scales over a static structural connectome: Models and mechanisms. NeuroImage, 160, 84–96. https://doi.org/10.1016/j.neuroimage.2017.03.045

Cai, H., Zhu, J., & Yu, Y. (2020). Robust prediction of individual personality from brain functional connectome. Social Cognitive and Affective Neuroscience, 15(3), 359–369. https://doi.org/10.1093/scan/nsaa044

Clayton, M. S., Yeung, N., & Cohen Kadosh, R. (2018). The many characters of visual alpha oscillations. The European Journal of Neuroscience, 48(7), 2498–2508. https://doi.org/10.1111/ejn.13747

de Souza Rodrigues, J., Ribeiro, F. L., Sato, J. R., Mesquita, R. C., & Júnior, C. E. B. (2019). Identifying individuals using fNIRS-based cortical connectomes. Biomedical Optics Express, 10(6), 2889–2897. https://doi.org/10.1364/BOE.10.002889

Desikan, R. S., Ségonne, F., Fischl, B., Quinn, B. T., Dickerson, B. C., Blacker, D., Buckner, R. L., Dale, A. M., Maguire, R. P., Hyman, B. T., Albert, M. S., & Killiany, R. J. (2006). An automated labeling system for subdividing the human cerebral cortex on MRI scans into gyral based regions of interest. NeuroImage, 31(3), 968–980. https://doi.org/10.1016/j.neuroimage.2006.01.021

Dubois, J., & Adolphs, R. (2016). Building a Science of Individual Differences from fMRI. Trends in Cognitive Sciences, 20(6), 425–443. https://doi.org/10.1016/j.tics.2016.03.014

Finn, E. S., Shen, X., Scheinost, D., Rosenberg, M. D., Huang, J., Chun, M. M., Papademetris, X., & Constable, R. T. (2015). Functional connectome fingerprinting: Identifying individuals using patterns of brain connectivity. Nature Neuroscience, 18(11), Article 11. https://doi.org/10.1038/nn.4135

Fischl, B. (2012). FreeSurfer. NeuroImage, 62(2), 774–781. https://doi.org/10.1016/j.neuroimage.2012.01.021

Florin, E., & Baillet, S. (2015). The brain's resting-state activity is shaped by synchronized cross-frequency coupling of neural oscillations. NeuroImage, 111, 26–35. https://doi.org/10.1016/j.neuroimage.2015.01.054

Foster, J. J., & Awh, E. (2019). The role of alpha oscillations in spatial attention: Limited evidence for a suppression account. Current Opinion in Psychology, 29, 34–40. https://doi.org/10.1016/j.copsyc.2018.11.001

Fraschini, M., Hillebrand, A., Demuru, M., Didaci, L., & Marcialis, G. L. (2015). An EEG-Based Biometric System Using Eigenvector Centrality in Resting State Brain Networks. IEEE Signal Processing Letters, 22(6), 666–670. https://doi.org/10.1109/LSP.2014.2367091

Glahn, D. C., Winkler, A. M., Kochunov, P., Almasy, L., Duggirala, R., Carless, M. A., Curran, J. C., Olvera, R. L., Laird, A. R., Smith, S. M., Beckmann, C. F., Fox, P. T., & Blangero, J. (2010). Genetic control over the resting brain. Proceedings of the National Academy of Sciences, 107(3), Article 3. https://doi.org/10.1073/pnas.0909969107

Greene, A. S., Gao, S., Scheinost, D., & Constable, R. T. (2018). Task-induced brain state manipulation improves prediction of individual traits. Nature Communications, 9(1), Article 1. https://doi.org/10.1038/s41467-018-04920-3

Gross, J., Baillet, S., Barnes, G. R., Henson, R. N., Hillebrand, A., Jensen, O., Jerbi, K., Litvak, V., Maess, B., Oostenveld, R., Parkkonen, L., Taylor, J. R., van Wassenhove, V., Wibral, M., & Schoffelen, J.-M. (2013). Good practice for conducting and reporting MEG research. NeuroImage, 65, 349–363. https://doi.org/10.1016/j.neuroimage.2012.10.001

Haegens, S., Cousijn, H., Wallis, G., Harrison, P. J., & Nobre, A. C. (2014). Inter- and intra-individual variability in alpha peak frequency. NeuroImage, 92, 46–55. https://doi.org/10.1016/j.neuroimage.2014.01.049

Harmelech, T., & Malach, R. (2013). Neurocognitive biases and the patterns of spontaneous correlations in the human cortex. Trends in Cognitive Sciences, 17(12), 606–615. https://doi.org/10.1016/j.tics.2013.09.014

Haufe, S., DeGuzman, P., Henin, S., Arcaro, M., Honey, C. J., Hasson, U., & Parra, L. C. (2018). Elucidating relations between fMRI, ECoG, and EEG through a common natural stimulus. NeuroImage, 179, 79–91. https://doi.org/10.1016/j.neuroimage.2018.06.016

Hodgkinson, C. A., Enoch, M.-A., Srivastava, V., Cummins-Oman, J. S., Ferrier, C., Iarikova, P., Sankararaman, S., Yamini, G., Yuan, Q., Zhou, Z., Albaugh, B., White, K. V., Shen, P.-H., & Goldman, D. (2010). Genome-wide association identifies candidate genes that influence the human electroencephalogram. Proceedings of the National Academy of Sciences of the United States of America, 107(19), 8695–8700. https://doi.org/10.1073/pnas.0908134107

Horien, C., Shen, X., Scheinost, D., & Constable, R. T. (2019). The individual functional connectome is unique and stable over months to years. NeuroImage, 189, 676–687. https://doi.org/10.1016/j.neuroimage.2019.02.002

Hunt, B. A. E., Tewarie, P. K., Mougin, O. E., Geades, N., Jones, D. K., Singh, K. D., Morris, P. G., Gowland, P. A., & Brookes, M. J. (2016). Relationships between cortical myeloarchitecture and electrophysiological networks. Proceedings of the National Academy of Sciences, 113(47), 13510–13515. https://doi.org/10.1073/pnas.1608587113

Iemi, L., Busch, N. A., Laudini, A., Haegens, S., Samaha, J., Villringer, A., & Nikulin, V. V. (2019). Multiple mechanisms link prestimulus neural oscillations to sensory responses. eLife, 8, e43620. https://doi.org/10.7554/eLife.43620

Kaufmann, T., Alnæs, D., Brandt, C. L., Bettella, F., Djurovic, S., Andreassen, O. A., & Westlye, L. T. (2018). Stability of the Brain Functional Connectome Fingerprint in Individuals With Schizophrenia. JAMA Psychiatry, 75(7), 749–751. https://doi.org/10.1001/jamapsychiatry.2018.0844

Kaufmann, T., Alnæs, D., Doan, N. T., Brandt, C. L., Andreassen, O. A., & Westlye, L. T. (2017). Delayed stabilization and individualization in connectome development are related to psychiatric disorders. Nature Neuroscience, 20(4), Article 4. https://doi.org/10.1038/nn.4511

Kong, R., Tan, Y. R., Wulan, N., Ooi, L. Q. R., Farahibozorg, S.-R., Harrison, S., Bijsterbosch, J. D., Bernhardt, B. C., Eickhoff, S., & Thomas Yeo, B. T. (2023). Comparison between gradients and parcellations for functional connectivity prediction of behavior. NeuroImage, 273, 120044. https://doi.org/10.1016/j.neuroimage.2023.120044

Korgaonkar, M. S., Ram, K., Williams, L. M., Gatt, J. M., & Grieve, S. M. (2014). Establishing the resting state default mode network derived from functional magnetic resonance imaging tasks as an endophenotype: A twins study. Human Brain Mapping, 35(8), 3893–3902. https://doi.org/10.1002/hbm.22446

Lennert, T., Samiee, S., & Baillet, S. (2021). Coupled oscillations enable rapid temporal recalibration to audiovisual asynchrony. Communications Biology, 4(1), Article 1. https://doi.org/10.1038/s42003-021-02087-0

Leppäaho, E., Renvall, H., Salmela, E., Kere, J., Salmelin, R., & Kaski, S. (2019). Discovering heritable modes of MEG spectral power. Human Brain Mapping, 40(5), 1391–1402. https://doi.org/10.1002/hbm.24454

Logothetis, N. K., Pauls, J., Augath, M., Trinath, T., & Oeltermann, A. (2001). Neurophysiological investigation of the basis of the fMRI signal. Nature, 412(6843), 150–157. https://doi.org/10.1038/35084005

Marcus, D. S., Harwell, J., Olsen, T., Hodge, M., Glasser, M. F., Prior, F., Jenkinson, M., Laumann, T., Curtiss, S. W., & Van Essen, D. C. (2011). Informatics and data mining tools and strategies for the human connectome project. Frontiers in Neuroinformatics, 5, 4. https://doi.org/10.3389/fninf.2011.00004

Mars, R. B., Passingham, R. E., & Jbabdi, S. (2018). Connectivity Fingerprints: From Areal Descriptions to Abstract Spaces. Trends in Cognitive Sciences, 22(11), 1026–1037. https://doi.org/10.1016/j.tics.2018.08.009

McIntosh, A. R., & Lobaugh, N. J. (2004). Partial least squares analysis of neuroimaging data: Applications and advances. NeuroImage, 23, S250–S263. https://doi.org/10.1016/j.neuroimage.2004.07.020

McIntosh, A. R., & Mišić, B. (2013). Multivariate statistical analyses for neuroimaging data. Annual Review of Psychology, 64, 499–525. https://doi.org/10.1146/annurev-psych-113011-143804

MEG, myself, and I: individual identification from neurophysiological brain activity. (n.d.). Retrieved October 23, 2023, from https://zenodo.org/records/5181836

Michalareas, G., Vezoli, J., van Pelt, S., Schoffelen, J.-M., Kennedy, H., & Fries, P. (2016). Alpha-Beta and Gamma Rhythms Subserve Feedback and Feedforward Influences among Human Visual Cortical Areas. Neuron, 89(2), 384–397. https://doi.org/10.1016/j.neuron.2015.12.018

Miller, M. B., & Van Horn, J. D. (2007). Individual variability in brain activations associated with episodic retrieval: A role for large-scale databases. International Journal of Psychophysiology: Official Journal of the International Organization of Psychophysiology, 63(2), 205–213. https://doi.org/10.1016/j.ijpsycho.2006.03.019

Miranda-Dominguez, O., Feczko, E., Grayson, D. S., Walum, H., Nigg, J. T., & Fair, D. A. (2018). Heritability of the human connectome: A connectotyping study. Network Neuroscience, 02(02), 175–199. https://doi.org/10.1162/netn_a_00029

Miranda-Dominguez, O., Mills, B. D., Carpenter, S. D., Grant, K. A., Kroenke, C. D., Nigg, J. T., & Fair, D. A. (2014). Connectotyping: Model Based Fingerprinting of the Functional Connectome. PLoS ONE, 9(11), e111048. https://doi.org/10.1371/journal.pone.0111048

Mišić, B., & Sporns, O. (2016). From regions to connections and networks: New bridges between brain and behavior. Current Opinion in Neurobiology, 40, 1–7. https://doi.org/10.1016/j.conb.2016.05.003

Morillon, B., & Baillet, S. (2017). Motor origin of temporal predictions in auditory attention. Proceedings of the National Academy of Sciences, 114(42), E8913–E8921. https://doi.org/10.1073/pnas.1705373114

Mosher, J. C., Baillet, S., & Leahy, R. M. (2003). Equivalence of linear approaches in bioelectromagnetic inverse solutions. IEEE Workshop on Statistical Signal Processing, 2003, 294–297. https://doi.org/10.1109/SSP.2003.1289402

Mowinckel, A. M., & Vidal-Piñeiro, D. (2022). ggseg: Plotting Tool for Brain Atlases (1.6.5) [Computer software]. https://cran.r-project.org/web/packages/ggseg/index.html

Nentwich, M., Ai, L., Madsen, J., Telesford, Q. K., Haufe, S., Milham, M. P., & Parra, L. C. (2020). Functional connectivity of EEG is subject-specific, associated with phenotype, and different from fMRI. NeuroImage, 218, 117001. https://doi.org/10.1016/j.neuroimage.2020.117001

Niso, G., Rogers, C., Moreau, J. T., Chen, L.-Y., Madjar, C., Das, S., Bock, E., Tadel, F., Evans, A. C., Jolicoeur, P., & Baillet, S. (2016). OMEGA: The Open MEG Archive. NeuroImage, 124, 1182–1187. https://doi.org/10.1016/j.neuroimage.2015.04.028

Noble, S., Spann, M. N., Tokoglu, F., Shen, X., Constable, R. T., & Scheinost, D. (2017). Influences on the Test-Retest Reliability of Functional Connectivity MRI and its Relationship with Behavioral Utility. Cerebral Cortex (New York, N.Y.: 1991), 27(11), 5415–5429. https://doi.org/10.1093/cercor/bhx230

Nottage, J. F., & Horder, J. (2015). State-of-the-Art Analysis of High-Frequency (Gamma Range) Electroencephalography in Humans. Neuropsychobiology, 72(3–4), 219–228. https://doi.org/10.1159/000382023

Parkinson, C., Kleinbaum, A. M., & Wheatley, T. (2018). Similar neural responses predict friendship. Nature Communications, 9(1), Article 1. https://doi.org/10.1038/s41467-017-02722-7

Poldrack, R. A., & Gorgolewski, K. J. (2014). Making big data open: Data sharing in neuroimaging. Nature Neuroscience, 17(11), Article 11. https://doi.org/10.1038/nn.3818

R Core Team. (2022). R: A Language and Environment for Statistical Computing. R Foundation for Statistical Computing. https://www.R-project.org/

Rocca, D. L., Campisi, P., Vegso, B., Cserti, P., Kozmann, G., Babiloni, F., & Fallani, F. D. V. (2014). Human brain distinctiveness based on EEG spectral coherence connectivity. IEEE Transactions on Bio-Medical Engineering, 61(9), 2406–2412. https://doi.org/10.1109/TBME.2014.2317881

Rosenberg, M. D., Finn, E. S., Scheinost, D., Constable, R. T., & Chun, M. M. (2017). Characterizing Attention with Predictive Network Models. Trends in Cognitive Sciences, 21(4), Article 4. https://doi.org/10.1016/j.tics.2017.01.011

Rosenberg, M. D., Finn, E. S., Scheinost, D., Papademetris, X., Shen, X., Constable, R. T., & Chun, M. M. (2016). A neuromarker of sustained attention from whole-brain functional connectivity. Nature Neuroscience, 19(1), Article 1. https://doi.org/10.1038/nn.4179

Rosenberg, M. D., Scheinost, D., Greene, A. S., Avery, E. W., Kwon, Y. H., Finn, E. S., Ramani, R., Qiu, M., Constable, R. T., & Chun, M. M. (2020). Functional connectivity predicts changes

in attention observed across minutes, days, and months. Proceedings of the National Academy of Sciences, 117(7), 3797–3807. https://doi.org/10.1073/pnas.1912226117

Sadaghiani, S., Brookes, M. J., & Baillet, S. (2022). Connectomics of human electrophysiology. NeuroImage, 247, 118788. https://doi.org/10.1016/j.neuroimage.2021.118788

Salmela, E., Renvall, H., Kujala, J., Hakosalo, O., Illman, M., Vihla, M., Leinonen, E., Salmelin, R., & Kere, J. (2016). Evidence for genetic regulation of the human parieto-occipital 10-Hz rhythmic activity. The European Journal of Neuroscience, 44(3), 1963–1971. https://doi.org/10.1111/ejn.13300

Samaha, J., Iemi, L., Haegens, S., & Busch, N. A. (2020). Spontaneous Brain Oscillations and Perceptual Decision-Making. Trends in Cognitive Sciences, 24(8), 639–653. https://doi.org/10.1016/j.tics.2020.05.004

Sareen, E., Zahar, S., Ville, D. V. D., Gupta, A., Griffa, A., & Amico, E. (2021). Exploring MEG brain fingerprints: Evaluation, pitfalls, and interpretations. NeuroImage, 240, 118331. https://doi.org/10.1016/j.neuroimage.2021.118331

Shrout, P. E., & Fleiss, J. L. (1979). Intraclass correlations: Uses in assessing rater reliability. Psychological Bulletin, 86(2), 420–428. https://doi.org/10.1037/0033-2909.86.2.420

Smith, S. M., Vidaurre, D., Beckmann, C. F., Glasser, M. F., Jenkinson, M., Miller, K. L., Nichols, T. E., Robinson, E. C., Salimi-Khorshidi, G., Woolrich, M. W., Barch, D. M., Uğurbil, K., & Van Essen, D. C. (2013). Functional connectomics from resting-state fMRI. Trends in Cognitive Sciences, 17(12), 666–682. https://doi.org/10.1016/j.tics.2013.09.016

Stein, R. B., Gossen, E. R., & Jones, K. E. (2005). Neuronal variability: Noise or part of the signal? Nature Reviews Neuroscience, 6(5), Article 5. https://doi.org/10.1038/nrn1668

Tadel, F., Baillet, S., Mosher, J. C., Pantazis, D., & Leahy, R. M. (2011). Brainstorm: A User-Friendly Application for MEG/EEG Analysis. Computational Intelligence and Neuroscience, 2011, 1–13. https://doi.org/10.1155/2011/879716

Uddin, L. Q. (2020). Bring the Noise: Reconceptualizing Spontaneous Neural Activity. Trends in Cognitive Sciences, 24(9), 734–746. https://doi.org/10.1016/j.tics.2020.06.003

Valizadeh, S. A., Liem, F., Mérillat, S., Hänggi, J., & Jäncke, L. (2018). Identification of individual subjects on the basis of their brain anatomical features. Scientific Reports, 8(1), Article 1. https://doi.org/10.1038/s41598-018-23696-6

Van Horn, J. D., Grafton, S. T., & Miller, M. B. (2008). Individual Variability in Brain Activity: A Nuisance or an Opportunity? Brain Imaging and Behavior, 2(4), 327–334. https://doi.org/10.1007/s11682-008-9049-9

Wachinger, C., Golland, P., Kremen, W., Fischl, B., & Reuter, M. (2015). BrainPrint: A Discriminative Characterization of Brain Morphology. NeuroImage, 109, 232–248. https://doi.org/10.1016/j.neuroimage.2015.01.032

Welch, P. (1967). The use of fast Fourier transform for the estimation of power spectra: A method based on time averaging over short, modified periodograms. IEEE Transactions on Audio and Electroacoustics, 15(2), 70–73. https://doi.org/10.1109/TAU.1967.1161901

Whitham, E. M., Pope, K. J., Fitzgibbon, S. P., Lewis, T., Clark, C. R., Loveless, S., Broberg, M., Wallace, A., DeLosAngeles, D., Lillie, P., Hardy, A., Fronsko, R., Pulbrook, A., & Willoughby, J. O. (2007). Scalp electrical recording during paralysis: Quantitative evidence that EEG frequencies above 20 Hz are contaminated by EMG. Clinical Neurophysiology: Official Journal of the International Federation of Clinical Neurophysiology, 118(8), 1877–1888. https://doi.org/10.1016/j.clinph.2007.04.027

Yamashita, M., Yoshihara, Y., Hashimoto, R., Yahata, N., Ichikawa, N., Sakai, Y., Yamada, T., Matsukawa, N., Okada, G., Tanaka, S. C., Kasai, K., Kato, N., Okamoto, Y., Seymour, B., Takahashi, H., Kawato, M., & Imamizu, H. (2018). A prediction model of working memory across health and psychiatric disease using whole-brain functional connectivity. eLife, 7, e38844. https://doi.org/10.7554/eLife.38844

Yarkoni, T. (2015). Neurobiological substrates of personality: A critical overview. In APA handbook of personality and social psychology, Volume 4: Personality processes and individual differences (pp. 61–83). American Psychological Association. https://doi.org/10.1037/14343-003

Yeo, B. T. T., Krienen, F. M., Sepulcre, J., Sabuncu, M. R., Lashkari, D., Hollinshead, M., Roffman, J. L., Smoller, J. W., Zöllei, L., Polimeni, J. R., Fischl, B., Liu, H., & Buckner, R. L. (2011). The

organization of the human cerebral cortex estimated by intrinsic functional connectivity. Journal of Neurophysiology, 106(3), 1125–1165. https://doi.org/10.1152/jn.00338.2011

Yoo, K., Rosenberg, M. D., Hsu, W.-T., Zhang, S., Li, C.-S. R., Scheinost, D., Constable, R. T., & Chun, M. M. (2018). Connectome-based predictive modeling of attention: Comparing different functional connectivity features and prediction methods across datasets. NeuroImage, 167, 11–22. https://doi.org/10.1016/j.neuroimage.2017.11.010

Yuval-Greenberg, S., Tomer, O., Keren, A. S., Nelken, I., & Deouell, L. Y. (2008). Transient induced gamma-band response in EEG as a manifestation of miniature saccades. Neuron, 58(3), 429–441. https://doi.org/10.1016/j.neuron.2008.03.027

# Chapter 3

# Inter-individual differences in neurophysiology vary with increasing age

## Preface

In the previous chapter, I demonstrated in a cohort of mostly young adults that patterns of electrophysiological brain activity are unique to individuals. To date, there has been limited investigation into how aging may influence these so-called spectral brain-fingerprints. Aging is associated with significant neurobiological changes in both brain structure and function and therefore the average brains of young and older adults are vastly different. Although I found little evidence that participant differentiability scales with age, the previous participant sample was imbalanced (i.e., has fewer older adults than young adults), and is ill-equipped to comprehensively address such questions. In this chapter, I investigated how characteristic brain activity varies across the adult lifespan. I established that spectral brain-fingerprints enabled individual differentiation with >90% accuracy across all ages. Yet, aging is associated with a shift in the most salient brain regions for participant differentiation. This manuscript therefore argues for the robustness of spectral brain-fingerprints in older adults.

The manuscript is being prepared for submission as:

da Silva Castanheira, J., Wiesman, A., et al. Inter-individual differences in neurophysiology vary with increasing age. (2023).

## Abstract

Aging is associated with significant neurobiological changes in both brain structure and function, resulting in substantial differences between the brains of young and older adults, on average. Recent research in young adults has demonstrated distinct electrophysiological brain activity patterns that are unique to individuals and can predict behaviour. However, there has been limited investigation into how aging may influence inter-individual variations in neurophysiological activity. For example, brain activity features that best differentiate between young adults may not generalize to older adults. To address this knowledge gap, we characterized how inter-individual differences in brain activity evolve across the adult lifespan in a cross-sectional cohort. We used magnetoencephalographic imaging to derive the brain-fingerprints of 606 individuals between 18 and 89 years old. These brain-fingerprints enabled individual differentiation with >90% accuracy across all ages. We found that the most differentiating electrophysiological features changed with age along a dorsal-to-ventral gradient: Older adults were better differentiated from neurophysiological activity in superior unimodal cortices, and younger adults from inferior transmodal regions. The brain-fingerprint of older adults maps to regions most affected by cortical thinning and neurochemical systems known to change with age. Our study showcases the robustness of neurophysiological individual differentiation throughout the adult lifespan and emphasizes the significance of considering how inter-individual differences in brain activity may evolve across populations—particularly when studying populations of varying ages and cognitive abilities.



Keywords: Aging, older adults, neural oscillations, spectral parametrization, individual differences, brain-behaviour relationship, magnetoencephalography, brain fingerprinting.



Lay summary:

Aging brain is accompanied by substantial changes in both the brain's function and structure. These changes include the thinning of the outer layer of the brain (i.e., the cerebral cortex) and the slowing of brain activity. This line of research, however, has largely focused on average changes across an entire age-group. In contrast, recent findings support the idea that brain activity is characteristic of individuals. The authors, therefore, sought to investigate how person-specific brain activity changes throughout healthy aging. To do so, the authors used a novel

approach: brain-fingerprinting. The study demonstrates that older adults can be differentiated from one another, based on their brain activity, as accurately as young adults. However, the specific brain regions most useful for differentiating individuals diverge between young and older adults. The authors demonstrate that young adults are better differentiated from brain regions that support cognition and abstract thought. On the other hand, brain regions more typical of older adults are responsible for sensory and motor functions, show the greatest structural changes with age, and are sparse in specific neurochemical systems. Taken together, our study demonstrates the importance of considering how aging may alter individual differences in brain activity. The authors discuss the relevance of considering divergence in inter-individual differences when researching individuals of various demographics and cognitive abilities.

## Introduction

Changes in brain structure and neurophysiological activity across healthy aging are well documented. For instance, the dominant activity in the alpha band (8-12 Hz) tends to slow down with age (Babiloni et al., 2006; Merkin et al., 2022; Moretti et al., 2013; Scally et al., 2018; Thuwal et al., 2021). The aging brain also exhibits increased broadband background brain activity which is related to cognitive abilities like visual working memory (Thuwal et al., 2021; Voytek et al., 2015b; Voytek & Knight, 2015). In addition, older adults exhibit decreases in the variability of the blood-oxygen-level-dependent (BOLD) response, a metric that similarly scales with cognitive performance (Baracchini et al., 2023; Garrett et al., 2011; Garrett, Kovacevic, et al., 2013; Garrett, Samanez-Larkin, et al., 2013; Rieck et al., 2022; Uddin, 2020).

Older adults also show wide-spread reductions of cortical thickness (Bethlehem et al., 2022; Provencher et al., 2016; Salat et al., 2004). Indeed, it is hypothesized that late-maturing brain regions (i.e., transmodal brain areas) are the most vulnerable to age-related loss of structural integrity (McGinnis et al., 2011; Raz & Rodrigue, 2006). Furthermore, the regional concentration of acetylcholine and monoamines receptors change with age (Araujo et al., 2005; Karrer et al., 2019; Meltzer et al., 1998; Schliebs & Arendt, 2011; *The Cholinergic Hypothesis of Geriatric Memory Dysfunction | Science*, n.d.). Alterations in the cholinergic system are hypothesized to underly age-related declines in memory performance (Dumas & Newhouse, 2011; Nemy et al., 2020; *The Cholinergic Hypothesis of Geriatric Memory Dysfunction | Science*,

n.d.), while shifts in serotonergic signalling is hypothesized to mediate age-related mood disturbances (Karrer et al., 2019; Meltzer et al., 1998; Rodríguez et al., 2012; Sultzer et al., 2022). These findings and the rest of the vast literature on neurobiological aging corroborate that substantial differences exist between the average brains of young and older adults.

This extant research, however, has primarily focused on average differences between the brains of young and older adults, leaving the question of how inter-individual variations are expressed across age largely unchartered.

The brain-fingerprinting method has advanced our understanding of the neurobiological correlates of individual traits (Finn et al., 2015a; Niso et al., 2016b; Taylor et al., 2017; Van Essen et al., 2012). This growing literature supports the idea that brain activity is distinctive of individuals (da Silva Castanheira et al., 2021; Finn et al., 2015a; Sareen et al., 2021a). Nevertheless, a majority of the work on individual differences in brain activity and brain-behaviour relationships, however, has focused on young adults. No study to date, however, has directly compared inter-individual differences in brain activity between young and older adults. Brain-fingerprints serve as valuable features for training machine learning and statistical models that link individual neuroimaging data to behavioural, demographic, or cognitive traits (da Silva Castanheira et al., 2021; Finn et al., 2015a; Rosenberg et al., 2017a). Investigating how aging may impact brain-fingerprinting is therefore important for future research on brain-behaviour relationships in older adults.

The question of how inter-individual differences vary across population has become particularly relevant as novel findings (Greene et al., 2022; J. Li et al., 2022) suggest that the brain-behaviour relationships may not generalize across populations. Models trained to predict individual behaviours from brain activity recorded from young adults do not necessarily generalize to older adults (M. Gao et al., 2020; J. Yu & Fischer, 2022). Collectively, these results interrogate whether the same brain activity features that best stratify older adults from one another can equally differentiate young adults.

To address this question, we derived the neurophysiological brain-fingerprints of individuals in a cross-sectional sample of adult participants (N = 606; 18- 89 years old). First, we tested if our ability to differentiate individuals from brain activity varied across three age groups

(young adults: 18-45 years old, adults: 45-65 years old, and older adults: 65-89 years old). We hypothesized that neurophysiological brain-fingerprints enable inter-individual differentiation regardless of age (da Silva Castanheira et al., 2023-- see Chapter 4; Sorrentino et al., 2021a; Troisi Lopez et al., 2023). Second, we identified the most salient features of individual brain-fingerprints and tested whether they would change with age. We hypothesized that the brain activity features characteristic of older adults would differ from young adults given the substantial neurobiological changes related to aging. Last, we explored whether brain regions characteristic of older adults were spatially aligned with specific functional, structural, and neurochemical systems. We hypothesized that previously reported neurochemical and structural changes associated with aging correlate spatially with brain regions characteristic of older adults. Together the results of this experiment establish how unique neurophysiological activity varies across aging populations.

## Results

We used task-free MEG (8 minutes) and structural MRI data from 606 healthy participants available from the Cambridge-Center for Aging Neuroscience (CamCAN) dataset (Taylor et al., 2017) (demographics are presented in Supplemental Table S1; for detailed information about data acquisition see Taylor et al., 2017). We replicated the approach proposed by da Silva Castanheira et al., 2021 (Chapter 2) to derive individual neurophysiological brain-fingerprints from the power spectrum density (PSD) of MEG source activity within all parcels of the Desikan-Killiany atlas (see Methods). The brain-fingerprinting procedure per se assessed the similarity within and between individual brain-fingerprints derived from two distinct segments of the MEG data (i.e., self- and other- similarity). We defined age groups as follows, to maximize the number of participants in each group: 204 young adults (18-45 years old), 194 adults (45-65 years old), and 208 older adults (65-89 years old).

### Brain-fingerprints differentiate between individuals across the lifespan

We obtained an individual differentiation accuracy score of 89.6% ([88.0, 91.1] 95% CI) between the brain-fingerprints of the entire cohort, with little variations across age groups: 91.8% between young adults ([88.6, 94.9] 95% CI), 89.2% between adults ([87.4, 91.4] 95% CI), and

93.3% between older adults ([91.4, 95.4] 95% CI; Figure 1a). Our observations were similar using brain-fingerprints defined within limited bands of the neurophysiological power spectrum, its arrhythmic components, and from MEG task data (see Supplemental Information: Individuals are differentiable regardless of age group & Figure S2-S4).

Next, we quantified the stability of individual brain-fingerprints between data segments using a self-similarity index, which did not change linearly with age (β=-4.62, SE= 2.45, 95% CI [-9.43, 0.20], $r^2$= 0.006, p=0.06, $BF_{01}$= 1.96, see Table S2 and Figure 1b). Individual differentiability (da Silva Castanheira et al., 2021), a metric that quantifies the ease by which we can differentiate an individual from a cohort, did change with age, but only in weak proportions (β= 6.14, SE= 1.12, 95% CI [3.94, 8.34], p< 0.001, $BF_{01}$= 6.38 $10^{-6}$, 4,6% of total variance explained; Table S3 & Figure S1).

We replicated these analyses using brain-fingerprints derived from shorter 30-second data segments and obtained an overall 67.0% differentiation accuracy (computed 95% CI [64.9, 69.0]) between all 606 individuals. We note that differentiation accuracy derived from shorter segments did not differ per age group (Figure 1a, points).

Note, the above results were robust to various environmental and physiological artifacts (see Supplemental Material: Brain-fingerprints are robust against data recording artifacts).

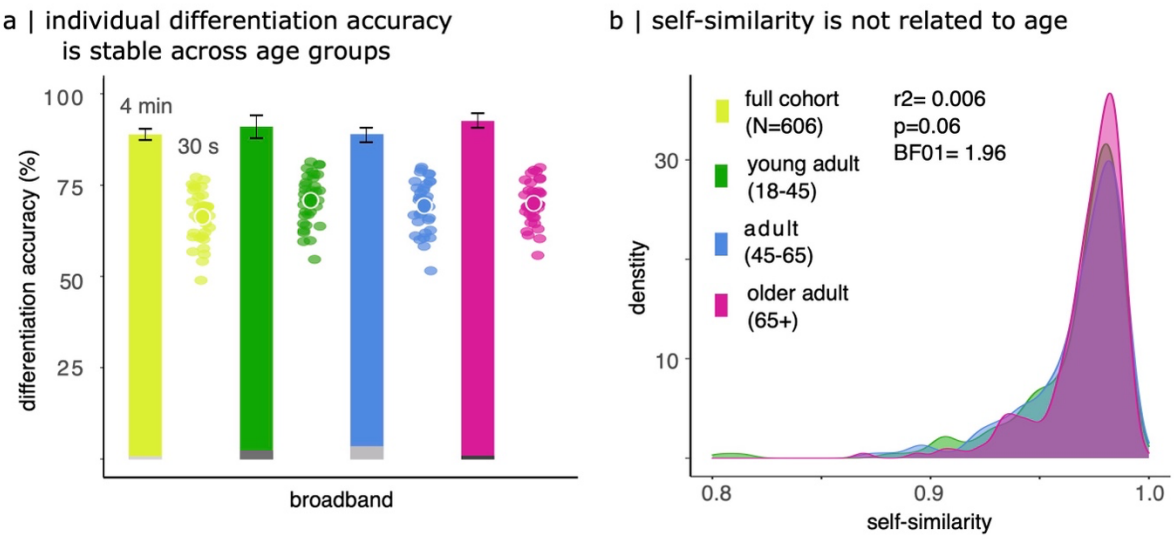


Chapter 3 Figure 1 Participants are differentiable regardless of age group

(a) Differentiation accuracy using (broadband) spectral brain-fingerprints derived from ~4-min data lengths (bars) and from 30-s segments (individual points). The error bars show bootstrapped 95% confidence intervals. The grey segments at the foot of each bar plot indicate the differentiation accuracies from empty-room MEG recordings around the participants' visits. (b) Self-similarity of participants' broadband spectral brain-fingerprints. The self-similarity of brain-fingerprints do not relate to age.

## Prediction of fluid intelligence traits from brain-fingerprints

We used estimates of intra-class correlation (ICC) to define the most salient features that differentiate individuals (Amico & Goñi, 2018a; da Silva Castanheira et al., 2021) (see Methods). Across all ages, these features mapped to the caudal aspects of the anterior cingulate cortex bilaterally (ICC= 0.88; see Figure S5).

Based on previous work in fMRI (Finn et al., 2015a), we hypothesized that salient spectral features for participant differentiation could predict fluid intelligence scores akin to their functional connectome counterparts. To test this we trained support vector regression (SVR) models where we decoded fluid intelligence scores from i) all resting-state brain activity features after applying feature reduction (see Methods), and ii) from the power spectral densities at each parcel of the Desikan-Killiany atlas (Desikan et al., 2006a).

First, we found that fluid intelligence scores can be inferred from resting-state brain activity across regions (observed vs. predicted fluid intelligence scores: r= 0.54, t=15.6, p < 2.2e-16, See Figure 3a). We note that chronological age is related to fluid intelligence performance (r=-0.67, t=-22.1, p < 2.2e-16); we similarly observed that participants' decoded fluid intelligence related to age (r=-0.71, t=-24.9, p-value < 2.2e-16).

Second, we aimed to relate regional differences in our ability to decode fluid intelligence to the spatial distribution of the most salient brain regions for individual differentiation. To achieve this, we trained SVR models to decode individual's fluid intelligence scores from the power spectrum at each parcel of the Desikan-Killiany atlas (Desikan et al., 2006a). The decoding of fluid intelligence performance was driven by a broad set of cortical regions, especially from the right peri-calcarine cortex (Figure 2b). The cortical topography of fluid intelligence performance decoding overlaps with that of the regional saliency of the brain-fingerprint (Figure 2c; r= 0.40, $p_{spin}$= 0.002)—a finding that was robust to differences in the cross-validation method used for designing the SVR models (Figure S6).

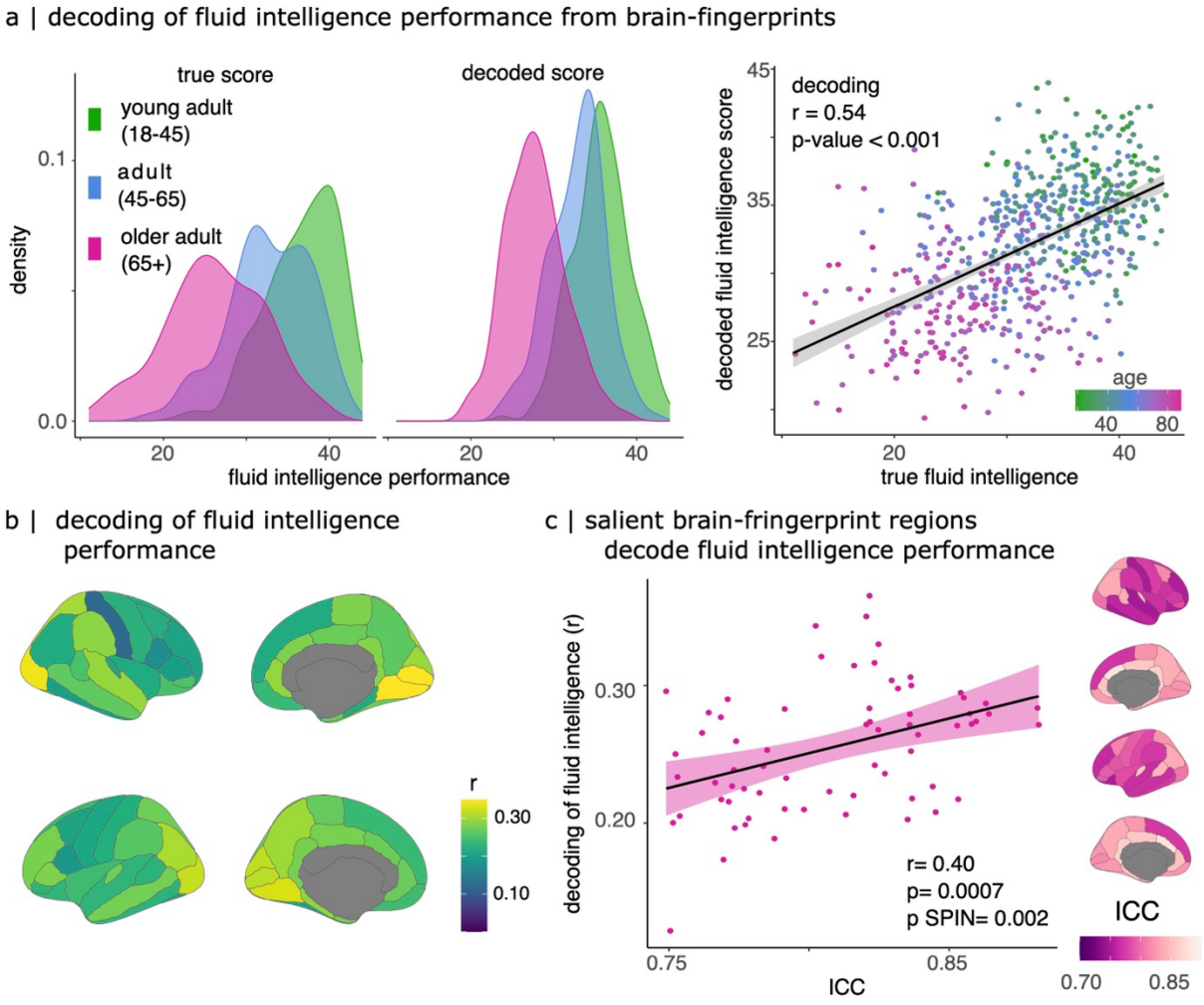


Chapter 3 Figure 2 Cortical region-wise decoding of fluid intelligence performance.

(a) Left panel: the spectral brain-fingerprint features that differentiate individuals were used to train Support Vector Regression models (SVR). We show that brain-fingerprint features decode fluid intelligence performance. Right panel: decoded fluid intelligence performance from brain-fingerprints. (b) Decoded fluid intelligence performance from brain-fingerprint features at each ROI of the Desikan-Killiany atlas, plotted as correlations between the observed and decoded scores. (c) Scatterplot of the colocalization of decoding performance of fluid intelligence scores at each cortical parcel with the brain-fingerprint saliency of the neurophysiological features of each cortical parcel (ICC). The ability to decode intelligence performance from a cortical region (left panel) is linearly associated with its saliency for the spectral brain-fingerprint (right panel).

## The salient features of the brain-fingerprint change across the adult lifespan

We then tested whether the most salient features of the brain-fingerprints changed with age. We mapped the difference between the respective ICC regional scores of the older and younger age groups. We found that lateral frontal and temporal regions are the most salient brain-fingerprint features of young adults, and that lateral parietal regions are the most salient regions of the brain-fingerprints of older adults (Figure 3a). The relative topography of these age-related disparities in salient brain-fingerprint features follows an inferior-to-superior gradient (β= 0.13, SE= 0.05, 95% CI [0.03, 0.23], p=0.012, $BF_{01}$= 0.17, $p_{spin}$= 0.013; Figure 3b).

We tested the impact of these age-related disparities in salient features on our ability to differentiate individuals (e.g., differentiation accuracy). We differentiated individuals from each of the three age groups based on the top 10% of features for differentiating young adults and the top 10% of features of older adults. We scaled the differentiation accuracy scores obtained for the young and older groups by those obtained from the adult group (see Methods). We observed that older adults were differentiated 22.9% more accurately from their respective top ICC features, whereas, young adults were differentiated 13.7% more accurately from their respective top ICC features (Figure 3a right).

We then computed the self-similarity of brain-fingerprints derived only from these top 10% of features for differentiating older and younger adults and related these self-similarity metrics to age. We observed a meager positive linear relationship between age and the self-similarity of brain-fingerprints derived from the top 10% of spectral features for older adult differentiation (r= 0.16, t= 3.94, p< 0.001). In contrast, we observed a larger negative linear relationship between age and the self-similarity of brain-fingerprints derived from young adult features (r=-0.32, t=-8.32, p< 0.001). These results suggest that aging lowers the self-similarity of brain-fingerprints specifically in orbitofrontal brain regions (Figure 3a).

In Figure 3b we plot an example power spectrum at the parcel showing the largest difference in salient features for participant differentiation (i.e., ΔICC). We observed polyrhythmic differences between the spectra of older adults compared to that of young adults, most evidently in the beta (13-30 Hz) and theta (4-8 Hz) bands.

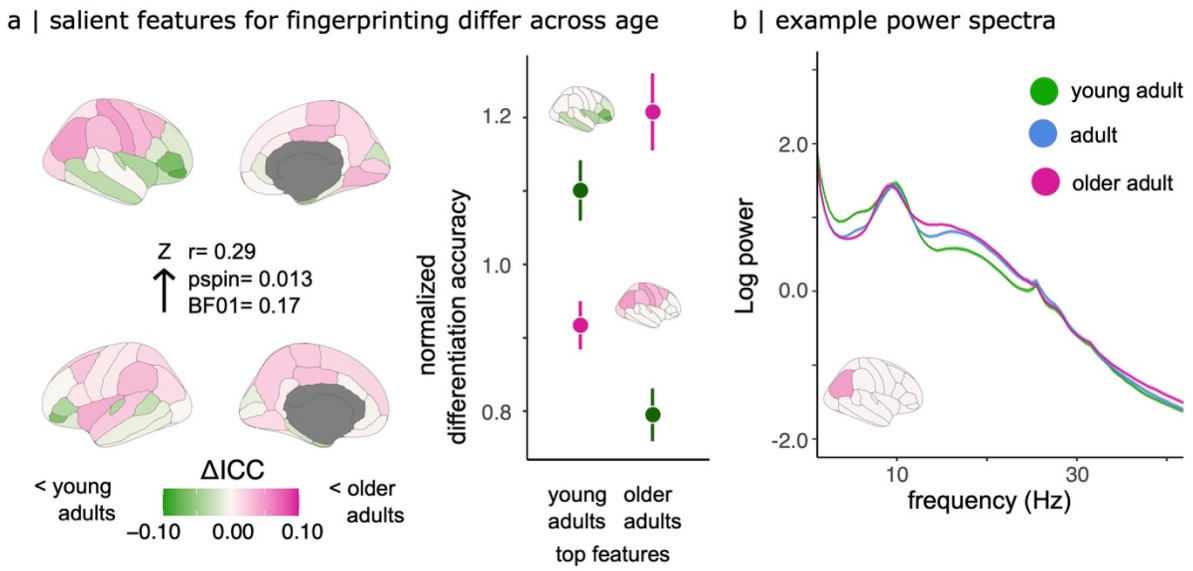


Chapter 3 Figure 3 Salient brain-fingerprinting features differ between young and older adults. (a) Topographic gradient of the age-related differences in self-similarity of brain-fingerprint features (brain maps). The topography of these differences between young and older adults follows a superior-to-inferior gradient (inlaid arrow). Right panel: differentiation accuracies obtained as a function of the most salient features for differentiating young and older adults. When we use the top features for differentiating older adults (i.e., lowest ΔICC), we obtain higher differentiation accuracies for older adults in comparison to young adults. The pattern is reversed when we use the top features for differentiating young adults (i.e., highest ΔICC). (b) Example spectra from the right inferior parietal cortex: the region that showed highest age-related differences in ICC. Shaded areas represent standard error of the mean.

## Alignment of the older-adult brain-fingerprint with cortical thinning and neurotransmitter systems

Prior research has hypothesized that late-maturing cortical regions, including the association cortices, are more vulnerable to age-related loss of structural integrity (McGinnis et al., 2011; Raz & Rodrigue, 2006). We, therefore, investigated if the observed dorsal-to-ventral gradient of differentiable brain activity (Figure 3a) was topographically related to the cortical distribution of i) cortical thinning observed with aging, ii) the cortical hierarchy, and iii) normative distributions of neurochemical systems.

First, we computed regional changes in cortical thickness for older adults relative to young adults (see Methods). We observed age-related thinning in most cortical regions, with more pronounced effects in the dorsolateral cortex (Figure 4a), which we previously identified as a salient region of the brain-fingerprint of older adults (r=-0.48, t(66)=-4.49, $p < 0.001$, $p_{spin}$= *0*.008; Figure 4a).

Second, we examined the alignment between older adult differentiable features with the unimodal-to-transmodal gradient of the functional hierarchy of the cortex (Margulies et al., 2016). We found that the salient regions that differentiate young adults are aligned with transmodal regions of that functional hierarchy, whereas regions that better differentiate older adults were aligned with unimodal cortical regions (r=-0.45, t(66)=-4.13, $p < 0.001$, $p_{spin} < 0.001$; Figure 4a).

Finally, we contextualized the dorsal-to-ventral gradient of differentiable brain activity with cortical atlases of neurochemical systems (Markello et al., 2022a) (see Methods). We found that the brain-fingerprint of young adults mapped to cortical regions rich with serotonin-2a (r=-0.40, pFDR = 0.004, $p_{spin}$= 0.003) and serotonin-4 (r=-0.49, pFDR= 0.0004, $p_{spin}$= 0.002) receptors, and serotonin (r=- 0.40, pFDR= 0.004, $p_{spin} <$ 0.001) transporters. In contrast, regions that differentiated older adults the best were enriched in norepinephrine (r= 0.42, pFDR= 0.003, $p_{spin}$= 0.003) transporters (Figure 4c-d).

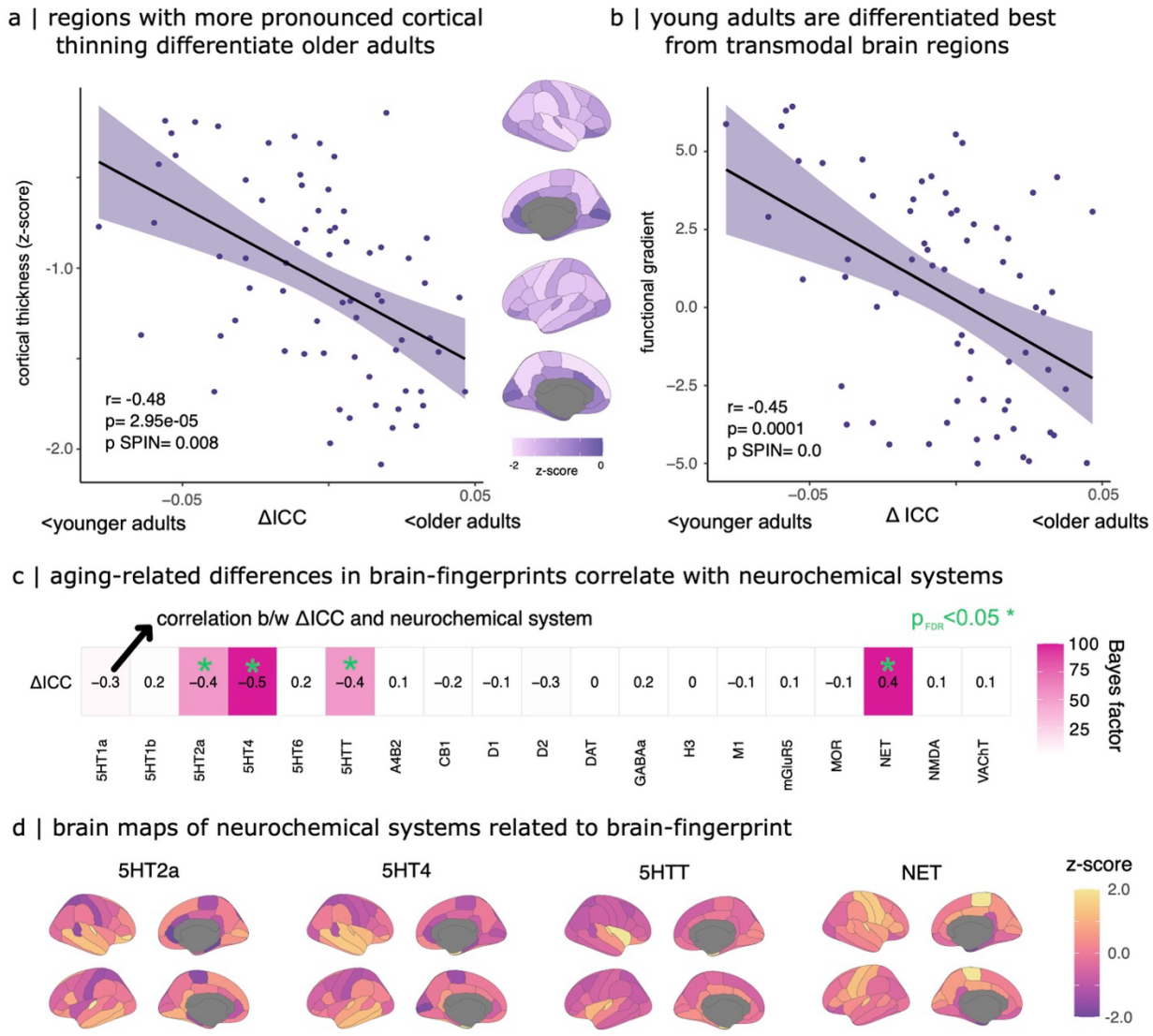


Chapter 3 Figure 4 Age-related differences in salient fingerprinting features colocalize with functional and neurochemical gradients.

(a) The topography of age-related differences in salient brain-fingerprint features (Figure 3a) is linearly associated with age-related changes in cortical thickness. Right panel: brain map of z-score age-related changes in cortical thickness. (b) The topography of age-related differences in salient brain-fingerprint features (Figure 4a) is linearly associated with the unimodal-transmodal functional gradient of the human brain. The size of the points are proportional to ΔICC. (c) Bayes factor analyses of the topographical alignment between the topography of age-related differences in salient brain-fingerprint features and atlases of cortical neurochemical systems

shows strong alignment with serotonin and norepinephrine systems. (d) Topographies of selected neurochemical cortical atlases.

# Discussion

Brain-fingerprinting has demonstrated great promise in quantifying distinctive patterns of inter-individual brain activity associated with complex traits (Amico & Goñi, 2018a; da Silva Castanheira et al., 2021; Finn et al., 2015a; Rosenberg et al., 2017a; Sareen et al., 2021a). In this study, we demonstrate, in the largest participant cohort to date, that individuals spanning the entire adult lifespan remain differentiable from spectral brain-fingerprints derived from brief neurophysiological recordings (Figure 1a). Salient brain regions for individual differentiation are similarly useful for decoding fluid intelligence test performance (Figure 2). However, it is noteworthy that salient features for participant differentiation differ between young and older adults (Figure 3a). We demonstrate that these disparities in differentiable features with age are topographically aligned with brain maps of cortical thinning, the unimodal-to-transmodal functional gradient, and the serotonin and norepinephrine neurochemical systems. Our results emphasize the importance of considering how inter-individual differences may vary across study populations and how these differences may inform models of brain-behaviour relationships.

## Neurophysiological recordings accurately differentiate individuals and decode fluid intelligence test performance

Individuals, irrespective of their age, can be differentiated from 605 other individuals with approximately 90% accuracy based on spatially-resolved broadband neurophysiological features (Figure 1a). These findings remain robust regardless of the frequency band in which we define the brain-fingerprint and hold when deriving arrhythmic brain-fingerprints (Figure S2-S3). Prior research has reported group-level neurophysiological changes associated with healthy aging (Babiloni et al., 2006; Heinrichs-Graham et al., 2018; Heinrichs-Graham & Wilson, 2016; Merkin et al., 2023; Rempe et al., 2023; Rossiter et al., 2014; Voytek et al., 2015b; L. E. Wilson et al., 2022), including a decrease in the moment-to-moment brain signal variability with age (Garrett et al., 2010; Garrett, Kovacevic, et al., 2013). Our present results suggest that despite these

group-level neurophysiological differences between age groups, older adults remain accurately differentiable from their brain activity. Indeed, we only observe a small effect of differentiability (~ 4% variance explained) in our sample (see Figure S1).

Additionally, we observed that brief segments of neurophysiological recordings are sufficient for distinguishing individuals (Figure 2b). These findings replicate our previous findings (da Silva Castanheira et al., 2021) in a substantially larger cohort of varying ages and support the growing body of evidence that suggests spectral resting-state brain activity estimates may be robustly estimated within 30 to 120 seconds of clean data (Wiesman, da Silva Castanheira, et al., 2022a).

Notably, our investigation revealed that the moment-to-moment variability of spectral brain-fingerprints does not exhibit significant differences across healthy age groups across the entire cortex (Figure 2b). Instead, we observe decreases in self-similarity of brain-fingerprints in transmodal brain regions of older adults (Figure 3a). This finding dovetails with previous research on BOLD variability indicating that older adults tend to exhibit reduced moment-to-moment variability in BOLD signals across the brain (Garrett et al., 2010; Garrett, Kovacevic, et al., 2013). Our results expand upon this prior literature and suggest that age-related changes in brain activity variability (i.e., low self-similarity) may affect brain regions in distinct ways, and potentially reflect unique manifestations of variability across various imaging modalities (Baracchini et al., 2023). Future research can leverage brain-fingerprinting methodologies as a complementary tool to address outstanding questions on intra-individual variability of brain activity, an emerging area of research in the neuroimaging field.

Moreover, our results expand upon recent work exploring the neurophysiological brain-fingerprints of clinical populations. In comparison to healthy older adults, the brain-fingerprints of mild cognitive impairment (MCI) and Parkinson's disease show greater intra-session variability across the entire brain, leading to reduced differentiability (da Silva Castanheira et al., 2023; Sorrentino et al., 2021a; Stampacchia et al., 2021; Troisi Lopez et al., 2023). In the case of Parkinson’s disease, previous work has argued that the arrhythmic component of brain activity selectively shows greater moment-to-moment variability (da Silva Castanheira et al., 2023 see Chapter 4). Future work can leverage the potential of clinical brain-fingerprinting approaches to

establish how intra-individual variability in brain-fingerprints may be a risk factor for neurological diseases by tracking brain activity variability longitudinally.

Previous work on brain-fingerprinting has emphasized that different brain networks are characteristic of individuals, depending on the specific brain signal recorded (e.g., BOLD vs. electrophysiology) (Amico & Goñi, 2018a; da Silva Castanheira et al., 2021; Finn et al., 2015a). We reaffirm these findings and suggest that several medial and caudal cortical areas are the most prominent electrophysiological features for distinguishing between all individuals in the cohort. Perhaps fast electrophysiological signals that contribute to individual differentiation with MEG have hemodynamic counterparts that are not as salient for fingerprinting, leading to a divergence between imaging modalities. This interpretation is substantiated by research on cross-modal fingerprinting (Sareen et al., 2021b)—yet warrants further investigation. Moreover, these findings suggest that fMRI and electrophysiological brain-fingerprints are complementary approaches that may independently contribute to brain-behavior relationships.

Limited research has explored how brain-fingerprints derived from electrophysiology may relate to inter-individual differences in behaviours (da Silva Castanheira et al., 2021; Sareen et al., 2021b). In addition, the literature has predominantly concentrated on associations between functional connectome brain-fingerprints and inter-individual differences in cognition (Amico & Goñi, 2018a; Finn et al., 2015a; Rosenberg et al., 2017a; Sareen et al., 2021a). In the present study, we extend these findings and demonstrate that simpler measures of local brain activity can not only robustly differentiate individuals from one another, but can also be used to train brain-behaviour models. These results expand our brain-behaviour research toolkit and underscore the utility of the spectral brain-fingerprinting approach in studying inter-individual differences.

### The saliency of neurophysiological brain-fingerprint features changes throughout the course of healthy aging

While individual differences in brain activity can characterize people regardless of age, the most useful features for differentiating between individuals vary with age. Specifically, we find that older adults are more differentiable from neurophysiological features of superior cortical regions, while younger adults are more differentiable from those of inferior cortices (Figure 3a).

The divergence of salient features for individual differentiation across age groups correlated spatially with the first component of the unimodal-to-transmodal functional gradient (Margulies et al., 2016). Transmodal regions are more characteristic of young adults (Figure 3a & Figure 4b), while unimodal regions are more salient for older adults. We posit that diminished functional responses to sensory stimuli observed in older adults (Stothart & Kazanina, 2016; Strömmer et al., 2017; Takahashi et al., 2009) may underly the observation that unimodal sensory regions are more distinctive of older individuals. Takahashi and colleagues, for instance, demonstrated that the entropy of EEG signals after a photic stimulus was higher in young adults compared to baseline but did not significantly vary from baseline in older adults (Takahashi et al., 2009). Consistent with Takahashi and colleagues' findings, better differentiation and higher self-similarity of brain-fingerprints derived from sensory regions (Figure 3a) may indicate different compensatory mechanisms to account for sensory-loss associated with increasing age, rendering brain activity in these regions more distinctive to individuals.

Apart from changes in sensory processing, aging has also been linked to the de-differentiation of brain networks, i.e., a reduction in the specialized modular structure of the brain (Chong et al., 2019; Goh, 2011; Koen & Rugg, 2019; Park et al., 2004). We speculate that the loss of specialization of higher-order brain regions may explain the reduced individual differentiation of older adults in transmodal brain regions. This interpretation is in line with the "last in, first out" hypothesis of brain aging, which posits that late-maturing brain regions (i.e., transmodal brain areas) are the most vulnerable to age-related loss of structural integrity (McGinnis et al., 2011; Raz & Rodrigue, 2006). Future research on the neurobiology of aging should substantiate this interpretation.

Moreover, we observed that the brain regions most salient for fingerprinting older adults are aligned with cortical areas that exhibit the most significant decrease in cortical thickness (Figure 4a). While previous work has documented cortical thinning with age, little research has explored how local changes in cortical thickness relate to neurophysiological changes observed in healthy aging (Moretti et al., 2013; Provencher et al., 2016; Rempe et al., 2022). Additionally, no study to date has documented how changes in differentiable electrophysiological brain activity relates to cortical thinning. Our results suggest that changes in brain structure may play a role in

shaping distinctive electrophysiological signals, where regions undergoing the most cortical thinning may be more characteristic of specific populations because of anatomical alterations. These results align with recent findings that propose the geometry of the brain constrains its function (Pang et al., 2023). The extent to which unique brain structure gives rise to characteristic electrophysiological signals observed with MEG remains an open question.

We contextualized the observed differences in salient brain-fingerprint features with normative atlases of neurochemical systems (Markello et al., 2022a). We observed a spatial overlap in the age-related differences in salient features for individual differentiation and the monoamine neurochemical systems, specifically the serotonin and norepinephrine systems (Figure 4c-d).

Previous research has hypothesized that age-related loss of serotonergic neurotransmission may explain, in part, age-related changes in behaviours including mood disturbances (Alexopoulos, 2019; Deza-Araujo et al., 2021; Meltzer et al., 1998), sleep (Myers & Badia, 1995), and cognition (Karrer et al., 2019; Peters, 2006). Yet the effects of aging on serotonergic neurotransmission, its effects on local electrophysiology, and behaviour are less well understood. Our results suggest that cortical regions with higher concentrations of serotonin receptors and transporters also correspond to cortical regions characteristic of younger adults, thus warrant further investigation into how serotonergic functioning may influence distinctive electrophysiological signals.

The norepinephrine neurochemical system is affected by neurodegenerative diseases. In particular, pathology of the locus coeruleus (LC) relates to cognitive deficits observed in Parkinson's disease (Del Tredici & Braak, 2013). Moreover, recent evidence suggests that early norepinephrine interventions in MCI may slow the progression of AD (Chalermpalanupap et al., 2013). These results have led to the neuroprotective hypothesis whereby norepinephrine may help to preserve cognitive reserve (Robertson, 2013). Given the important role the LC plays in attention processes (*Noradrenergic Modulation of Rhythmic Neural Activity Shapes Selective Attention - ScienceDirect*, n.d.), regional changes in electrophysiological signals may indirectly reflect the functioning of the norepinephrine neurochemical system in the aging brain, which, in turn, may explain individual differences in cognitive abilities.

## Brain-fingerprinting for population neuroscience

The current body of findings suggest that electrophysiological spectral features are a robust neurophysiological phenotype that may aid the goal of population neuroscience. On the other hand, our results also underscore the importance of multi-omic data repositories sampled across multiple dimensions of socio-economic, age, and geographic factors(Ricard et al., 2023).

Recent work has postulated that functional connectomes derivatives are limited in their ability to generalize brain-behaviour relationships across subgroups. Greene and colleagues[27], for example, argue that brain-behaviour models fail to generalize as they may not reflect unitary neurocognitive constructs; rather, brain models may instead represent cognitive constructs embedded in clinical and socioeconomic demographic groups. The brain-fingerprinting approach provides a means to investigate and understand the failed generalization of brain-behaviour models. With brain-fingerprinting approaches, researchers can investigate whether the failed generalization of a brain-behaviour model to another population is, in part, related to diverging characteristic brain activity.

Bethlehem and colleagues have suggested that age-related changes in brain structure and function can be assessed using *brain-charts* (Bethlehem et al., 2022). These charts are analogous to growth charts in medicine and were expanded to include morphological brain-charts across the lifespan. A goal behind this initiative is to measure how individuals differ in brain morphology relative to developmental norms, which may be extended to measures of brain function in future research. However, this approach fails to capture neurodevelopmental norms in the moment-to-moment variability of brain activity. Brain-fingerprinting, among other measures of variability in brain activity, may complement such brain-chart approaches and provide neurodevelopmental norms of moment-to-moment variability of brain activity. Given previous work on intra-individual variability in brain-fingerprints, its relationship to neurological diseases, and our present work on healthy aging, establishing developmental norms of intra-individual variability in brain function may be informative for clinical prognosis and diagnosis. This effort, however, would require large longitudinal datasets of neuroimaging phenotypes, which are currently limited.

The interpretation of these results should be considered alongside important methodological limitations. The current study only considers changes in brain-fingerprinting cross-sectionally. Future work with longitudinal data across several decades can better ascertain the neurodevelopmental trajectory of an individual's brain-fingerprint. In addition, the normative neurochemical system maps used for contextualizing our results were obtained from a mostly young adult sample. Therefore, future research should replicate these results utilizing normative atlases of neurochemical systems in older adults—data which is currently not openly available.

Like the prints left by our fingers, neurophysiological features differentiate individuals even in older populations. Unlike fingerprints, however, we show that brain-fingerprints change in salient features for individual differentiation between younger and older adults. Our results underscore the importance of considering variability in the most characteristic features of neurophysiological brain activity in heterogeneous populations with varying cognitive abilities. We propose that a one-size-fits-all approach to understanding brain-phenotype relationships is limited by changes in inter-individual differences in brain activity across the adult life span.

# Methods

**Participants.** Data from 606 healthy individuals (18-89 years old; mean age= 54.69; SD= 18.28; 299 of whom were Female) were collected from the Cambridge-Centre for Aging Neuroscience repository (Cam-CAN Taylor et al., 2017). The sample consisted of individuals spanning the adult lifespan (18 years old to 89) approximately uniformly sampled across decades. All participants completed a home-interview, underwent a resting-state eye-closed MEG recording using a 306-channel VectorView MEG system (Elekta Neuromag, Helsinki), a sensorimotor task MEG recording, and a structural T1 MRI. MEG data was collected from 102 magnetometers and 204 orthogonal planar gradiometers at 1,000Hz sampling rate and a 0.03-330 Hz bandpass filter. The head position of participants was continuously monitored using four Head-Position Indicator (HPI) coils, while ocular (EOG) and cardiac (ECG) external electrodes were used to monitor physiological artifacts. All MEG recordings were conducted at the same site. Resting-state recordings lasted approximately 8 minutes (Wiesman, da Silva Castanheira, et al., 2022b). See (Taylor et al., 2017) for details on the dataset and data acquisition.

**Preprocessing and source modeling of empirical MEG data.** MEG data were preprocessed using Brainstorm (Tadel et al., 2011) March 2021 distribution, running MATLAB 2020b (Mathworks, Inc., Massachusetts, USA) following good-practice guidelines (Gross et al., 2013). The preprocessing pipeline followed our previously published work on brain-fingerprinting (da Silva Castanheira et al., 2021). Line noise artifact (50 Hz; with 10 harmonics) and 88 Hz noise—a common artifact characteristic to the Cam-CAN dataset—were removed using a notch filter bank. Slow-wave and DC-offset artifacts were removed with a high-pass FIR filter with a 0.3-Hz cut-off. We derived Signal-Space Projectors (SSPs) to remove cardiac artifacts and attenuate low-frequency (1–7 Hz) and high-frequency noisy components (40–400 Hz) due to saccades and muscle activity, respectively.

We subsequently derived brain source models constrained to the individual T1-weighted MRI data available for each participant. The MRI volumes of each participant were automatically segmented and labelled using Freesurfer (Fischl, 2012) and co-registered to the MEG recording using approximately 100 digitized head points. We computed head models for each participant using the Brainstorm overlapping-spheres approach with default parameters. Cortical source models were computed using the Brainstorm implementation of linearly-constrained minimum-variance (LCMV) beamforming with default parameters (2018 version for source estimation processes). MEG source orientations at 15,000 locations were constrained normal to the surface of the cortex. The first principal component of all signals within each of the 68 cortical regions of the Desikan-Killiany atlas (Desikan et al., 2006a) was extracted, and used to compute neural power spectra using the Welch method (2 second, 50% overlapping windows).

We repeated the above preprocessing steps separately for the resting-state and sensorimotor task MEG recordings (see Figure S4). Note, we treated the sensorimotor task data continuously, such that we could compare brain-fingerprints to those derived from the resting-state data.

The resulting frequency range of PSDs was 0–150 Hz, with a frequency resolution of 1/2 Hz. This yielded a matrix of 68x300 features per participant and data segment for fingerprinting. Spectral features were exported to R (4.2.2) (R Core Team, 2022) for fingerprinting analyses.

**Fingerprinting and differentiability**. Our MEG spectral brain-fingerprinting approached followed previous work (Amico & Goñi, 2018a; da Silva Castanheira et al., 2021; Finn et al., 2015a). Brain-fingerprints are defined as the correlational differentiability of participants between data segments, taken from the first and second half of the resting-state MEG recording. We compute the Pearson correlation between the spectral features of participant$_i$ at the first time-point (i.e., data segment 1) and all other individuals at a second time-point (data segment 2). We repeat this procedure for all participants yielding an asymmetric correlation matrix spanning all participants in the cohort across data at two separate time-points. Participant$_i$ is said to be correctly differentiated from the cohort if the largest correlation coefficient to the second timepoint is the data segment of participant$_i$ at the second timepoint (i.e., their self-similarity is higher than their other-similarity to other participants). The percent of participants correctly differentiated from the cohort corresponds to the differentiation accuracy (i.e., the total number of correctly differentiated participants divided by the total number of individuals in the cohort).

We report the percent of correctly differentiated participants across four subgroups of interest: i) a young adult cohort (N= 204; 18-45 years old), ii) an adult cohort (N= 194; 45-65 years old), iii) an older adult cohort (N= 208; 65+ years old) and the iv) entire cohort of individuals (N=606). We selected these three age groups such that each group would have an approximately equal number of participants to fingerprint. We report the demographics of our sample in Supplemental Table S1.

**Shortened 30-second brain-fingerprinting.** We similarly derived spectral brain-fingerprints using brief 30-second non-overlapping segments taken from the resting state MEG recording. Here, we computed differentiation accuracy for all pairs of brain-fingerprints derived from these short recordings.

**Differentiability.** We compute a metric of differentiability, as per our previous work (da Silva Castanheira et al., 2021), to describe how easy any given participant is to differentiate from a cohort of individuals. This measure consists of the self-similarity of the spectral brain-fingerprint of participant$_i$ (data segment 1 to data segment 2), z-scored to the mean and standard deviation of the other-similarity of participant$_i$ data segment 1 with the data segment 2 of all others in the

cohort (see (da Silva Castanheira et al., 2021) for details). A participant with a high differentiability score will have a higher self-similarity relative to their other-similarity to others in the cohort, and therefore be easier to accurately identify.

**Bootstrapping differentiation accuracy.** We derived bootstrapped 95% confidence intervals for all of the reported differentiation accuracies. For each bootstrap iteration, we randomly selected a sub-sample of our desired cohort such that we fingerprinted only these individuals (i.e., for the entire cohort we subsampled 485 individuals, and 175 for each age group). We repeated this process 1000 times and computed the $2.5^{th}$ and $97.5^{th}$ percentile from the resulting distribution of differentiation accuracies. Note that because our confidence intervals were obtained by bootstrapping, they are not necessarily symmetric around the mean.

**Band-limited spectral fingerprinting.** We replicated all fingerprinting analyses using spectral features averaged over canonical frequency bands (delta: 1–4 Hz, theta: 4–8 Hz, alpha: 8–13 Hz, beta: 13–30 Hz, gamma: 30–50 Hz, and high gamma: 50–150 Hz).

**Recording artifacts and differentiability.** We investigated how common recording artifacts affect our ability to fingerprint. To do so, we related individual differentiability with the average L2 norm of measured ocular (VEOG and HEOG electrodes), cardiac (ECG electrode), and head movement artifacts (3 HLU channels) over the duration of the entire recording. We correlated these measures with differentiability in our full-cohort. To further verify that recording artifacts were not related to individual differentiation, we regressed these physiological artifacts from the brain-fingerprints of individuals, and used the residuals of this regression to differentiate the cohort (see Brain-fingerprints are robust against data recording artefacts in Supplemental Materials).

Empty-room fingerprinting. We verified that environmental and instrument noise on the day of the MEG recording could not differentiate individuals. Empty-room recordings from the day of each participants visit were used to differentiate their resting-state brain-fingerprints (see **Fingerprinting and differentiability**). The empty-room data was pre-processed similarly to the participant data (except physiological artifact removal using SSPs), source imaged with the above-

described imaging kernel, and frequency-transformed. We report the average differentiation accuracies using these empty-room brain-fingerprints, which represent baseline performance of the brain-fingerprinting approach (da Silva Castanheira et al., 2021).

***Specparam* modeling**. We estimated how much differentiation accuracy was driven by arrhythmic neural activity by parametrizing participants' neurophysiological power spectra with *ms-specparam* in Brainstorm (Tadel et al., 2011). Settings for *ms-specparam* were: frequency range: [1 to 40 Hz]; peak width limits: [0.5-12 Hz]; maximum number of peaks: 6; minimum peak amplitude: 3 a.u.; peak threshold: 2 standard deviations; proximity threshold: 0.75 standard deviations; aperiodic mode: fixed. Participants were differentiated from the resulting aperiodic fits following the described brain-fingerprinting procedure.

**Relative contribution of features for fingerprinting.** We calculated intraclass correlations (ICC) to quantify the contribution of each neurophysiological (frequency * cortical region) feature towards differentiating between individuals. ICC quantifies the ratio of within-participant variance and between-participant variance, such that high values of ICC indicate that said neurophysiological feature corresponds to high within-participant similarity and low between-participant similarity. Features with high ICC values therefore contribute the most to participant differentiation. We computed the ICC saliency of brain fingerprint features separately within the i) full cohort, the ii) young adult cohort, and the iii) older adult cohort to quantify how the contents of the brain fingerprint may change with age. The brain maps presented in Figures S5 were obtained by first averaging ICC values within each canonical frequency band, and then averaging across all six frequency band maps. This was done to equate the contribution of each frequency band to the broadband saliency topography, regardless of their respective definitions (e.g., the delta bandwidth is 4Hz, while high-gamma is 100 Hz). To measure differences in the most salient features for participant differentiation contents across the adult lifespan, we computed ΔICC brain maps by subtracting the broadband ICC maps obtained for the young and older adult cohort.

**Decoding of fluid intelligence performance.** Based on previous literature in fMRI (Finn et al., 2015a), we hypothesized that spectral neurophysiological features that differentiate individuals could be used to decode individuals' fluid intelligence test performance, as measured by the Cattell test (Cattell, 1963, 1971; Taylor et al., 2017). To test this, we decoded individuals' Cattell scores from their resting-state neurophysiological features. We first applied principal component analysis (PCA) on the neurophysiological features to reduce the number of dimensions (reduced from 68*300 features down to 68 components which explained 100% of the variance). We then trained Support Vector Regressions (SVR) on these features in R, using default parameters, to distinguish individuals' Cattell scores. We trained SVR models using a random subset of participants (i.e., 80% of the participants) and tested its performance on a held-out 20% of participants, and iterated this process 1000 times before taking the average decoded Cattell score per participant across iterations.

Next, we aimed to assess the spatial correspondence across cortical ROIs between the saliency of the broadband brain-fingerprint features and our ability to decode Cattell scores. We trained SVR models separately on the broadband spectra of each ROI using 80% of participants for training and held-out the remaining 20% participants to test the performance of the model. We iterated this process 1000 times per ROI to generate a topography of classification performance across the cortex. Decoding performance was assessed by correlating the true Cattell scores of the held-out participants to the predicted ones. We repeated these analyses for different cross-validation strategies (i.e., 70% training, 30% held-out; and 90% training, 10% held-out) to ensure the robustness of our results. To test for spatial concordance between the saliency of brain regions for fingerprinting and their importance for decoding fluid intelligence performance, we correlated the Cattell decoding performance and the broadband ICC values across ROIs (Figure S6). We estimated the p-value of this relationship based on spatially constrained permutation tests (1000 autocorrelation-preserving permutation tests; Hungarian method) (Markello & Misic, 2021; Váša & Mišić, 2022).

**Correspondence of brain-fingerprint features with the functional hierarchy of the cortex.** We aimed to determine whether age differences in brain-fingerprint contents related to the unimodal-to-transmodal functional gradient of brain organization (Margulies et al., 2016), taken from the

*neuromaps* toolbox (Markello et al., 2022b). We used a similar approach for spatial correspondence as in **Decoding of fluid intelligence performance**. We computed the Bayesian evidence (i.e., $BF_{01}$) for this relationship using the *correlationBF* function in R and corrected for the spatial autocorrelation of the atlas data using 1000 autocorrelation-preserving permutation tests (Hungarian method) (Markello & Misic, 2021; Váša & Mišić, 2022).

**Cortical thinning analysis.** We extracted cortical thickness measures from the Freesurfer processed data made available through Cam-CAN (Taylor et al., 2017). We imported the Freesurfer folder for each individual and averaged cortical thickness estimates at each parcel of the Desikan-Killiany atlas (Desikan et al., 2006a) using brainstorm (Tadel et al., 2011). We computed z-scored changes in cortical thickness from controls for the older adult age group by subtracting the mean and dividing by the standard deviation of the cortical thickness of young adults. We used the resulting z-scored map (Figure 5a) to measure how changes in the brain-fingerprints of older adults colocalize with the observed age-related cortical thinning effects. See **Correspondence of brain-fingerprint features with the functional hierarchy of the cortex** for details.

**Correspondence of brain-fingerprint features with cortical neurotransmitter systems.** We followed a similar approach, as outlined above, to test the spatial correspondence of the age-differences in brain-fingerprint contents normative neurochemical atlases. We obtained normative atlas maps of 19 receptors and transporters from 9 neurotransmitter systems from *neuromaps,* parcellated using the 68 regions of the Desikan-Killiany atlas (Desikan et al., 2006a). These consisted of: dopamine (D1: 13 adults, [11C]SCH23390 PET; D2: 92, [11C]FLB-457, DAT: 174, [123I]-FP-CIT), serotonin (5-HT1a: 36, [11C]WAY-100635; 5-HT1b: 88, [11C]P943; 5-HT2a: 29, [11C]Cimbi-36; 5-HT4: 59, [11C]SB207145; 5-HT6: 30, [11C]GSK215083; 5-HTT: 100, [11C]DASB), acetylcholine (α4β2: 30, [18F]flubatine; M1: 24, [11C]LSN3172176; VAChT: 30, [18F]FEOBV), GABA (GABAa: 16, [11C]flumazenil), glutamate (NMDA: 29, [18F]GE-179; mGluR5: 123, [11C]ABP688), norepinephrine (NET: 77, [11C]MRB), histamine (H3: 8, [11 C]GSK189254), cannabinoid (CB1: 77, [11 C]OMAR), and opioid (MOR: 204, [11 C]carfentanil).

We corrected for multiple comparisons using a False Discovery Rate (FDR) as implemented in the R function *p.*adjust and derived Bayes factors to quantify the evidence in

favour of the topographic relationship using the *correlationBF* function in R. For each significant spatial correspondence observed, we also estimated p-values based on spatially constrained permutation tests (Markello & Misic, 2021; Váša & Mišić, 2022).

## Data availability

Data used in the preparation of this work are available through the Cam-CAN repository (https://camcan-archive.mrc-cbu.cam.ac.uk/ ) (Niso et al., 2016b). Normative neurotransmitter density data are available from *neuromaps* (https://github.com/netneurolab/neuromaps) (Markello et al., 2022b).

## Code availability

All codes for preprocessing, data analysis, and data visualization can be found on the project's GitHub https://github.com/jasondsc/brainfingerprintsR4ever.

## Acknowledgements

The Brainstorm app is supported by funding to SB from the NIH (R01-EB026299), a Discovery grant from the Natural Science and Engineering Research Council of Canada (436355-13), the CIHR Canada research Chair in Neural Dynamics of Brain Systems, the Brain Canada Foundation with support from Health Canada, and the Innovative Ideas program from the Canada First Research Excellence Fund, awarded to McGill University for the HBHL initiative. This work was supported by a grant F32-NS119375 (AIW) from the National Institutes of Health and a doctoral fellowship from NSERC (JDSC).

## References

Alexopoulos, G. S. (2019). Mechanisms and treatment of late-life depression. Translational Psychiatry, 9(1), 188. https://doi.org/10.1038/s41398-019-0514-6

Amico, E., & Goñi, J. (2018). The quest for identifiability in human functional connectomes. Scientific Reports, 8(1), Article 1. https://doi.org/10.1038/s41598-018-25089-1

Araujo, J. A., Studzinski, C. M., & Milgram, N. W. (2005). Further evidence for the cholinergic hypothesis of aging and dementia from the canine model of aging. Progress in Neuro-Psychopharmacology and Biological Psychiatry, 29(3), 411–422. https://doi.org/10.1016/j.pnpbp.2004.12.008

Babiloni, C., Binetti, G., Cassarino, A., Dal Forno, G., Del Percio, C., Ferreri, F., Ferri, R., Frisoni, G., Galderisi, S., Hirata, K., Lanuzza, B., Miniussi, C., Mucci, A., Nobili, F., Rodriguez, G., Luca Romani, G., & Rossini, P. M. (2006). Sources of cortical rhythms in adults during physiological aging: A multicentric EEG study. Human Brain Mapping, 27(2), 162–172. https://doi.org/10.1002/hbm.20175

Baracchini, G., Zhou, Y., Castanheira, J. D. S., Hansen, J. Y., Rieck, J., Turner, G. R., Grady, C. L., Misic, B., Nomi, J., Uddin, L. Q., & Spreng, R. N. (2023). The biological role of local and global fMRI BOLD signal variability in human brain organization [Preprint]. Neuroscience. https://doi.org/10.1101/2023.10.22.563476

Bethlehem, R. a. I., Seidlitz, J., White, S. R., Vogel, J. W., Anderson, K. M., Adamson, C., Adler, S., Alexopoulos, G. S., Anagnostou, E., Areces-Gonzalez, A., Astle, D. E., Auyeung, B., Ayub, M., Bae, J., Ball, G., Baron-Cohen, S., Beare, R., Bedford, S. A., Benegal, V., … Alexander-Bloch, A. F. (2022). Brain charts for the human lifespan. Nature, 604(7906), Article 7906. https://doi.org/10.1038/s41586-022-04554-y

Cattell, R. B. (1963). Theory of fluid and crystallized intelligence: A critical experiment. Journal of Educational Psychology, 54(1), 1–22. https://doi.org/10.1037/h0046743

Cattell, R. B. (1971). Abilities: Their structure, growth, and action (pp. xxii, 583). Houghton Mifflin.

Chalermpalanupap, T., Kinkead, B., Hu, W. T., Kummer, M. P., Hammerschmidt, T., Heneka, M. T., Weinshenker, D., & Levey, A. I. (2013). Targeting norepinephrine in mild cognitive impairment and Alzheimer's disease. Alzheimer's Research & Therapy, 5(2), 21. https://doi.org/10.1186/alzrt175

Chong, J. S. X., Ng, K. K., Tandi, J., Wang, C., Poh, J.-H., Lo, J. C., Chee, M. W. L., & Zhou, J. H. (2019). Longitudinal Changes in the Cerebral Cortex Functional Organization of Healthy Elderly. Journal of Neuroscience, 39(28), 5534–5550. https://doi.org/10.1523/JNEUROSCI.1451-18.2019

da Silva Castanheira, J., Orozco Perez, H. D., Misic, B., & Baillet, S. (2021). Brief segments of neurophysiological activity enable individual differentiation. Nature Communications, 12(1), Article 1. https://doi.org/10.1038/s41467-021-25895-8

da Silva Castanheira, J., Wiesman, A. I., Hansen, J. Y., Misic, B., Baillet, S., PREVENT-AD Research Group, & Quebec Parkinson Network. (2023). Neurophysiological brain-fingerprints of motor and cognitive decline in Parkinson's disease. medRxiv: The Preprint Server for Health Sciences, 2023.02.03.23285441. https://doi.org/10.1101/2023.02.03.23285441

Del Tredici, K., & Braak, H. (2013). Dysfunction of the locus coeruleus-norepinephrine system and related circuitry in Parkinson's disease-related dementia. Journal of Neurology, Neurosurgery, and Psychiatry, 84(7), 774–783. https://doi.org/10.1136/jnnp-2011-301817

Desikan, R. S., Ségonne, F., Fischl, B., Quinn, B. T., Dickerson, B. C., Blacker, D., Buckner, R. L., Dale, A. M., Maguire, R. P., Hyman, B. T., Albert, M. S., & Killiany, R. J. (2006). An automated labeling system for subdividing the human cerebral cortex on MRI scans into gyral based regions of interest. NeuroImage, 31(3), 968–980. https://doi.org/10.1016/j.neuroimage.2006.01.021

Deza-Araujo, Y. I., Baez-Lugo, S., Vuilleumier, P., Chocat, A., Chételat, G., Poisnel, G., & Klimecki, O. M. (2021). Whole blood serotonin levels in healthy elderly are negatively associated with the functional activity of emotion-related brain regions. Biological Psychology, 160, 108051. https://doi.org/10.1016/j.biopsycho.2021.108051

Donoghue, T., Haller, M., Peterson, E. J., Varma, P., Sebastian, P., Gao, R., Noto, T., Lara, A. H., Wallis, J. D., Knight, R. T., Shestyuk, A., & Voytek, B. (2020). Parameterizing neural power spectra into periodic and aperiodic components. Nature Neuroscience, 23(12), 1655–1665. https://doi.org/10.1038/s41593-020-00744-x

Dumas, J. A., & Newhouse, P. A. (2011). The Cholinergic Hypothesis of Cognitive Aging Revisited Again: Cholinergic Functional Compensation. Pharmacology, Biochemistry, and Behavior, 99(2), 254–261. https://doi.org/10.1016/j.pbb.2011.02.022

Finn, E. S., Shen, X., Scheinost, D., Rosenberg, M. D., Huang, J., Chun, M. M., Papademetris, X., & Constable, R. T. (2015). Functional connectome fingerprinting: Identifying individuals

using patterns of brain connectivity. Nature Neuroscience, 18(11), Article 11. https://doi.org/10.1038/nn.4135

Fischl, B. (2012). FreeSurfer. NeuroImage, 62(2), 774–781. https://doi.org/10.1016/j.neuroimage.2012.01.021

Gao, M., Wong, C. H. Y., Huang, H., Shao, R., Huang, R., Chan, C. C. H., & Lee, T. M. C. (2020). Connectome-based models can predict processing speed in older adults. NeuroImage, 223, 117290. https://doi.org/10.1016/j.neuroimage.2020.117290

Garrett, D. D., Kovacevic, N., McIntosh, A. R., & Grady, C. L. (2010). Blood Oxygen Level-Dependent Signal Variability Is More than Just Noise. Journal of Neuroscience, 30(14), 4914–4921. https://doi.org/10.1523/JNEUROSCI.5166-09.2010

Garrett, D. D., Kovacevic, N., McIntosh, A. R., & Grady, C. L. (2011). The Importance of Being Variable. Journal of Neuroscience, 31(12), 4496–4503. https://doi.org/10.1523/JNEUROSCI.5641-10.2011

Garrett, D. D., Kovacevic, N., McIntosh, A. R., & Grady, C. L. (2013). The modulation of BOLD variability between cognitive states varies by age and processing speed. Cerebral Cortex (New York, N.Y.: 1991), 23(3), 684–693. https://doi.org/10.1093/cercor/bhs055

Garrett, D. D., Samanez-Larkin, G. R., MacDonald, S. W. S., Lindenberger, U., McIntosh, A. R., & Grady, C. L. (2013). Moment-to-moment brain signal variability: A next frontier in human brain mapping? Neuroscience and Biobehavioral Reviews, 37(4), 610–624. https://doi.org/10.1016/j.neubiorev.2013.02.015

Goh, J. O. S. (2011). Functional Dedifferentiation and Altered Connectivity in Older Adults: Neural Accounts of Cognitive Aging. Aging and Disease, 2(1), 30–48.

Greene, A. S., Shen, X., Noble, S., Horien, C., Hahn, C. A., Arora, J., Tokoglu, F., Spann, M. N., Carrión, C. I., Barron, D. S., Sanacora, G., Srihari, V. H., Woods, S. W., Scheinost, D., & Constable, R. T. (2022). Brain–phenotype models fail for individuals who defy sample stereotypes. Nature, 609(7925), Article 7925. https://doi.org/10.1038/s41586-022-05118-w

Gross, J., Baillet, S., Barnes, G. R., Henson, R. N., Hillebrand, A., Jensen, O., Jerbi, K., Litvak, V., Maess, B., Oostenveld, R., Parkkonen, L., Taylor, J. R., van Wassenhove, V., Wibral, M., &

Schoffelen, J.-M. (2013). Good practice for conducting and reporting MEG research. NeuroImage, 65, 349–363. https://doi.org/10.1016/j.neuroimage.2012.10.001

Heinrichs-Graham, E., McDermott, T. J., Mills, M. S., Wiesman, A. I., Wang, Y.-P., Stephen, J. M., Calhoun, V. D., & Wilson, T. W. (2018). The lifespan trajectory of neural oscillatory activity in the motor system. Developmental Cognitive Neuroscience, 30, 159–168. https://doi.org/10.1016/j.dcn.2018.02.013

Heinrichs-Graham, E., & Wilson, T. W. (2016). Is an absolute level of cortical beta suppression required for proper movement? Magnetoencephalographic evidence from healthy aging. NeuroImage, 134, 514–521. https://doi.org/10.1016/j.neuroimage.2016.04.032

Karrer, T. M., McLaughlin, C. L., Guaglianone, C. P., & Samanez-Larkin, G. R. (2019). Reduced serotonin receptors and transporters in normal aging adults: A meta-analysis of PET and SPECT imaging studies. Neurobiology of Aging, 80, 1–10. https://doi.org/10.1016/j.neurobiolaging.2019.03.021

Koen, J. D., & Rugg, M. D. (2019). Neural Dedifferentiation in the Aging Brain. Trends in Cognitive Sciences, 23(7), 547–559. https://doi.org/10.1016/j.tics.2019.04.012

Li, J., Bzdok, D., Chen, J., Tam, A., Ooi, L. Q. R., Holmes, A. J., Ge, T., Patil, K. R., Jabbi, M., Eickhoff, S. B., Yeo, B. T. T., & Genon, S. (2022). Cross-ethnicity/race generalization failure of behavioral prediction from resting-state functional connectivity. Science Advances, 8(11), eabj1812. https://doi.org/10.1126/sciadv.abj1812

Margulies, D. S., Ghosh, S. S., Goulas, A., Falkiewicz, M., Huntenburg, J. M., Langs, G., Bezgin, G., Eickhoff, S. B., Castellanos, F. X., Petrides, M., Jefferies, E., & Smallwood, J. (2016). Situating the default-mode network along a principal gradient of macroscale cortical organization. Proceedings of the National Academy of Sciences, 113(44), 12574–12579. https://doi.org/10.1073/pnas.1608282113

Markello, R. D., Hansen, J. Y., Liu, Z.-Q., Bazinet, V., Shafiei, G., Suárez, L. E., Blostein, N., Seidlitz, J., Baillet, S., Satterthwaite, T. D., Chakravarty, M. M., Raznahan, A., & Misic, B. (2022a). neuromaps: Structural and functional interpretation of brain maps. Nature Methods, 19(11), Article 11. https://doi.org/10.1038/s41592-022-01625-w

Markello, R. D., Hansen, J. Y., Liu, Z.-Q., Bazinet, V., Shafiei, G., Suárez, L. E., Blostein, N., Seidlitz, J., Baillet, S., Satterthwaite, T. D., Chakravarty, M. M., Raznahan, A., & Misic, B. (2022b). neuromaps: Structural and functional interpretation of brain maps [Preprint]. Neuroscience. https://doi.org/10.1101/2022.01.06.475081

Markello, R. D., & Misic, B. (2021). Comparing spatial null models for brain maps. NeuroImage, 236, 118052. https://doi.org/10.1016/j.neuroimage.2021.118052

McGinnis, S. M., Brickhouse, M., Pascual, B., & Dickerson, B. C. (2011). Age-Related Changes in the Thickness of Cortical Zones in Humans. Brain Topography, 24(3–4), 279–291. https://doi.org/10.1007/s10548-011-0198-6

Meltzer, C. C., Smith, G., DeKosky, S. T., Pollock, B. G., Mathis, C. A., Moore, R. Y., Kupfer, D. J., & Reynolds, C. F. (1998). Serotonin in Aging, Late-Life Depression, and Alzheimer's Disease: The Emerging Role of Functional Imaging. Neuropsychopharmacology, 18(6), Article 6. https://doi.org/10.1016/S0893-133X(97)00194-2

Merkin, A., Sghirripa, S., Graetz, L., Smith, A. E., Hordacre, B., Harris, R., Pitcher, J., Semmler, J., Rogasch, N. C., & Goldsworthy, M. (2022). Do age-related differences in aperiodic neural activity explain differences in resting EEG alpha? Neurobiology of Aging. https://doi.org/10.1016/j.neurobiolaging.2022.09.003

Merkin, A., Sghirripa, S., Graetz, L., Smith, A. E., Hordacre, B., Harris, R., Pitcher, J., Semmler, J., Rogasch, N. C., & Goldsworthy, M. (2023). Do age-related differences in aperiodic neural activity explain differences in resting EEG alpha? Neurobiology of Aging, 121, 78–87. https://doi.org/10.1016/j.neurobiolaging.2022.09.003

Moretti, D. V., Paternicò, D., Binetti, G., Zanetti, O., & Frisoni, G. B. (2013). EEG upper/low alpha frequency power ratio relates to temporo-parietal brain atrophy and memory performances in mild cognitive impairment. Frontiers in Aging Neuroscience, 5, 63. https://doi.org/10.3389/fnagi.2013.00063

Myers, B. L., & Badia, P. (1995). Changes in circadian rhythms and sleep quality with aging: Mechanisms and interventions. Neuroscience & Biobehavioral Reviews, 19(4), 553–571. https://doi.org/10.1016/0149-7634(95)00018-6

Nemy, M., Cedres, N., Grothe, M. J., Muehlboeck, J.-S., Lindberg, O., Nedelska, Z., Stepankova, O., Vyslouzilova, L., Eriksdotter, M., Barroso, J., Teipel, S., Westman, E., & Ferreira, D. (2020). Cholinergic white matter pathways make a stronger contribution to attention and memory in normal aging than cerebrovascular health and nucleus basalis of Meynert. NeuroImage, 211, 116607. https://doi.org/10.1016/j.neuroimage.2020.116607

Niso, G., Rogers, C., Moreau, J. T., Chen, L.-Y., Madjar, C., Das, S., Bock, E., Tadel, F., Evans, A. C., Jolicoeur, P., & Baillet, S. (2016). OMEGA: The Open MEG Archive. NeuroImage, 124, 1182–1187. https://doi.org/10.1016/j.neuroimage.2015.04.028

Noradrenergic modulation of rhythmic neural activity shapes selective attention—ScienceDirect. (n.d.). Retrieved May 8, 2023, from https://www.sciencedirect.com/science/article/pii/S1364661321002643?via%3Dihub

Pang, J. C., Aquino, K. M., Oldehinkel, M., Robinson, P. A., Fulcher, B. D., Breakspear, M., & Fornito, A. (2023). Geometric constraints on human brain function. Nature, 618(7965), Article 7965. https://doi.org/10.1038/s41586-023-06098-1

Park, D. C., Polk, T. A., Park, R., Minear, M., Savage, A., & Smith, M. R. (2004). Aging reduces neural specialization in ventral visual cortex. Proceedings of the National Academy of Sciences, 101(35), 13091–13095. https://doi.org/10.1073/pnas.0405148101

Peters, R. (2006). Ageing and the brain: This article is part of a series on ageing edited by Professor Chris Bulpitt. Postgraduate Medical Journal, 82(964), 84–88. https://doi.org/10.1136/pgmj.2005.036665

Provencher, D., Hennebelle, M., Cunnane, S. C., Bérubé-Lauzière, Y., & Whittingstall, K. (2016). Cortical Thinning in Healthy Aging Correlates with Larger Motor-Evoked EEG Desynchronization. Frontiers in Aging Neuroscience, 8. https://www.frontiersin.org/articles/10.3389/fnagi.2016.00063

R Core Team. (2022). R: A Language and Environment for Statistical Computing. R Foundation for Statistical Computing. https://www.R-project.org/

Raz, N., & Rodrigue, K. M. (2006). Differential aging of the brain: Patterns, cognitive correlates and modifiers. Neuroscience and Biobehavioral Reviews, 30(6), 730–748. https://doi.org/10.1016/j.neubiorev.2006.07.001

Rempe, M. P., Lew, B. J., Embury, C. M., Christopher-Hayes, N. J., Schantell, M., & Wilson, T. W. (2022). Spontaneous sensorimotor beta power and cortical thickness uniquely predict motor function in healthy aging. NeuroImage, 263, 119651. https://doi.org/10.1016/j.neuroimage.2022.119651

Rempe, M. P., Ott, L. R., Picci, G., Penhale, S. H., Christopher-Hayes, N. J., Lew, B. J., Petro, N. M., Embury, C. M., Schantell, M., Johnson, H. J., Okelberry, H. J., Losh, K. L., Willett, M. P., Losh, R. A., Wang, Y.-P., Calhoun, V. D., Stephen, J. M., Heinrichs-Graham, E., Kurz, M. J., & Wilson, T. W. (2023). Spontaneous cortical dynamics from the first years to the golden years. Proceedings of the National Academy of Sciences, 120(4), e2212776120. https://doi.org/10.1073/pnas.2212776120

Ricard, J. A., Parker, T. C., Dhamala, E., Kwasa, J., Allsop, A., & Holmes, A. J. (2023). Confronting racially exclusionary practices in the acquisition and analyses of neuroimaging data. Nature Neuroscience, 26(1), Article 1. https://doi.org/10.1038/s41593-022-01218-y

Rieck, J. R., DeSouza, B., Baracchini, G., & Grady, C. L. (2022). Reduced modulation of BOLD variability as a function of cognitive load in healthy aging. Neurobiology of Aging, 112, 215–230. https://doi.org/10.1016/j.neurobiolaging.2022.01.010

Robertson, I. H. (2013). A noradrenergic theory of cognitive reserve: Implications for Alzheimer's disease. Neurobiology of Aging, 34(1), 298–308. https://doi.org/10.1016/j.neurobiolaging.2012.05.019

Rodríguez, J. J., Noristani, H. N., & Verkhratsky, A. (2012). The serotonergic system in ageing and Alzheimer's disease. Progress in Neurobiology, 99(1), 15–41. https://doi.org/10.1016/j.pneurobio.2012.06.010

Rosenberg, M. D., Finn, E. S., Scheinost, D., Constable, R. T., & Chun, M. M. (2017). Characterizing Attention with Predictive Network Models. Trends in Cognitive Sciences, 21(4), Article 4. https://doi.org/10.1016/j.tics.2017.01.011

Rossiter, H. E., Davis, E. M., Clark, E. V., Boudrias, M.-H., & Ward, N. S. (2014). Beta oscillations reflect changes in motor cortex inhibition in healthy ageing. NeuroImage, 91, 360–365. https://doi.org/10.1016/j.neuroimage.2014.01.012

Salat, D. H., Buckner, R. L., Snyder, A. Z., Greve, D. N., Desikan, R. S. R., Busa, E., Morris, J. C., Dale, A. M., & Fischl, B. (2004). Thinning of the Cerebral Cortex in Aging. Cerebral Cortex, 14(7), 721–730. https://doi.org/10.1093/cercor/bhh032

Sareen, E., Zahar, S., Ville, D. V. D., Gupta, A., Griffa, A., & Amico, E. (2021a). Exploring MEG brain fingerprints: Evaluation, pitfalls, and interpretations. NeuroImage, 240, 118331. https://doi.org/10.1016/j.neuroimage.2021.118331

Sareen, E., Zahar, S., Ville, D. V. D., Gupta, A., Griffa, A., & Amico, E. (2021b). Exploring MEG brain fingerprints: Evaluation, pitfalls, and interpretations. NeuroImage, 240, 118331. https://doi.org/10.1016/j.neuroimage.2021.118331

Scally, B., Burke, M. R., Bunce, D., & Delvenne, J.-F. (2018). Resting-state EEG power and connectivity are associated with alpha peak frequency slowing in healthy aging. Neurobiology of Aging, 71, 149–155. https://doi.org/10.1016/j.neurobiolaging.2018.07.004

Schliebs, R., & Arendt, T. (2011). The cholinergic system in aging and neuronal degeneration. Behavioural Brain Research, 221(2), 555–563. https://doi.org/10.1016/j.bbr.2010.11.058

Sorrentino, P., Rucco, R., Lardone, A., Liparoti, M., Troisi Lopez, E., Cavaliere, C., Soricelli, A., Jirsa, V., Sorrentino, G., & Amico, E. (2021). Clinical connectome fingerprints of cognitive decline. NeuroImage, 238, 118253. https://doi.org/10.1016/j.neuroimage.2021.118253

Stampacchia, S., Asadi, S., Ribaldi, F., Tomczyk, S., Altomare, D., Pievani, M., Frisoni, G., Amico, E., & Garibotto, V. (2021). Towards fingerprinting and identifiability within the Alzheimer's continuum using resting-state functional connectivity. Alzheimer's & Dementia, 17(S4), e057724. https://doi.org/10.1002/alz.057724

Stothart, G., & Kazanina, N. (2016). Auditory perception in the aging brain: The role of inhibition and facilitation in early processing. Neurobiology of Aging, 47, 23–34. https://doi.org/10.1016/j.neurobiolaging.2016.06.022

Strömmer, J. M., Põldver, N., Waselius, T., Kirjavainen, V., Järveläinen, S., Björksten, S., Tarkka, I. M., & Astikainen, P. (2017). Automatic auditory and somatosensory brain responses in relation to cognitive abilities and physical fitness in older adults. Scientific Reports, 7(1), Article 1. https://doi.org/10.1038/s41598-017-14139-9

Sultzer, D. L., Lim, A. C., Gordon, H. L., Yarns, B. C., & Melrose, R. J. (2022). Cholinergic receptor binding in unimpaired older adults, mild cognitive impairment, and Alzheimer's disease dementia. Alzheimer's Research & Therapy, 14(1), 25. https://doi.org/10.1186/s13195-021-00954-w

Tadel, F., Baillet, S., Mosher, J. C., Pantazis, D., & Leahy, R. M. (2011). Brainstorm: A User-Friendly Application for MEG/EEG Analysis. Computational Intelligence and Neuroscience, 2011, 1–13. https://doi.org/10.1155/2011/879716

Takahashi, T., Cho, R. Y., Murata, T., Mizuno, T., Kikuchi, M., Mizukami, K., Kosaka, H., Takahashi, K., & Wada, Y. (2009). Age-related variation in EEG complexity to photic stimulation: A multiscale entropy analysis. Clinical Neurophysiology : Official Journal of the International Federation of Clinical Neurophysiology, 120(3), 476–483. https://doi.org/10.1016/j.clinph.2008.12.043

Taylor, J. R., Williams, N., Cusack, R., Auer, T., Shafto, M. A., Dixon, M., Tyler, L. K., Cam-CAN, & Henson, R. N. (2017). The Cambridge Centre for Ageing and Neuroscience (Cam-CAN) data repository: Structural and functional MRI, MEG, and cognitive data from a cross-sectional adult lifespan sample. NeuroImage, 144, 262–269. https://doi.org/10.1016/j.neuroimage.2015.09.018

The Cholinergic Hypothesis of Geriatric Memory Dysfunction | Science. (n.d.). Retrieved August 15, 2023, from https://www.science.org/doi/abs/10.1126/science.7046051

Thuwal, K., Banerjee, A., & Roy, D. (2021). Aperiodic and Periodic Components of Ongoing Oscillatory Brain Dynamics Link Distinct Functional Aspects of Cognition across Adult Lifespan. eNeuro, 8(5), ENEURO.0224-21.2021. https://doi.org/10.1523/ENEURO.0224-21.2021

Troisi Lopez, E., Minino, R., Liparoti, M., Polverino, A., Romano, A., De Micco, R., Lucidi, F., Tessitore, A., Amico, E., Sorrentino, G., Jirsa, V., & Sorrentino, P. (2023). Fading of brain

network fingerprint in Parkinson's disease predicts motor clinical impairment. Human Brain Mapping, 44(3), 1239–1250. https://doi.org/10.1002/hbm.26156

Uddin, L. Q. (2020). Bring the Noise: Reconceptualizing Spontaneous Neural Activity. Trends in Cognitive Sciences, 24(9), 734–746. https://doi.org/10.1016/j.tics.2020.06.003

Van Essen, D. C., Ugurbil, K., Auerbach, E., Barch, D., Behrens, T. E. J., Bucholz, R., Chang, A., Chen, L., Corbetta, M., Curtiss, S. W., Della Penna, S., Feinberg, D., Glasser, M. F., Harel, N., Heath, A. C., Larson-Prior, L., Marcus, D., Michalareas, G., Moeller, S., … Yacoub, E. (2012). The Human Connectome Project: A data acquisition perspective. NeuroImage, 62(4), Article 4. https://doi.org/10.1016/j.neuroimage.2012.02.018

Váša, F., & Mišić, B. (2022). Null models in network neuroscience. Nature Reviews Neuroscience, 23(8), 493–504. https://doi.org/10.1038/s41583-022-00601-9

Voytek, B., & Knight, R. T. (2015). Dynamic Network Communication as a Unifying Neural Basis for Cognition, Development, Aging, and Disease. Biological Psychiatry, 77(12), 1089–1097. https://doi.org/10.1016/j.biopsych.2015.04.016

Voytek, B., Kramer, M. A., Case, J., Lepage, K. Q., Tempesta, Z. R., Knight, R. T., & Gazzaley, A. (2015). Age-Related Changes in 1/f Neural Electrophysiological Noise. Journal of Neuroscience, 35(38), 13257–13265. https://doi.org/10.1523/JNEUROSCI.2332-14.2015

Wiesman, A. I., da Silva Castanheira, J., & Baillet, S. (2022a). Stability of spectral estimates in resting-state magnetoencephalography: Recommendations for minimal data duration with neuroanatomical specificity. NeuroImage, 247, 118823. https://doi.org/10.1016/j.neuroimage.2021.118823

Wiesman, A. I., da Silva Castanheira, J., & Baillet, S. (2022b). Stability of spectral estimates in resting-state magnetoencephalography: Recommendations for minimal data duration with neuroanatomical specificity. NeuroImage, 247, 118823. https://doi.org/10.1016/j.neuroimage.2021.118823

Wilson, L. E., da Silva Castanheira, J., & Baillet, S. (2022). Time-resolved parameterization of aperiodic and periodic brain activity. eLife, 11, e77348. https://doi.org/10.7554/eLife.77348

Yu, J., & Fischer, N. L. (2022). Age-specificity and generalization of behavior-associated structural and functional networks and their relevance to behavioral domains. Human Brain Mapping, 43(8), 2405–2418. https://doi.org/10.1002/hbm.25759

# Chapter 4

# The neurophysiological brain-fingerprint of Parkinson's disease

## Preface

There has been limited research to date on how neurodegenerative diseases impact the unique brain activity of patients (i.e., brain-fingerprints). In this Chapter, I explore how neurodegenerative diseases like Parkinson's disease alter inter-individual differences. We explore the clinical utility of the brain-fingerprinting approach. I report that the rhythmic brain-fingerprints of Parkinson's disease are specific to patients and decode disease staging. In contrast, arrhythmic brain activity is less characteristic of patients and challenges participant differentiation. The findings of this Chapter clarify previous negative results in the clinical brain-fingerprinting literature.

The manuscript was submitted to eBioMedicine as:

da Silva Castanheira, J., Wiesman, A., et al. The neurophysiological brain-fingerprint of Parkinson's disease. (2023). https://doi.org/10.1101/2023.02.03.23285441

## Abstract

In this study, we investigate the clinical potential of brain-fingerprints derived from electrophysiological brain activity for diagnostics and progression monitoring of Parkinson's disease (PD). We obtained brain-fingerprints from PD patients and age-matched healthy controls using short, task-free magnetoencephalographic recordings. The rhythmic components of the individual brain-fingerprint distinguished between patients and healthy participants with

approximately 90% accuracy. The most prominent cortical features of the Parkinson's brain-fingerprint mapped to polyrhythmic activity in unimodal sensorimotor regions. Leveraging these features, we also show that Parkinson's disease stages can be decoded directly from cortical neurophysiological activity. Additionally, our study reveals that the cortical topography of the Parkinson's brain-fingerprint aligns with that of neurotransmitter systems affected by the disease's pathophysiology. We further demonstrate that the arrhythmic components of cortical activity are more variable over short periods of time in patients with Parkinson's disease than in healthy controls, making individual differentiation between patients based on these features more challenging and explaining previous negative published results. Overall, we outline patient-specific rhythmic brain signalling features that provide insights into both the neurophysiological signature and clinical staging of Parkinson's disease. For this reason, the proposed definition of a rhythmic brain-fingerprint of Parkinson's disease may contribute to novel, refined approaches to patient stratification, identification, and testing of therapeutic neurostimulation targets.

Keywords: Movement disorders, Parkinson's disease, neural dynamics, oscillations, arrhythmic brain activity, magnetoencephalography, brain-fingerprinting.

Lay summary: We propose a new method to help diagnose and monitor Parkinson's disease (PD) using patients' unique *brain-fingerprint*. These fingerprints are based on the brain's electrical activity, which we measured without any specific tasks, using a technique called magnetoencephalography. Remarkably, we found that these brain-fingerprints can differentiate between people with Parkinson's and those without, with about 90% accuracy. Specifically, we noticed that certain rhythmic patterns in the brain, particularly in areas involved in sensory and motor functions, were key indicators of Parkinson's. Interestingly, these patterns also helped us identify the different stages of the disease.

Additionally, our research shows that the arrangement of these brain-fingerprints in Parkinson's patients corresponds to how the neurochemistry of the brain is impacted by the disease. We also observed that certain irregular patterns in the brain's activity, which vary more from moment to moment in Parkinson's patients, make it harder to distinguish between

individuals based on these features alone. This finding shed light on why previous studies reported challenges with similar approaches.

Overall, our study offers new insights into the unique brain activity patterns in Parkinson's disease and suggests that individual brain-fingerprints could be valuable in tailoring treatment plans and developing new therapies for this condition.

## Introduction

The neurophysiological underpinnings of Parkinson's disease (PD) are characterized by a spectrum of motor and non-motor symptoms that vary widely among patients, and their fundamental nature continues to be a subject of extensive research (Bosboom et al., 2006; Stoffers et al., 2007, 2008b). This variation in symptoms is paralleled by PD's diverse structural alterations (Hanganu et al., 2014; Jubault et al., 2011; Pereira et al., 2014; H. Wilson et al., 2019), along with changes in hemodynamic and electrophysiological brain activity compared to healthy individuals (Olde Dubbelink et al., 2013; Stoffers et al., 2007; Tinkhauser et al., 2017; Torrecillos et al., 2018; Wiesman, Castanheira, et al., 2022; Y. Yu et al., 2021). Notably, electrophysiological changes in PD concern both the rhythmic and arrhythmic components of neurophysiological signals (Clark et al., 2023; Darmani et al., 2023; Olde Dubbelink et al., 2013; Tinkhauser et al., 2017; Torrecillos et al., 2018; Wiesman, da Silva Castanheira, et al., 2023). Brain-network characteristics, as highlighted in previous studies using functional connectome analysis with functional magnetic resonance imaging (fMRI) and other brain mapping techniques, also deviate from those in health and correlate with PD's hallmark motor and cognitive impairments (Díez-Cirarda et al., 2018; Fiorenzato et al., 2019; J. Kim et al., 2017; Zhu et al., 2019).

Recent methodological advances have employed fMRI connectomes to derive *brain-fingerprints*, providing biometric differentiation based on individual neuroimaging phenotypes (Amico & Goñi, 2018b; Finn et al., 2015b; Greene et al., 2018b; Rosenberg et al., 2017b). This concept posits that the neuroimaging phenotypes of an individual remain relatively stable over time, forming the basis for distinctive brain-fingerprints (Amico & Goñi, 2018b; da Silva Castanheira et al., 2021; Finn et al., 2015b). The brain-fingerprinting method has enabled the exploration of the neurophysiological bases of complex traits and behaviours in healthy participants (Amico &

Goñi, 2018b; da Silva Castanheira et al., 2021; Finn et al., 2015b; Greene et al., 2018b; Rosenberg et al., 2017a; Sareen et al., 2021c; Sorrentino et al., 2021b).

However, subsequent studies have indicated an increased variability (lower self-similairty/ Iself ) in brain-fingerprints of clinical populations (Kaufmann et al., 2017b, 2018b; Sorrentino et al., 2021b), which challenges the differentiation between patients based on this neuroimaging phenotype. This has been reported in both neuropsychiatric conditions as well as neurological diseases with motor symptoms. For example, a recent study with magnetoencephalography (MEG) showed that the differentiation accuracy between the brain-fingerprints of patients with PD, derived from connectomes, declines with the severity of their motor symptoms (Troisi Lopez et al., 2023). This investigation focused on beta band (13-30 Hz) activity, yet polyrhythmic alterations in neurophysiology are reported in Parkinson's disease. No study to date has explored whether these connectome effects are equally present in brain-fingerprints derived from hemodynamic signals.

Brain activity is composed of both rhythmic (oscillatory) and arrhythmic (1/f) components which both independently relate to cognitive task performance (Donoghue et al., 2020b; R. Gao et al., 2017) and are impacted by disease. Distinguishing between rhythmic and arrhythmic effects is critical as both components of neurophysiological signals represent distinct physiological mechanisms. The slope of the arrhythmic component (i.e., 1/f) is thought to reflect the local balance of excitatory and inhibitory currents (Donoghue et al., 2020b; R. Gao et al., 2017). Conflating one component for another negatively impacts the interpretability of genuine rhythmic signals.A comprehensive understanding of whether increased variability is driven by rhythmic or arrhythmic brain-fingerprints remains unexplored.

A plausible explanation for the de-individualization of brain activity and subsequent difficulty in differentiation of patients with Parkinson's disease may be an inherent instability in the brain activity of PD patients over short periods. For instance, previous work has shown that hemodynamic signals from functional near-infrared spectroscopy (fNIRS) are more variable in patients with severe PD symptoms (Maidan et al., 2022). This suggests that electrophysiological activity in PD is also likely to exhibit greater temporal variability, especially in brain regions with strong coupling between electrophysiological and hemodynamic signals (Shafiei et al., 2022).

This short-term variability within patients challenges the definition of a stable brain-fingerprint profile that would accurately characterize an individual's disease stage. Further research is needed to determine whether this increased variability affects the entire frequency spectrum of electrophysiological activity or is confined to specific rhythmic or arrhythmic components (Donoghue et al., 2020b; R. Gao et al., 2017).

In a recent study with healthy young adult participants, we showed that frequency-specific measures of electrophysiological activity across the cortex, derived from brief, task-free MEG data, define *spectral* brain-fingerprints that are specific to each individual over remarkably prolonged periods of time.

In the present study, we extend this approach and confirm that the electrophysiological brain-fingerprint of patients with PD exhibits greater variability over time compared to that of healthy controls. However, this variability is predominantly driven by the arrhythmic component of the neurophysiological power spectrum. In contrast, rhythmic features of the PD brain-fingerprint remain remarkably stable, enabling effective differentiation between PD patients and healthy controls, and among patients themselves. We highlight the clinical significance of these stable features by relating them to individual disease stages, and their cortical topography to the functional hierarchy of the cortex (Margulies et al., 2016) and atlas maps of cortical neurotransmitter systems relevant to PD neuropathophysiology (Markello et al., 2022a).

# Methods

**Participants:** Participants for this study were selected from a diverse age group (40-82 years) and included healthy controls as well as patients with mild to moderate idiopathic Parkinson's Disease (PD). We aggregated data from multiple sources. We utilized data from 79 PD patients who were part of the Quebec Parkinson Network (QPN; https://rpq-qpn.ca (Gan-Or et al., 2020)). These patients had undergone extensive clinical, neurophysiological, and biological profiling. All enrolled patients in the QPN study were on a stable dose of antiparkinsonian medication and demonstrated satisfactory clinical responses. They were instructed to continue their medication regimen as prescribed before any data collection. We included data from QPN participants who had complete

and usable Magnetoencephalography (MEG; 275 channels whole-head CTF; Port Coquitlam, British Columbia, Canada) clinical, and demographic data.

Our main control group comprised demographically matched participants from the PREVENT-AD (N=50) (Tremblay-Mercier et al., 2021) and OMEGA (N=4) (Niso et al., 2016b) studies, ensuring a comparison group that mirrors the age and demographic characteristics of the PD group. We replicated our observations using a second sample of healthy controls from the Cambridge Center for Aging Neuroscience (CamCAN) dataset (N= 370 healthy adults, 40-78 years old, 58.67, SD= 11.04; 185 Females) recorded on a different MEG instrument. See "Methods: CamCAN sample of healthy controls" and Chapter 3 for more details.

All participants underwent resting-state eyes-open MEG recordings. These recordings were conducted using a 275-channel whole-head CTF system (Port Coquitlam, British Columbia, Canada) at a sampling rate of 2400 Hz, with a 600-Hz antialiasing filter. We also applied systems built-in third-order gradient filters to the recordings. Consistency in data collection was maintained by conducting all recordings at the same site, each lasting a minimum of 10 minutes.

**Preprocessing of MEG Data**: We preprocessed the MEG data using Brainstorm (Tadel et al., 2011), March-2021 distribution, on MATLAB 2019b (Mathworks, Inc., Massachusetts, USA). We adhered to established good practice guidelines (Gross et al., 2013) and replicated the following pre-processing steps following previously published studies applied to similar data (Wiesman, da Silva Castanheira, et al., 2023; Wiesman, Donhauser, et al., 2023).

We filtered the MEG sensor signals between 1–200 Hz to minimize slow-wave drifts and high-frequency noise. Then, we removed line noise artifacts at 60 Hz and harmonic frequencies, with a notch filter bank. We corrected for cardiac and ocular artifacts using Signal-Space Projectors (SSPs), derived from electro-cardiogram and electro-oculogram recordings, using an automated procedure in Brainstorm (Tadel et al., 2011). We segmented the MEG recordings into non-overlapping 6-second epochs and downsampled them to 600 Hz. Lastly, we screened and excluded data segments with peak-to-peak signal amplitude or maximum signal gradient exceeding ±3 absolute deviations from the median across all epochs.

**MEG source mapping**. We derived brain source models from each participant's individual T1-weighted MRI data. We segmented and labeled the MRI volumes using Freesurfer (Fischl, 2012). We coregistered the MEG data to these segmented MRIs using approximately 100 head points that were digitized on the day of the MEG sessions. For 14 PD patients and 3 controls who lacked usable MRI data, we warped the default Freesurfer anatomy using Brainstorm procedures to match their available head digitization points and anatomical landmarks.

We created biophysical head models for each participant using the Brainstorm overlapping-spheres model with default parameters. The MEG cortical maps consisted of 15,000 elementary dipole sources, constrained to the cortical surface, with free orientation. We computed source maps for each participant and each 6-second epoch using dynamic statistical parametric mapping (dSPM) with Brainstorm's default parameters. To model environmental noise statistically, we processed with the same approach the two-minute empty-room recordings collected around the time of each participant's visit.

For all epochs, we extracted individual source time series at each cortical location from the first principal component of the three elementary time courses of each triplet of elementary sources at each cortical vertex. Finally, we clustered the resulting 15,000 time series according to the Desikan-Killiany cortical parcellation (Desikan et al., 2006b) into 68 regions of interest (ROIs), obtaining one representative time series per parcel from the first principal component of all source signals within each ROI.

**Derivation of spectral brain-fingerprints**: We derived brain-fingerprints from the power spectrum of the ROI source time series. We calculated the Power Spectrum Density (PSD) for each parcel using Welch's method, with a time window of 3 seconds and 50% overlap. This approach yielded PSDs in the frequency range of 0–150 Hz, at a frequency resolution of 1/3 Hz.

Each individual's spectral brain-fingerprint was composed of the PSDs of all 68 cortical parcels, averaged across all 6-second epochs. As detailed in Results, we derived two sets of spectral brain-fingerprints based on epochs from either the first or second half of the entire MEG session recordings. We also produced spectral brain-fingerprints from shorter datasets comprising 30-second non-overlapping segments.

The feature count in each spectral brain-fingerprint totaled 68*451. We performed subsequent analyses using in-house developed code in Python (version 3.7.6) and R (version 4.2.1).

**Individual differentiation from spectral brain-fingerprints:** We replicated a previously published fingerprinting approach based on the correlational differentiability of participants between data segments (as illustrated in Figure 1a-b) (da Silva Castanheira et al., 2021-; see Chapter 2). For each participant, we calculated all Pearson's correlation coefficients between their first spectral brain-fingerprint and the second brain-fingerprint of every individual in the same cohort, including the participant being analyzed. The fingerprinting process per se involved a simple lookup along the rows or columns of the symmetrical interindividual correlation matrix. The highest correlation coefficient in this matrix indicated the matching participant.

We repeated this approach for all participants in the cohort, resulting in a confusion matrix across all participants based on the two instances of their respective brain-fingerprints. We determined the overall differentiation accuracy of the brain-fingerprinting procedure by calculating the percent ratio of correctly differentiated individuals.

We addressed three types of differentiation challenges: i) differentiation among healthy participants, ii) differentiation among Parkinson's disease patients, and iii) differentiation of each PD patient against all healthy controls (as shown in Figure 1c). Differentiating healthy participants aimed to replicate our earlier study with younger adults (da Silva Castanheira et al., 2021) in an older participant group, providing a benchmark differentiation accuracy for the patient participants' age group.

We defined individual differentiability as the ability to distinguish a participant from others in the cohort based on their brain-fingerprint. We calculated this measure as the z-scored Pearson's correlation between the two brain-fingerprints of a given participant (self-similarity), relative to the mean and standard deviation of the correlations between this participant's first brain-fingerprint and the second brain-fingerprints of all other participants (other-similarity).

**Bootstrapping differentiation accuracy scores:** To establish confidence intervals for the average differentiation accuracy scores obtained from the fingerprinting procedure, we employed a bootstrapping method across the tested cohorts. This involved randomly selecting a subset of

participants, constituting 90% of the cohort, and performing brain-fingerprinting on their data to obtain a differentiation accuracy score for that subset.

We repeated this process 1,000 times, each time with a different random subset of participants from the cohort. From the empirical distribution of these differentiation accuracies, we derived a 95% confidence interval, using the $2.5^{th}$ and $97.5^{th}$ percentiles.

**Addressing biophysical and environmental artifacts:** We examined the potential impact of environmental noise and biophysical recording artifacts on the differentiation of individual participants. To do this, we correlated individual differentiability scores with the root-mean-squares (RMS) of ocular, cardiac, and head movement signals that were recorded simultaneously with MEG. These signals included data from electrocardiogram (ECG), horizontal electrooculogram (HEOG), vertical electrooculogram (VEOG), and head-coils triplet channels.

We analyzed the correlations between these three measures and the individual differentiability of each participant from the entire cohort. Additionally, we included the head motion RMS measure as a nuisance covariate in our regression model that explored self-similarity with increasing gap durations.

To assess if environmental and instrument noise, which can vary daily, could have biased individual differentiation, we utilized the empty-room recordings collected alongside each MEG session. From these recordings, we derived pseudo-brain fingerprints for each participant, based on the cortical source maps of the noise recordings. We then calculated the differentiation accuracies from these pseudo brain-fingerprints, following the same procedure as above.

**Arrhythmic/rhythmic spectral parametrization**: To evaluate the contribution of arrhythmic and rhythmic spectral components to individual differentiation, we first identified the best-fitting arrhythmic components of each individual's brain-fingerprint spectral features in the 2-40 Hz range using *specparam* in Brainstorm. The parameters for *specparam* were set as follows: peak width limits between 0.5 and 12 Hz, a maximum of 3 peaks, a minimum peak amplitude of 3 arbitrary units (a.u.), a peak threshold of 2 standard deviations, a proximity threshold of 2 standard deviations, and a fixed aperiodic mode.

The specparam algorithm defines neural power spectra as the sum of arrhythmic and rhythmic brain activity, with arrythmic brain activty modeled as a Lorentzian function:

$$Arrythmic = b - \log\left(F^{\alpha}\right)$$

Where b represents the broadband offset of the neural power spectrum and α represents the arrhythmic exponent (or slope) of the power spectrum which approximates a linear fit in log-log space.

Rhythmic brain activity is modelled as a series of Gaussian peaks that sit atop the background arrhythmic brain activity with the following three parameters: the center frequency of the Gaussian peak in Hz, the standard deviation of the Gaussian peak (Hz) and the height of the gaussian peak above the background arrhythmic activity (arbitrary units).

Using these arrhythmic models, we derived brain-fingerprints based solely on their features. Symmetrically, we removed the arrhythmic components from the original brain-fingerprints to isolate the rhythmic residuals and assess their contribution to inter-individual differentiation.

We then conducted the same brain-fingerprinting analyses as previously described, applying them separately to both arrhythmic and rhythmic brain-fingerprints.

**Temporal variability of the PD brain-fingerprint:** To investigate the temporal variability of PD brain-fingerprint, we utilized brain-fingerprints derived from 30-second recordings of data. This approach builds on our previous work, which demonstrated the robustness of spectral brain-fingerprints derived from brief recordings (Wiesman, da Silva Castanheira, et al., 2022c).

To predict the Fisher z-transformed self-similarity (i.e., autocorrelation) of successive brain-fingerprints, we employed second-order polynomial hierarchical regression models constructed using the *lme4* package in R.

In our modeling, we nested the slope of gap duration within each subject, allowing for second-order polynomial fits for gap duration between brain fingerprints.

$$artanh(self - similairty) \sim poly(gap\ duration, 2) * Group\ (PD\ vs\ CTL) + head\ motion + random\ effect(1 + poly(gap\ duration, 2)\ |SubjId)$$

**Saliency of brain-fingerprint features:** We quantified the contribution of each cortical region to individual differentiation using intraclass correlations (ICC). ICC assess the agreement between two measures, in this context, indicating how consistent a particular brain-fingerprint feature is across the two brain-fingerprints of each individual compared to others in the cohort. A higher ICC for a given brain-fingerprint feature implies greater consistency across an individual's brain-fingerprints relative to the cohort.

To illustrate the saliency of these features, we created ΔICC maps, as shown in Figure 3b. We first averaged the ΔICC values within each of the canonical frequency bands and then averaged these across all bands. This process involved averaging ΔICC within specified frequency ranges: delta (1–4 Hz), theta (4–8 Hz), alpha (8–13 Hz), beta (13–30 Hz), and gamma (30–50 Hz). This resulted in six ΔICC maps, one for each frequency band, which were then averaged to obtain a broadband ΔICC map.

The rationale behind this method was to give equal weight to each frequency band in the derivation of the broadband ΔICC, irrespective of their respective bandwidths. For example, while the delta band has a bandwidth of 4 Hz, the high-gamma band encompasses 100 Hz. This approach ensures a balanced representation of all frequency bands in assessing the contribution of cortical regions to individual differentiation based on brain-fingerprint features. In addition, this method allowed for a direct comparison to the CamCAN dataset whose power spectrum was computed using 2 second windows and therefore has a different spectral resolution (i.e., ½ Hz).

**CamCAN sample of healthy controls**: For verifying the robustness of the ΔICC cortical map, we utilized an independent sample of healthy age-matched controls from the Cambridge Center for Aging Neuroscience (CamCAN) dataset. This data consisted of resting-state, eye-closed MEG recordings using a 306-channel VectorView MEG system (Elekta Neuromag, Helsinki). We processed the data of 370 healthy adults, aged between 40 and 78 years, from the CamCAN dataset using a pipeline similar to the one described in this paper.

The CamCAn data were preprocessed for a separate project and therefore was preprocessed with some differences from the other data reported herein. For this reason, and the

different recording technology, we do not make any direct comparisons between the CamCAN control sample and the PD sample on participant differentiation accuracies or self-similarity.

We preprocessed the CamCAN dataset in a similar fashion to the other data reported herein using a standardized pipeline based on24. The differences in the preprocessing include the notch filter (50Hz), linearly constrained beamformer in Brainstorm with default parameters to brain map sensor data, and time windows of 2 seconds with a 50% overlap for power spectrum estimates of source time series.

We computed PSD estimates at each of the 68 parcels in the Desikan-Killiany atlas. We calculated ICC values for each specified frequency band. Using these ICC values, we constructed a cortical map of broadband ΔICC, following the method outlined above in Saliency of Brain-fingerprint Features.

Given that the ICC approach relies on participants as their own 'rater', the computation of salient features for participant differentiation in the two control samples should not be biased by the preprocessing of the MEG datasets. Taken together, we believe that the differences in the preprocessing of the two control samples and MEG recording technologies are a strength of our approach.

**Computational neuroanatomy analysis:** We ensured that neuroanatomical features, including those altered by Parkinson's disease, did not influence the differentiation of participants based on their spectral brain-fingerprints. To achieve this, we measured z-scored deviations in cortical thickness for each cortical parcel in PD patients. These deviations were calculated using FreeSurfer's recon-all, based on the mean and standard deviation of cortical thickness observed in the age-matched healthy controls.

We employed linear regression models to investigate two aspects: i) whether patients who were most differentiable based on their brain-fingerprints also exhibited greater deviations in cortical thickness, and ii) the relationship between deviations in regional cortical thickness and regional ΔICC (as depicted in Figure 3b, left panel).

**Decoding disease stage from brain-fingerprints:** We used individual Hoehn & Yahr scores as markers for disease staging in PD patients (Goetz et al., 2004; Hoehn & Yahr, 1967). We binarized these scores around a value of 2, creating two distinct groups to differentiate patients with unilateral symptoms from those with bilateral symptoms.

We trained a linear support vector machine (SVM) classifier in R, using default parameters to identify each patient's disease stage category from their respective spectral brain-fingerprint features.

We conducted SVM classification for each cortical parcel independently. To train the SVM classifier, we used data from a random sample of 80% of the patients, and the remaining 20% of patients served as a test set. We recorded the percentage of these held-out patients for whom the classifier accurately identified their Hoehn & Yahr category. We repeated this classification process 1,000 times for each cortical parcel, generating an empirical distribution of disease stage classification accuracy across the cortex.

Next, we examined the spatial correlation between the cortical topographies of disease stage decoding accuracy and the regional ΔICC values from the brain-fingerprints (as discussed above in Saliency of Brain-fingerprint Features). Specifically, we correlated the differences in ICC values—subtracted between the PD-cohort fingerprinting challenge and the control-cohort challenge—across cortical ROIs with the decoding accuracies obtained from Hoehn & Yahr score decoding.

**Correspondence with cortical functional hierarchy:** We examined whether the brain-fingerprints of individuals with Parkinson's Disease (PD) align with the cortical topography of functional hierarchies in the cortex (Margulies et al., 2016). To investigate this, we focused on the spatial relationship between the ΔICC brain-fingerprint topography and the first gradient of the cortical functional hierarchy.

We calculated Pearson's spatial correlation between the ΔICC topography of brain-fingerprints and the atlas map of the first gradient of the cortical functional hierarchy. The functional gradient map, obtained from (Margulies et al., 2016), we accessed from *neuromaps* (Markello et al., 2022a) and was parcellated into the 68 regions of the Desikan-Killiany atlas.

To statistically evaluate the significance of these correlations, we computed Bayes factors using the *correlationBF* function in R. Additionally, we estimated p-values using permutation tests that accounted for the spatial autocorrelation inherent in the data(Markello & Misic, 2021; Váša & Mišić, 2022).

**Correlation with cortical neurotransmitter systems:** Using a similar approach, we assessed the spatial correlation between the ΔICC values of brain-fingerprints and the normative atlas maps of various neurotransmitter systems. These systems were represented by maps for 19 receptors and transporters across 9 neurotransmitter systems, obtained from *neuromaps*. The neurotransmitter systems and their corresponding receptors and transporters included: Dopamine (D1, D2, DAT); Serotonin (5-HT1a, 5-HT1b, 5-HT2a, 5-HT4, 5-HT6, 5-HTT); Acetylcholine (α4β2, M1, VAChT); GABA (GABAa); Glutamate (NMDA, mGluR5); Norepinephrine (NET); Histamine (H3); Cannabinoid (CB1) and Opioid (MOR).

Each neurotransmitter system map was parcellated using the 68 regions of the Desikan-Killiany atlas. We then calculated Pearson's spatial correlations between these neurochemical maps and the regional ΔICC values of brain-fingerprints.

To determine statistical significance, we corrected for multiple comparisons using the False Discovery Rate (FDR) method implemented in R's *p.adjust* function(R Core Team, 2022). We also computed Bayes factors using the *correlationBF* function in R to quantify evidence in favor of the alternative hypothesis that a spatial correlation exists.

For each significant spatial correspondence observed, we estimated p-values based on spatially constrained permutation tests (Markello & Misic, 2021; Váša & Mišić, 2022). We conducted 1,000 permutations of the neurochemical atlases using the Hungarian method. It is important to note that the reported effects might be stronger than what was observed in the spin tests from the permuted data, leading to a null $p_{spin}$ value.

# Results

We collected at least two task-free MEG recordings, each lasting 5 minutes with participants' eyes open, from 79 PD patients and 54 age-matched healthy controls (Prevent-AD sample; demographic

details in Table S1). We then applied source-imaging to the MEG sensor data, using individual cortical surfaces derived from T1-weighted structural MRI scans (Baillet, 2017). For each participant, we estimated the power spectrum density (PSD) of their cortical MEG time series in the 0-150 Hz frequency range, across the cortical regions defined by the Desikan-Killiany atlas (Desikan et al., 2006b). This process generated one spectral brain-fingerprint for each participant's MEG recordings (see Methods).

Our goal with brain-fingerprinting was to quantify the distinctiveness of individual features in the brain-fingerprints of patients and healthy controls. We therefore compared the cortical spectral features from each participant's MEG recordings with those of all other participants in our sample. Subsequently, we applied the same analysis to differentiate PD patients. Finally, we examined if this method could reliably distinguish PD patients from their age-matched healthy counterparts (Figure 1). For the differentiation accuracy scores obtained, we calculated bootstrapped confidence intervals (CIs), as detailed in the Methods section.

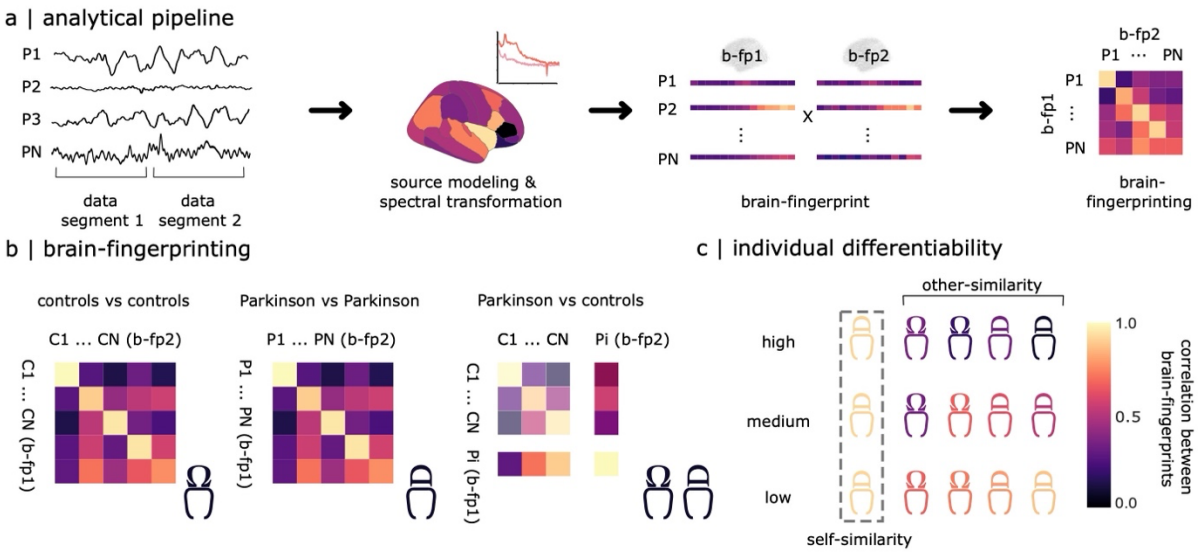


Chapter 4 Figure 1 Brain-fingerprinting pipeline and study design.

(a) From each participant, the power spectrum density of MEG source time series is computed for each region defined by the Desikan-Killiany atlas. This is done for two data segments (datasets 1 and 2), each containing approximately 4 minutes of clean data. The power spectra from these segments form two spectral brain-fingerprints (b-fp1 and b-fp2) for each participant (Desikan et

al., 2006b). A confusion matrix, using self- and other-similarity measures of these brain-fingerprints across participants, enables inter-individual differentiation assessment. (b) We evaluated the effectiveness of this approach in differentiating individuals among three groups: i) healthy controls, ii) patients with Parkinson's Disease (PD), and iii) each PD patient compared to healthy controls. (c) We derived an individual differentiability score for each participant, based on the self-similarity of their two brain-fingerprints. This score is z-scored against the other-similarity of their fingerprints with those of other participants in the study.

### Brain-Fingerprinting Accuracy in Differentiating Healthy and PD Participants

We found that healthy participants can be differentiated from each other with 89.8% accuracy (CI [88.0, 94.0]; Figure 2a), patients with PD from each other with 77.2% accuracy (CI [74.7, 81.7]), and patients from healthy controls with 81.1% accuracy (CI [81.0, 83.5]; Figure 2a) using full spectral features.

To assess the respective contributions to this inter-individual differentiation from *arrhythmic* versus *rhythmic* neurophysiology, we parametrized the regional power spectra of the cortical time series into its background (scale-free 1/f) and oscillatory (band-limited) components and used these data to recompute brain-fingerprints. The accuracy of inter-individual differentiation based on *arrhythmic* brain-fingerprints decreased to 74.1% between healthy controls (CI [72.0, 78.0]), 66.5% between patients (CI [62.9, 71.4]), and 71.5% accuracy individual patients and healthy controls (CI [69.6, 75.9]; Figure S1 and Supplemental Information). In contrast, the accuracy of inter-individual differentiation based on *rhythmic* brain-fingerprints increased to 92.6% (CI [90.0, 96.0]) among healthy participants, 86.7% (CI [82.9, 91.4]) between patients, and 90.5% (CI [89.9, 92.4]) between individual patients and healthy controls (Figure 2a bar plots).

We then sought to determine whether the present participants could be similarly differentiated based on brief, 30-second segments, thereby replicating our previous observations in younger healthy participants with older healthy adults and patients (da Silva Castanheira et al., 2021). We observed a similar pattern of differentiation accuracies: differentiation between healthy participants reached 84.9% (computed 95% CI [83.1, 86.7]), 77.2% for between patients (95% CI [74.4, 79.9]), and 81.2% for between patients and healthy controls (95% CI [78.7, 83.7]) for full spectral features. These results demonstrate the robustness of the spectral brain-fingerprinting

approach with respect to data length (scatter plots in Figure 2a). Both brain-fingerprints of the arrhythmic and rhythmic components derived from brief segments of 30 seconds exhibited similar patterns, with arrhythmic brain-fingerprints differentiating between patients with lower accuracy than healthy participants.

### Moment-to-moment arrhythmic fluctuations are increased in Parkinson's disease

We aimed to understand why the accuracy of differentiating PD patients from healthy controls varied so significantly, both with full spectral brain-fingerprints (77.2% vs. 89.8% accuracy) and arrhythmic ones (66.5% vs. 74.1% accuracy). To do this, we compared the similarity of brain-fingerprints within each dataset (self-similarity) to the similarity with fingerprints from other participants (other-similarity). Our analysis revealed no significant difference in *other-similarity* among healthy participants and PD patients when comparing full spectral brain-fingerprints (see Figure S2). However, we noted a significant reduction in the *self-similarity* of the patients' full spectral brain-fingerprints ($t=2.24$, $p=0.02$; permutation t-tests; Figure 2b).

To better understand this effect, we analyzed the impact of arrhythmic versus rhythmic neurophysiological spectral components on self-similarity. We observed that *arrhythmic* brain-fingerprints in patients demonstrated reduced self-similarity ($t=4.86$, $p<0.01$; permutation t-tests), unlike *rhythmic* brain-fingerprints ($t=1.77$, $p=0.09$; permutation t-tests; Figure 2b).

Further, we investigated if this discrepancy could be linked to the increased moment-to-moment variability in the brain activity of PD patients within the recording session (as detailed in Methods under 'Temporal variability of the PD brain-fingerprint'; see Table S2-S4 and Figure 2c). Using the shorter 30-second data segments, we discovered that for full spectrum brain-fingerprints, the self-similarity decreases more rapidly in patients than in healthy controls as the duration of the gap between the data segments increases ($\beta=-3.77$, $SE=1.73$, 95% CI [-7.16,-0.38], $p= 0.029$; detailed in Table S2). This pattern was not significant for arrhythmic brain-fingerprints ($\beta=-3.67$, $SE=2.33$, 95% CI [-8.25, 0.92], $p= 0.117$; Table S3) but showed a similar trend. Conversely, *rhythmic* brain-fingerprints revealed a different pattern: for shorter time gaps between data segments, the neurophysiological activity in patients with PD was more self-similar than that of controls, becoming comparable over longer durations ($\beta=-3.33$, $SE=1.69$, 95% CI [-6.65,-0.02],

p=0.049; Table S4). Together, these results suggest that the decreased differentiation accuracy observed in PD is related to an increased moment-to-moment variability of *arrhythmic* brain-fingerprints in PD.

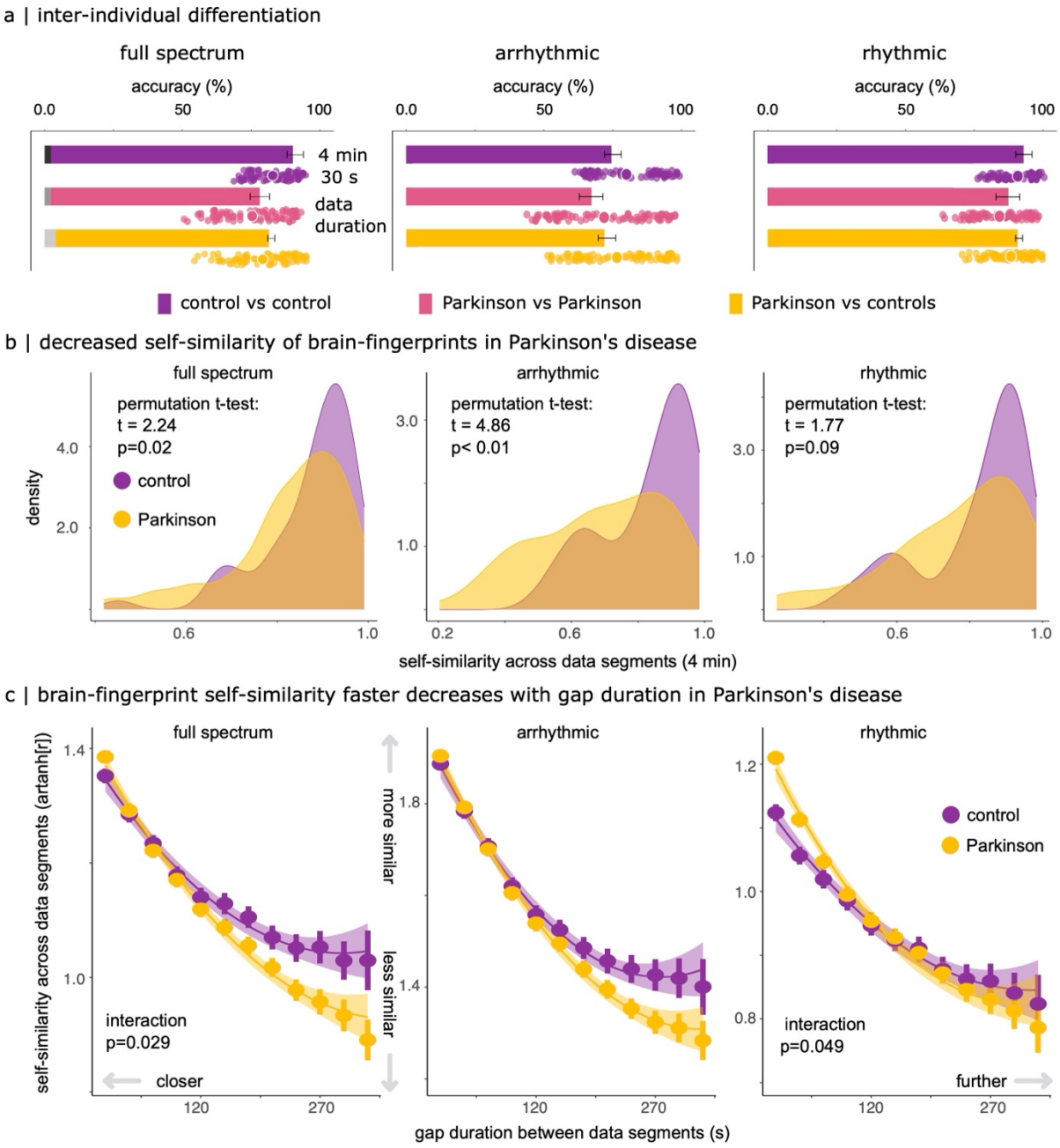


Chapter 4 Figure 2 Differentiating Patients with Parkinson's Disease from Healthy Controls Using Spectral Brain-Fingerprints.

(a) Accuracy in distinguishing participants from their brain-fingerprints derived from full, arrhythmic, and rhythmic neurophysiological power spectra, estimated from 4-minute (bar plots)

and 30-second (scatter plots) data segments. Scatter plots indicate differentiation accuracy for all brain-fingerprint pairs derived from all possible contiguous 30-second segments derived from the original 4-minute recordings. Grey segments at the base of the bar plots indicate control differentiation performances based on empty-room MEG recordings collected during each participant' visit (refer to Methods). Error bars represent bootstrapped 95% confidence intervals. (b) Self-similarity statistics within participants for full spectral, rhythmic, and arrhythmic brain-fingerprints. The plots show the empirical density of self-similarity statistics between two consecutive brain-fingerprints in control and PD cohorts, with the PD group showing a wider distribution, suggesting more variability in patients for full spectral and aperiodic features.
(c) Self-similarity of brain-fingerprints from brief (30-second) brain data segments across full spectral, rhythmic, and arrhythmic features. PD patients show lower self-similarity with increased gap durations between recordings (y-intercept shift downwards). The self-similarity of patient full spectrum brain-fingerprints decreases more rapidly as the gap duration between recordings increases. In contrast, the self-similarity of patient brain-fingerprints from rhythmic components was more self-similar than controls at short gap durations, and became comparable at longer durations. Shaded regions indicate the standard error on the mean.

### The Parkinson's brain-fingerprint indicates disease stages

Given the noted temporal stability of rhythmic neurophysiological features in patients with Parkinson's Disease (PD), we calculated the intraclass correlation (ICC) scores for each cortical region to identify the most consistent neurophysiological features in the rhythmic spectral brain-fingerprints across individuals (Amico & Goñi, 2018b; Shrout & Fleiss, 1979b). We found distinctive patterns of rhythmic neurophysiology in varying brain regions between healthy controls and PD patients. The highest ICC values were in frontal and medial cortical regions for healthy controls (Figure S3a), and in the right pre- and post-central regions for PD patients (Figure 3a and Figures S3b).

We replicated these findings with an external sample of healthy age-matched controls from the Cambridge Center for Aging Neuroscience (CamCAN) dataset(Taylor et al., 2017) (Figure 3a, see Methods). We computed a cortical map of ICC values for the independent sample of healthy older controls and contrasted this map with the topography of patients with PD (i.e., ΔICC map).

The cortical maps of the distinctive patterns of the PD brain-fingerprint obtained from using the two separate control samples were strongly correlated across control samples (r= 0.75, p< 0.001, $p_{spin}$< 0.001).

To gauge how the spatial divergence between the rhythmic brain-fingerprints relates to individual differentiation, we created brain-fingerprints for both PD patients and healthy controls using the top 10% of ICC features specific to each group (Figure 3a). Utilizing the most distinctive features of the brain-fingerprints of PD patients, we achieved a differentiation accuracy of 78.7% ([76.6, 80.8] CI; Figure 2a) among healthy participants, and 88.7% ([85.5, 91.8] CI; Figure 3b) among PD patients. In contrast, using the features most salient in healthy control brain-fingerprints, we differentiated healthy participants with 92.7% accuracy ([90.6, 94.9] CI; Figure 3b), and PD patients with only 66.9% accuracy ([62.4, 71.5] CI; Figure 3b).

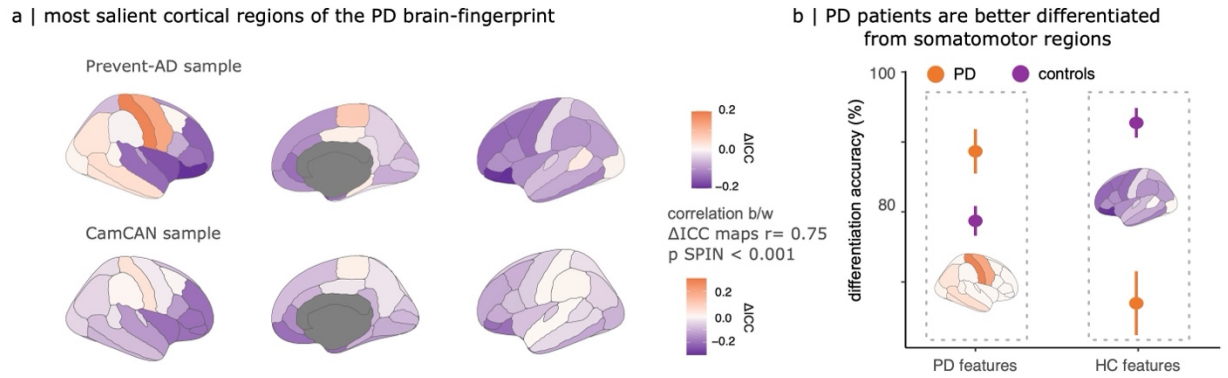


*Chapter 4 Figure 3 Comparative Analysis of Brain-Fingerprint Differentiation in Parkinson's Disease and Control Groups*

(a) Cortical maps comparing ICC scores for differentiating between patients and controls. Orange areas show regions where differentiation of individual patients is more effective than in controls. We replicated this finding in two independent samples of healthy controls: the Prevent-AD dataset (top panel) and the CamCAN dataset (bottom panel). (b) Differentiation accuracy from brain-fingerprints defined by top features for differentiating patients (left, cortical areas shown in orange) and top features for differentiating controls (right, cortical areas shown in blue).

We then explored if the rhythmic brain-fingerprint of a patient could be indicative of their clinical disease stage. For this purpose, we developed binary classifiers to decode the disease stage based on rhythmic spectral features at each cortical parcel (detailed in Methods under 'Decoding

disease staging from brain-fingerprints'). We classified the disease stage as either "early" or "advanced" according to the patients' scores on the Hoehn & Yahr clinical scale (HY< 2 and HY≥ 2, respectively) (Goetz et al., 2004; Hoehn & Yahr, 1967).

The cortical map of regional decoding accuracies revealed that it is possible to distinguish early from advanced clinical stages, exceeding chance levels, through electrophysiological brain activity. The most notable brain regions enabling this decoding were the right post-central and left caudal middle frontal gyri, showing decoding accuracies of 69.6% and 68.8%, respectively (Figure 4a). This data-driven approach uncovered that in these specific regions, there is a suppression of faster brain activity above 15Hz and an increase in slower activity (6-9 Hz) in the more advanced disease stages (Figure 4a, right panel).

Moreover, we found that the cortical map for disease-stage decoding aligns with the map of ICC difference scores (Figure 4b) and replicated this alignment using the CamCAN sample of healthy controls r= 0.36 (p< 0.01, $p_{spin}$< 0.001) and r= 0.51 (p>0.001, $p_{spin}$< 0.001), respectively. This consistency in findings was robust regardless of the cross-validation method employed for training the disease-stage classifiers (Figure S6).

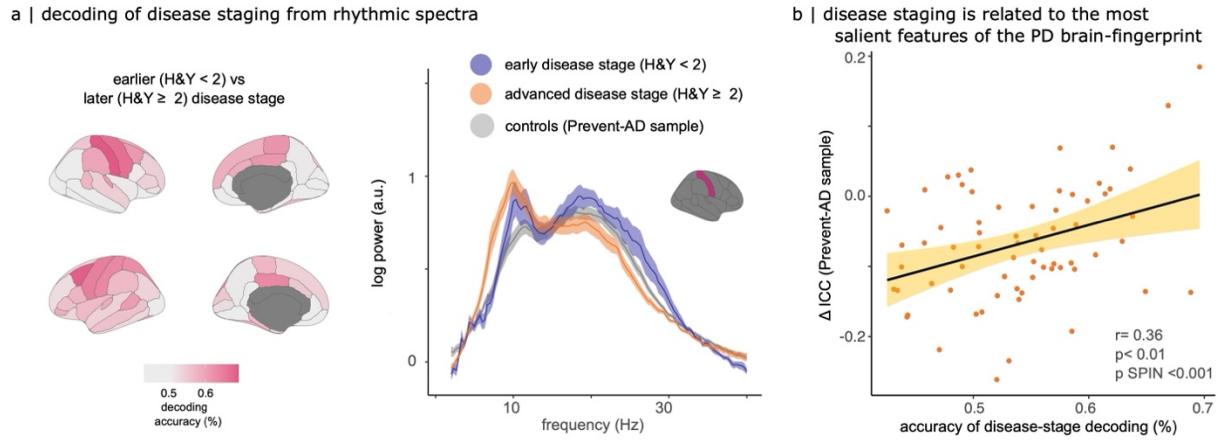


*Chapter 4 Figure 4 Decoding Stages of Parkinson's Disease from Brain-Fingerprints.*
(a) Cortical topography of decoding accuracies for Parkinson's disease stages (based on binarized Hoehn & Yahr scores). On the right, power spectra of resting-state neurophysiological activity in the right postcentral gyrus, the cortical region with the highest accuracy in disease stage decoding. Plots represent the average power spectrum for each group: healthy controls, early and advanced disease stages, with shaded areas indicating standard errors across groups.

(b) Scatter plot showing how the decoding accuracy of Parkinson's disease stages from brain-fingerprint features of each cortical parcel correlates with the saliency of each parcel, as determined by its ΔICC score.

## Aligning Parkinson's Disease Brain-Fingerprints with Cortical Functional Gradients and Neurotransmitter Systems

We found that the regional disparities in prominent features of the rhythmic brain-fingerprint between Parkinson's Disease (PD) patients and controls (indicated by ΔICC; see Figure 3a) were aligned with the unimodal-to-transmodal functional gradient of the cortical hierarchy (Margulies et al., 2016) ($r=-0.49$, $p< 0.001$, $p_{spin}<0.001$; Figure 5a, with details in Methods). The most notable *rhythmic* brain-fingerprint features in healthy adults were associated with transmodal cortical regions. Conversely, the distinct features of the Parkinson *rhythmic* brain-fingerprint were more closely related to unimodal (i.e., primary sensorimotor) areas within the functional hierarchy of the cortex. Again, we replicated this effect using the CamCAN sample of healthy controls ($r=-0.53$, $tp< 0.001$, $p_{spin}<0.001$; Figure S7).

We further investigated if the most prominent features of the Parkinson's brain-fingerprint were topographically related to the cortical distribution of major neurotransmitter systems. Using *neuromaps* (Markello et al., 2022a), we obtained 19 normative cortical maps representing 9 neurotransmitter systems (Figure 5b bottom) and assessed their spatial correlation with the cortical map of ICC difference scores (Figure 3a Prevent-AD sample; see Methods). Our analysis revealed significant correlations with several neurotransmitter systems, including serotonin-2a ($r=-0.39$, $p_{FDR}=0.006$, $p_{spin}<0.001$), serotonin-4 ($r=-0.37$, $p_{FDR}=0.008$, $p_{spin}=0.008$), cannabinoid-1 ($r=-0.41$, $p_{FDR}=0.00045$, $p_{spin}<0.001$), mu-opioid ($r=-0.34$, $p_{FDR}=0.018$, $p_{spin}=0.007$) receptors, and the norepinephrine transporter ($r=0.43$, $p_{FDR}=0.0040$, $p_{spin}<0.001$). Notably, the cannabinoid, opioid, and serotonin systems, concentrated in temporal and frontal cortical regions, and corresponded with the most salient *rhythmic* brain-fingerprint features in healthy controls (Figure 5b & Figure S3a). Conversely, the pronounced presence of norepinephrine transporters in the somato-motor cortices mirrored the significance of *rhythmic* neurophysiology in these areas in PD patients (Figure 5b & Figure 3a).

This effect replicated using the CamCAN sample of healthy controls (Figure 3a). We found alignments with the cortical distributions of serotonin-2a (r=-0.31, $p_{FDR}$ =0.02, $p_{spin}$ =0.005), serotonin-4 (r=-0.43, $p_{FDR}$ =0.002, $p_{spin}$ =0.002), cannabinoid-1 (r=-0.35, $p_{FDR}$ =0.01, $p_{spin}$ =0.003), mu-opioid (r=-0.37, $p_{FDR}$ =0.007, $p_{spin}$ =0.002) receptors, and the norepinephrine transporter (r=0.52, $p_{FDR}$ <0.001, $p_{spin}$<0.001). Additionally, we observed correspondence with the dopamine-1 (r=-0.31, $p_{FDR}$ =0.02, $p_{spin}$ =0.005), dopamine-2 (r=-0.28, $p_{FDR}$ =0.04, $p_{spin}$ =0.035), and serotonin transporter maps (r=-0.43, $p_{FDR}$ =0.001, $p_{spin}$ =0.003; Figure 5b).

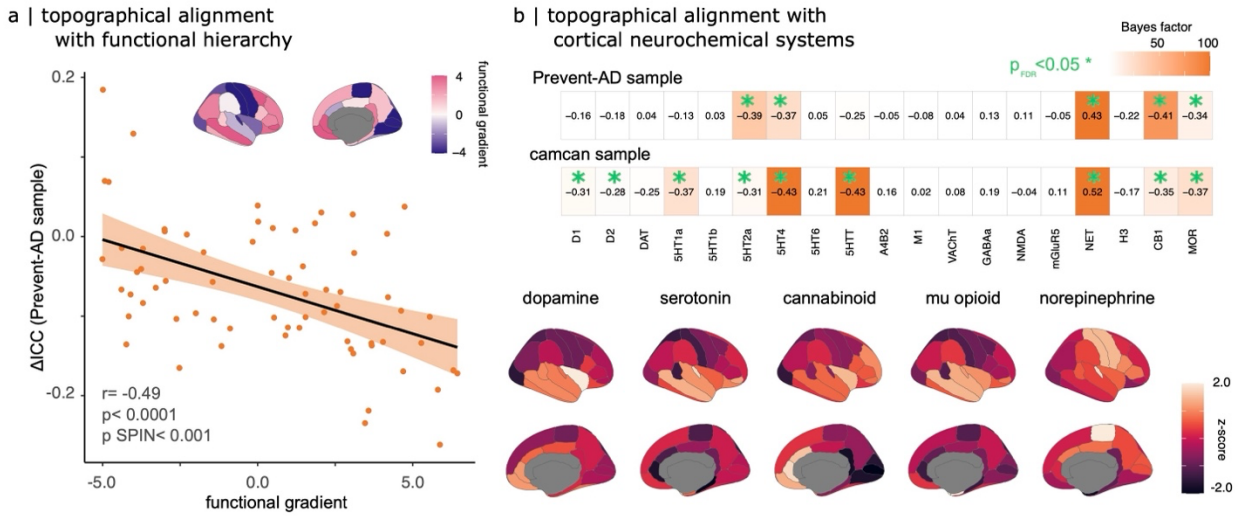


*Chapter 4 Figure 5 Correlation of Spectral Brain-Fingerprints with Cortical Functional Hierarchy and Neurotransmitter Systems.*

(a) Top: Cortical map illustrating the first unimodal-to-transmodal functional gradient, sourced from *neuromaps* (Markello et al., 2022a). Bottom: Linear association between the weights of cortical regions in this functional gradient (as per *neuromaps*) and their prominence in the PD brain-fingerprint (Figure 3a, top).

(b) Top: Bayes factor analysis of the topographical alignment between PD brain-fingerprint features (from Figure 3a) and atlases of various cortical neurochemical systems, highlighting strong correlations particularly with serotonin, cannabinoid, mu-opioid, and norepinephrine systems. Each row represents data from different control samples. Bottom: Selected neurochemical cortical atlases, as obtained from *neuromaps*.

## Robustness of Spectral Brain-Fingerprints Against Environmental and Physiological Artifacts

To ensure the reliability of spectral brain-fingerprints, we tested their robustness against environmental and physiological artifacts. We first evaluated environmental factors, specifically those related to the recording conditions on different days. To that effect, we used empty-room MEG recordings conducted around each participant's visit. By processing these recordings in a manner similar to the participant data and mapping them onto the participant's cortical surfaces with the same imaging procedure used for their MEG data, we established that environmental factors did not significantly contribute to individual differentiation. Notably, the differentiation accuracy based on these empty-room recordings was substantially lower than that achieved with actual spectral brain-fingerprints (<5%; see Figure 2a & Figure S1).

Further, we evaluated the influence of common physiological artifacts in MEG recordings, such as head motion, heart-rate variability, and eye blinks, on brain-fingerprinting. Our findings indicated that inter-individual differentiability was not significantly affected by cardiac or ocular artifacts (r=-0.04, p= 0.71 and r=-0.08, p= 0.46, respectively). However, there was a modest association with head movements in the PD cohort (r= 0.24, p= 0.04; Bayesian post-hoc analysis BF= 2.04; Figure S5). Consequently, we included head motion as a nuisance covariate in all subsequent regression analyses (detailed in Methods). We note that there were no significant differences in physiological artifact profiles between healthy controls and PD patients (head motion: t(64.34)= 0.41, p= 0.68; EOG: t(123.88)=-0.91, p=0.36; ECG: t(64.41)=-1.24, p=0.22).

Lastly, considering previous reports of cortical thickness abnormalities in PD (Hanganu et al., 2014; Jubault et al., 2011; Pereira et al., 2014; H. Wilson et al., 2019), we investigated whether these structural changes could partly explain the differentiability of PD patients from healthy controls. We derived cortical thickness measures from the structural MRI data of both groups, when available (n=134; Figure S4a). We standardized the patients' cortical thickness maps using z-score transforms based on healthy controls. Our analysis revealed no significant linear relationship between individual differentiability and the average standardized cortical thickness in PD patients (b=-0.03, SE= 0.07, 95% CI [-0.16, 0.11], p= 0.69; Figure S4b). Additionally, the cortical topography of the most salient Parkinson's brain-fingerprint features did not align with the cortical thickness changes observed in patients (Pearson's correlation: r=0.04, t(66)=0.34, p=0.73, $p_{spin}$ =0.36). Thus, we conclude that the individual differentiability observed in PD patients based on their spectral

brain-fingerprints is not significantly influenced by cortical thickness alterations associated with the disease.

# Discussion

Our study demonstrates the application and relevance of brain fingerprinting to Parkinson's disease (PD) research. We derived brain-fingerprints from task-free MEG recordings and replicated the prior observation that the brain-fingerprints of patients with PD present increased variability over short periods of time compared to healthy controls (Maidan et al., 2022; Troisi Lopez et al., 2023). We identified that this effect is due in large part to the enhanced temporal variability of the *arrhythmic* component of the neurophysiological brain activity of PD patients, making them less distinguishable from one another. However, we observed that PD patients can be accurately differentiated from each other and from healthy controls based on brain-fingerprints derived from the *rhythmic* components of their ongoing electrophysiological brain activity. We further show that the distinct features of these rhythmic fingerprints correlate with disease staging and align with neurochemical systems impacted in PD, underscoring the potential for targeting neuromodulation therapies based on rhythmic cortical neurophysiology in PD.

## Alterations of Cortical Signaling in Parkinson's Disease

Previous studies highlighted frequency-specific signaling abnormalities in PD, particularly in motor and subcortical structures (Geraedts et al., 2018; Oswal et al., 2013). Our findings align with this literature (Guerra et al., 2020; Underwood & Parr-Brownlie, 2021; Y. Yu et al., 2021), showing that the most distinctive brain-fingerprint features in PD patients localize to the primary sensorimotor cortex (Figure 3b left panel & Figure S3c), which correlates with their disease stages (Figure 3b). In particular, we found evidence of a link between atypical beta and theta band activities in the postcentral gyrus and disease stages. This aligns with previous findings linking beta-bursting in the motor network and sensorimotor cortex with symptom severity and treatment response to medication (Tinkhauser et al., 2017; Y. Yu et al., 2021) and deep brain stimulation of the subthalamic nucleus (Harmsen et al., 2018).

The role of midline theta-band activity in PD (Chen et al., 2016; Parker et al., 2015; Singh et al., 2018a, 2021a), thought to reflect cognitive processes (Cavanagh & Frank, 2014; Singh et al.,

2018b) and dopaminergic signaling (Y.-C. Kim et al., 2017, p. 4; Parker et al., 2014), was also confirmed in our study (Figure 4a). These findings are supported by previous research on theta neurostimulation's effectiveness in alleviating motor symptoms, including when targeting the precentral gyrus (Chou et al., 2015; Chung & Mak, 2016; Horn et al., 2020).

### Functional Decoupling of the Default Mode Network in Parkinson's Disease

We observed that the most salient brain-fingerprint features of healthy controls align with regions of the default-mode network (DMN; Figure 5a & Figure S3a). Prior studies have noted functional decoupling of the DMN in PD during rest and task-based recordings (Lucas-Jiménez et al., 2016; Ruppert et al., 2021; Tessitore et al., 2012; van Eimeren et al., 2009), often linked to the dopaminergic system (Lucas-Jiménez et al., 2016; Ruppert et al., 2021; Tessitore et al., 2012; van Eimeren et al., 2009). Yet, our data from patients on stable antiparkinsonian medication regimens may have moderated the saliency of DMN regions in the patients' brain-fingerprints (Figure 3). Thus, our observation that the DMN, transmodal brain regions of the functional hierarchy do not contribute substantially to the Parkinson's brain-fingerprint (Figure 5a) may reflect a normalization effect of medications (Delaveau et al., 2010; Krajcovicova et al., 2012). These observations prompt further investigation into how responsiveness to medications relates to brain-fingerprints in transmodal brain regions.

### Neurochemical correlates of the PD brain-fingerprint

Our data suggest that monoamine neurotransmitters are closely associated with the brain-fingerprint of PD (Figure 5b). Specifically, we found that the cortical topography of serotonin 2a and 4 receptor densities is inversely related to the PD brain-fingerprint, while there is a direct association with the norepinephrine transporter.

This finding is in agreement with previous observations of the degradation of monoamines in PD (Narayanan et al., 2013). We report negative relationships between the brain-fingerprint of PD and dopamine systems (Figure 5b). This effect was weak and inconsistent, possibly because changes in dopaminergic signalling caused by PD may primarily affect subcortical structures (Poewe et al., 2017) rather than the cortex, where our analyses were restricted. Further, the normative neurochemical system maps available in *neuromaps* were derived from an independent

sample of adults, who were younger than the PD patients and aged-matched controls of the present study. Future research should explore these effects across subcortical structures and with normative atlases of neurochemical systems in older adults.

We also observed a negative alignment of the Parkinson's brain-fingerprint with the cannabinoid receptor-1 (CB1) system (Figure 5b), supporting prior research that documents elevated CB1 receptor concentrations in PD[61], and highlighting CB1 as a potential therapeutic target in PD(Brotchie, 2003). Our present results also highlight the potential participation of the cannabinoid system in the neuropathophysiology of PD and encourage more research in this area.

### Enhanced Temporal Fluctuation of Arrhythmic Brain Activity in Parkinson's Disease

Our study revealed that the brain-fingerprints of patients with Parkinson's disease fluctuate more over short time spans compared to age-matched healthy individuals. This finding aligns with the decreased accuracy observed originally in differentiating individuals within the patient group (Figures 2b &c).

We anticipated greater variability in PD brain activity based on previous fNIRS research, which suggested a correlation between symptom severity and hemodynamic signal variability (Maidan et al., 2022). Additionally, studies using fMRI connectome brain-fingerprinting indicated reduced self-similarity in individuals at risk of or with mental health disorders (Kaufmann et al., 2017b),(Kaufmann et al., 2018b) and in PD patients (Troisi Lopez et al., 2023). Our data extend these findings to electrophysiology, pointing at increased within-subject variability of *arrhythmic* brain activity in PD as a possible source of such variability. We noted that differentiation accuracy using full spectral and arrhythmic brain-fingerprints in PD patients was lower compared to *rhythmic* brain-fingerprints, which achieved similar differentiation as seen in healthy controls (Figure 2a).

Recent research has linked alterations in PD patients' arrhythmic brain activity to symptom severity (Belova et al., 2021; J. Kim et al., 2022; Wiesman, da Silva Castanheira, et al., 2023). Preliminary studies further suggest that baseline arrhythmic activity in the subthalamic nucleus may predict responses to neuro-stimulation protocols (Clark et al., 2023; Darmani et al., 2023). While these studies focused on group-level mean differences, our findings emphasize the significance of within-patient variability of arrhythmic brain activity in understanding individual

disease manifestations. We hope our results promote further research into optimizing personalized rhythmic stimulation protocols for PD management by normalizing cortical dynamics.

Previous studies have also documented increased intra-individual variability in cognitive task performance in PD (Burton et al., 2006a; Costa et al., 2019b; Kuntsi & Klein, 2011a), correlating with cognitive symptom severity (Burton et al., 2006a; Costa et al., 2019b; Singh et al., 2021a). The biological basis of this behavioral variability increase remains poorly understood (J. D. Jones et al., 2022). fMRI research has linked moment-to-moment brain activity variability with cognitive performance (Garrett et al., 2010; Garrett, Kovacevic, et al., 2013; Nomi et al., 2017), and recent studies have related BOLD signal variability to the arrhythmic components of electrophysiology (Baracchini et al., 2023). Consequently, we hypothesize that the heightened variability in PD behavioural markers may be associated with the observed increased temporal variability in arrhythmic brain activity.

The arrhythmic and rhythmic components of the neurophysiological spectrum indicate distinct neural mechanisms (Donoghue et al., 2020b; R. Gao et al., 2017; L. E. Wilson et al., 2022). The arrhythmic spectrum's slope is conceived as reflecting the balance of neuronal excitation versus inhibition (Donoghue et al., 2020b; R. Gao et al., 2017). Therefore, our findings tentatively suggest greater fluctuating dynamics in cortical excitability in PD. This construct is in line with emerging insights that dynamics of spectral aperiodic components are key to understanding healthy aging and behaviours (L. E. Wilson et al., 2022).

### Potential Clinical Impact of Brain-Fingerprinting in Personalized Neuromodulation Therapies

The clinical utility of brain-fingerprinting hinges on its capacity to refine patient stratification, reveal novel disease characteristics, and inspire new treatment strategies.

Our findings demonstrate that brief brain recordings can distinguish individuals (da Silva Castanheira et al., 2021), including those with Parkinson’s disease. We highlight the consistent within-participant stability of rhythmic brain-fingerprints in both patients and healthy controls (see Figure 2c), offering a unique insight into individual-specific brain activity. This consistency aligns with prior research showing the stabilization of spectral content in resting-state brain activity within 30 to 120 seconds of MEG recording (Wiesman, da Silva Castanheira, et al., 2022c). This

rapid stabilization is especially beneficial for clinical applications, particularly for patients with cognitive or motor impairments who may find longer recording sessions challenging.

The present study also suggests that personalized neuromodulation therapies should primarily concentrate on *rhythmic* neurophysiology, the most consistent electrophysiological characteristic within individuals, reflective of each patient and related to disease traits. Specifically, theta- and beta-frequency rhythms in the fronto-motor cortices emerge as potential prime targets for neurostimulation protocols aimed at normalizing disease-related neurophysiological changes (Chase et al., 2019; Chou et al., 2015; Clark et al., 2023; Harmsen et al., 2018). Conversely, *arrhythmic* neurophysiological activity displayed less stability and individual specificity in Parkinson's disease patients (Figure 2). This suggests that tracking the longitudinal variability of arrhythmic brain-fingerprints could enhance the definition and understanding of patient trajectories, as indicated here in Figure 2c. Incorporating this variability into adaptive neurostimulation therapies could potentially enhance clinical outcomes in Parkinson's disease by reducing moment-to-moment fluctuations of core dynamics of brain activity related to the disease.

We also highlight the need to account for increased intra-individual variability of brain activity in disease states when developing statistical and machine-learning models for disease classification. This consideration is crucial to ensure the scalability and generalizability of patient stratification methods.

The results of the present study may transfer to other existing electrophysiological techniques such as electroencephalography (EEG), which promises to be more affordable and accessible, and optically pumped magnetometers (OPMs). Future work should explore this possibility as it would offer researchers and clinicians the flexibility of recording patients at the bedside.

In conclusion, our study underscores the clinical significance of brain-fingerprinting based on rapid neurophysiological activity dynamics. It sheds light on the clinical aspects of Parkinson's disease, identifying specific brain regions and rhythms where disease impacts neurophysiological stability. We anticipate these insights will catalyze further research in population neuroscience and the development of personalized neuromodulation therapies for Parkinson's disease and other neurodegenerative conditions.

## Data availability

The data are available through the Clinical Biospecimen Imaging and Genetic (C-BIG) repository (https://www.mcgill.ca/neuro/open-science/c-big-repository)(Gan-Or et al., 2020), the PREVENT-AD open resource (https://openpreventad.loris.ca/ and https://registeredpreventad.loris.ca) (Tremblay-Mercier et al., 2021), and the OMEGA repository (https://www.mcgill.ca/bic/resources/omega) (Niso et al., 2016b). Normative neurotransmitter density data are available from *neuromaps* (https://github.com/netneurolab/neuromaps) (Markello et al., 2022a).

## Code availability

All in-house code used for data analysis and visualization is available on GitHub https://github.com/jasondsc/PDneuralfingerprinting.

## Acknowledgements

Data collection and sharing for this project was provided by the Quebec Parkinson Network (QPN), the Pre-symptomatic Evaluation of Novel or Experimental Treatments for Alzheimer's Disease (PREVENT-AD; release 6.0) program, and the Open MEG Archives (OMEGA). The funders had no role in study design, data collection and analysis, decision to publish, or preparation of the manuscript. The QPN is funded by a grant from Fonds de recherche du Québec-Santé (FRQS). PREVENT-AD was launched in 2011 as a $13.5 million, 7-year public-private partnership using funds provided by McGill University, the FRQS, an unrestricted research grant from Pfizer Canada, the Levesque Foundation, the Douglas Hospital Research Centre and Foundation, the Government of Canada, and the Canada Fund for Innovation. Private sector contributions are facilitated by the Development Office of the McGill University Faculty of Medicine and by the Douglas Hospital Research Centre Foundation (http://www.douglas.qc.ca/). The Brainstorm project is supported by funding to SB from the NIH (R01-EB026299-05). Further funding to SB for this study included Discovery grant from the Natural Science and Engineering Research Council of Canada (436355-13), and the CIHR Canada research Chair in Neural Dynamics of Brain Systems

(CRC-2017-00311). This work was also supported by a grant F32-NS119375 (AIW) from the National Institutes of Health and a doctoral fellowship from NSERC (JDSC, JYH).

## References

Amico, E., & Goñi, J. (2018). The quest for identifiability in human functional connectomes. Scientific Reports, 8(1), 8254. https://doi.org/10.1038/s41598-018-25089-1

Baillet, S. (2017). Magnetoencephalography for brain electrophysiology and imaging. Nature Neuroscience, 20(3), Article 3. https://doi.org/10.1038/nn.4504

Baracchini, G., Zhou, Y., Castanheira, J. D. S., Hansen, J. Y., Rieck, J., Turner, G. R., Grady, C. L., Misic, B., Nomi, J., Uddin, L. Q., & Spreng, R. N. (2023). The biological role of local and global fMRI BOLD signal variability in human brain organization [Preprint]. Neuroscience. https://doi.org/10.1101/2023.10.22.563476

Belova, E. M., Semenova, U., Gamaleya, A. A., Tomskiy, A. A., & Sedov, A. (2021). Voluntary movements cause beta oscillations increase and broadband slope decrease in the subthalamic nucleus of parkinsonian patients. European Journal of Neuroscience, 53(7), 2205–2213. https://doi.org/10.1111/ejn.14715

Bosboom, J. L. W., Stoffers, D., Stam, C. J., van Dijk, B. W., Verbunt, J., Berendse, H. W., & Wolters, E. Ch. (2006). Resting state oscillatory brain dynamics in Parkinson's disease: An MEG study. Clinical Neurophysiology, 117(11), 2521–2531. https://doi.org/10.1016/j.clinph.2006.06.720

Brotchie, J. (2003). CB cannabinoid receptor signalling in Parkinson's disease. Current Opinion in Pharmacology, 3(1), 54–61. https://doi.org/10.1016/S1471-4892(02)00011-5

Burton, C. L., Strauss, E., Hultsch, D. F., Moll, A., & Hunter, M. A. (2006). Intraindividual Variability as a Marker of Neurological Dysfunction: A Comparison of Alzheimer's Disease and Parkinson's Disease. Journal of Clinical and Experimental Neuropsychology, 28(1), 67–83. https://doi.org/10.1080/13803390490918318

Cavanagh, J. F., & Frank, M. J. (2014). Frontal theta as a mechanism for cognitive control. Trends in Cognitive Sciences, 18(8), 414–421. https://doi.org/10.1016/j.tics.2014.04.012

Chase, H., Boudewyn, M., Carter, C., & Phillips, M. (2019). Transcranial direct current stimulation: A roadmap for research, from mechanism of action to clinical implementation. Molecular Psychiatry, 25. https://doi.org/10.1038/s41380-019-0499-9

Chen, K.-H., Okerstrom, K. L., Kingyon, J. R., Anderson, S. W., Cavanagh, J. F., & Narayanan, N. S. (2016). Startle Habituation and Midfrontal Theta Activity in Parkinson Disease. Journal of Cognitive Neuroscience, 28(12), 1923–1932. https://doi.org/10.1162/jocn_a_01012

Chou, Y., Hickey, P. T., Sundman, M., Song, A. W., & Chen, N. (2015). Effects of Repetitive Transcranial Magnetic Stimulation on Motor Symptoms in Parkinson Disease. JAMA Neurology, 72(4), 432–440. https://doi.org/10.1001/jamaneurol.2014.4380

Chung, C. L., & Mak, M. K. Y. (2016). Effect of Repetitive Transcranial Magnetic Stimulation on Physical Function and Motor Signs in Parkinson's Disease: A Systematic Review and Meta-Analysis. Brain Stimulation, 9(4), 475–487. https://doi.org/10.1016/j.brs.2016.03.017

Clark, D. L., Khalil, T., Kim, L. H., Noor, M. S., Luo, F., & Kiss, Z. HT. (2023). Aperiodic subthalamic activity predicts motor severity and stimulation response in Parkinson disease. Parkinsonism & Related Disorders, 110, 105397. https://doi.org/10.1016/j.parkreldis.2023.105397

Costa, A. S., Dogan, I., Schulz, J. B., & Reetz, K. (2019). Going beyond the mean: Intraindividual variability of cognitive performance in prodromal and early neurodegenerative disorders. The Clinical Neuropsychologist, 33(2), 369–389. https://doi.org/10.1080/13854046.2018.1533587

da Silva Castanheira, J., Orozco Perez, H. D., Misic, B., & Baillet, S. (2021). Brief segments of neurophysiological activity enable individual differentiation. Nature Communications, 12(1), Article 1. https://doi.org/10.1038/s41467-021-25895-8

Darmani, G., Drummond, N. M., Ramezanpour, H., Saha, U., Hoque, T., Udupa, K., Sarica, C., Zeng, K., Cortez Grippe, T., Nankoo, J.-F., Bergmann, T. O., Hodaie, M., Kalia, S. K., Lozano, A. M., Hutchison, W. D., Fasano, A., & Chen, R. (2023). Long-Term Recording of Subthalamic Aperiodic Activities and Beta Bursts in Parkinson's Disease. Movement Disorders, 38(2), 232–243. https://doi.org/10.1002/mds.29276

Delaveau, P., Salgado-Pineda, P., Fossati, P., Witjas, T., Azulay, J.-P., & Blin, O. (2010). Dopaminergic modulation of the default mode network in Parkinson's disease. European Neuropsychopharmacology, 20(11), 784–792. https://doi.org/10.1016/j.euroneuro.2010.07.001

Desikan, R. S., Ségonne, F., Fischl, B., Quinn, B. T., Dickerson, B. C., Blacker, D., Buckner, R. L., Dale, A. M., Maguire, R. P., Hyman, B. T., Albert, M. S., & Killiany, R. J. (2006). An automated labeling system for subdividing the human cerebral cortex on MRI scans into gyral based regions of interest. NeuroImage, 31(3), 968–980. https://doi.org/10.1016/j.neuroimage.2006.01.021

Díez-Cirarda, M., Strafella, A. P., Kim, J., Peña, J., Ojeda, N., Cabrera-Zubizarreta, A., & Ibarretxe-Bilbao, N. (2018). Dynamic functional connectivity in Parkinson's disease patients with mild cognitive impairment and normal cognition. NeuroImage: Clinical, 17, 847–855. https://doi.org/10.1016/j.nicl.2017.12.013

Donoghue, T., Haller, M., Peterson, E. J., Varma, P., Sebastian, P., Gao, R., Noto, T., Lara, A. H., Wallis, J. D., Knight, R. T., Shestyuk, A., & Voytek, B. (2020). Parameterizing neural power spectra into periodic and aperiodic components. Nature Neuroscience, 23(12), Article 12. https://doi.org/10.1038/s41593-020-00744-x

Finn, E. S., Shen, X., Scheinost, D., Rosenberg, M. D., Huang, J., Chun, M. M., Papademetris, X., & Constable, R. T. (2015). Functional connectome fingerprinting: Identifying individuals using patterns of brain connectivity. Nature Neuroscience, 18(11), 1664–1671. https://doi.org/10.1038/nn.4135

Fiorenzato, E., Strafella, A. P., Kim, J., Schifano, R., Weis, L., Antonini, A., & Biundo, R. (2019). Dynamic functional connectivity changes associated with dementia in Parkinson's disease. Brain, 142(9), 2860–2872. https://doi.org/10.1093/brain/awz192

Fischl, B. (2012). FreeSurfer. NeuroImage, 62(2), 774–781. https://doi.org/10.1016/j.neuroimage.2012.01.021

Gan-Or, Z., Rao, T., Leveille, E., Degroot, C., Chouinard, S., Cicchetti, F., Dagher, A., Das, S., Desautels, A., Drouin-Ouellet, J., Durcan, T., Gagnon, J.-F., Genge, A., Karamchandani, J., Lafontaine, A.-L., Sun, S. L. W., Langlois, M., Levesque, M., Melmed, C., … Fon, E. A. (2020).

The Quebec Parkinson Network: A Researcher-Patient Matching Platform and Multimodal Biorepository. Journal of Parkinson's Disease, 10(1), 301–313. https://doi.org/10.3233/JPD-191775

Gao, R., Peterson, E. J., & Voytek, B. (2017). Inferring synaptic excitation/inhibition balance from field potentials. NeuroImage, 158, 70–78. https://doi.org/10.1016/j.neuroimage.2017.06.078

Garrett, D. D., Kovacevic, N., McIntosh, A. R., & Grady, C. L. (2010). Blood Oxygen Level-Dependent Signal Variability Is More than Just Noise. Journal of Neuroscience, 30(14), 4914–4921. https://doi.org/10.1523/JNEUROSCI.5166-09.2010

Garrett, D. D., Kovacevic, N., McIntosh, A. R., & Grady, C. L. (2013). The modulation of BOLD variability between cognitive states varies by age and processing speed. Cerebral Cortex (New York, N.Y.: 1991), 23(3), 684–693. https://doi.org/10.1093/cercor/bhs055

Geraedts, V. J., Boon, L. I., Marinus, J., Gouw, A. A., van Hilten, J. J., Stam, C. J., Tannemaat, M. R., & Contarino, M. F. (2018). Clinical correlates of quantitative EEG in Parkinson disease: A systematic review. Neurology, 91(19), 871–883. https://doi.org/10.1212/WNL.0000000000006473

Gerdeman, G. L., Ronesi, J., & Lovinger, D. M. (2002). Postsynaptic endocannabinoid release is critical to long-term depression in the striatum. Nature Neuroscience, 5(5), 446–451. https://doi.org/10.1038/nn832

Goetz, C. G., Poewe, W., Rascol, O., Sampaio, C., Stebbins, G. T., Counsell, C., Giladi, N., Holloway, R. G., Moore, C. G., Wenning, G. K., Yahr, M. D., & Seidl, L. (2004). Movement Disorder Society Task Force report on the Hoehn and Yahr staging scale: Status and recommendations The Movement Disorder Society Task Force on rating scales for Parkinson's disease. Movement Disorders, 19(9), 1020–1028. https://doi.org/10.1002/mds.20213

Greene, A. S., Gao, S., Scheinost, D., & Constable, R. T. (2018). Task-induced brain state manipulation improves prediction of individual traits. Nature Communications, 9(1), 2807. https://doi.org/10.1038/s41467-018-04920-3

Gross, J., Baillet, S., Barnes, G. R., Henson, R. N., Hillebrand, A., Jensen, O., Jerbi, K., Litvak, V., Maess, B., Oostenveld, R., Parkkonen, L., Taylor, J. R., van Wassenhove, V., Wibral, M., & Schoffelen, J.-M. (2013). Good practice for conducting and reporting MEG research. NeuroImage, 65, 349–363. https://doi.org/10.1016/j.neuroimage.2012.10.001

Guerra, A., Asci, F., D'Onofrio, V., Sveva, V., Bologna, M., Fabbrini, G., Berardelli, A., & Suppa, A. (2020). Enhancing Gamma Oscillations Restores Primary Motor Cortex Plasticity in Parkinson's Disease. The Journal of Neuroscience, 40(24), 4788–4796. https://doi.org/10.1523/JNEUROSCI.0357-20.2020

Hanganu, A., Bedetti, C., Degroot, C., Mejia-Constain, B., Lafontaine, A.-L., Soland, V., Chouinard, S., Bruneau, M.-A., Mellah, S., Belleville, S., & Monchi, O. (2014). Mild cognitive impairment is linked with faster rate of cortical thinning in patients with Parkinson's disease longitudinally. Brain: A Journal of Neurology, 137(Pt 4), 1120–1129. https://doi.org/10.1093/brain/awu036

Harmsen, I. E., Rowland, N. C., Wennberg, R. A., & Lozano, A. M. (2018). Characterizing the effects of deep brain stimulation with magnetoencephalography: A review. Brain Stimulation, 11(3), 481–491. https://doi.org/10.1016/j.brs.2017.12.016

Hoehn, M. M., & Yahr, M. D. (1967). Parkinsonism: Onset, progression, and mortality. Neurology, 17(5), 427–427. https://doi.org/10.1212/WNL.17.5.427

Hohmann, A. G., & Herkenham, M. (2000). Localization of cannabinoid CB1 receptor mRNA in neuronal subpopulations of rat striatum: A double-label in situ hybridization study. Synapse, 37(1), 71–80. https://doi.org/10.1002/(SICI)1098-2396(200007)37:1<71::AID-SYN8>3.0.CO;2-K

Horn, M. A., Gulberti, A., Gülke, E., Buhmann, C., Gerloff, C., Moll, C. K. E., Hamel, W., Volkmann, J., & Pötter-Nerger, M. (2020). A New Stimulation Mode for Deep Brain Stimulation in Parkinson's Disease: Theta Burst Stimulation. Movement Disorders: Official Journal of the Movement Disorder Society, 35(8), 1471–1475. https://doi.org/10.1002/mds.28083

Jones, J. D., Valenzuela, Y. G., Uribe, C., Bunch, J., & Kuhn, T. P. (2022). Intraindividual variability in neuropsychological performance predicts longitudinal cortical volume loss in early Parkinson's disease. Neuropsychology, 36, 513–519. https://doi.org/10.1037/neu0000809

Jubault, T., Gagnon, J.-F., Karama, S., Ptito, A., Lafontaine, A.-L., Evans, A. C., & Monchi, O. (2011). Patterns of cortical thickness and surface area in early Parkinson's disease. NeuroImage, 55(2), 462–467. https://doi.org/10.1016/j.neuroimage.2010.12.043

Kaufmann, T., Alnæs, D., Brandt, C. L., Bettella, F., Djurovic, S., Andreassen, O. A., & Westlye, L. T. (2018). Stability of the Brain Functional Connectome Fingerprint in Individuals With Schizophrenia. JAMA Psychiatry, 75(7), 749. https://doi.org/10.1001/jamapsychiatry.2018.0844

Kaufmann, T., Alnæs, D., Doan, N. T., Brandt, C. L., Andreassen, O. A., & Westlye, L. T. (2017). Delayed stabilization and individualization in connectome development are related to psychiatric disorders. Nature Neuroscience, 20(4), 513–515. https://doi.org/10.1038/nn.4511

Kim, J., Criaud, M., Cho, S. S., Díez-Cirarda, M., Mihaescu, A., Coakeley, S., Ghadery, C., Valli, M., Jacobs, M. F., Houle, S., & Strafella, A. P. (2017). Abnormal intrinsic brain functional network dynamics in Parkinson's disease. Brain, 140(11), 2955–2967. https://doi.org/10.1093/brain/awx233

Kim, J., Lee, J., Kim, E., Choi, J. H., Rah, J.-C., & Choi, J.-W. (2022). Dopamine depletion can be predicted by the aperiodic component of subthalamic local field potentials. Neurobiology of Disease, 168, 105692. https://doi.org/10.1016/j.nbd.2022.105692

Kim, Y.-C., Han, S.-W., Alberico, S. L., Ruggiero, R. N., De Corte, B., Chen, K.-H., & Narayanan, N. S. (2017). Optogenetic Stimulation of Frontal D1 Neurons Compensates for Impaired Temporal Control of Action in Dopamine-Depleted Mice. Current Biology, 27(1), 39–47. https://doi.org/10.1016/j.cub.2016.11.029

Krajcovicova, L., Mikl, M., Marecek, R., & Rektorova, I. (2012). The default mode network integrity in patients with Parkinson's disease is levodopa equivalent dose-dependent. Journal of Neural Transmission, 119(4), 443–454. https://doi.org/10.1007/s00702-011-0723-5

Kuntsi, J., & Klein, C. (2011). Intraindividual Variability in ADHD and Its Implications for Research of Causal Links. In C. Stanford & R. Tannock (Eds.), Behavioral Neuroscience of Attention

Deficit Hyperactivity Disorder and Its Treatment (Vol. 9, pp. 67–91). Springer Berlin Heidelberg. https://doi.org/10.1007/7854_2011_145

Lucas-Jiménez, O., Ojeda, N., Peña, J., Díez-Cirarda, M., Cabrera-Zubizarreta, A., Gómez-Esteban, J. C., Gómez-Beldarrain, M. Á., & Ibarretxe-Bilbao, N. (2016). Altered functional connectivity in the default mode network is associated with cognitive impairment and brain anatomical changes in Parkinson's disease. Parkinsonism & Related Disorders, 33, 58–64. https://doi.org/10.1016/j.parkreldis.2016.09.012

Maidan, I., Hacham, R., Galperin, I., Giladi, N., Holtzer, R., Hausdorff, J. M., & Mirelman, A. (2022). Neural Variability in the Prefrontal Cortex as a Reflection of Neural Flexibility and Stability in Patients With Parkinson Disease. Neurology, 98(8), e839–e847. https://doi.org/10.1212/WNL.0000000000013217

Margulies, D. S., Ghosh, S. S., Goulas, A., Falkiewicz, M., Huntenburg, J. M., Langs, G., Bezgin, G., Eickhoff, S. B., Castellanos, F. X., Petrides, M., Jefferies, E., & Smallwood, J. (2016). Situating the default-mode network along a principal gradient of macroscale cortical organization. Proceedings of the National Academy of Sciences, 113(44), 12574–12579. https://doi.org/10.1073/pnas.1608282113

Markello, R. D., Hansen, J. Y., Liu, Z.-Q., Bazinet, V., Shafiei, G., Suárez, L. E., Blostein, N., Seidlitz, J., Baillet, S., Satterthwaite, T. D., Chakravarty, M. M., Raznahan, A., & Misic, B. (2022). neuromaps: Structural and functional interpretation of brain maps. Nature Methods, 19(11), Article 11. https://doi.org/10.1038/s41592-022-01625-w

Markello, R. D., & Misic, B. (2021). Comparing spatial null models for brain maps. NeuroImage, 236, 118052. https://doi.org/10.1016/j.neuroimage.2021.118052

Narayanan, N. S., Rodnitzky, R. L., & Uc, E. Y. (2013). Prefrontal dopamine signaling and cognitive symptoms of Parkinson's disease. Reviews in the Neurosciences, 24(3). https://doi.org/10.1515/revneuro-2013-0004

Niso, G., Rogers, C., Moreau, J. T., Chen, L.-Y., Madjar, C., Das, S., Bock, E., Tadel, F., Evans, A. C., Jolicoeur, P., & Baillet, S. (2016). OMEGA: The Open MEG Archive. NeuroImage, 124, 1182–1187. https://doi.org/10.1016/j.neuroimage.2015.04.028

Nomi, J. S., Bolt, T. S., Ezie, C. E. C., Uddin, L. Q., & Heller, A. S. (2017). Moment-to-Moment BOLD Signal Variability Reflects Regional Changes in Neural Flexibility across the Lifespan. Journal of Neuroscience, 37(22), 5539–5548. https://doi.org/10.1523/JNEUROSCI.3408-16.2017

Olde Dubbelink, K. T. E., Stoffers, D., Deijen, J. B., Twisk, J. W. R., Stam, C. J., & Berendse, H. W. (2013). Cognitive decline in Parkinson's disease is associated with slowing of resting-state brain activity: A longitudinal study. Neurobiology of Aging, 34(2), Article 2. https://doi.org/10.1016/j.neurobiolaging.2012.02.029

Oswal, A., Brown, P., & Litvak, V. (2013). Synchronized neural oscillations and the pathophysiology of Parkinson's disease: Current Opinion in Neurology, 26(6), 662–670. https://doi.org/10.1097/WCO.0000000000000034

Parker, K. L., Chen, K.-H., Kingyon, J. R., Cavanagh, J. F., & Narayanan, N. S. (2014). D1-Dependent 4 Hz Oscillations and Ramping Activity in Rodent Medial Frontal Cortex during Interval Timing. The Journal of Neuroscience, 34(50), 16774–16783. https://doi.org/10.1523/JNEUROSCI.2772-14.2014

Parker, K. L., Chen, K.-H., Kingyon, J. R., Cavanagh, J. F., & Narayanan, N. S. (2015). Medial frontal ∼4-Hz activity in humans and rodents is attenuated in PD patients and in rodents with cortical dopamine depletion. Journal of Neurophysiology, 114(2), 1310–1320. https://doi.org/10.1152/jn.00412.2015

Pereira, J. B., Svenningsson, P., Weintraub, D., Brønnick, K., Lebedev, A., Westman, E., & Aarsland, D. (2014). Initial cognitive decline is associated with cortical thinning in early Parkinson disease. Neurology, 82(22), 2017–2025. https://doi.org/10.1212/WNL.0000000000000483

Poewe, W., Seppi, K., Tanner, C. M., Halliday, G. M., Brundin, P., Volkmann, J., Schrag, A.-E., & Lang, A. E. (2017). Parkinson disease. Nature Reviews Disease Primers, 3(1), Article 1. https://doi.org/10.1038/nrdp.2017.13

R Core Team. (2022). R: A Language and Environment for Statistical Computing. R Foundation for Statistical Computing. https://www.R-project.org/

Rosenberg, M. D., Finn, E. S., Scheinost, D., Constable, R. T., & Chun, M. M. (2017a). Characterizing Attention with Predictive Network Models. Trends in Cognitive Sciences, 21(4), 290–302. https://doi.org/10.1016/j.tics.2017.01.011

Rosenberg, M. D., Finn, E. S., Scheinost, D., Constable, R. T., & Chun, M. M. (2017b). Characterizing Attention with Predictive Network Models. Trends in Cognitive Sciences, 21(4), Article 4. https://doi.org/10.1016/j.tics.2017.01.011

Ruppert, M. C., Greuel, A., Freigang, J., Tahmasian, M., Maier, F., Hammes, J., van Eimeren, T., Timmermann, L., Tittgemeyer, M., Drzezga, A., & Eggers, C. (2021). The default mode network and cognition in Parkinson's disease: A multimodal resting-state network approach. Human Brain Mapping, 42(8), 2623–2641. https://doi.org/10.1002/hbm.25393

Sareen, E., Zahar, S., Ville, D. V. D., Gupta, A., Griffa, A., & Amico, E. (2021). Exploring MEG brain fingerprints: Evaluation, pitfalls, and interpretations. NeuroImage, 240, 118331. https://doi.org/10.1016/j.neuroimage.2021.118331

Shafiei, G., Baillet, S., & Misic, B. (2022). Human electromagnetic and haemodynamic networks systematically converge in unimodal cortex and diverge in transmodal cortex. PLoS Biology, 20(8), e3001735. https://doi.org/10.1371/journal.pbio.3001735

Shrout, P. E., & Fleiss, J. L. (1979). Intraclass correlations: Uses in assessing rater reliability. Psychological Bulletin, 86(2), 420–428. https://doi.org/10.1037/0033-2909.86.2.420

Singh, A., Cole, R. C., Espinoza, A. I., Evans, A., Cao, S., Cavanagh, J. F., & Narayanan, N. S. (2021). Timing variability and midfrontal ~4 Hz rhythms correlate with cognition in Parkinson's disease. Npj Parkinson's Disease, 7(1), 14. https://doi.org/10.1038/s41531-021-00158-x

Singh, A., Richardson, S. P., Narayanan, N., & Cavanagh, J. F. (2018a). Mid-frontal theta activity is diminished during cognitive control in Parkinson's disease. Neuropsychologia, 117, 113–122. https://doi.org/10.1016/j.neuropsychologia.2018.05.020

Singh, A., Richardson, S. P., Narayanan, N., & Cavanagh, J. F. (2018b). Mid-frontal theta activity is diminished during cognitive control in Parkinson's disease. Neuropsychologia, 117, 113–122. https://doi.org/10.1016/j.neuropsychologia.2018.05.020

Sorrentino, P., Rucco, R., Lardone, A., Liparoti, M., Troisi Lopez, E., Cavaliere, C., Soricelli, A., Jirsa, V., Sorrentino, G., & Amico, E. (2021). Clinical connectome fingerprints of cognitive decline. NeuroImage, 238, 118253. https://doi.org/10.1016/j.neuroimage.2021.118253

Stoffers, D., Bosboom, J. L. W., Deijen, J. B., Wolters, E. C., Berendse, H. W., & Stam, C. J. (2007). Slowing of oscillatory brain activity is a stable characteristic of Parkinson's disease without dementia. Brain, 130(7), 1847–1860. https://doi.org/10.1093/brain/awm034

Stoffers, D., Bosboom, J. L. W., Wolters, E. Ch., Stam, C. J., & Berendse, H. W. (2008). Dopaminergic modulation of cortico-cortical functional connectivity in Parkinson's disease: An MEG study. Experimental Neurology, 213(1), 191–195. https://doi.org/10.1016/j.expneurol.2008.05.021

Tadel, F., Baillet, S., Mosher, J. C., Pantazis, D., & Leahy, R. M. (2011). Brainstorm: A User-Friendly Application for MEG/EEG Analysis. Computational Intelligence and Neuroscience, 2011, 1–13. https://doi.org/10.1155/2011/879716

Taylor, J. R., Williams, N., Cusack, R., Auer, T., Shafto, M. A., Dixon, M., Tyler, L. K., Cam-CAN, & Henson, R. N. (2017). The Cambridge Centre for Ageing and Neuroscience (Cam-CAN) data repository: Structural and functional MRI, MEG, and cognitive data from a cross-sectional adult lifespan sample. NeuroImage, 144, 262–269. https://doi.org/10.1016/j.neuroimage.2015.09.018

Tessitore, A., Esposito, F., Vitale, C., Santangelo, G., Amboni, M., Russo, A., Corbo, D., Cirillo, G., Barone, P., & Tedeschi, G. (2012). Default-mode network connectivity in cognitively unimpaired patients with Parkinson disease. Neurology, 79(23), 2226–2232. https://doi.org/10.1212/WNL.0b013e31827689d6

Tinkhauser, G., Pogosyan, A., Tan, H., Herz, D. M., Kühn, A. A., & Brown, P. (2017). Beta burst dynamics in Parkinson's disease OFF and ON dopaminergic medication. Brain: A Journal of Neurology, 140(11), 2968–2981. https://doi.org/10.1093/brain/awx252

Torrecillos, F., Tinkhauser, G., Fischer, P., Green, A. L., Aziz, T. Z., Foltynie, T., Limousin, P., Zrinzo, L., Ashkan, K., Brown, P., & Tan, H. (2018). Modulation of Beta Bursts in the Subthalamic Nucleus Predicts Motor Performance. The Journal of Neuroscience: The Official Journal of

the Society for Neuroscience, 38(41), 8905–8917. https://doi.org/10.1523/JNEUROSCI.1314-18.2018

Tremblay-Mercier, J., Madjar, C., Das, S., Pichet Binette, A., Dyke, S. O. M., Étienne, P., Lafaille-Magnan, M.-E., Remz, J., Bellec, P., Louis Collins, D., Natasha Rajah, M., Bohbot, V., Leoutsakos, J.-M., Iturria-Medina, Y., Kat, J., Hoge, R. D., Gauthier, S., Tardif, C. L., Mallar Chakravarty, M., … Breitner, J. C. S. (2021). Open science datasets from PREVENT-AD, a longitudinal cohort of pre-symptomatic Alzheimer's disease. NeuroImage: Clinical, 31, 102733. https://doi.org/10.1016/j.nicl.2021.102733

Troisi Lopez, E., Minino, R., Liparoti, M., Polverino, A., Romano, A., De Micco, R., Lucidi, F., Tessitore, A., Amico, E., Sorrentino, G., Jirsa, V., & Sorrentino, P. (2023). Fading of brain network fingerprint in Parkinson's disease predicts motor clinical impairment. Human Brain Mapping, 44(3), 1239–1250. https://doi.org/10.1002/hbm.26156

Underwood, C. F., & Parr-Brownlie, L. C. (2021). Primary motor cortex in Parkinson's disease: Functional changes and opportunities for neurostimulation. Neurobiology of Disease, 147, 105159. https://doi.org/10.1016/j.nbd.2020.105159

van Eimeren, T., Monchi, O., Ballanger, B., & Strafella, A. P. (2009). Dysfunction of the Default Mode Network in Parkinson Disease: A Functional Magnetic Resonance Imaging Study. Archives of Neurology, 66(7), 877–883. https://doi.org/10.1001/archneurol.2009.97

Váša, F., & Mišić, B. (2022). Null models in network neuroscience. Nature Reviews Neuroscience, 23(8), 493–504. https://doi.org/10.1038/s41583-022-00601-9

Wiesman, A. I., Castanheira, J. da S., Degroot, C., Fon, E. A., Baillet, S., Group, P.-A. R., & Network, Q. P. (2022). A sagittal gradient of pathological and compensatory effects of neurophysiological slowing in Parkinson's disease (p. 2022.08.05.22278436). medRxiv. https://doi.org/10.1101/2022.08.05.22278436

Wiesman, A. I., da Silva Castanheira, J., & Baillet, S. (2022). Stability of spectral estimates in resting-state magnetoencephalography: Recommendations for minimal data duration with neuroanatomical specificity. NeuroImage, 247, 118823. https://doi.org/10.1016/j.neuroimage.2021.118823

Wiesman, A. I., da Silva Castanheira, J., Degroot, C., Fon, E. A., Baillet, S., & Network, Q. P. (2023). Adverse and compensatory neurophysiological slowing in Parkinson's disease. Progress in Neurobiology, 231, 102538. https://doi.org/10.1016/j.pneurobio.2023.102538

Wiesman, A. I., Donhauser, P. W., Degroot, C., Diab, S., Kousaie, S., Fon, E. A., Klein, D., & Baillet, S. (2023). Aberrant neurophysiological signaling associated with speech impairments in Parkinson's disease. Npj Parkinson's Disease, 9(1), Article 1. https://doi.org/10.1038/s41531-023-00495-z

Wilson, H., Niccolini, F., Pellicano, C., & Politis, M. (2019). Cortical thinning across Parkinson's disease stages and clinical correlates. Journal of the Neurological Sciences, 398, 31–38. https://doi.org/10.1016/j.jns.2019.01.020

Wilson, L. E., da Silva Castanheira, J., & Baillet, S. (2022). Time-resolved parameterization of aperiodic and periodic brain activity. eLife, 11, e77348. https://doi.org/10.7554/eLife.77348

Yu, Y., Escobar Sanabria, D., Wang, J., Hendrix, C. M., Zhang, J., Nebeck, S. D., Amundson, A. M., Busby, Z. B., Bauer, D. L., Johnson, M. D., Johnson, L. A., & Vitek, J. L. (2021). Parkinsonism Alters Beta Burst Dynamics across the Basal Ganglia-Motor Cortical Network. The Journal of Neuroscience: The Official Journal of the Society for Neuroscience, 41(10), 2274–2286. https://doi.org/10.1523/JNEUROSCI.1591-20.2021

Zhu, H., Huang, J., Deng, L., He, N., Cheng, L., Shu, P., Yan, F., Tong, S., Sun, J., & Ling, H. (2019). Abnormal Dynamic Functional Connectivity Associated With Subcortical Networks in Parkinson's Disease: A Temporal Variability Perspective. Frontiers in Neuroscience, 13. https://www.frontiersin.org/articles/10.3389/fnins.2019.00080

# Chapter 5

# Heritable traits of brain electrophysiology for individual differentiation

## Preface

The previous chapters explored how the spatial distribution of neurophysiological spectral signal power differentiates individuals across healthy and clinical populations. Yet, whether the salient spectral features characteristic of individuals are similarly heritable remains unexplored. In this Chapter, I use a combination of twin study and brain-fingerprinting methodology to explore the genetic and micro-scale correlates of electrophysiological brain-fingerprints. I demonstrated that the most salient features for participant differentiation are similarly heritable and differentiate monozygotic twin pairs. I further explored how differentiable electrophysiological brain activity covaries with ventromedial-to-dorsolateral cortical gradient of gene expression. The results presented within this chapter shed light on the micro-scale biological factors that underlie person-specific spectral brain activity.

The manuscript is being prepared for submission as:

da Silva Castanheira, J., Poli, J., et al. Heritable traits of brain electrophysiology for individual differentiation. (2023).

## Abstract

The significant diversity in personality traits and behaviours is, at least in part, reflected in the brain activity of every individual. Previous research has demonstrated the ability of brain-

fingerprints, derived from either neuroimaging or electrophysiological data, to differentiate individuals from one another and predict behaviours. In this study, our objective was to determine the extent to which electrophysiological brain-fingerprints are heritable and to identify how they relate to cortical gene expression. To achieve this, we used task-free brain activity data using magnetoencephalography from a cohort of 89 participants, including 17 pairs of monozygotic twins and 11 pairs of dizygotic twins. Our findings revealed that the brain-fingerprints of monozygotic twins are remarkably more similar than dizygotic twins, suggesting the importance of genetics in shaping electrophysiological brain-fingerprints. Furthermore, our investigation unveiled that the most differentiable features of brain-fingerprints are heritable. We found that differentiable electrophysiological brain activity covaries with ventromedial-to-dorsolateral cortical gradient of gene expression enriched for ion transport genes, which is predominantly expressed in neurons. This signature becomes more pronounced throughout neurodevelopment. In sum, our results shed light on the micro-scale biological factors that underlie variations in neurophysiology among individuals. These findings pave the way for future research that can establish connections between genetic variation, brain activity, and behaviour.

Keywords: neural oscillations, individual differences, magnetoencephalography, brain fingerprinting, heritability, gene expression

Lay summary:

Human behavior and personality traits exhibit considerable diversity, yet the underlying biological causes responsible for these variations continue to be a subject of ongoing scientific investigation. Recent advancements in neuroscience have proposed that task-free brain activity is characteristic of individuals, much like a fingerprint. However, the connection between these brain-fingerprints and genetics remains poorly understood. This study aimed to assess the extent to which genetics contribute to the formation of these brain-fingerprints. The research findings indicate that monozygotic twins, who share approximately 100% of their genes, have remarkably similar brain-fingerprints unlike dizygotic twins, who share only 50% of their genes. The authors demonstrate that the most distinctive brain activity, which enables the differentiation of

individuals, is associated with a cortical gradient of gene expression. Notably, genes associated with the electrical signalling between neurons play a crucial role in this gene-differentiation relationship. Furthermore, the identified gene signature becomes more pronounced throughout neurodevelopment. Collectively, this research not only quantifies the significance of genetics in shaping the unique brain activity of individuals but also introduces a novel framework for understanding the biological basis of behavioural variations among individuals.

## Introduction

Personality traits and complex behaviours are expressed with considerable diversity between individuals (da Silva Castanheira et al., 2021; Dubois & Adolphs, 2016; Finn et al., 2015a; *APA Handbook of Personality and Social Psychology, Volume 4*, 2015; Van Horn et al., 2008; Waschke, Kloosterman, et al., 2021). Integrative neuroscience is actively engaged in the endeavour to link brain structure and brain activity with individual traits, employing increasingly sophisticated methods and larger, more diverse datasets (Amico & Goñi, 2018a; da Silva Castanheira et al., 2021; Finn et al., 2015a; Niso et al., 2016a; Taylor et al., 2017; Van Essen et al., 2012). Within this context, a pivotal, yet unanswered question is the extent to which genetics contribute to inter-individual variations in electrophysiological brain activity and how these variations manifest as diverse behaviours.

To investigate the genetic contribution to phenotypic variability, researchers have computed heritability measures of brain structure, function, and behaviours (Falconer, 1965). Several large-scale imaging consortia have consistently reported that brain structure is heritable (Lee et al., 2016; Pizzagalli et al., 2020; Posthuma et al., 2005; Schmitt et al., 2020). Moreover, research has shown that regional gene expression can predict the functional connectivity between distinct cortical regions (Betzel et al., 2019, 2019; Fulcher et al., 2019; Hansen et al., 2021; Richiardi et al., 2015).

In the realm of electrophysiology, brain rhythms have also been identified as heritable phenotypes (De Gennaro et al., 2008; Hodgkinson et al., 2010; Malone et al., 2014; Markovic et al., 2018; Salmela et al., 2016; C. M. Smit et al., 2006; D. J. A. Smit et al., 2005; Zietsch et al., 2007), with alpha power and peak frequency (8-12 Hz) being one of the most consistently

reported heritable brain rhythm (Salmela et al., 2016; C. M. Smit et al., 2006; Zietsch et al., 2007). Concerning behaviour, cognitive abilities, especially in domains such as attention, reading, and intelligence test performance, are recognized as highly heritable traits, with genetic factors accounting for up to 50% of their variability(Bouchard & McGue, 2003; Haworth et al., 2010; Mollon et al., 2021; R. A. Power & Pluess, 2015; Zwir et al., 2020).

Together this body of work demonstrates that phenotypes and individual behaviours are influenced by genetics to different degrees. However, the precise relationship between heritable brain phenotypes, and individual differences in brain activity remains a topic of inquiry. To what extent are heritable brain phenotypes characteristic of individuals?

A body of research has collectively demonstrated that features of both task-related and task-free brain activity are unique to each individual, often described metaphorically as brain-fingerprints (Amico & Goñi, 2018a; da Silva Castanheira et al., 2021; Finn et al., 2015a; Sareen et al., 2021a). Brain-fingerprints are unique to individuals, relate to individual cognitive abilities, including attention and intelligence test performance (Finn et al., 2015a; Rosenberg et al., 2017a; Rosenberg, Scheinost, et al., 2020; Yamashita et al., 2018), and have been reported to be altered by disease (da Silva Castanheira et al., 2023; Kaufmann et al., 2017a, 2018a; Sorrentino et al., 2021c; Troisi Lopez et al., 2023). Consequently, we aimed to investigate the role of genetics in shaping brain phenotypes characteristic of individuals.

Our hypotheses revolved around the notions that MZ twins can be more accurately distinguished from their siblings based on their brain-fingerprints than DZ twin pairs and that prominent features contributing to individual differentiation are associated with heritable brain phenotypes.

To this end, we utilized a combination of twin-study (Mayhew & Meyre, 2017) and brain-fingerprinting methodologies. If a phenotype is influenced by genetics, the similarity between monozygotic twins (MZ), who share approximately 100% of their genes, should be more pronounced than that of dizygotic twins (DZ), who share only about 50% of their genes. We hypothesized that if genetics contribute to variation in brain-fingerprints, then MZ twins can be more accurately distinguished (i.e., matched) based on their sibling's brain-fingerprint than DZ twin pairs. In addition, we predicted that the distinctive brain phenotype features contributing to

individual differentiation would similarly be heritable. In our final analysis, we sought to bridge macroscale inter-individual differences in neurophysiological brain activity with microscale neural gene expression gradients. Here, we characterized how differentiable neurophysiological brain activity relates to cortical gene expression, and brain activation patterns of psychological-processes. In this manner, our study triangulates cortical gene expression, inter-individual differences in brain activity, and brain activations of psychological processes, to explore the biological underpinnings of inter-individual variability.

# Results

We used task-free magnetoencephalography recordings available from the Human Connectome Project (Van Essen et al., 2012). Three approximately 6-minute recordings were used for each of the 89 individuals (17 pairs of monozygotic twins, 11 pairs of dizygotic twins, and 33 unrelated individuals) to derive anatomically specific brain-fingerprints. Brain-fingerprints consisted of frequency-specific power spectra density (PSD) estimates within each parcel of the Schaefer 200 7-network atlas (see Methods and Figure 1a).

## Brain-fingerprints differentiate Monozygotic twin pairs

The brain-fingerprinting procedure consisted of assessing the similarity between the cortical spectral features derived from the three datasets from the same individual. If a participant's brain-fingerprint from the first dataset was most similar to their second dataset, the individual would be considered correctly differentiated. We bootstrapped differentiation accuracy to obtain confidence intervals (see Methods). We derived broadband (1-150Hz) and narrow-band brain-fingerprints based on the six canonical neurophysiological bands: delta (1–4 Hz), theta (4–8 Hz), alpha (8–13 Hz), beta (13–30 Hz), gamma (30–50 Hz), and high gamma (50–150 Hz). Note we repeated this procedure for all pairs of recordings and reported the mean accuracy (see Methods for details).

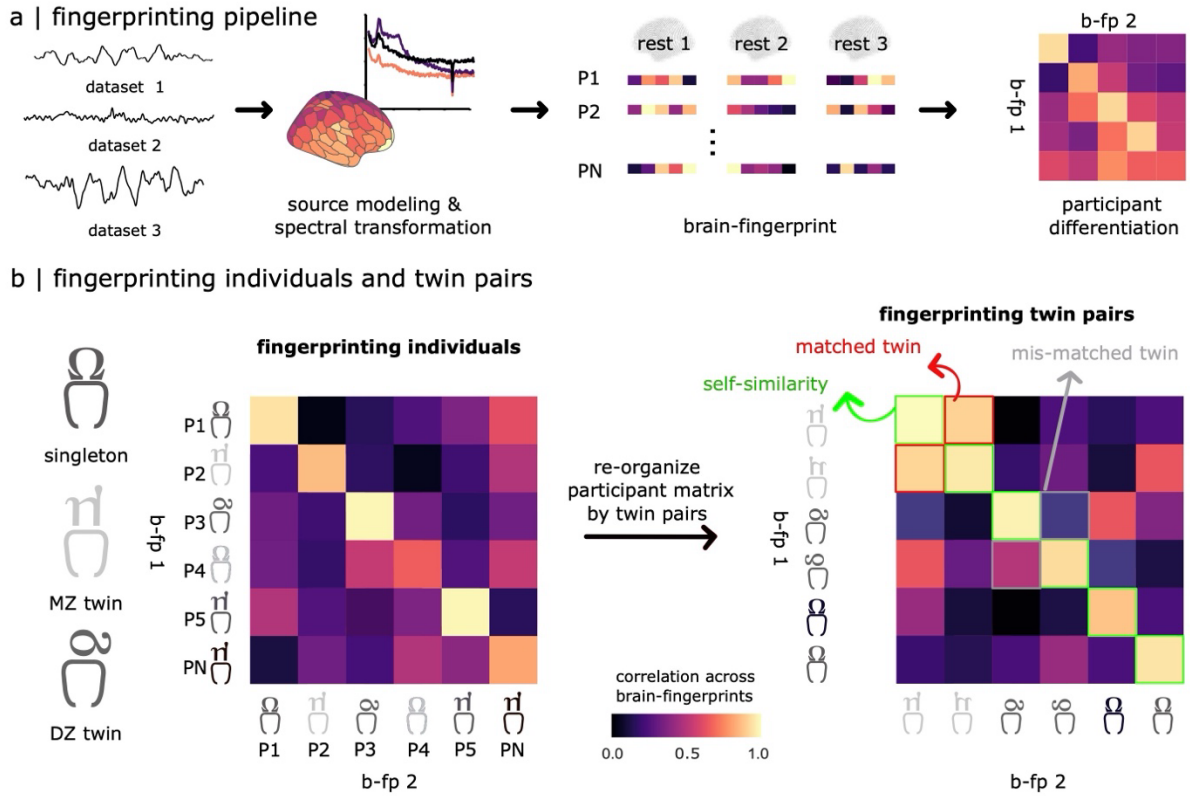


Chapter 5 Figure 1 Spectral brain-fingerprinting pipeline and study design.

(a) The spectral power of MEG source time series is estimated from each parcel of the Schaefer 200 7-network atlas, from each recording (dataset 1,2 and 3) for all participants. The resulting power spectra define the three spectral brain-fingerprints for each individual (e.g., b-fp 1 and b-fp 2). A confusion matrix of the self- and other similarity between participants' brain-fingerprints determines their respective differentiation. (b) We used the resulting spectral brain-fingerprints to differentiate i) between singletons (i.e., individual differentiation). We similarly used brain-fingerprints to match ii) MZ twin pairs, and iii) DZ twin pairs. A participant who is correctly differentiated from the cohort has a higher self-similarity of brain-fingerprints than other-similarity. A correctly matched twin pair shows greater similarity to their sibling than to all other individuals in the cohort.

The brain-fingerprint differentiation accuracy for all participants using broadband neurophysiological signals was 83.4% ([73.8, 90.0] 95% CI). Individual differentiation accuracy

varied across frequency bands: differentiation accuracy was highest for the high gamma band 87.4% ([80.0, 92.5] 95% CI), and lowest for the delta band 59.7% ([57.5, 73.8] 95% CI; Figure 2a).

We assessed whether we could differentiate (i.e., match) twin pairs from their sibling's brain phenotype. Here, we compared the similarity of brain-fingerprints across twins, i.e., was the brain-fingerprint of *twin i* most similar to that of *twin ii*, ignoring the self-similarity of participants (see Methods and Figure 1b). We matched MZ twin pairs with 61.5% ([46.7, 76.7] 95% CI) accuracy. In contrast, we failed to match DZ twins from their sibling's brain-fingerprint (5.2% [0.0, 15.0] 95% CI; See Figure 2a). We repeated this twin differentiation procedure for each electrophysiological narrow band.

In line with previous literature, we observed the largest decrease in twin-pair matching accuracy between MZ and DZ twins in the alpha (MZ 47.8% [33.3, 66.7] 95% CI; DZ 1.2% [0.0, 5.0] 95% CI) and beta band (MZ 52.1% [33.3, 70.0] 95% CI; DZ 7.1% [0.0, 20.0] 95% CI) indicating that the brain-fingerprints derived from these bands are heritable. High gamma brain-fingerprints showed the smallest difference between MZ and DZ twin-pair matching (MZ 19.9% [10.0, 36.7] 95% CI; DZ 16.4% [10.0, 25.0] 95% CI; see Figure 2a).

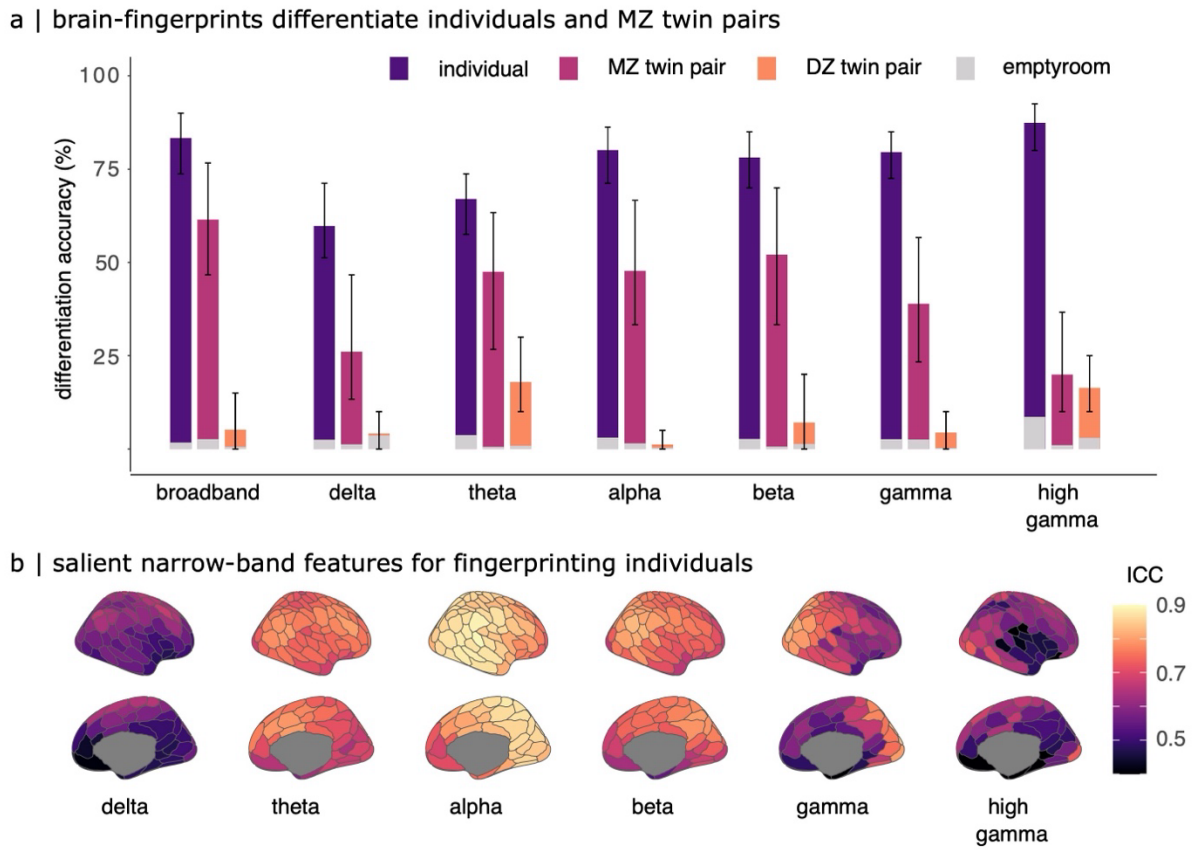


Chapter 5 Figure 2 Spectral brain-fingerprinting differentiate individuals and MZ twin pairs.

(a) Differentiation accuracy using broadband and narrow-band spectral brain-fingerprints derived from ~5-min data lengths. Purple bars represent the accuracy for differentiating all individuals, magenta and orange bars represent the accuracy for matching MZ and DZ twins from their sibling's brain fingerprint, respectively. The error bars show bootstrapped 95% confidence intervals. The grey segments at the foot of each bar plot indicate the null differentiation accuracy obtained from empty-room MEG recordings. (b) Topographic brain maps of the most salient features for differentiating all individuals (ICC) for each of the narrow bands. High values for ICC represent important features for individual differentiation.

## The most salient features of the brain-fingerprint are heritable

To identify the most salient brain phenotypes for individual differentiation, we used intra-class correlations (ICC) (Amico & Goñi, 2018a; da Silva Castanheira et al., 2021, 2023). We bootstrapped individuals such that only one sibling was present in the bootstrapped sample. This

procedure eliminated any potential sibling bias: In each bootstrapped sample all individuals were unrelated (see Methods). We report that the alpha, theta, and beta bands were the most salient features for individual differentiation (mean ICC across cortex: alpha = 0.83, theta= 0.74, beta= 0.74; Figure 2b). Notably, we observed the highest ICC among caudal and medial regions across bands, and the lowest ICC values in orbital frontal regions.

We then computed the heritability of these brain phenotypes using Falconer's method (see Methods). Heritability compares the similarity of MZ twin pairs on a phenotype to the similarity of DZ twin pairs—with higher values of heritability indicating that a variance in a phenotype is driven by genetics. We observed that neurophysiology in the alpha, theta, and beta, bands showed the highest heritability across the cortex (mean $H^2$: theta= 0.85, alpha= 0.76, and beta= 0.77). Neurophysiology of the lateral- temporal, lateral-frontal regions, and caudal regions showed the highest influence of genetics (see Figure 3a). Indeed, the visual Yeo-Krienen network (Yeo et al., 2011) showed the highest overall heritability score; this contrasts with the limbic network which showed the lowest influence of genetics (Figure 3a right).

Next, we examined the linear relationship between the salient brain-fingerprint features for individual differentiation and heritable brain phenotypes. We found a moderate positive correlation between broadband ICC brain-fingerprint features and the heritability of broadband neurophysiology of the region (r= 0.28, $p_{spin}$= 0.026; see Figure 3b & Figure S3). We similarly correlated narrow-band heritability and ICC brain-fingerprint brain maps. We observed strong positive spatial relationships in the alpha (r=0.62, $p_{spin}$= 0.0009) and beta bands (r=0.58, $p_{spin}$= 0.0009; see Figure 3b). While heritable regions in the gamma band were also important for participant differentiation (r=0.41, $p_{spin}$= 0.069), this relationship did not survive spatial auto-correlation correction. Taken together, these results indicate that salient features for differentiating individuals, also tend to be heritable—this is principally true for the alpha and beta bands.

Note we verified the robustness of our differentiation effects against common environmental and physiological artifacts (see Supplemental materials)

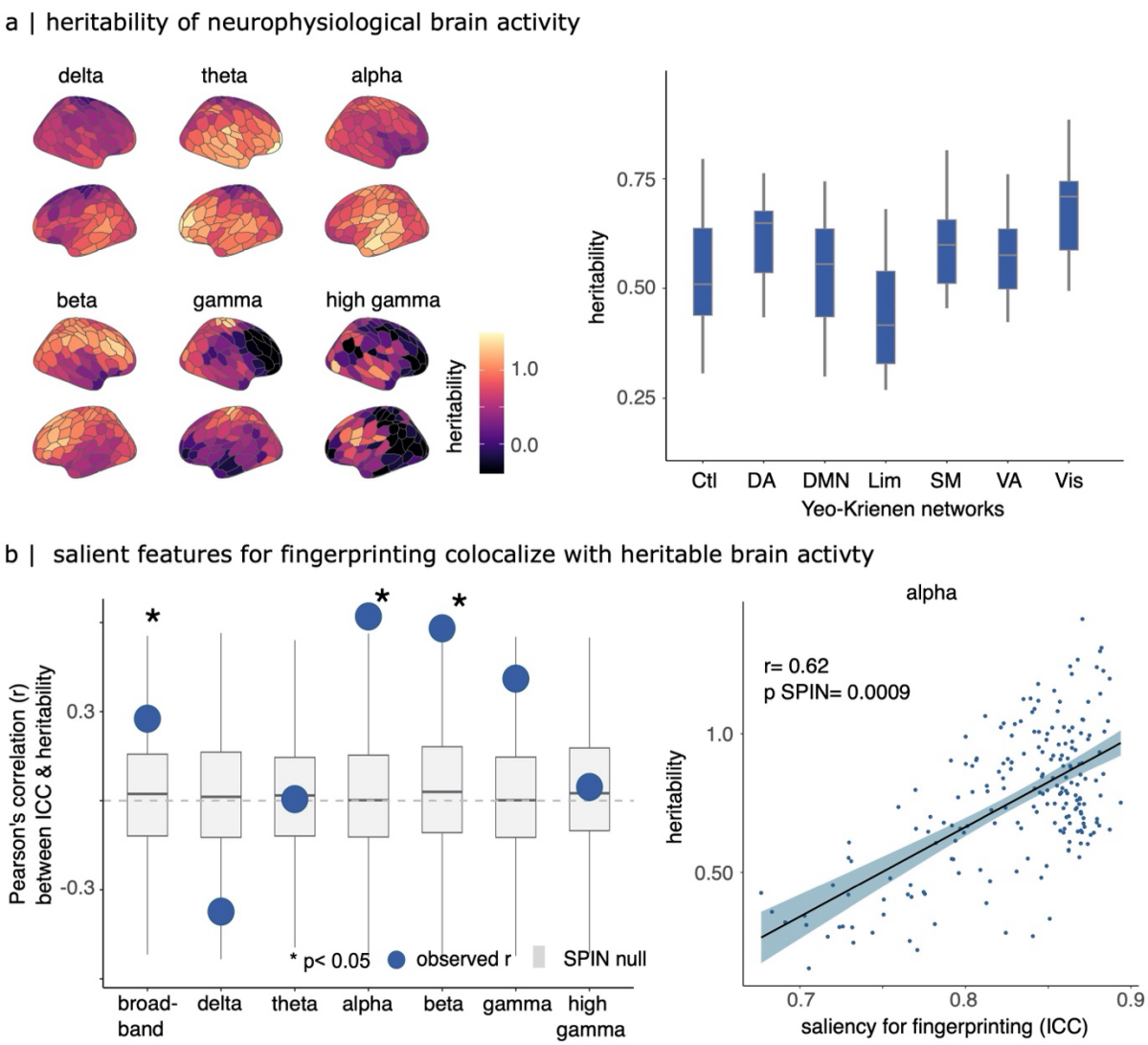


Chapter 5 Figure 3 Differentiable brain-fingerprint features are heritable.

(a) Left panel: topographic brain maps of the heritability of brain-phenotypes. High values of heritability represent brain-phenotypes under stronger genetic influence. Right panel: broadband brain-phenotype heritability scores organized by Yeo-Krienen 7 resting-state networks(Yeo et al., 2011). (b) Left panel: Linear relationship between salient features for participant differentiation and their heritability across each of the narrow bands. Points represent the strength of the correlation, and grey boxplots represent null relationship obtained from SPIN permutations. Right panel: Scatter plot of alpha heritability-differentiation relationship. Each point represents a region of the Schaefer atlas. Salient features for participant differentiation in the alpha band are linearly related to heritable broadband brain-phenotypes.

## Salient brain-fingerprint features covary along a gene expression gradient

Next, we investigated the relationship between participant differentiation and cortical gene expression using data obtained from the Allan Human Brain Atlas (ABHA) (M. J. Hawrylycz et al., 2012) in a Partial Least Squares (PLS) analysis. To facilitate the interpretation and comparison of our results with previous work, we focused our analyses on genes with a differential stability greater than 0.1 (see Methods) (Burt et al., 2018; Hansen et al., 2021; M. Hawrylycz et al., 2015; M. J. Hawrylycz et al., 2012; Markello et al., 2021).

PLS relates the covariance between two observed matrices—e.g., salient features for fingerprinting (regions by frequency bands) and gene expression (regions by genes)—using latent components (see Figure 4a). We observed a single statistically significant latent variable relating gene expression to salient features for fingerprinting (85.2% covariance explained, $P_{SPIN}$= 0.01, 95% CI = [73.4, 90.1]; Figure 4b left panel).

Each latent variable includes singular values (proportional to the amount of covariance explained), and weight patterns reflecting the relative importance of genes and frequency bands for individual differentiation. We computed scores and loadings to describe the significant multivariate pattern of covariance (i.e., the first latent variable) by multiplying the original gene expression matrix (regions by genes) with the gene weights of the first latent variable (genes by 1), and vice versa for salient features for fingerprinting. Gene and ICC brain scores indicate which brain regions exhibit the pattern of covariance described by the latent component. Brain regions with positive scores display covariance between positively loaded genes and frequency bands (refer to the paragraph below for a description of PLS loadings).

We observed a gradient from dorsolateral to ventromedial regions in both gene and ICC scores. The visual and somatomotor network exhibited the highest positive gene brain scores, covarying with broadband differentiable brain activity in the dorsal attention and somatomotor networks (Figure 4b). In contrast, the limbic network had the most negative brain score for both gene expression and ICC.

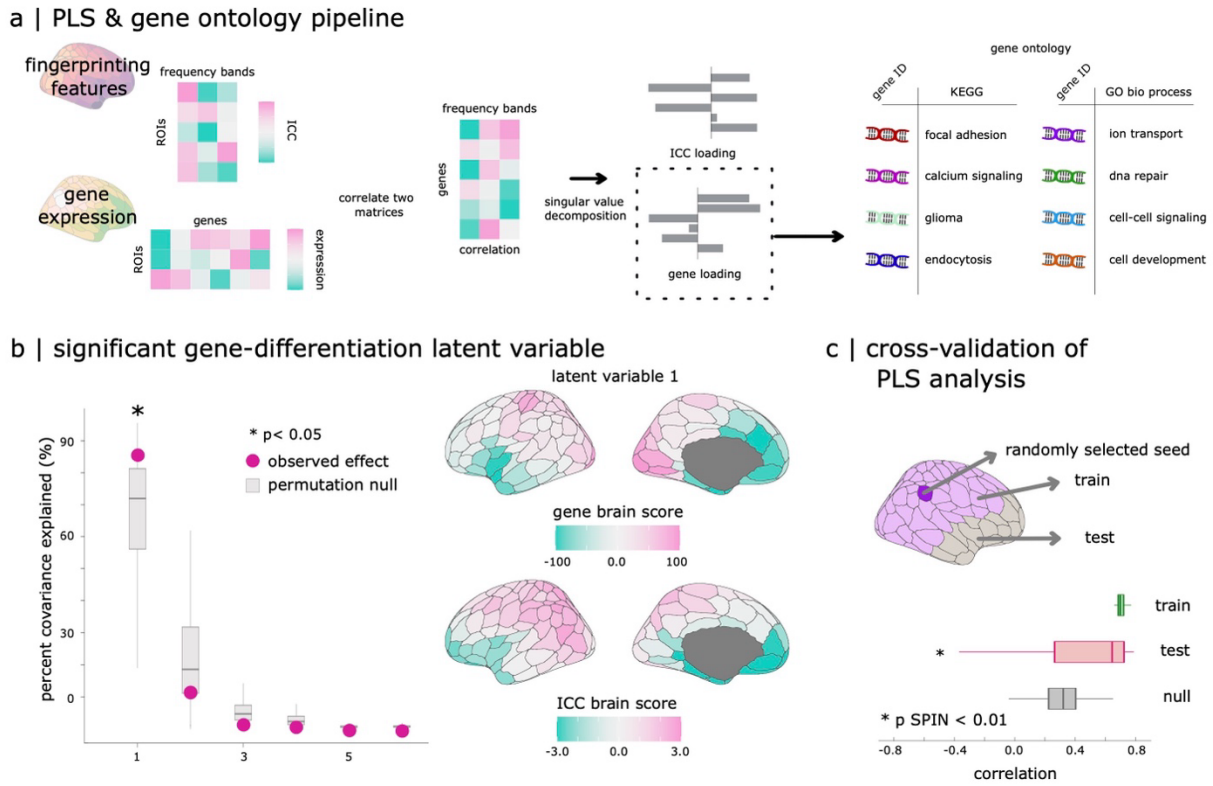


Chapter 5 Figure 4 Gene-differentiation PLS analysis pipeline and latent component.

(a) Analysis pipeline for PLS and gene ontology. Two data matrices were defined: i) one representing the most salient features for brain-fingerprinting and ii) a matrix of gene expression across each of the defined ROIs of the Schaefer atlas(Schaefer et al., 2018). PLS decomposes the covariance of these two matrices to describe latent components that reflect modes of highest covariance between the observed datasets. We then used the top loadings of the significant latent component to conduct a gene ontology analysis. Gene ontology analyses describe if the observed genes contributing to the latent component of the PLS are enriched for specific molecular processes. (b) Left panel: Latent components from the PLS analysis are ordered according to effect size and shown as pink points. Statistical significance of the latent components was computed by permuting the observed data (1000 permutations). The first latent component was the only statistically significant component after correction for spatial autocorrelation. Right panel: Topography of gene and ICC scores obtained by projecting the first latent component back onto the observed data. (c) Cross-validation of gene-differentiability PLS analysis by training the model with 75% of brain regions closest in Euclidean distance to a

randomly chosen source node (dark purple), and testing the relationship between gene and ICC scores. The median out-of-sample relationship was ($r= 0.64$, $p_{SPIN}= 0.002$).

To evaluate the relative contribution of each frequency and gene to the first significant latent component, we computed each item's loading (see Methods). Loadings were determined as the Pearson correlation between the brain map of gene expression and the opposite brain score pattern (e.g., correlate gene expression & ICC brain score) and vice versa. These loadings provided interpretable values ranging from-1 to 1, where larger absolute loadings indicate a higher correlation with the observed score pattern and a greater contribution to the observed latent pattern of covariance.

We observed that all differentiable features across frequency bands, with the exception of theta, contributed to the observed gene-differentiation latent component (see Figure 5a). Consequently, the observed gene-differentiation latent component reflects the capacity to differentiate between individuals from a wide range of frequencies. Note, that we did not observe any negative frequency loadings. We interpret this finding as follows: ventromedial brain areas, with negative ICC brain scores (Figure 4b middle), represent regions of poor individual neurophysiological differentiation that covary with the gene expression in the limbic network.

To validate our PLS analysis, we conducted a cross-validation process by randomly dividing brain regions into training and test sets. We randomly selected a seed region 100 times and picked the closest 75% of brain regions in Euclidean distance, leaving the remaining 25% out for validation. At each iteration, we computed Pearson's correlation between gene and ICC scores. We assessed the significance of the out-of-sample cross-validation using spatial auto-correlation correction (1,000 times). The median out-of-sample correlation between gene and ICC scores was r=0.64 (pSPIN= 0.002).

### Biological correlates of gene expression signature

We then aimed to gain insight into the genetic contribution of the latent component. We analogously computed loadings of each gene (see Methods). In summary, we divided genes into those with positive and negative loadings and identified the top 50% of genes within both the

positive and negative loading categories. This resulted in 2,272 genes contributing positively to the observed latent component and 2,280 negatively loaded genes.

Subsequently, we conducted a gene ontology analysis to quantify the biological processes associated with these sets of positively and negatively loaded genes. We utilized the ShinyGO analysis pipeline, which employs both the KEGG and GO biological process databases (Ge et al., 2020) (see Methods for details and Supplemental Data for a full list of biological processes). In brief, gene ontology analyses reveal which biological processes are enriched within a specified list of genes. We conducted separate gene ontology analyses for the genes with positive and negative loadings.

We present a selection of the significant biological processes from the gene ontology analyses in Figure 5b (see Supplemental Data for a complete list of biological processes). Genes with positive loadings, which covary with individual differentiation along the regions depicted in Figure 4b, were notably enriched for processes related to ion transportation, including potassium and sodium, cell signalling, and neurotransmitter transport (see Figure 5b right). Genes with negative loadings, which covary with low individual electrophysiological differentiation, were enriched for processes related to neurogenesis, and cell morphology. We provide the results of the KEGG gene ontology analyses in the supplement (see Supplemental Figure S4).

We then investigated whether the identified positive and negative gene lists were specifically expressed in certain cell types of the brain. To achieve this, we relied on gene sets previously identified as being preferentially expressed in seven distinct cell types based on postmortem single-cell and single-nucleus RNA sequencing studies (Darmanis et al., 2015; Habib et al., 2017; Lake et al., 2018; M. Li et al., 2018; McKenzie et al., 2018; Zhang et al., 2016). We computed the ratio of positively and negatively loaded genes in each cell-specific set including astrocytes, microglia, oligodendrocyte precursors (OPC), oligodendrocytes, endothelial cells, excitatory neurons, and inhibitory neurons (Figure 5b). The statistical significance of the cell-specific ratios was determined using permutation tests: We permuted genes 1,000 times to create null distributions of cell-specific ratios for positive and negative loaded genes (two-tailed; false discovery rate corrected). The results showed that positively loaded genes were preferentially expressed in excitatory ($p_{FDR}$ = 0.002) and inhibitory neurons ($p_{FDR}$ = 0.006) and

significantly under-expressed in astrocytes ($p_{FDR}$ = 0.002) and OPCs ($p_{FDR}$= 0.03). Conversely, negatively loaded genes were preferentially expressed in astrocytes ($p_{FDR}$ = 0.002), microglia ($p_{FDR}$ = 0.004), and oligodendrocytes ($p_{FDR}$ = 0.002), and significant under-expressed in OPCs ($p_{FDR}$ = 0.002). Taken together, these results corroborate that the identified positive gene expression signature is expressed in neurons, whereas genes that negatively covary with differentiation are expressed in neuron support cells like astrocytes and microglia.

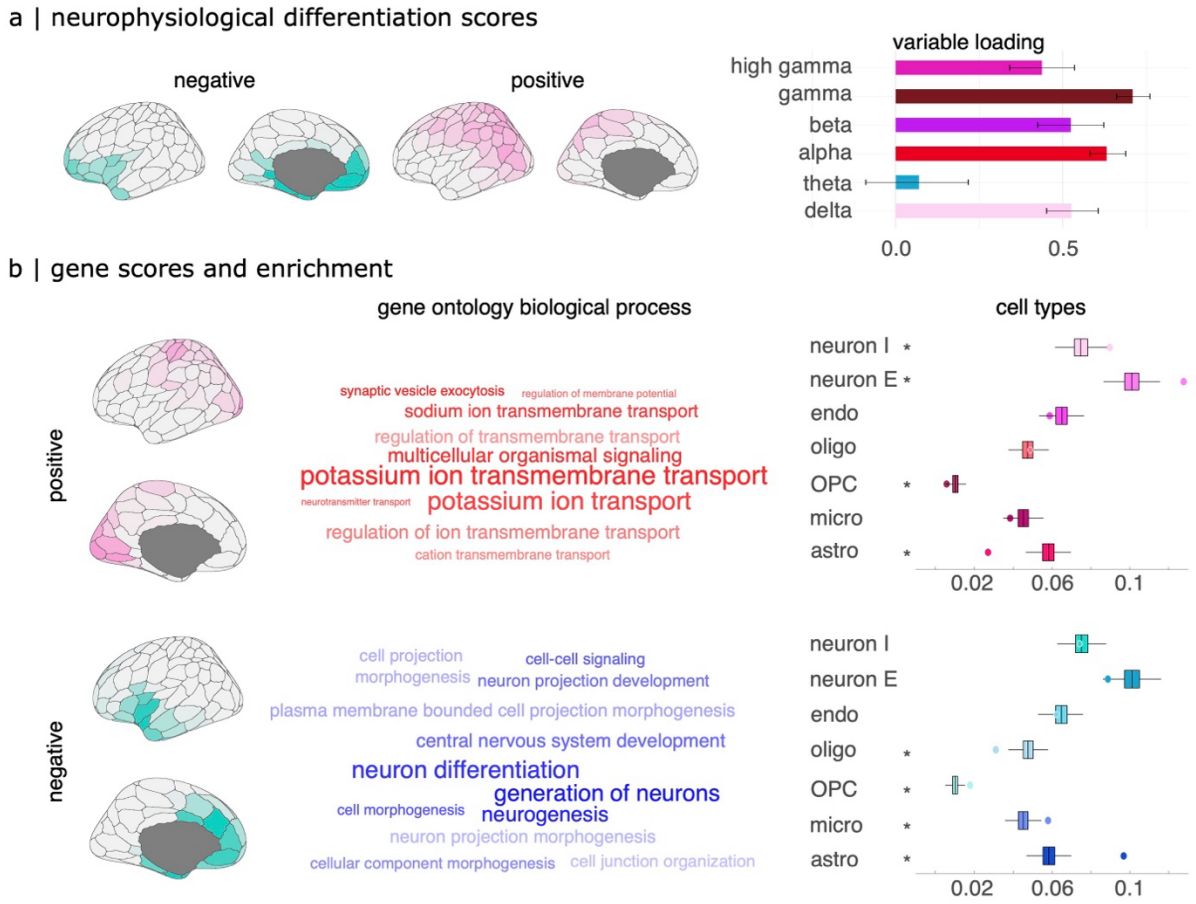


Chapter 5 Figure 5 Genes enriched for ion transporters and preferentially expressed in neurons covary with broadband neurophysiological differentiation.

(a) Differentiable neurophysiological features that contribute most to the latent component. Left panel: neurophysiological brain score pattern for positive and negative loadings. Right panel: frequency bands that contribute the most to the observed latent component. Brain scores reflect which brain regions demonstrate the observed pattern of covariance described by

the latent component. Loadings correspond to which variables contribute the most to the latent component. (b) Genes that contribute to the reported PLS latent component was assessed by computing loadings. Left panel: gene brain score pattern for positive and negative loadings. Molecular processes were inferred from the genes with the top 50% of positive (red) and negative (blue) loadings using a gene enrichment analysis (see Methods). Middle panel: Biological processes gene ontology analysis for positive and negative loadings. Word size and colour correspond to the relative importance of the term for the respective loadings. Right panel: Cell-type deconvolution analyses report the ratio of genes in each gene set (positive and negative) preferentially expressed in seven distinct cell types as defined by previous single-cell and single-nucleus RNA sequencing (Darmanis et al., 2015; Habib et al., 2017; Lake et al., 2018; M. Li et al., 2018; Seidlitz et al., 2020; Zhang et al., 2016). The significance of the ratios was determined based on permutation tests (* $p< 0.05$). Points represent observed ratios, box plots depict the ratios obtained from permuting gene sets.  Neuron I, inhibitory neurons; Neuron E, excitatory neurons; Endo, endothelial cells; Oligo, oligodendrocyte; OPC, oligodendrocyte precursor cell; Micro, microglia; Astro, astrocyte.

### Gene-differentiation gradient correlates with psychological processes

Having identified a gradient of gene expression that covaries with differentiable neurophysiological brain activity, we sought to contextualize our results with a previously reported gene expression-phycological processes gradient (Hansen et al., 2021). Hansen and colleagues reported that cortical gene expression covaries with brain activations related to specific psychological-processes (Hansen et al., 2021). They observed that brain activations associated with cognitive tasks like attention covary strongly with gene expression in dorsolateral cortexes. Previous work has argued that brain-fingerprints can predict individual differences in cognitive task performance. We therefore sought to assess the similarity between gene signatures overlap between brain gene expression patterns.

To accomplish this, we conducted a separate PLS analysis to assess the covariance between gene expression and probabilistic measures of brain activation (measured using fMRI) associated with psychological processes (e.g., attention, emotion, sleep). We observed a single

significant latent component that explained 67.2% of covariance (PSPIN= 0.002, 95% CI = [54.7, 72.2%), between gene expression and psychological processes. This component loaded negatively onto psychological processes associated with emotions, mood, and risk; and loaded positively onto terms associated with attention, planning, and multi-sensory processes (Figure 6a).

Next, we quantified the similarity between the identified gene-differentiability and the gene-psychological processes latent variables. We observed a strong significant correlation between the two gene brain scores (r=0.99, p spin< 0.001; see Figure 6b), and a strong linear relationship between both gene loadings (r= 0.99, p < 0.001; see Figure 6c). Note we verified that differentiability covaries with the identified psychological-processes signature in an independent PLS analysis (see Supplemental Information Psychological activations and differentiation PLS analysis). In summary, these results indicate that electrophysiological signals characteristic of individuals covaries with cognitive task brain activations and gene expression in caudal brain regions.

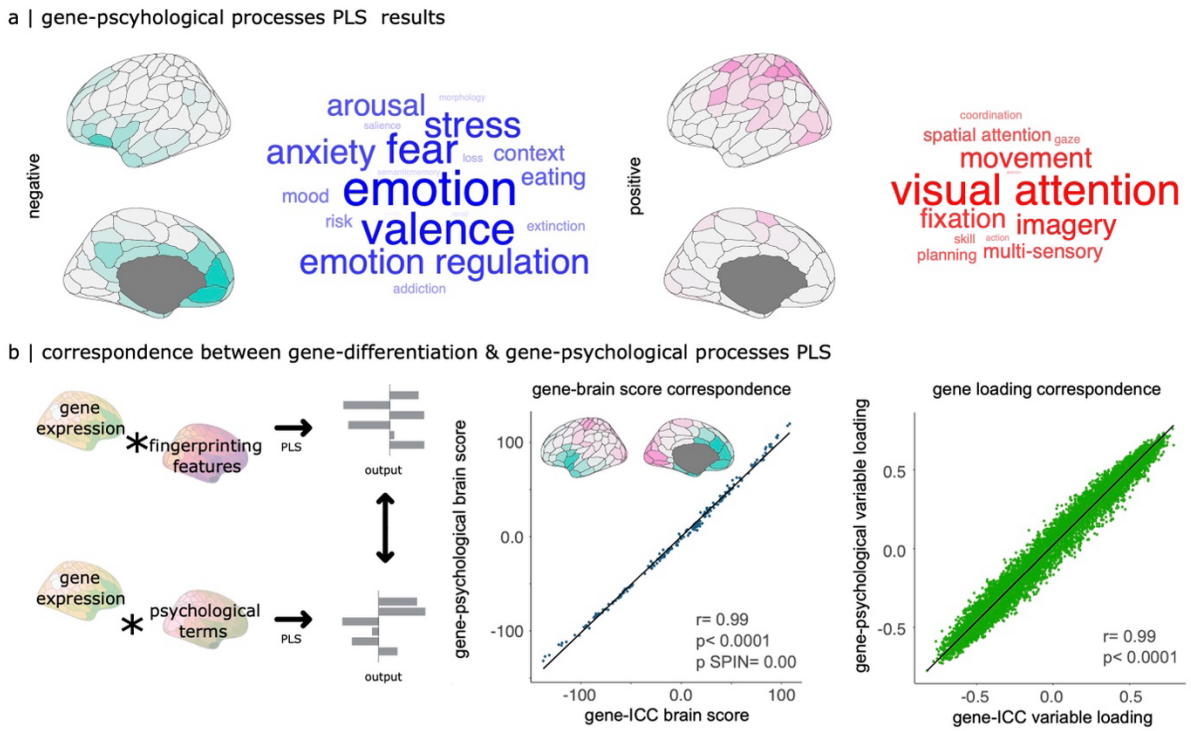


Chapter 5 Figure 6 Genes latent component covaries with psychological processes and neurophysiological differentiation.

(a) Psychological terms that contribute most to the gene-psychological processes PLS latent component. Brain map of psychological term brain score pattern for positive and negative loadings. Word size and colour correspond to relative importance of the term for the respective loadings. Terms with the top 25% most positively (red) and negatively (blue) loadings form a cognitive–affective gradient. (b) Correspondence between the gene-differentiation and gene-psychological process PLS analyses. Middle panel: scatter plot of gene brain scores for the two PLS analyses depicts a strong linear relationship between gene brain score patterns. Left panel: scatter plot of gene loadings for the genetic -psychological processes and -differentiation PLS analyses. Genes that loaded strongly onto the gene-behaviour PLS similarly contributed the most to the gene-differentiation PLS analysis.

### Gene-differentiation signature matures along neurodevelopment

Next, we explored the possibility that the identified gene signature is enriched for genes related to the cortical expansion of higher-order cognitive areas throughout human evolution (Driessens et al., 2023; Girskis et al., 2021; Guardiola-Ripoll & Fatjó-Vilas, 2023; Wei et al., 2019). We relied on human accelerated regions (HAR) of the genome to address this question. First, we found a significant overrepresentation of HAR-Brain genes (Wei et al., 2019) (see Supplemental data 2 Wei et al. 2019) in our identified gene signature ($p = 0.004$). Second, we examined the spatial relationship between the identified gene brain score and the topography of HAR brain gene expression. There was a negative relationship between local HAR gene expression and the identified gene brain score from the gene-differentiability PLS analysis ($r=-0.63$, $p_{spin}= 0.001$; Figure 7a).

Finally, we sought to quantify the neurodevelopmental trajectory of the identified gene signature, with the hypothesis that it would become more pronounced with neurodevelopmental maturation akin to cognitive abilities. To achieve this, we used data from BrainSpan which provides gene expression estimates from 16 cortical regions across neurodevelopment: from 8 weeks post-conception to 40 years old (J. A. Miller et al., 2014). First, we computed gene expression of the identified top 50% positive and negative loading genes across five life stages: fetal, infant, child, adolescent and adult (see Methods for details). We observed that positive

loading genes, covarying with participant differentiation, increased across development, whereas negative loading genes decreased across development (Figure 7b). We compared the trajectory of the positive and negative gene sets to a random set of genes (gray line Figure7b; see Methods for details). We then derived gene scores by projecting the BrainSpan data onto the previously defined gene weights from our PLS analysis for each cortical region separately (Figure 7c). The genetic signature, which covaries with participant differentiation, becomes more pronounced throughout neurodevelopment. We compared the linear trajectory (i.e., slope) of the defined gene score to that of 1,000 null models obtained from first randomly permuting the gene expression data used to compute the PLS before projecting the BrainSpan data. All cortical regions except for the hippocampus demonstrated a significant positive slope of gene scores (i.e., more pronounced with maturation; Figure 7c).

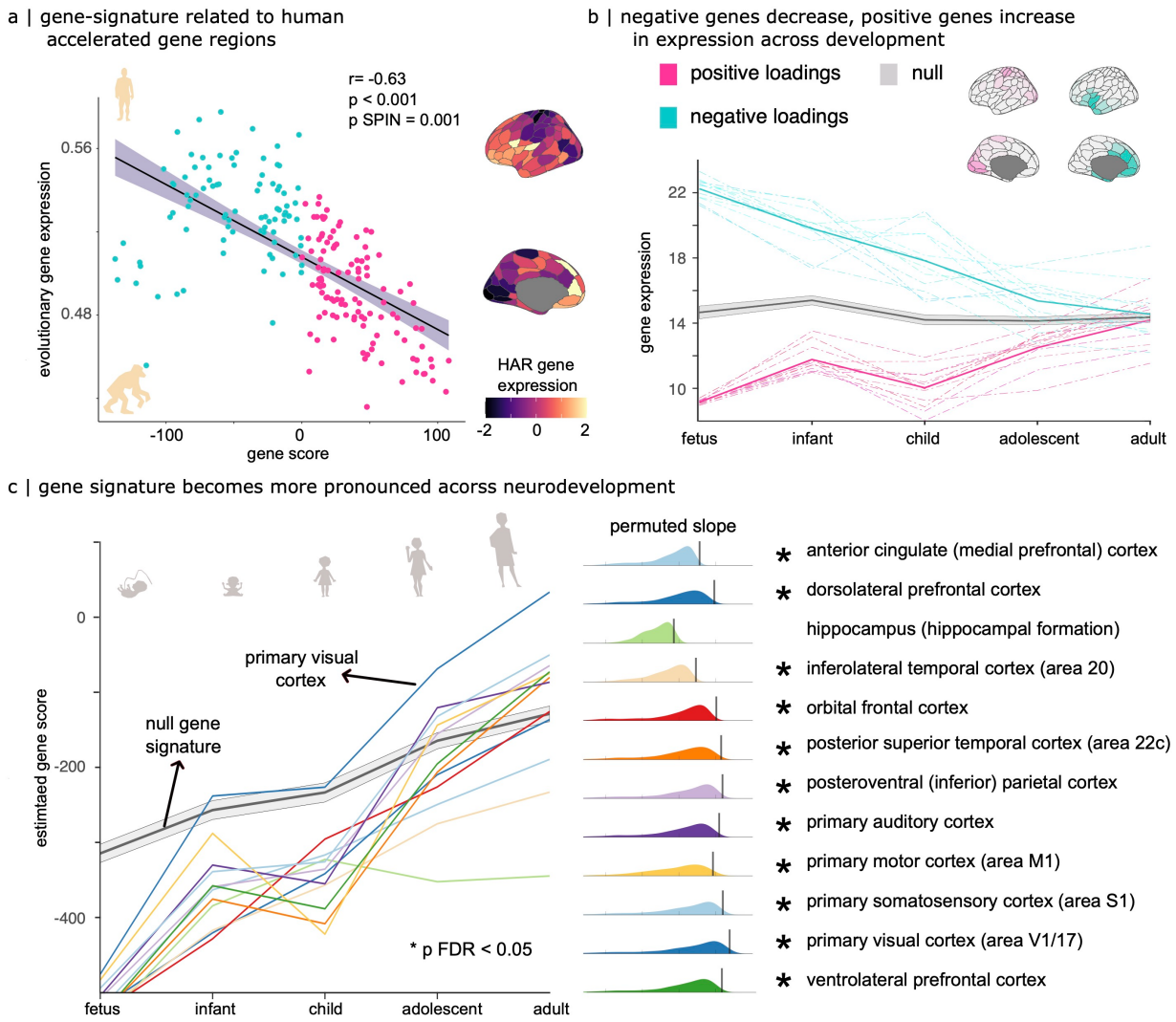


Chapter 5 Figure 7 Genes signature relates to human accelerated expansion and becomes more pronounced with neurodevelopment.

(a) Left panel: Scatter plot of the gene score derived from the PLS analysis (Figure 4b) against the gene expression of evolutionary expanded genes (HAR-brain genes). Pink points represent regions with positive gene scores, whereas blue regions depict negative gene scores. Gene scores are linearly negatively related to HAR brain gene expression. Right panel: z-score brain map of HAR brain gene expression across cortical regions. (b) Gene expression data from various life stages were used to compute the neurodevelopment of the identified gene signature. Gene expression values for the top 50% of negatively loaded genes (blue) and positively loaded genes (pink) across the 5 developmental periods. Dotted lines represent individual cortical regions, whereas solid lines represent the mean across regions. We computed

the trajectory of randomly selected genes (grey line) for comparison. (c) Left panel: Gene scores became more pronounced with maturation across the 12 brain regions of the BrainSpan data. The grey line depicts the trajectory of permutated gene scores. We fit linear slopes to the trajectory of observed and permuted data per region. Right panel: histograms of permuted slopes per cortical region. The vertical line represents the observed slope of gene score across development (*p <0.05).

# Discussion

Large neuroimaging datasets have allowed scientists to demonstrate that individuals can be differentiated from their brain activity, like a fingerprint (Amico & Goñi, 2018a; da Silva Castanheira et al., 2021; Finn et al., 2015a; Sareen et al., 2021a). But unlike a fingerprint left by your hand, the brain-fingerprint contains relevant information about demographics and cognition (da Silva Castanheira et al., 2021; Finn et al., 2015a; Rosenberg et al., 2017a; Rosenberg, Scheinost, et al., 2020), is altered by disease (da Silva Castanheira et al., 2023; Sorrentino et al., 2021c; Troisi Lopez et al., 2023), and tracks healthy aging (see Chapter 3). Despite this growing body of research, little is known about the genetic origins of electrophysiological brain-fingerprints.

## Neurophysiological activity is differentiable and heritable

Here, we demonstrate that MZ twins have significantly similar brain-fingerprints to their siblings enabling the differentiation of a MZ twin from their sibling's brain-fingerprint (Figure 2a). In contrast, DZ twins cannot be matched—these results suggest that brain-fingerprints, principally in the alpha and beta bands, are likely driven by genetics. We come to this conclusion based on the methodologies of twin studies: MZ twins are considerably more similar in terms of their genomes than DZ twins, all else being equal (e.g., the twins were raised in similar environments).

We similarly observed that the most salient features for differentiating individuals were also heritable brain phenotypes (Figure 3). This finding was most evident in the alpha and beta bands, and dovetails with previous work on individual alpha peak frequency (Salmela et al., 2016; C. M. Smit et al., 2006), suggesting that it is a heritable trait. Our work builds on this literature

and suggests that posterior alpha brain rhythms similarly differentiate individuals from one another. While we do not explicitly explore the relationship between brain rhythms and behaviours, our work proposes that polyrhythmic brain activity covaries with brain transcriptome gradients and brain activations during cognitive tasks (Figure 6).

### Genes related to ion transport relate to characteristic brain activity

Gene expression is reportedly associated with the structural and functional architecture of the brain, including cortical folding (Lee et al., 2016; Pizzagalli et al., 2020; Posthuma et al., 2005; Schmitt et al., 2020), and patterns of functional communication between brain regions (Fornito et al., 2011; Fu et al., 2015; Posthuma et al., 2005). Yet, the relationship between gene transcription, brain activity, and behaviour is less clear.

Previous work describes how brain activations for different psychological-processes relate to gene transcription (Hansen et al., 2021). Yet this prior work exclusively considered group-level average brain activity. Our results extend these findings by demonstrating that the gene-psychological processes gradient is associated with differentiable brain activity, and add to a growing literature demonstrating that the molecular organization of the brain may represent an important axis that shapes regional functional specialization (Alexander-Bloch et al., 2020; Fulcher & Fornito, 2016; Hansen et al., 2021; Krienen et al., 2016; Markello et al., 2022a; Seidlitz et al., 2020; Whitaker et al., 2016). Deviations from this gene expression gradient and/or genetic variation in the specific genes of this gradient may simultaneously lead to differentiable brain activity and variation in behaviour.

Genes positively related to neurophysiological differentiation were enriched for biological processes related to ion transport and neurotransmission (Figure 5). Prior work on the genetics of neural oscillations, has in large part focused on the genetic variants and their relationship to alpha rhythms. This literature has identified several candidate genetic variants—including the catechol-O-methyltransferase (COMT) enzyme responsible for the metabolism of cortical dopamine (Bodenmann et al., 2009), adenosine A2Areceptor gene (Rétey et al., 2005), adenosine deaminase gene, glutamatergic signaling (Salmela et al., 2016), and the GABAB receptor (GABABR1) (Winterer et al., 2003) which control, in part, neurochemical communication in the

brain. Moreover, we observed that the gene signature related to participant differentiation was preferentially expressed in excitatory and inhibitory neurons (Figure 5b). These results would suggest that inter-individual differences in neurochemical systems that lead to variations in neuron signalling are measurable at the mesoscale level. Our findings are in line with the hypothesized microscale origins of MEG signals (i.e., post-synaptic potentials of thousands of neurons) (Baillet, 2017; Baillet et al., 2001; Hämäläinen et al., 1993).

These results contrast with genes responsible for the morphology of cells and neurogenesis in limbic regions, which negatively covary with individual differentiation (Figure 4b) and are preferentially expressed in neuron support cells. Altogether, these results suggest that neurophysiological brain-fingerprints specifically capture differences in the neurochemical communication of thousands of neurons independently of heritable anatomical features.

We envision that our results will inform future research on inter-individual differences, offering novel biologically driven hypotheses to explain inter-individual variation in behaviour. For example, future work could link, from the bottom-up, how variation among sub-sets of genes shape brain microstructure and neuron signalling, which in turn manifest as differentiable mesoscale brain activity, and cognition.

While we demonstrate a link between gene expression and differentiable brain activity in the present study, our results do not suggest that diversity in brain activity is entirely driven by genetics. The environment in which one develops plays a significant role in shaping our behaviours, and therefore likely shapes our so-called brain-fingerprint. A case in point is our ability to differentiate twin pairs. We achieve high, but not ceiling, accuracies for differentiating MZ twin pairs (Figure 2a). We anticipate that future work can replicate the results presented herein to a large sample and better disambiguate the role of shared environmental factors on brain-fingerprints.

### Cognitive behaviours covary with gene expression and differentiable brain activity

We demonstrate for the first time that cognitive psychological processes brain activations and our ability to differentiate individuals from neurophysiology covary with a cortical genetic gradient (Figure 6). This ventromedial-dorsolateral psychological-processes gradient divides brain

activations between those related to cognitive processes like attention from activations related to affect (Figure 6a). The distinction between cognitive and affective psychological processes (i.e., thinking vs feeling) has long been debated: With some scholars suggesting that the distinction is more phenomenological rather than ontological (Duncan & Barrett, 2007). While our results indicate that brain activations fall along a gradient, this does not suggest that the two ends of the psychological processes do not interact, nor does it support their ontological distinction.

Our work suggests that cognitive processes like attention are more closely intertwined with gene expression associated with neuron communication, which in turn is related to inter-individual variation in neurophysiology. These results dovetail with recent reports that observed larger effect sizes in decoding cognition from brain activity than personality and mental health measures(Kong et al., 2023). Our results, despite utilizing different neuroimaging technology, provide a tentative biological explanation for these findings.

In contrast, psychological-processes more related to affect appear to be under the purview of genes responsible for cell morphology and expressed preferentially in astrocytes and microglia, which electrophysiological brain-fingerprinting may be ill-equipped to measure. This distinction may explain why neurophysiology is poor at disambiguating individuals from one another using these signals.

Brain regions that scored negatively on the identified significant latent variable include the anterior cingulate cortex: an area that has been disproportionally reported as vulnerable to mental illness (Bush et al., 2000; Goodkind et al., 2015; Shafiei et al., 2020; Tanti et al., 2022). Some of this work indeed suggests the important role of neuron support cells, like OPCs and microglia, in mental health (Salter & Stevens, 2017; Tanti et al., 2022; Tay et al., 2017; Wang et al., 2022; Wohleb & Delpech, 2017). We also note that prior work hypothesizes that adult neurogenesis may play a critical role in mental health (Madsen et al., 2000; Sahay & Hen, 2007; Schoenfeld & Cameron, 2015) which aligns with our gene ontology results. Taken together, the findings presented herein suggest that electrophysiological signals from regions related to emotional psychological-processes, and specifically vulnerable to mental illness, differentiate individuals with lower accuracy. These findings have important implications for personalized medicine research and should be further expanded upon in future studies.

### Neurodevelopmental trajectory of brain-fingerprints

Previous work reports that brain-fingerprints defined from functional connectomes become more pronounced with age, and their trajectory is stunted by mental illness (Kaufmann et al., 2017a, 2018a). We extend these results by offering a possible biological explanation: The gene expression signature associated with differentiable brain activity similarly becomes more pronounced with neurodevelopmental maturation (Figure 7). In line with these findings, the influence of genetics on cognition appears to increase throughout neurodevelopment (Briley & Tucker-Drob, 2017; Haworth et al., 2010; Mollon et al., 2021). Taken together these results suggest that cortical gene expression may drive both observations: making an individuals' brain activity more unique and by consequence influencing cognition more strongly. This interpretation requires further investigation.

Previous work in fMRI suggests that inter-individual differences in fMRI functional connectomes relate to gene expression enriched for the development of the central nervous system, and related positively to HAR gene expression (L. Li et al., 2021). In line with this observation, it has been reported that the most salient brain regions of the functional connectome brain-fingerprint are within the frontoparietal network. This contrasts with electrophysiological differentiation reported herein and elsewhere which emphasizes posterior sensory regions (e.g., Figure 2b and Chapter 3). These opposing findings emphasize the potential differences in the biological origins of hemodynamic and electrophysiological fingerprints, with the latter being potentially driven by neuron communication. Researchers can leverage these two salient signals for participant differentiation to explore brain-behaviour relationships and their genetic origins.

The conclusions of this work should be interpreted alongside important methodological considerations. First, we estimated heritability using the Falconer's formula as a relative measure of the importance of genetics for a given phenotype. We do not, however, explore the proportion of variance related to environmental factors—which would require a much larger sample of twin pairs. Second, the gene expression gradient is computed from a small sample of post-mortem brain tissue which is biased to the left hemisphere and imbalanced for sex. Third, the results reported herein are correlational in nature. Experimental manipulations of gene expression and

gene variants in animal models will afford neuroscientists a comprehensive understanding of how microscale gene expression may influence mesoscale neurophysiology and behaviour. Fourth, the molecular-psychological signature is based on brain activation patterns taken from the Neurosynth (Yarkoni et al., 2011) meta-analytic approach. While this method is useful for synthesizing data, scientists cannot draw strong conclusions about the neural basis of behaviours. In addition, Neurosynth assays a restricted scope of behaviours studied, the methods used to generate these activation maps are limited, and the activation maps lack information about individual variation.

Taken together, our study investigated the biological origins of inter-individual differences. We demonstrated using a twin-study-like approach that electrophysiological brain activity characteristic of individuals is influenced by genetics. We identify a ventromedial–dorsolateral gradient of gene expression that relates to person-specific neurophysiological brain activity. Together, our results highlight the potential of multi-scale data science approaches to understand the biological origins of individual variation.

# Methods

**Participants.** Data from 89 healthy young adults (22-35 years old; mean= 28.6, SD= 3.8 years old) were collected from the Human connectome project (HCP)(Van Essen et al., 2012). Of these 89 participants, 34 were monozygotic twins, 22 were dizygotic twins. The zygosity of the participants were confirmed with genotyping tests. All participants enrolled in the study and underwent three approximately six-minute resting-state eyes-open MEG recordings using a 248 magnetometers whole-head Magnes 3600 system (4DNeuroimaging, San Diego, CA). All scans were performed at the same site with a sampling rate of 2034.5 Hz (see (Van Essen et al., 2012)for detailed Methods of data collection).

**MEG data preprocessing**. MEG data were preprocessed following good practice guidelines (Gross et al., 2013) using Brainstorm (Tadel et al., 2011) March 2023 distribution running in MATLAB 2020b (Mathworks, Inc., Massachusetts, USA). Our preprocessing pipeline was adapted from our previous work (da Silva Castanheira et al., 2021, 2023). Line noise artifacts (60Hz) along with its

first 9 harmonics were removed using a notch filter. Slow-wave and DC artifacts were attenuated with a high-pass 0.3 FIR filter. To remove ocular and cardiac physiological artifacts, we defined Signal-Space Projections (SSPs) based on the activity of external electro-cardiogram and-oculogram recordings. We additionally attenuated low-frequency saccade (1-7 Hz) and high-frequency (40-240 Hz) muscle noise components with SSPs.

**MEG source mapping.** We source imaged the resting-state MEG using the coregistered anatomy folder provided by HCP (Van Essen et al., 2012). We computed MEG biophysical head models for each participant using the *Brainstorm* overlapping-spheres model (default parameters) applied to 15,000 locations of the cortex. Source maps for each participants' recoding were computed using linearly-constrained minimum-variance (LCMV) beamforming (using Brainstorm default parameters: 2018 version). Noise statistics for the respective day of the MEG recording were estimated from empty-room recordings. Participant source models were projected into the default anatomy of Brainstorm(Tadel et al., 2011), spatially smoothed (3mm) and clustered into the 200 cortical ROIs defined from the Schaefer 200 7-network atlas (Schaefer et al., 2018) using the first principal component within each ROI. Brain-fingerprints were derived from the power spectrum of these ROI source timeseries.

**Spectral brain-fingerprints**. We derived power spectrum density (PSD) estimates at each parcel of the Schaefer atlas using the Welch's method (time window of 2 s, 50% overlap). The resulting data for brain fingerprinting consisted of a feature matrix of 301 frequencies (0-150Hz; ½ Hz resolution) per each of the 200 ROIs. We derived a brain-fingerprint for each of the three MEG recordings per participant. We similarly defined brain-fingerprints using shorter 30-s non-overlapping segments of data.

**Individual differentiation from spectral brain-fingerprints.** The brain-fingerprinting method followed from our previous work (Figure 1a) (da Silva Castanheira et al., 2021; Chapter 2), and is based on the correlational similarity of participants between data recordings. For each participant in the cohort, we compute the Pearson correlation coefficient between the spectral brain-fingerprint of the first recording and the second brain-fingerprint of all participants in the

cohort, including the probe participant. Participant differentiation, thus, consists of a lookup procedure along the rows or columns of the inter-individual correlation matrix. A participant is said to be correctly differentiated if the largest correlation coefficient between the first brain-fingerprint and the second matches the probe participant. This approach is repeated for all participants. We compute a percent ratio of the number of participants correctly differentiated across the cohort (i.e., differentiation accuracy). We repeated the brain-fingerprinting procedure for all possible pairs of data recordings, and report the mean differentiation accuracy.

**Twin pair matching from spectral brain-fingerprints.** We extended participant differentiation to twin pairs. Similar to individual differentiation, for a given MZ twin, we compute the Pearson correlation coefficient between the spectral brain-fingerprint of the first recording and the second brain-fingerprint of all participants in the cohort. We exceptionally ignore the Pearson correlation coefficient of the probe participant to their second brain-fingerprint for the twin pair differentiation procedure (i.e., self-similarity; see Figure 1a). Instead, a twin pair is said to be correctly matched if the largest correlation coefficient between the first brain-fingerprint and the second matches the probe twin's sibling. We repeat the twin pair matching procedure for all twin pairs in the cohort and report the percent ratio of correctly matched pairs separately for MZ and DZ twin pairs.

**Band-limited spectral fingerprinting.** We replicated the individual and twin pair brain-fingerprinting analyses using spectral features averaged over canonical frequency bands (delta: 1–4 Hz, theta: 4–8 Hz, alpha: 8–13 Hz, beta: 13–30 Hz, gamma: 30–50 Hz, and high gamma: 50–150 Hz).

**Bootstrapping of differentiation accuracy scores.** To derive confidence intervals for the reported differentiation accuracies, we bootstrapped participants. We randomly selected a subset of participants representing ~90% of the tested full cohort (i.e., 30 MZ, 20 DZ, and 30 non-twins), derived differentiation accuracy score, and repeated the procedure 1000 times with random subsamples of participants. We report 95-% confidence interval from the $2.5^{th}$ and $97.5^{th}$ percentiles of the resulting empirical distribution of differentiation accuracies. To derive

confidence intervals for the differentiation of twin pairs, we randomly subsample 15 MZ twin pairs, and 10 DZ twin pairs for each iteration of the random subsampling.

**Saliency of brain-fingerprint features.** We calculated intraclass correlations (ICC) to quantify the contribution of each region and frequency band towards differentiating between individuals across the entire cohort. ICC quantifies the ratio of within-rater variance and between-rater variance. We define raters as participants, such that high values of ICC indicate that said brain-fingerprint feature corresponds to high within-participant similarity, and low between-participant similarity. To avoid any potential bias due to twin pairs, we computed ICC across all individuals in the cohort and across 100 random subsamples of participants such that we did not include twin pairs (i.e., for each subsample we would randomly select twin A or B to include in the calculation of ICC). Note that the resulting ICC values obtained from bootstrapping were 98.6% correlated to those obtained from the entire cohort. We proceeded with the ICC averaged across bootstraps for all analyses below.

**Heritability of brain phenotypes.** We calculated the heritability of brain phenotypes using the Falconer formula (Falconer, 1965). This method estimates the relative contribution of genetics against environmental factors in determining a phenotype. Heritability compares MZ twin pairs—who share approximately 100% of their genome— against DZ twin pairs —who share 50% of their genome. If the similarity in a phenotype between MZ is greater than DZ, a trait is said to be heritable:

$$H^2 = 2(r_{MZ} - r_{DZ})$$

where $r_{MZ}$ is the intraclass correlation between MZ twin pairs on a given phenotype and $r_{DZ}$ is the correlation among DZ twin. Note that the intra-class correlation used for defining salient features for differentiating individuals is defined independently of heritability. Heritability reflects the similarity within twin pairs on a given phenotype, whereas ICC reflects the stability of a phenotype within a person relative to others in the cohort (see Saliency of brain-fingerprint features).

**Correspondence of salient brain-fingerprint features and heritable brain phenotypes.** We aimed to determine if the salient features for participant differentiation colocalized with heritable brain phenotypes. We computed the Pearson's spatial correlation of ICC brain-fingerprint topographies with the brain maps obtained from the heritability analyses (see **Heritability of brain phenotypes**) across the 200 regions of the Schaefer atlas (Schaefer et al., 2018). We controlled for the spatial autocorrelation of the data using spin tests (see **Correction for spatial autocorrelation of brain maps**).

**Neuroanatomy.** We verified that our ability to differentiate MZ twin pairs was not driven predominantly by heritable anatomical features. To do so, we extracted anatomical features for each region of the Desikan-Killiany atlas provided by the Freesurfer segmentation procedure (Fischl, 2012). We then i) computed the heritability of these anatomical features following the procedure described above, and ii) computed the linear relationship between anatomical and spectral similarity for twin pairs. We report the results of the linear relationship separately for MZ, and DZ twin pairs (see Supplemental information).

**Biophysical and environmental artifacts.** We investigated whether biophysical recording artifacts might enhance our ability to differentiate individuals and twin pairs. First, we computed the root-mean-squares (RMS) of ocular, and cardiac signals collected simultaneously with MEG (ECG, HEOG, VEOG, respectively). Second, we linearly regressed the measured physiological artifacts from the brain-fingerprints, and used the residuals of this regression to differentiate individuals.

We tested whether day-to-day environmental and instrument noise biased our ability to differentiate individuals based on our previously published approach (da Silva Castanheira et al., 2021). To do so, we used the empty-room recordings collected on the same day of the MEG session for each participant to derive pseudo brain-fingerprints based on the imaging kennel of each participant's resting-state data. The empty-room recordings were preprocessed using the same filters as the resting-state data. We computed the differentiation accuracies obtained based on these pseudo brain-fingerprints.

**Gene expression data.** Gene expression data was obtained from the six postmortem brains provided by the AHBA (http://human.brain-map.org/) (M. J. Hawrylycz et al., 2012) using the *abagen* python package (Markello et al., 2021). Our analyses followed a similar pipeline to (Hansen et al., 2021). In brief, we first used microarray probes with the highest differential stability to represent gene expression for each gene (20,232 in total). Tissue samples were assigned to each of the 200 brain regions of the Schaefer atlas using Montreal Neurological Institute (MNI) coordinates generated via nonlinear registrations, with a maximum distance to of up to 2 mm away. To reduce potential misassignment, sample-to-region matching was constrained by hemisphere and to the cortex. If a region of the Schaefer atlas was not assigned a sample, the closest sample in Euclidian distance to the centroid of the region was selected. Gene expression was normalized across tissue samples and subjects to facilitate comparison with a robust sigmoid function (Fulcher et al., 2013). Gene expression for each of the retained genes was obtained by averaging across donors. We retained 9104 genes with differential stability above 0.1 for all future analyses following good-practice guidelines and previous literature (Arnatkevičiūtė et al., 2019; Hansen et al., 2021; M. Hawrylycz et al., 2015; Markello et al., 2021).

**Gene expression & differentiable neurophysiological PLS analysis.** We related salient features for participant differentiation to gene expression gradients using a partial least squares analysis (PLS) (Krishnan et al., 2011; McIntosh et al., 1996; McIntosh & Mišić, 2013). PLS is an unsupervised multivariate analyses method that relates two data matrices based on latent components of maximal covariance. We z-scored the columns both data matrices: the salient fingerprinting features matrix (ICC values; 6 columns represented each frequency band of interest & rows 200 ROIs of the Schaefer atlas) and the gene expression matrix (9104 columns represented genes & rows 200 ROIs of the Schaefer atlas), Y and X respectively. We applied singular value decomposition to the covariation matrix of X and Y such that:

$$(Y'X)' = USV'$$

where the *U* 9104 by 6 matrix, and the V 6 by 6 matrix, are orthonormal matrices with each column representing a latent component. The S matrix is a diagonal matrix of the singular values, with each value corresponding to the amount of covariance explained by each latent component(Krishnan et al., 2011; McIntosh & Mišić, 2013). Values of *U* and *V* at column i represent how much genes and frequency bands, respectively, contribute to the latent component (i.e., the weights of each gene and frequency band respectively). Positively weighted genes covary with positively weighted frequency bands.

Gene and ICC brain scores are computed for each brain region, by projecting the original data matrices X and Y onto the singular vector weights. These scores represent how much a given region demonstrates the pattern of covariance described the latent component. Positively scored brain regions exhibit covariance between the positively weighted genes and the positively weighted frequency bands for participant differentiation.

Loadings for genes and frequency bands were computed as the Pearson correlation between each variable's regional spatial distribution over the cortex (i.e., gene expression and ICC data) and the opposing brain score pattern (i.e., correlate gene expression & ICC brain score). Note, we used Pearson correlation as our loadings as they are easier to interpret and are bounded between-1 and 1. Variables with large absolute loadings are highly correlated to the observed score pattern, and relate strongly to the latent component of covariance.

To assess the significance of the latent components, we conducted spatial autocorrelation-preserving permutation tests (see **Correction for spatial autocorrelation of brain maps**). We conducted 1,000 spin tests and computed a null distribution of singular values. P values were computed as the proportion of null singular values that achieved a greater magnitude than the empirical singular values. Bootstrapped confidence intervals for the singular values were computed by randomly resampling the rows (brain regions) of both data matrices 1,000 times. We report the $2.5^{th}$ and $97.5^{th}$ percentile of the resulting distribution of singular values.

**Gene ontology analysis.** To determine the biological processes which strongly contributed to the set of positively and negatively loaded genes, we ran an enrichment analysis. Gene ontology is a framework for categorizing gene product molecular function and its associated biological process

by computing if a set of genes overrepresent specific biological functions relative to a random set of genes.

For negative and positive genes, we separately selected the 50% largest loadings (e.g., genes with the 50% most negative loadings) and entered these genes into the ShinyGO V 0.77 gene ontology tool (Ge et al., 2020). Genes with no EnrtezIds were ignored. Fold enrichment for each biological process was computed by comparing the frequency of a given biological process in the set of positive genes against the number of genes in the entire genome related to said biological process. P values associated with fold enrichment for all terms were FDR corrected. We conducted the fold-enrichment analysis using the KEGG (Kanehisa et al., 2017) and GO biological processes pathway databases (Thomas, 2017). See Supplemental Data for a list of all biological processes and their corresponding fold enrichment.

**Gene expression & psychological-processes PLS analysis.** We repeated the above-described PLS analysis to relate gene expression to psychological-processes as indexed by brain activation maps obtained from Neurosynth (Yarkoni et al., 2011). This analysis replicated Hansen and colleagues (Hansen et al., 2021) using the Schaefer 200 atlas (Schaefer et al., 2018).

Psychological-processes brain activation maps represent probabilistic association between a given term reported in a study (e.g., attention) and brain activation observed at a that specific voxel. This meta-analytic approach combines data from more than 15,000 published fMRI studies to create brain activation maps for each psychological term. We focused our analyses on the 123 terms reported in Hansen and colleagues (Hansen et al., 2021), which represent the subset of terms that exist both within Neurosynth (Yarkoni et al., 2011) and the Cognitive Atlas (Poldrack et al., 2011), a public ontology of cognitive science. Note that this big-data approach does not distinguish between activations and deactivations, nor does it represent the degree of activation of a given brain area. We parcellated the probabilistic functional association maps according to the Schaefer atlas(Schaefer et al., 2018).

We assessed the overlap between the identified gene latent components observed for the gene-differentiation and gene-psychological processes PLS analyses by computing the Pearson correlation between i) the gene brain score and ii) the gene weights of between both PLS analyses.

**Cross-validation of PLS analysis.** We assessed the robustness of our PLS model through cross-validation of the correlation between the observed gene scores and ICC scores (Pearson's correlation). We followed the same cross-validation procedures as Hansen and colleagues (Hansen et al., 2021) which creates a training and testing set of data by splitting spatially distant brain regions. A random seed is used to determine the training set—75% of brain regions closest in Euclidian distance to the seed location are used to train the PLS model. The remaining 25% of regions are held out, to test the PLS model by computing the correlation between predicted gene and ICC scores [*Corr(XtestUtrain, YtestVtrain*)]. This procedure was repeated 100 times to produce a distribution of correlations. The significance of the cross-validation procedure was assessed against a null model: We computed spatially autocorrelation-preserving permutations of the gene expression matrix and repeated the cross-validation procedure 1,000 times (see Figure 4c).

**Cell-type deconvolution analyses.** To determine if the identified gene signature is preferentially expressed in certain cell-types, we performed a cell-type deconvolution analysis. We aggregated cell-specific gene sets for 7 cell-types using five human adult postmortem single-cell and single-nucleus RNA sequencing studies (Darmanis et al., 2015; Habib et al., 2017; Lake et al., 2018; M. Li et al., 2018; Seidlitz et al., 2020; Zhang et al., 2016). The 7 cell classes were previously determined based on hierarchical clustering which resulted in the following cell types: astrocytes, endothelial cells, microglia, excitatory neurons, inhibitory neurons, oligodendrocytes, and oligodendrocyte precursors cells (OPC). We assessed the preferential expression of cell-specific gene sets by i) computing the ratio of positively (and negatively separately) loaded genes which overlapped with the cell-specific gene set and ii) permuting gene sets 1,000 times to assess statistical significance.

**Development of the gene signature.** We used brain gene expression data available from the BrainSpan (J. A. Miller et al., 2014). Gene expression levels from different developmental stages

ranging from 8 post-conception weeks to 40 years of age from 16 cortical regions. We binned gene expression data into five life stages: fetal (8–37 post-conception weeks), infant (4 months–1 year), child (2–8 years), adolescent (11–19 years) and adult (21–40 years) (Werling et al., 2020). For each life stage, we first computed the gene expression of the top 50% of positive and negatively loaded genes for every cortical region. We similarly compute gene expression at every neurodevelopmental stage for a random set of genes. Note that of the 16 cortical regions with gene expression data, four regions only had samples for the fetal stage—we, therefore, report data for the 12 cortical regions with data across all neurodevelopmental stages. We then computed gene scores for the 12 cortical regions across all neurodevelopmental stages by multiplying the gene expression matrix obtained from BrainSpan with the PLS-derived gene weights (columns of $U$). We fitted linear slopes—using the MATLAB polyfit() function—to the gene scores across neurodevelopment for every cortical region separately. We compared these slopes to null slope values obtained by first performing spatially autocorrelation-preserving permutations, running the PLS analysis, and multiplying the null gene weights with BrainSpan gene expression data. This resulted in a null distribution of slopes (1000 permutations).

**Human accelerated region analyses.** We defined genes associated with human accelerated regions (HARs) based on Wei et al.(Wei et al., 2019). Of the 1711 genes present in AHBA, Wei and colleagues reported that 415 genes were significantly more expressed in brain tissues than other available body samples (see (Wei et al., 2019) Supplementary Data 2). We based our analyses on these 415 HAR-brain genes for all further analyses. Of these 415 genes, 313 genes were considered differential stable in our analysis (see **Gene expression data**). We first assessed the overrepresentation of HAR-brain genes in the identified gene signature (top 50% positive and negative loadings) through permutation analyses. We then assessed the spatial correspondence of gene expression of HAR-brain genes and the computed gene brain score (see **Correction for spatial autocorrelation of brain maps**).

**Visualization.** We plotted brain maps of ICC, heritability, and PLS brain scores using the ggSchaefer and ggseg R packages. All other plots were generated using the ggplot2 package in R (R Core Team, 2022).

**Correction for spatial autocorrelation of brain maps**. We corrected for spatial autocorrelation of brain map data—where applicable—using SPIN tests. SPIN tests preserve the spatial autocorrelation of a brain map while permuting the indices of said map. The resulting relationship represents a null relationship, controlled for autocorrelation. We conducted 1000 SPIN permutations of our brain maps using the Hungarian method (Markello & Misic, 2021; Váša & Mišić, 2022).

## Data availability

This project relied on openly available data. The data are available through the Human connectome Project (HCP) repository (https://www.humanconnectome.org/study/hcp-young-adult). Gene expression data are available through the Allan Human Brain atlas (ABHA; http://human.brain-map.org/). The Neurosynth database is available at https://neurosynth.org/.

## Code availability

All in-house code used for data analysis and visualization is available on GitHub https://github.com/Epideixx/Fingerprints_Twins.

## Acknowledgements

The funders had no role in study design, data collection and analysis, decision to publish, or preparation of the manuscript. The Brainstorm app is supported by funding to SB from the NIH (R01-EB026299), a Discovery grant from the Natural Science and Engineering Research Council of Canada (436355-13), the CIHR Canada Research Chair in Neural Dynamics of Brain Systems, the Brain Canada Foundation with support from Health Canada, and the Innovative Ideas program from the Canada First Research Excellence Fund, awarded to McGill University for the HBHL initiative. This work was supported by a doctoral fellowship from NSERC (JDSC, JYH).

# References


Alexander-Bloch, A. F., Raznahan, A., Vandekar, S. N., Seidlitz, J., Lu, Z., Mathias, S. R., Knowles, E., Mollon, J., Rodrigue, A., Curran, J. E., Görring, H. H. H., Satterthwaite, T. D., Gur, R. E., Bassett, D. S., Hoftman, G. D., Pearlson, G., Shinohara, R. T., Liu, S., Fox, P. T., … Glahn, D. C. (2020). Imaging local genetic influences on cortical folding. Proceedings of the National Academy of Sciences, 117(13), 7430–7436. https://doi.org/10.1073/pnas.1912064117

Amico, E., & Goñi, J. (2018). The quest for identifiability in human functional connectomes. Scientific Reports, 8(1), Article 1. https://doi.org/10.1038/s41598-018-25089-1

Arnatkevičiūtė, A., Fulcher, B. D., & Fornito, A. (2019). A practical guide to linking brain-wide gene expression and neuroimaging data. NeuroImage, 189, 353–367. https://doi.org/10.1016/j.neuroimage.2019.01.011

Baillet, S. (2017). Magnetoencephalography for brain electrophysiology and imaging. Nature Neuroscience, 20(3), Article 3. https://doi.org/10.1038/nn.4504

Baillet, S., Mosher, J. C., & Leahy, R. M. (2001). Electromagnetic brain mapping. IEEE Signal Processing Magazine, 18(6), 14–30. https://doi.org/10.1109/79.962275

Betzel, R. F., Medaglia, J. D., Kahn, A. E., Soffer, J., Schonhaut, D. R., & Bassett, D. S. (2019). Structural, geometric and genetic factors predict interregional brain connectivity patterns probed by electrocorticography. Nature Biomedical Engineering, 3(11), Article 11. https://doi.org/10.1038/s41551-019-0404-5

Bodenmann, S., Rusterholz, T., Dürr, R., Stoll, C., Bachmann, V., Geissler, E., Jaggi-Schwarz, K., & Landolt, H.-P. (2009). The Functional Val158Met Polymorphism of COMT Predicts Interindividual Differences in Brain α Oscillations in Young Men. Journal of Neuroscience, 29(35), 10855–10862. https://doi.org/10.1523/JNEUROSCI.1427-09.2009

Bouchard, T. J., & McGue, M. (2003). Genetic and environmental influences on human psychological differences. Journal of Neurobiology, 54(1), 4–45. https://doi.org/10.1002/neu.10160

Briley, D. A., & Tucker-Drob, E. M. (2017). Comparing the Developmental Genetics of Cognition and Personality over the Lifespan. Journal of Personality, 85(1), 51–64. https://doi.org/10.1111/jopy.12186

Burt, J. B., Demirtaş, M., Eckner, W. J., Navejar, N. M., Ji, J. L., Martin, W. J., Bernacchia, A., Anticevic, A., & Murray, J. D. (2018). Hierarchy of transcriptomic specialization across human cortex captured by structural neuroimaging topography. Nature Neuroscience, 21(9), 1251–1259. https://doi.org/10.1038/s41593-018-0195-0

Bush, G., Luu, P., & Posner, M. I. (2000). Cognitive and emotional influences in anterior cingulate cortex. Trends in Cognitive Sciences, 4(6), 215–222. https://doi.org/10.1016/s1364-6613(00)01483-2

da Silva Castanheira, J., Orozco Perez, H. D., Misic, B., & Baillet, S. (2021). Brief segments of neurophysiological activity enable individual differentiation. Nature Communications, 12(1), Article 1. https://doi.org/10.1038/s41467-021-25895-8

da Silva Castanheira, J., Wiesman, A. I., Hansen, J. Y., Misic, B., Baillet, S., PREVENT-AD Research Group, & Quebec Parkinson Network. (2023). Neurophysiological brain-fingerprints of motor and cognitive decline in Parkinson's disease. medRxiv: The Preprint Server for Health Sciences, 2023.02.03.23285441. https://doi.org/10.1101/2023.02.03.23285441

Darmanis, S., Sloan, S. A., Zhang, Y., Enge, M., Caneda, C., Shuer, L. M., Hayden Gephart, M. G., Barres, B. A., & Quake, S. R. (2015). A survey of human brain transcriptome diversity at the single cell level. Proceedings of the National Academy of Sciences, 112(23), 7285–7290. https://doi.org/10.1073/pnas.1507125112

De Gennaro, L., Marzano, C., Fratello, F., Moroni, F., Pellicciari, M. C., Ferlazzo, F., Costa, S., Couyoumdjian, A., Curcio, G., Sforza, E., Malafosse, A., Finelli, L. A., Pasqualetti, P., Ferrara, M., Bertini, M., & Rossini, P. M. (2008). The electroencephalographic fingerprint of sleep is genetically determined: A twin study. Annals of Neurology, 64(4), 455–460. https://doi.org/10.1002/ana.21434

Driessens, S. L. W., Galakhova, A. A., Heyer, D. B., Pieterse, I. J., Wilbers, R., Mertens, E. J., Waleboer, F., Heistek, T. S., Coenen, L., Meijer, J. R., Idema, S., De Witt Hamer, P. C., Noske, D. P., De Kock, C. P. J., Lee, B. R., Smith, K., Ting, J. T., Lein, E. S., Mansvelder, H. D., & Goriounova, N. A. (2023). Genes associated with cognitive ability and HAR show overlapping expression patterns in human cortical neuron types. Nature Communications, 14(1), 4188. https://doi.org/10.1038/s41467-023-39946-9

Dubois, J., & Adolphs, R. (2016). Building a Science of Individual Differences from fMRI. Trends in Cognitive Sciences, 20(6), 425–443. https://doi.org/10.1016/j.tics.2016.03.014

Duncan, S., & Barrett, L. F. (2007). Affect is a form of cognition: A neurobiological analysis. Cognition & Emotion, 21(6), 1184–1211. https://doi.org/10.1080/02699930701437931

Falconer, D. S. (1965). The inheritance of liability to certain diseases, estimated from the incidence among relatives. Annals of Human Genetics, 29(1), 51–76. https://doi.org/10.1111/j.1469-1809.1965.tb00500.x

Finn, E. S., Shen, X., Scheinost, D., Rosenberg, M. D., Huang, J., Chun, M. M., Papademetris, X., & Constable, R. T. (2015). Functional connectome fingerprinting: Identifying individuals using patterns of brain connectivity. Nature Neuroscience, 18(11), Article 11. https://doi.org/10.1038/nn.4135

Fischl, B. (2012). FreeSurfer. NeuroImage, 62(2), 774–781. https://doi.org/10.1016/j.neuroimage.2012.01.021

Fornito, A., Zalesky, A., Bassett, D. S., Meunier, D., Ellison-Wright, I., Yucel, M., Wood, S. J., Shaw, K., O'Connor, J., Nertney, D., Mowry, B. J., Pantelis, C., & Bullmore, E. T. (2011). Genetic Influences on Cost-Efficient Organization of Human Cortical Functional Networks. Journal of Neuroscience, 31(9), Article 9. https://doi.org/10.1523/JNEUROSCI.4858-10.2011

Fu, Y., Ma, Z., Hamilton, C., Liang, Z., Hou, X., Ma, X., Hu, X., He, Q., Deng, W., Wang, Y., Zhao, L., Meng, H., Li, T., & Zhang, N. (2015). Genetic influences on resting-state functional networks: A twin study: Genetic Influences on Resting-State Functional Networks. Human Brain Mapping, 36(10), Article 10. https://doi.org/10.1002/hbm.22890

Fulcher, B. D., & Fornito, A. (2016). A transcriptional signature of hub connectivity in the mouse connectome. Proceedings of the National Academy of Sciences, 113(5), 1435–1440. https://doi.org/10.1073/pnas.1513302113

Fulcher, B. D., Little, M. A., & Jones, N. S. (2013). Highly comparative time-series analysis: The empirical structure of time series and their methods. Journal of The Royal Society Interface, 10(83), 20130048. https://doi.org/10.1098/rsif.2013.0048

Fulcher, B. D., Murray, J. D., Zerbi, V., & Wang, X.-J. (2019). Multimodal gradients across mouse cortex. Proceedings of the National Academy of Sciences, 116(10), 4689–4695. https://doi.org/10.1073/pnas.1814144116

Ge, S. X., Jung, D., & Yao, R. (2020). ShinyGO: A graphical gene-set enrichment tool for animals and plants. Bioinformatics, 36(8), 2628–2629. https://doi.org/10.1093/bioinformatics/btz931

Girskis, K. M., Stergachis, A. B., DeGennaro, E. M., Doan, R. N., Qian, X., Johnson, M. B., Wang, P. P., Sejourne, G. M., Nagy, M. A., Pollina, E. A., Sousa, A. M. M., Shin, T., Kenny, C. J., Scotellaro, J. L., Debo, B. M., Gonzalez, D. M., Rento, L. M., Yeh, R. C., Song, J. H. T., … Walsh, C. A. (2021). Rewiring of human neurodevelopmental gene regulatory programs by human accelerated regions. Neuron, 109(20), 3239-3251.e7. https://doi.org/10.1016/j.neuron.2021.08.005

Goodkind, M., Eickhoff, S. B., Oathes, D. J., Jiang, Y., Chang, A., Jones-Hagata, L. B., Ortega, B. N., Zaiko, Y. V., Roach, E. L., Korgaonkar, M. S., Grieve, S. M., Galatzer-Levy, I., Fox, P. T., & Etkin, A. (2015). Identification of a common neurobiological substrate for mental illness. JAMA Psychiatry, 72(4), 305–315. https://doi.org/10.1001/jamapsychiatry.2014.2206

Gross, J., Baillet, S., Barnes, G. R., Henson, R. N., Hillebrand, A., Jensen, O., Jerbi, K., Litvak, V., Maess, B., Oostenveld, R., Parkkonen, L., Taylor, J. R., van Wassenhove, V., Wibral, M., & Schoffelen, J.-M. (2013). Good practice for conducting and reporting MEG research. NeuroImage, 65, 349–363. https://doi.org/10.1016/j.neuroimage.2012.10.001

Guardiola-Ripoll, M., & Fatjó-Vilas, M. (2023). A Systematic Review of the Human Accelerated Regions in Schizophrenia and Related Disorders: Where the Evolutionary and Neurodevelopmental Hypotheses Converge. International Journal of Molecular Sciences, 24(4), 3597. https://doi.org/10.3390/ijms24043597

Habib, N., Avraham-Davidi, I., Basu, A., Burks, T., Shekhar, K., Hofree, M., Choudhury, S. R., Aguet, F., Gelfand, E., Ardlie, K., Weitz, D. A., Rozenblatt-Rosen, O., Zhang, F., & Regev, A. (2017). Massively parallel single-nucleus RNA-seq with DroNc-seq. Nature Methods, 14(10), Article 10. https://doi.org/10.1038/nmeth.4407

Hämäläinen, M., Hari, R., Ilmoniemi, R. J., Knuutila, J., & Lounasmaa, O. V. (1993). Magnetoencephalography—Theory, instrumentation, and applications to noninvasive studies of the working human brain. Reviews of Modern Physics, 65(2), 413–497. https://doi.org/10.1103/RevModPhys.65.413

Hansen, J. Y., Markello, R. D., Vogel, J. W., Seidlitz, J., Bzdok, D., & Misic, B. (2021). Mapping gene transcription and neurocognition across human neocortex. Nature Human Behaviour, 5(9), Article 9. https://doi.org/10.1038/s41562-021-01082-z

Haworth, C., Wright, M., Luciano, M., Martin, N., de Geus, E., van Beijsterveldt, C., Bartels, M., Posthuma, D., Boomsma, D., Davis, O., Kovas, Y., Corley, R., DeFries, J., Hewitt, J., Olson, R., Rhea, S.-A., Wadsworth, S., Iacono, W., McGue, M., … Plomin, R. (2010). The heritability of general cognitive ability increases linearly from childhood to young adulthood. Molecular Psychiatry, 15(11), 1112–1120. https://doi.org/10.1038/mp.2009.55

Hawrylycz, M. J., Lein, E. S., Guillozet-Bongaarts, A. L., Shen, E. H., Ng, L., Miller, J. A., van de Lagemaat, L. N., Smith, K. A., Ebbert, A., Riley, Z. L., Abajian, C., Beckmann, C. F., Bernard, A., Bertagnolli, D., Boe, A. F., Cartagena, P. M., Chakravarty, M. M., Chapin, M., Chong, J., … Jones, A. R. (2012). An anatomically comprehensive atlas of the adult human brain transcriptome. Nature, 489(7416), Article 7416. https://doi.org/10.1038/nature11405

Hawrylycz, M., Miller, J. A., Menon, V., Feng, D., Dolbeare, T., Guillozet-Bongaarts, A. L., Jegga, A. G., Aronow, B. J., Lee, C.-K., Bernard, A., Glasser, M. F., Dierker, D. L., Menche, J., Szafer, A., Collman, F., Grange, P., Berman, K. A., Mihalas, S., Yao, Z., … Lein, E. (2015). Canonical genetic signatures of the adult human brain. Nature Neuroscience, 18(12), Article 12. https://doi.org/10.1038/nn.4171

Hodgkinson, C. A., Enoch, M.-A., Srivastava, V., Cummins-Oman, J. S., Ferrier, C., Iarikova, P., Sankararaman, S., Yamini, G., Yuan, Q., Zhou, Z., Albaugh, B., White, K. V., Shen, P.-H., & Goldman, D. (2010). Genome-wide association identifies candidate genes that influence the human electroencephalogram. Proceedings of the National Academy of Sciences of the United States of America, 107(19), 8695–8700. https://doi.org/10.1073/pnas.0908134107

Kanehisa, M., Furumichi, M., Tanabe, M., Sato, Y., & Morishima, K. (2017). KEGG: New perspectives on genomes, pathways, diseases and drugs. Nucleic Acids Research, 45(D1), D353–D361. https://doi.org/10.1093/nar/gkw1092

Kaufmann, T., Alnæs, D., Brandt, C. L., Bettella, F., Djurovic, S., Andreassen, O. A., & Westlye, L. T. (2018). Stability of the Brain Functional Connectome Fingerprint in Individuals With Schizophrenia. JAMA Psychiatry, 75(7), 749–751. https://doi.org/10.1001/jamapsychiatry.2018.0844

Kaufmann, T., Alnæs, D., Doan, N. T., Brandt, C. L., Andreassen, O. A., & Westlye, L. T. (2017). Delayed stabilization and individualization in connectome development are related to psychiatric disorders. Nature Neuroscience, 20(4), Article 4. https://doi.org/10.1038/nn.4511

Kong, R., Tan, Y. R., Wulan, N., Ooi, L. Q. R., Farahibozorg, S.-R., Harrison, S., Bijsterbosch, J. D., Bernhardt, B. C., Eickhoff, S., & Thomas Yeo, B. T. (2023). Comparison between gradients and parcellations for functional connectivity prediction of behavior. NeuroImage, 273, 120044. https://doi.org/10.1016/j.neuroimage.2023.120044

Krienen, F. M., Yeo, B. T. T., Ge, T., Buckner, R. L., & Sherwood, C. C. (2016). Transcriptional profiles of supragranular-enriched genes associate with corticocortical network architecture in the human brain. Proceedings of the National Academy of Sciences, 113(4), E469–E478. https://doi.org/10.1073/pnas.1510903113

Krishnan, A., Williams, L. J., McIntosh, A. R., & Abdi, H. (2011). Partial Least Squares (PLS) methods for neuroimaging: A tutorial and review. NeuroImage, 56(2), 455–475. https://doi.org/10.1016/j.neuroimage.2010.07.034

Lake, B. B., Chen, S., Sos, B. C., Fan, J., Kaeser, G. E., Yung, Y. C., Duong, T. E., Gao, D., Chun, J., Kharchenko, P. V., & Zhang, K. (2018). Integrative single-cell analysis of transcriptional and epigenetic states in the human adult brain. Nature Biotechnology, 36(1), Article 1. https://doi.org/10.1038/nbt.4038

Lee, P. H., Baker, J. T., Holmes, A. J., Jahanshad, N., Ge, T., Jung, J.-Y., Cruz, Y., Manoach, D. S., Hibar, D. P., Faskowitz, J., McMahon, K. L., de Zubicaray, G. I., Martin, N. H., Wright, M. J., Öngür, D., Buckner, R., Roffman, J., Thompson, P. M., & Smoller, J. W. (2016). Partitioning

heritability analysis reveals a shared genetic basis of brain anatomy and schizophrenia. Molecular Psychiatry, 21(12), Article 12. https://doi.org/10.1038/mp.2016.164

Li, L., Wei, Y., Zhang, J., Ma, J., Yi, Y., Gu, Y., Li, L. M. W., Lin, Y., & Dai, Z. (2021). Gene expression associated with individual variability in intrinsic functional connectivity. NeuroImage, 245, 118743. https://doi.org/10.1016/j.neuroimage.2021.118743

Li, M., Santpere, G., Imamura Kawasawa, Y., Evgrafov, O. V., Gulden, F. O., Pochareddy, S., Sunkin, S. M., Li, Z., Shin, Y., Zhu, Y., Sousa, A. M. M., Werling, D. M., Kitchen, R. R., Kang, H. J., Pletikos, M., Choi, J., Muchnik, S., Xu, X., Wang, D., … Sestan, N. (2018). Integrative functional genomic analysis of human brain development and neuropsychiatric risks. Science, 362(6420), eaat7615. https://doi.org/10.1126/science.aat7615

Madsen, T. M., Treschow, A., Bengzon, J., Bolwig, T. G., Lindvall, O., & Tingström, A. (2000). Increased neurogenesis in a model of electroconvulsive therapy. Biological Psychiatry, 47(12), 1043–1049. https://doi.org/10.1016/S0006-3223(00)00228-6

Malone, S. M., Burwell, S. J., Vaidyanathan, U., Miller, M. B., McGue, M., & Iacono, W. G. (2014). Heritability and Molecular-Genetic Basis of Resting EEG Activity: A Genome-Wide Association Study. Psychophysiology, 51(12), 1225–1245. https://doi.org/10.1111/psyp.12344

Markello, R. D., Arnatkeviciute, A., Poline, J.-B., Fulcher, B. D., Fornito, A., & Misic, B. (2021). Standardizing workflows in imaging transcriptomics with the abagen toolbox. eLife, 10, e72129. https://doi.org/10.7554/eLife.72129

Markello, R. D., Hansen, J. Y., Liu, Z.-Q., Bazinet, V., Shafiei, G., Suárez, L. E., Blostein, N., Seidlitz, J., Baillet, S., Satterthwaite, T. D., Chakravarty, M. M., Raznahan, A., & Misic, B. (2022). neuromaps: Structural and functional interpretation of brain maps. Nature Methods, 19(11), Article 11. https://doi.org/10.1038/s41592-022-01625-w

Markello, R. D., & Misic, B. (2021). Comparing spatial null models for brain maps. NeuroImage, 236, 118052. https://doi.org/10.1016/j.neuroimage.2021.118052

Markovic, A., Achermann, P., Rusterholz, T., & Tarokh, L. (2018). Heritability of Sleep EEG Topography in Adolescence: Results from a Longitudinal Twin Study. Scientific Reports, 8(1), Article 1. https://doi.org/10.1038/s41598-018-25590-7

Mayhew, A. J., & Meyre, D. (2017). Assessing the Heritability of Complex Traits in Humans: Methodological Challenges and Opportunities. Current Genomics, 18(4), 332–340. https://doi.org/10.2174/1389202918666170307161450

McIntosh, A. R., Bookstein, F. L., Haxby, J. V., & Grady, C. L. (1996). Spatial pattern analysis of functional brain images using partial least squares. NeuroImage, 3(3 Pt 1), 143–157. https://doi.org/10.1006/nimg.1996.0016

McIntosh, A. R., & Mišić, B. (2013). Multivariate statistical analyses for neuroimaging data. Annual Review of Psychology, 64, 499–525. https://doi.org/10.1146/annurev-psych-113011-143804

McKenzie, A. T., Wang, M., Hauberg, M. E., Fullard, J. F., Kozlenkov, A., Keenan, A., Hurd, Y. L., Dracheva, S., Casaccia, P., Roussos, P., & Zhang, B. (2018). Brain Cell Type Specific Gene Expression and Co-expression Network Architectures. Scientific Reports, 8(1), Article 1. https://doi.org/10.1038/s41598-018-27293-5

Mikulincer, M., Shaver, P. R., Cooper, M. L., & Larsen, R. J. (Eds.). (2015). APA handbook of personality and social psychology, Volume 4: Personality processes and individual differences (pp. xxviii, 727). American Psychological Association. https://doi.org/10.1037/14343-000

Miller, J. A., Ding, S.-L., Sunkin, S. M., Smith, K. A., Ng, L., Szafer, A., Ebbert, A., Riley, Z. L., Royall, J. J., Aiona, K., Arnold, J. M., Bennet, C., Bertagnolli, D., Brouner, K., Butler, S., Caldejon, S., Carey, A., Cuhaciyan, C., Dalley, R. A., … Lein, E. S. (2014). Transcriptional landscape of the prenatal human brain. Nature, 508(7495), Article 7495. https://doi.org/10.1038/nature13185

Mollon, J., Knowles, E. E. M., Mathias, S. R., Gur, R., Peralta, J. M., Weiner, D. J., Robinson, E. B., Gur, R. E., Blangero, J., Almasy, L., & Glahn, D. C. (2021). Genetic influence on cognitive development between childhood and adulthood. Molecular Psychiatry, 26(2), Article 2. https://doi.org/10.1038/s41380-018-0277-0

Niso, G., Rogers, C., Moreau, J. T., Chen, L.-Y., Madjar, C., Das, S., Bock, E., Tadel, F., Evans, A. C., Jolicoeur, P., & Baillet, S. (2016). OMEGA: The Open MEG Archive. NeuroImage, 124, 1182–1187. https://doi.org/10.1016/j.neuroimage.2015.04.028

Pizzagalli, F., Auzias, G., Yang, Q., Mathias, S. R., Faskowitz, J., Boyd, J. D., Amini, A., Rivière, D., McMahon, K. L., de Zubicaray, G. I., Martin, N. G., Mangin, J.-F., Glahn, D. C., Blangero, J., Wright, M. J., Thompson, P. M., Kochunov, P., & Jahanshad, N. (2020). The reliability and heritability of cortical folds and their genetic correlations across hemispheres. Communications Biology, 3(1), Article 1. https://doi.org/10.1038/s42003-020-01163-1

Poldrack, R. A., Kittur, A., Kalar, D., Miller, E., Seppa, C., Gil, Y., Parker, D. S., Sabb, F. W., & Bilder, R. M. (2011). The Cognitive Atlas: Toward a Knowledge Foundation for Cognitive Neuroscience. Frontiers in Neuroinformatics, 5, 17. https://doi.org/10.3389/fninf.2011.00017

Posthuma, D., de Geus, E. J. C., Mulder, E. J. C. M., Smit, D. J. A., Boomsma, D. I., & Stam, C. J. (2005). Genetic components of functional connectivity in the brain: The heritability of synchronization likelihood. Human Brain Mapping, 26(3), Article 3. https://doi.org/10.1002/hbm.20156

Power, R. A., & Pluess, M. (2015). Heritability estimates of the Big Five personality traits based on common genetic variants. Translational Psychiatry, 5(7), e604. https://doi.org/10.1038/tp.2015.96

R Core Team. (2022). R: A Language and Environment for Statistical Computing. R Foundation for Statistical Computing. https://www.R-project.org/

Rétey, J. V., Adam, M., Honegger, E., Khatami, R., Luhmann, U. F. O., Jung, H. H., Berger, W., & Landolt, H.-P. (2005). A functional genetic variation of adenosine deaminase affects the duration and intensity of deep sleep in humans. Proceedings of the National Academy of Sciences, 102(43), 15676–15681. https://doi.org/10.1073/pnas.0505414102

Richiardi, J., Altmann, A., Milazzo, A.-C., Chang, C., Chakravarty, M. M., Banaschewski, T., Barker, G. J., Bokde, A. L. W., Bromberg, U., Büchel, C., Conrod, P., Fauth-Bühler, M., Flor, H., Frouin, V., Gallinat, J., Garavan, H., Gowland, P., Heinz, A., Lemaître, H., … IMAGEN CONSORTIUM. (2015). Correlated gene expression supports synchronous activity in brain networks. Science, 348(6240), 1241–1244. https://doi.org/10.1126/science.1255905

Rosenberg, M. D., Finn, E. S., Scheinost, D., Constable, R. T., & Chun, M. M. (2017). Characterizing Attention with Predictive Network Models. Trends in Cognitive Sciences, 21(4), Article 4. https://doi.org/10.1016/j.tics.2017.01.011

Rosenberg, M. D., Scheinost, D., Greene, A. S., Avery, E. W., Kwon, Y. H., Finn, E. S., Ramani, R., Qiu, M., Constable, R. T., & Chun, M. M. (2020). Functional connectivity predicts changes in attention observed across minutes, days, and months. Proceedings of the National Academy of Sciences, 117(7), 3797–3807. https://doi.org/10.1073/pnas.1912226117

Sahay, A., & Hen, R. (2007). Adult hippocampal neurogenesis in depression. Nature Neuroscience, 10(9), Article 9. https://doi.org/10.1038/nn1969

Salmela, E., Renvall, H., Kujala, J., Hakosalo, O., Illman, M., Vihla, M., Leinonen, E., Salmelin, R., & Kere, J. (2016). Evidence for genetic regulation of the human parieto-occipital 10-Hz rhythmic activity. The European Journal of Neuroscience, 44(3), 1963–1971. https://doi.org/10.1111/ejn.13300

Salter, M. W., & Stevens, B. (2017). Microglia emerge as central players in brain disease. Nature Medicine, 23(9), Article 9. https://doi.org/10.1038/nm.4397

Sareen, E., Zahar, S., Ville, D. V. D., Gupta, A., Griffa, A., & Amico, E. (2021). Exploring MEG brain fingerprints: Evaluation, pitfalls, and interpretations. NeuroImage, 240, 118331. https://doi.org/10.1016/j.neuroimage.2021.118331

Schaefer, A., Kong, R., Gordon, E. M., Laumann, T. O., Zuo, X.-N., Holmes, A. J., Eickhoff, S. B., & Yeo, B. T. T. (2018). Local-Global Parcellation of the Human Cerebral Cortex from Intrinsic Functional Connectivity MRI. Cerebral Cortex, 28(9), 3095–3114. https://doi.org/10.1093/cercor/bhx179

Schmitt, J. E., Raznahan, A., Liu, S., & Neale, M. C. (2020). The Heritability of Cortical Folding: Evidence from the Human Connectome Project. Cerebral Cortex (New York, NY), 31(1), 702–715. https://doi.org/10.1093/cercor/bhaa254

Schoenfeld, T. J., & Cameron, H. A. (2015). Adult Neurogenesis and Mental Illness. Neuropsychopharmacology, 40(1), 113–128. https://doi.org/10.1038/npp.2014.230

Seidlitz, J., Nadig, A., Liu, S., Bethlehem, R. A. I., Vértes, P. E., Morgan, S. E., Váša, F., Romero-Garcia, R., Lalonde, F. M., Clasen, L. S., Blumenthal, J. D., Paquola, C., Bernhardt, B.,

Wagstyl, K., Polioudakis, D., de la Torre-Ubieta, L., Geschwind, D. H., Han, J. C., Lee, N. R., … Raznahan, A. (2020). Transcriptomic and cellular decoding of regional brain vulnerability to neurogenetic disorders. Nature Communications, 11(1), Article 1. https://doi.org/10.1038/s41467-020-17051-5

Shafiei, G., Markello, R. D., Makowski, C., Talpalaru, A., Kirschner, M., Devenyi, G. A., Guma, E., Hagmann, P., Cashman, N. R., Lepage, M., Chakravarty, M. M., Dagher, A., & Mišić, B. (2020). Spatial Patterning of Tissue Volume Loss in Schizophrenia Reflects Brain Network Architecture. Biological Psychiatry, 87(8), 727–735. https://doi.org/10.1016/j.biopsych.2019.09.031

Smit, C. M., Wright, M. J., Hansell, N. K., Geffen, G. M., & Martin, N. G. (2006). Genetic variation of individual alpha frequency (IAF) and alpha power in a large adolescent twin sample. International Journal of Psychophysiology: Official Journal of the International Organization of Psychophysiology, 61(2), 235–243. https://doi.org/10.1016/j.ijpsycho.2005.10.004

Smit, D. J. A., Posthuma, D., Boomsma, D. I., & Geus, E. J. C. (2005). Heritability of background EEG across the power spectrum. Psychophysiology, 42(6), Article 6. https://doi.org/10.1111/j.1469-8986.2005.00352.x

Sorrentino, P., Rucco, R., Lardone, A., Liparoti, M., Troisi Lopez, E., Cavaliere, C., Soricelli, A., Jirsa, V., Sorrentino, G., & Amico, E. (2021). Clinical connectome fingerprints of cognitive decline. NeuroImage, 238, 118253. https://doi.org/10.1016/j.neuroimage.2021.118253

Tadel, F., Baillet, S., Mosher, J. C., Pantazis, D., & Leahy, R. M. (2011). Brainstorm: A User-Friendly Application for MEG/EEG Analysis. Computational Intelligence and Neuroscience, 2011, 1–13. https://doi.org/10.1155/2011/879716

Tanti, A., Belliveau, C., Nagy, C., Maitra, M., Denux, F., Perlman, K., Chen, F., Mpai, R., Canonne, C., Théberge, S., McFarquhar, A., Davoli, M. A., Belzung, C., Turecki, G., & Mechawar, N. (2022). Child abuse associates with increased recruitment of perineuronal nets in the ventromedial prefrontal cortex: A possible implication of oligodendrocyte progenitor cells. Molecular Psychiatry, 27(3), Article 3. https://doi.org/10.1038/s41380-021-01372-y

Tay, T. L., Béchade, C., D'Andrea, I., St-Pierre, M.-K., Henry, M. S., Roumier, A., & Tremblay, M.-E. (2017). Microglia Gone Rogue: Impacts on Psychiatric Disorders across the Lifespan. Frontiers in Molecular Neuroscience, 10, 421. https://doi.org/10.3389/fnmol.2017.00421

Taylor, J. R., Williams, N., Cusack, R., Auer, T., Shafto, M. A., Dixon, M., Tyler, L. K., Cam-CAN, & Henson, R. N. (2017). The Cambridge Centre for Ageing and Neuroscience (Cam-CAN) data repository: Structural and functional MRI, MEG, and cognitive data from a cross-sectional adult lifespan sample. NeuroImage, 144, 262–269. https://doi.org/10.1016/j.neuroimage.2015.09.018

Thomas, P. D. (2017). The Gene Ontology and the meaning of biological function. Methods in Molecular Biology (Clifton, N.J.), 1446, 15. https://doi.org/10.1007/978-1-4939-3743-1_2

Troisi Lopez, E., Minino, R., Liparoti, M., Polverino, A., Romano, A., De Micco, R., Lucidi, F., Tessitore, A., Amico, E., Sorrentino, G., Jirsa, V., & Sorrentino, P. (2023). Fading of brain network fingerprint in Parkinson's disease predicts motor clinical impairment. Human Brain Mapping, 44(3), 1239–1250. https://doi.org/10.1002/hbm.26156

Van Essen, D. C., Ugurbil, K., Auerbach, E., Barch, D., Behrens, T. E. J., Bucholz, R., Chang, A., Chen, L., Corbetta, M., Curtiss, S. W., Della Penna, S., Feinberg, D., Glasser, M. F., Harel, N., Heath, A. C., Larson-Prior, L., Marcus, D., Michalareas, G., Moeller, S., … Yacoub, E. (2012). The Human Connectome Project: A data acquisition perspective. NeuroImage, 62(4), Article 4. https://doi.org/10.1016/j.neuroimage.2012.02.018

Van Horn, J. D., Grafton, S. T., & Miller, M. B. (2008). Individual Variability in Brain Activity: A Nuisance or an Opportunity? Brain Imaging and Behavior, 2(4), 327–334. https://doi.org/10.1007/s11682-008-9049-9

Váša, F., & Mišić, B. (2022). Null models in network neuroscience. Nature Reviews Neuroscience, 23(8), 493–504. https://doi.org/10.1038/s41583-022-00601-9

Wang, H., He, Y., Sun, Z., Ren, S., Liu, M., Wang, G., & Yang, J. (2022). Microglia in depression: An overview of microglia in the pathogenesis and treatment of depression. Journal of Neuroinflammation, 19(1), 132. https://doi.org/10.1186/s12974-022-02492-0

Waschke, L., Kloosterman, N. A., Obleser, J., & Garrett, D. D. (2021). Behavior needs neural variability. Neuron, 109(5), 751–766. https://doi.org/10.1016/j.neuron.2021.01.023

Wei, Y., de Lange, S. C., Scholtens, L. H., Watanabe, K., Ardesch, D. J., Jansen, P. R., Savage, J. E., Li, L., Preuss, T. M., Rilling, J. K., Posthuma, D., & van den Heuvel, M. P. (2019). Genetic mapping and evolutionary analysis of human-expanded cognitive networks. Nature Communications, 10(1), Article 1. https://doi.org/10.1038/s41467-019-12764-8

Werling, D. M., Pochareddy, S., Choi, J., An, J.-Y., Sheppard, B., Peng, M., Li, Z., Dastmalchi, C., Santpere, G., Sousa, A. M. M., Tebbenkamp, A. T. N., Kaur, N., Gulden, F. O., Breen, M. S., Liang, L., Gilson, M. C., Zhao, X., Dong, S., Klei, L., … Sestan, N. (2020). Whole-Genome and RNA Sequencing Reveal Variation and Transcriptomic Coordination in the Developing Human Prefrontal Cortex. Cell Reports, 31(1), 107489. https://doi.org/10.1016/j.celrep.2020.03.053

Whitaker, K. J., Vértes, P. E., Romero-Garcia, R., Váša, F., Moutoussis, M., Prabhu, G., Weiskopf, N., Callaghan, M. F., Wagstyl, K., Rittman, T., Tait, R., Ooi, C., Suckling, J., Inkster, B., Fonagy, P., Dolan, R. J., Jones, P. B., Goodyer, I. M., the NSPN Consortium, & Bullmore, E. T. (2016). Adolescence is associated with genomically patterned consolidation of the hubs of the human brain connectome. Proceedings of the National Academy of Sciences, 113(32), 9105–9110. https://doi.org/10.1073/pnas.1601745113

Winterer, G., Mahlberg, R., Smolka, M. N., Samochowiec, J., Ziller, M., Rommelspacher, H.-P., Herrmann, W. M., Schmidt, L. G., & Sander, T. (2003). Association Analysis of Exonic Variants of the GABAB-Receptor Gene and Alpha Electroencephalogram Voltage in Normal Subjects and Alcohol-Dependent Patients. Behavior Genetics, 33(1), 7–15. https://doi.org/10.1023/A:1021043315012

Wohleb, E. S., & Delpech, J.-C. (2017). Dynamic cross-talk between microglia and peripheral monocytes underlies stress-induced neuroinflammation and behavioral consequences. Progress in Neuro-Psychopharmacology & Biological Psychiatry, 79(Pt A), 40–48. https://doi.org/10.1016/j.pnpbp.2016.04.013

Yamashita, M., Yoshihara, Y., Hashimoto, R., Yahata, N., Ichikawa, N., Sakai, Y., Yamada, T., Matsukawa, N., Okada, G., Tanaka, S. C., Kasai, K., Kato, N., Okamoto, Y., Seymour, B., Takahashi, H., Kawato, M., & Imamizu, H. (2018). A prediction model of working memory

across health and psychiatric disease using whole-brain functional connectivity. eLife, 7, e38844. https://doi.org/10.7554/eLife.38844

Yarkoni, T., Poldrack, R. A., Nichols, T. E., Van Essen, D. C., & Wager, T. D. (2011). Large-scale automated synthesis of human functional neuroimaging data. Nature Methods, 8(8), 665–670. https://doi.org/10.1038/nmeth.1635

Yeo, B. T. T., Krienen, F. M., Sepulcre, J., Sabuncu, M. R., Lashkari, D., Hollinshead, M., Roffman, J. L., Smoller, J. W., Zöllei, L., Polimeni, J. R., Fischl, B., Liu, H., & Buckner, R. L. (2011). The organization of the human cerebral cortex estimated by intrinsic functional connectivity. Journal of Neurophysiology, 106(3), 1125–1165. https://doi.org/10.1152/jn.00338.2011

Zhang, Y., Sloan, S. A., Clarke, L. E., Caneda, C., Plaza, C. A., Blumenthal, P. D., Vogel, H., Steinberg, G. K., Edwards, M. S. B., Li, G., Duncan, J. A., Cheshier, S. H., Shuer, L. M., Chang, E. F., Grant, G. A., Gephart, M. G. H., & Barres, B. A. (2016). Purification and Characterization of Progenitor and Mature Human Astrocytes Reveals Transcriptional and Functional Differences with Mouse. Neuron, 89(1), 37–53. https://doi.org/10.1016/j.neuron.2015.11.013

Zietsch, B. P., Hansen, J. L., Hansell, N. K., Geffen, G. M., Martin, N. G., & Wright, M. J. (2007). Common and specific genetic influences on EEG power bands delta, theta, alpha, and beta. Biological Psychology, 75(2), 154–164. https://doi.org/10.1016/j.biopsycho.2007.01.004

Zwir, I., Arnedo, J., Del-Val, C., Pulkki-Råback, L., Konte, B., Yang, S. S., Romero-Zaliz, R., Hintsanen, M., Cloninger, K. M., Garcia, D., Svrakic, D. M., Rozsa, S., Martinez, M., Lyytikäinen, L.-P., Giegling, I., Kähönen, M., Hernandez-Cuervo, H., Seppälä, I., Raitoharju, E., … Cloninger, C. R. (2020). Uncovering the complex genetics of human character. Molecular Psychiatry, 25(10), Article 10. https://doi.org/10.1038/s41380-018-0263

# Chapter 6

# Discussion

Individuals exhibit a great diversity of personality traits and behaviors, yet the biological mechanisms underlying these differences remain incompletely understood. A likely contributor to such variability is the substantial heterogeneity in brain structure and function. How inter-individual variation of the brain relates to behaviours remains an open field of inquiry. This question is of particular interest as the neuroscientific field moves towards larger openly-available data volumes that approach the realm of population science (Niso et al., 2016a; Taylor et al., 2017; Van Essen et al., 2012). In this dissertation, I demonstrate how brain-fingerprinting can expand our neuroscientific toolkit to better understand the diversity of neurophysiological brain activity across individuals and ultimately explore the biological origins of the self.

## Inter-individual differences in brain activity evolve across the lifespan

Leveraging several large open datasets across four experiments, I investigated inter-individual differences in brain activity across populations and demonstrated that an individual's brain activity is characteristic of themselves. Much like a fingerprint left by your hand, brain activity can differentiate a person from a large cohort. But unlike a fingerprint left by your hand, the brain-fingerprint can predict behaviours and traits (Amico & Goñi, 2018a; da Silva Castanheira et al., 2021; Finn et al., 2015a; Rosenberg et al., 2017a), scales with disease progression (Chapter 4), and correlates to cortical gene expression (Chapter 5) allowing scientists to study the biological origins of behavioural variation.

Previous work on brain-fingerprinting (Amico & Goñi, 2018a; Finn et al., 2015a) exclusively studied healthy young adults. In this dissertation, I expand the concept of the brain-

fingerprint to various populations, demonstrating that individuals remain distinguishable across diverse groups, including older adults. The findings of Chapter 3 suggest that while individual differentiation remains accurate, the electrophysiological features that best differentiate between individuals evolve throughout healthy aging. Whether individuals remain equally differentiable across all of neurodevelopment remains an active area of research.

Kauffman and colleagues' demonstrate that functional connectome brain-fingerprints, as measured using fMRI scans, become increasingly stable throughout neurodevelopment (Kaufmann et al., 2017a), and suggest that delayed stabilization of the functional connectome may be a marker of abnormal neurodevelopment (Kaufmann et al., 2017a). Given the different origins of BOLD and electrophysiological signals, whether these findings translate to electrophysiological brain-fingerprints remains to be explored.

In Chapter 5 I demonstrate that the genetic signature which covaries with electrophysiological individual differentiation becomes more pronounced across neurodevelopment. These findings dovetail with the observation that older adults remain differentiable across the adult lifespan, previous fMRI literature reporting an increasingly stable brain-fingerprint with neurodevelopment, and imply that the influence of genetics on electrophysiology becomes increasingly important for inter-individual differences across neurodevelopment. These effects also align with the observations that cognitive processes develop over the lifespan and that genetics play an increasingly important role in cognition as one ages (Mollon et al., 2021).

In a separate project not presented in this dissertation, I compared the brain fingerprints of young children (4-12 years old) to that of adults (18+ years old). The findings reveal that the brain-fingerprints of children are more challenging to differentiate, showing increased similarity to other children's brain activity, specifically for arrhythmic brain activity (da Silva Castanheira et al., in preparation). These results tentatively explain previous findings in the fMRI literature (Kaufmann et al., 2017a), and aligns with the results of Chapter 5, where we observed that the gene-differentiation signature becomes more pronounced across neurodevelopment. A graphical representation of this effect is depicted in Figure 1. Together, these findings suggest that brain-

fingerprints may be stable within specific developmental periods, underscoring the importance of future research exploring brain-fingerprints with longitudinal data across the lifespan.

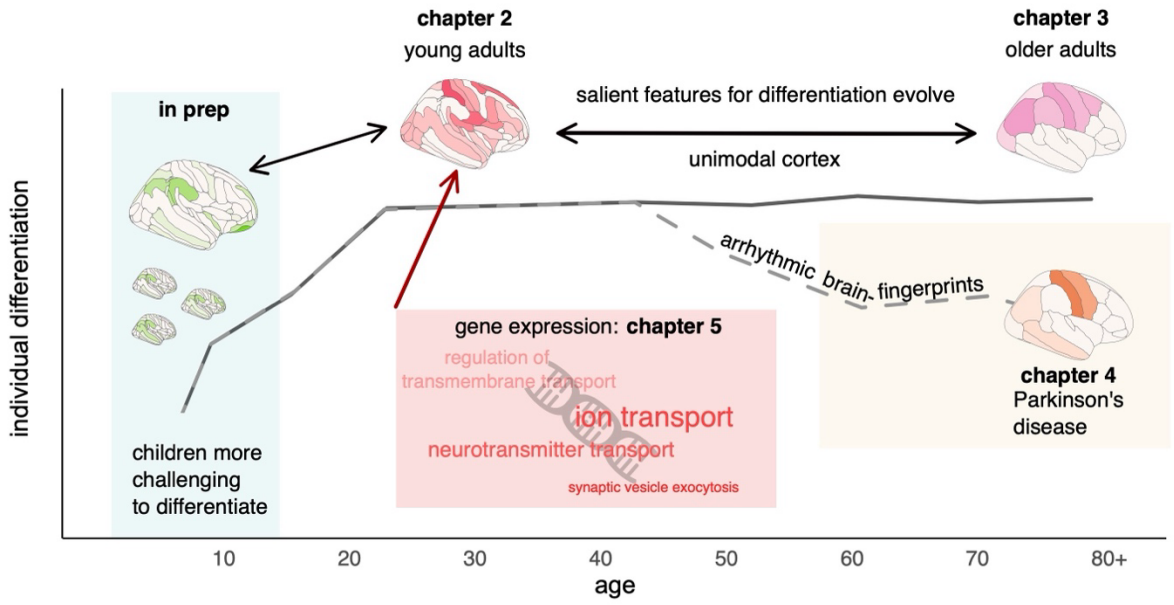


Chapter 6 Figure 1 Individual differentiation across the lifespan overview.

Summary figure of the results presented within this dissertation. Chapter 2 established the differentiation of young adults (18-35 years old) from spectral brain-fingerprints. The accuracy of individual differentiation remains high across the adult lifespan. Diseases, such as neurodegenerative diseases may lower participant self-similarity of brain-fingerprints and therefore lower participant differentiation. Young children on the other hand (4-12 years old) are more difficult to differentiate from one another due to higher other-similarity of brain activity features (data not presented in thesis da Silva Castanheira et al., in preparation). These finding are in line with the results presented in Chapter 5. Across these populations, the most differentiable brain activity features (depicted in brain maps) evolve across groups.

## Stability of rhythmic brain activity

In our analysis of different populations, we observed that arrhythmic brain activity differentiated individuals with a lower accuracy than its rhythmic counterpart. While we found little evidence for the impact of age on our ability to differentiate individuals, we observed that individual differentiation using arrhythmic brain features was remarkedly worse than rhythmic features

across all age groups (see Chapter 3). This effect is most evident when using the entire cohort: using brain-fingerprints defined from full spectral activity, 606 individuals were differentiated with 89.6% ([88.0, 91.1] 95% CI) accuracy, this dropped to 47.1% (CI [46.0, 48.0]) when using brain-fingerprints derived exclusively from arrhythmic brain activity. This effect is unsurprising as arrhythmic brain activity is derived from two spectral parameters across brain regions, reducing the complexity of the electrophysiological signal substantially.

Additionally, we observed that individuals with Parkinson's disease (PD) showed a pronounced destabilization of arrhythmic brain activity. Any differences in differentiation accuracy between healthy age-matched controls and patients with PD were mitigated when defining brain-fingerprints from rhythmic brain activity (Chapter 4). The latter findings tentatively explain why previous efforts to define brain-fingerprints of individuals with neurodegenerative diseases reported lower differentiation accuracies (Romano et al., 2022; Sorrentino et al., 2021c; Troisi Lopez et al., 2023).

Together these findings suggest that the arrhythmic component of brain activity may be less stable within a recording session and subsequently less characteristic of individuals, than its rhythmic counterpart. This finding is in line with the interpretation that arrhythmic brain activity may represent the local balance of excitatory and inhibitory activity (Chini et al., 2022; R. Gao et al., 2017; Waschke, Donoghue, et al., 2021) and fluctuates across different states of alertness including sleep stages and anesthetic-induced loss of consciousness (Colombo et al., 2019; Favaro et al., 2023; Lendner et al., 2020; Maschke et al., 2023). These results would tentatively suggest that arrythmic brain activty reflects more of a '*state'* than a '*trait'*. Future research should explore how fluctuating states of arousal during resting-state scans may impact brain-fingerprinting and be altered by diseases like neurodegeneration.

## Implications for future clinical research

The budding brain-fingerprint literature puts forward the notion that task-free brain activity is stable within individuals and deviations from this stability may index disease, cognitive decline, and neurodegeneration (Kaufmann et al., 2017a, 2018a; Sorrentino et al., 2021c; Troisi Lopez et al., 2023). The results of Chapter 4 elaborate on these findings and propose that arrhythmic brain activity exhibits an increase in moment-to-moment variability in PD hindering individual

differentiation. These findings challenge the notion of a general 'fading' brain-fingerprint associated with neurodegenerative diseases and suggest that specific components of brain activity may be selectively affected by disease, impacting individual differentiation.

The clinical utility of the brain-fingerprinting method lies in identifying patient-specific polyrhythmic biomarkers that are both characteristic of individuals and relate to the clinical presentation of diseases. These biomarkers may offer potential targets for neuromodulation therapies, providing researchers exploring such therapies with new avenues for investigation (Chase et al., 2019; Harmsen et al., 2018; Litvak et al., 2021; Thut & Pascual-Leone, 2010). In addition, documenting which neurological conditions specifically show greater within-session variability could aid in building more generalizable translational neuroimaging models (Woo et al., 2017).

In Chapter 4, I contextualize the PD brain-fingerprint with respect to normative atlases of neurochemical systems. These results open avenues for novel hypotheses and therapeutic targets beyond previously reported group-level aberrations. Exploring cellular and molecular correlates of increased variability in arrhythmic brain activity in animal models of neurodegenerative diseases could provide valuable insights.

The influence of genetics on brain-fingerprints, as discussed in Chapter 5, suggests that future clinical work could also use animal models to understand how gene expression may alter mesoscale differentiable brain activity. This approach could contribute to a deeper understanding of the microscale correlates of brain variability, the relationship between variability and symptom presentation, and ultimately help move the field toward the goal of personalized medicine.

### Exploring biological origins of unique brain activity

Novel large neuroscientific datasets and tools have afforded neuroscientists new methodologies to bridge across methodologies (e.g., fMRI, MEG, single-cell recordings, PET, and gene expression) and measurement scales (e.g., gene expression, neurochemistry, and mesoscale neurophysiology) (Hansen et al., 2021, 2022; Markello et al., 2022a). Inspired by these tools and databases, I contextualize the observed differentiable brain activity with the spatial distribution of neurochemical systems and cortical gene expression.

Cortical regions enriched for norepinephrine transporter were observed to also differentiate older adults better than young adults, and patients with PD better than age-matched healthy controls. These results emphasize the importance of the noradrenergic system in inter-individual differences. Extant literature emphasizes the role of the noradrenergic system on sensory processing, alertness, and attention (Borodovitsyna et al., 2017; Devilbiss et al., 2006; Holland et al., 2021; Vazey & Aston-Jones, 2014). I speculate that inter-individual differences in cognitive functions may relate to the noradrenergic system, and subsequently be observed as inter-individual differences in electrophysiology in noradrenergic enriched regions. In line with this hypothesis, the cognitive changes observed with healthy aging and in Parkinson's disease may relate to norepinephrine function and this may explain why electrophysiology of regions enriched in this neurochemical system best differentiates between older adults and between patients with PD. Future work may triangulate inter-individual differences in behaviours, including attention and sensory processing, differentiable neurophysiological activity, and the noradrenergic system.

These are among the first results to link within-participant stability of neurophysiological brain activity to neurochemistry. Despite this ambitious goal, the method is not without its limitations. Indeed, the normative atlases of neurochemical distribution aggregated data exclusively from healthy young adults (Markello et al., 2022a). Future work should aim to replicate these effects using cross-sectional Positron Emission Tomography scans. This data-science approach to neuroimaging is promising, but still in its infancy; future databases with more extensive characterization of the neurochemistry and microstructure of the brain across populations may expedite brain-behaviour research.

The results presented herein put forward the construal that brain morphology may play a limited role in shaping electrophysiological brain-fingerprints. While we observed a significant spatial alignment between age-related cortical thinning and diverging features for participant differentiation between age-groups (Chapter 3), we observed limited evidence for the role of cortical thickness in shaping the brain-fingerprints of patients with PD (Chapter 4). In addition, the anatomical similarity between monozygotic twins did not linearly scale with their spectral brain-fingerprint similarity (Chapter 5). Together, these mixed results contrast with recent

findings reporting that the brains geometry plays an important role in shaping its function as measured by fMRI (Pang et al., 2023). Future work should clarify the role anatomy plays in electrophysiological participant differentiation.

In addition, we reported that differentiable electrophysiological brain activity in healthy young adults covaries with gene expression enriched for ion homeostasis, and cell signalling. This gene signature was preferentially expressed in excitatory and inhibitory neurons (see Chapter 5) and corroborates the hypothesized microscale origins of MEG signals (i.e., post-synaptic potentials of thousands of neurons) (Baillet, 2017; Baillet et al., 2001; Hämäläinen et al., 1993). Together this dissertation provides evidence that inter-individual differences measurable at the mesoscale using electrophysiology may relate to inter-individual variations in neuron signaling, and are not a by-product of neural noise as previous work suggested (Başar, 1990; Stein et al., 2005).

There are well-recorded neurodevelopmental changes in the brain's transcriptome, and while these alterations are most notable throughout the prenatal and infancy periods, a small percentage of genes have been documented to change in late adulthood (see Ham & Lee (Ham & Lee, 2020) for review). Across cortical regions, age-dependent gene transcription alterations primarily reduce synaptic functions and increase the brain's immune response. The results of Chapters 5 and 3 tentatively propose that transcriptomic changes in synaptic function may drive the changes we observed in differentiable electrophysiological features of older adults.

Previous studies reported that microglial genes like complement component 1q A (C1QA) are increasingly expressed with age (Cribbs et al., 2012; Erraji-Benchekroun et al., 2005; Ham & Lee, 2020; Norden & Godbout, 2013; Soreq et al., 2017). These results corroborate the inflammation hypothesis of aging (Cribbs et al., 2012; Malva et al., 2021) which suggests that neuroinflammation may be an important risk factor in protecting against cognitive decline and neurodegenerative disease. Yet, the results of this dissertation suggest that differentiable electrophysiological activity may not be particularly sensitive to capture the macro-scale correlates of gene transcription alterations in neural support cells (Chapter 5). While the present body of work does not address this concern directly—due to limited available transcriptomic

data—it certainly represents a novel avenue for future studies exploring the link between neuroinflammation, aging, and inter-individual differences in electrorheological activity.

### Linking within-person variability of behaviours and brain activity

Most of the extant research on brain-behaviour relationships has largely focused on inter-individual variation in behaviours and how they relate to brain activity. Scant work explores how intra-individual variation in behaviours relates to intra-individual variation in brain activity.

Indeed, preliminary work on intra-individual variability in behaviours suggests that increased variation in behavioural responses may be an important index of participants' mental wellbeing (Burton et al., 2006b; Costa et al., 2019a; Kuntsi & Klein, 2011b; MacDonald et al., 2006; Singh et al., 2021b). Increased behavioural intra-individual variability specifically in neurodegenerative diseases has been related to the severity of cognitive symptoms (Burton et al., 2006b; Costa et al., 2019a; J. D. Jones et al., 2022; Singh et al., 2021b). Yet, the neurobiological foundations of such an effect are yet to be entirely understood. Some preliminary findings in fMRI report an association between the variability of brain activity and cognitive performance (Garrett et al., 2010; Garrett, Kovacevic, et al., 2013; Nomi et al., 2017).

Variability in neural signals, previously conceptualized as noise has recently been re-examined as a signal that can index task performance (Baracchini et al., 2023; Nomi et al., 2017; Uddin, 2020, 2021). Throughout neurodevelopment, brain signal variability appears to increase and correlate with cognitive task performance. BOLD variability appears to be an important signal related to cognition and several biological processes like the arrhythmic component of electrophysiology (Baracchini et al., 2023).

It is for these reasons I speculate that greater intra-individual variability of the arrhythmic component observed in PD may relate to variability in task performance, as discussed in Chapter 4. Note that greater intra-individual variability of brain activity (lower self-similarity) hinders participant differentiation. Bridging the brain-fingerprinting (Kaufmann et al., 2017a, 2018a; Sorrentino et al., 2021c; Troisi Lopez et al., 2023) and variability literature, the results of this dissertation tentatively suggest that brain-fingerprints may be a useful index of cognitive health and brain signal variability. Increased variability may be an important "*signal*" of interest in future neuroscientific research (Garrett et al., 2010; Garrett, Kovacevic, et al., 2013). Future work should

clarify this hypothesis and triangulate these fields of research to link cognitive decline to intra-individual variability of behaviours and brain activity.

## Methodological considerations for studying brain-behaviour relationships

Building on previous research on brain-fingerprints (Amico & Goñi, 2018a; Finn et al., 2015a; Rosenberg et al., 2017a), the results of this dissertation indicate a connection between inter-individual differences in cognition and electrophysiological brain-fingerprints. For example, salient electrophysiological features for individual differentiation predict inter-individual differences in fluid intelligence (Chapter 3). In addition, I observed an axis of psychological task-activations—from cognitive tasks to self-reported affect—that covaries with gene expression, and differentiable brain activity (Chapter 5).

The longstanding ontological debate surrounding the distinction between affect and cognition, rooted in ancient philosophy, persists to this day (Duncan & Barrett, 2007; Forgas, 2008). Recent arguments propose a phenomenological rather than an ontological distinction—individuals subjectively feel that paying attention is different than experiencing an emotion, but a true boundary between these brain processes may not exist (Duncan & Barrett, 2007). Following this perspective, research has documented cases where affect directly impacts cognitive processes such as attention (Ochsner & Gross, 2005; Veerapa et al., 2020), and cases where cognitive processes, like declarative memories, elicit emotional responses (Duncan & Barrett, 2007). Understanding the complex relationship between inter-individual differences in cognition and affect, and their connection to brain fingerprints, requires further investigation.

It is noteworthy that salient features in fMRI that predict individual differences in cognitive abilities overlap minimally with the salient brain regions of electrophysiological brain-fingerprints reported herein. The diverging salient features between imaging modalities for participant differentiation may help future research on brain-behaviour relationships.

Another crucial consideration when studying brain-behaviour relationships is how cognition and affect are often studied in the lab. Cognition is often measured through tasks that require participants to respond to stimuli, whereas affect is often measured through self-report questionnaires. Future work should investigate whether methodological considerations in how we measure behaviours in the field underlie this gradient of task-activations observed in the

Neurosynth data. While moderate to high test-rest reliability of personality questionnaires like the Big Five factor model suggest that participants on average can introspect their behaviours, certain socioeconomic factors may reduce the reliability of these questionnaires (Gnambs, 2014, 2016; Gurven et al., 2013; McCrae & Costa Jr., 1997). The discrepancy in how researchers measure cognition and affect may complicate interpretations of brain-behaviour research.

Earlier studies on social networks and friendships suggest that two friends who are closer in a social network show more similar brain activation patterns during resting state than two strangers—much like a brain-fingerprint (Baek et al., 2022; Parkinson et al., 2018). The authors speculate that the similarity in brain activity amongst friends at rest may reflect shared world views and beliefs that, like lenses, shape information processing (Parkinson et al., 2018). The results of Chapter 5 expand on these findings and tentatively suggest that monozygotic twin pairs, whose brain-fingerprints are strikingly similar, may similarly have overlapping cognitive abilities, beliefs, and personalities. Future research should expand on these results and explore how shared personalities and beliefs are similarly represented in the brain with brain-fingerprinting of siblings and unrelated participants. Taken together, this burgeoning literature demonstrates that novel methods inspired by brain-fingerprinting may help us better understand brain-behaviour relationships.

Brain-fingerprinting presents itself as a complementary approach for investigating brain-behavior relationships. In contrast with Brain Wide Association Studies (BWAS), the brain-fingerprinting approach considers both within- and between- participant variance of brain activity. Expanding the neuroscientific toolkit for brain-behaviour relationships is particularly important given recent concerns about the limited reproducibility of BWAS, including small effect-sizes, low reproducibility (Marek et al., 2022), and limited generalization across populations (Greene et al., 2022; J. Li et al., 2022).

Expanding upon previous fMRI results, I demonstrate that the most salient features for individual differentiation similarly decode inter-individual differences in fluid intelligence. By concentrating solely on differentiable brain activity and its relationship to behaviours, the brain-fingerprinting approach can potentially reduce the number of statical tests by reducing the feature space, and thereby render BWAS more amenable to smaller sample sizes. In addition,

brain-fingerprinting will likely afford scientists novel hypotheses to design brain-behaviour models.

## Individuals are differentiable from brief neurophysiological segments

One notable advantage of electrophysiological brain-fingerprints, in comparison to fMRI, is their relative stability within-individuals over brief 30-second recordings. Across multiple cohorts totalling ~1,000 total participants, and across various population demographics (e.g., young adults, older adults, and individuals with Parkinson's disease), I observed that brief 30-second neurophysiological recordings can differentiate between individuals based on fast brain dynamics. This observation is clinically useful and coincides with other work suggesting that within-participant estimates of spectral brain activity stabilize over a relatively short period of time (i.e., less than 2 minutes for most spectral features) (Wiesman, da Silva Castanheira, et al., 2022c). Together, these results suggest that the brain activity of healthy adults is relatively stable over brief segments in time.

This growing body of work, corroborating the stability of brief neurophysiological recordings, has important implications for the design and collection of population neuroscientific data. Future data-sharing efforts can benefit from these results by recording brief MEG recordings. Indeed, brief electrophysiological recordings from thousands of individuals will expedite data collection, and encourage the recruitment of participants from populations that were previously difficult to study in scanning environments. I foresee that brief neurophysiological recordings may catalyze innovation in the neuroscience of aging, neurological and mental illness, and neurodevelopment. Brief neurophysiological recording may also benefit brain-behaviour research, as scientists estimate that brain-wide association studies (BWAS) methods may require thousands of individuals to achieve adequate statistical power (Button et al., 2013; Marek et al., 2022; Spisak et al., 2023).

Novel wearable optically pumped magnetencephalography recording technology may further accelerate progress in naturalistic real-world scanning environments (Boto et al., 2018; Brookes et al., 2022; Hill et al., 2020) allowing researchers access to previously difficult-to-sample populations. Whether brief recordings of MEG brain activity are equally stable with optically pumped sensors remains an open question.

## Future of open neuroimaging data: longitudinal brain charts

Recent efforts have proposed the notion of brain-charts: Population norms of brain structure across neurodevelopment (Bethlehem et al., 2022). Like their pediatric growth-chart equivalents, the goal of brain-charts is early screening of neurological and mental health diseases based on age-matched norms of the brains morphology. The benefits of such an approach for functional brain imaging have yet to be explored. In addition, little work to date has examined developmental norms of brain variability. Brain-fingerprinting may complement such efforts.

I propose that longitudinal functional brain imaging data may help scientists in this screening endeavour. Beyond comparing individuals to population norms, assessing the trajectory of individuals and the relative stability of brain activity may index health. Preliminary evidence—some of which is reported within this dissertation—suggests that neurodegenerative disorders may destabilize brain activity in the short term, making individuals less differentiable from their brain activity (da Silva Castanheira et al., 2023; Kaufmann et al., 2017a, 2018a; Troisi Lopez et al., 2023). This research could be expanded to assess the utility of longitudinal brain-fingerprint assessments in pre-clinical screening of diseases. This is especially relevant for neurodegenerative diseases because older adults do not show an equivalent destabilization of their brain-fingerprints with age (Chapter 3), thus the decreased stability (increased variability) of brain activity may be a biomarker of neurodegeneration.

Beyond neurological conditions, longitudinal brain fingerprinting may clarify how major life events and stressors impact brain health. Previous work suggests that trauma, major stressors, and resulting chronic activation of the HPA axis alter brain structure and function (Bremner, 2006; Herringa, 2017; Karl et al., 2006; Shields et al., 2016). Brain-fingerprinting may offer a unique opportunity to study how life stressors may impact brain function and health. With large enough data volumes, population neuroscience could study how stress affects the brain-fingerprint, which in turn may predict the future well-being of an individual.

Like the fingerprints left by your hand, the brain-fingerprint is stable and differentiates between individuals. The brain-fingerprinting method, presented in this dissertation, shows great potential in exploring questions concerning the biological underpinnings of the self. The findings of this thesis expand upon the electrophysiological origins of characteristic brain activity, across

several populations, and demonstrate their utility in predicting behaviours and disease progression. I present evidence corroborating that diversity in brain activity across individuals is meaningful and should be studied. I bridge data across the microscale, mesoscale, and behaviour to demonstrate how genetics and neurochemistry relate to inter-individual variability of brain activity. Taken together, I anticipate that the results presented herein will inspire future research exploring the biological origins of the self, to answer the question: “What makes us unique?”.

# References


Alexander-Bloch, A. F., Raznahan, A., Vandekar, S. N., Seidlitz, J., Lu, Z., Mathias, S. R., Knowles, E., Mollon, J., Rodrigue, A., Curran, J. E., Görring, H. H. H., Satterthwaite, T. D., Gur, R. E., Bassett, D. S., Hoftman, G. D., Pearlson, G., Shinohara, R. T., Liu, S., Fox, P. T., … Glahn, D. C. (2020). Imaging local genetic influences on cortical folding. *Proceedings of the National Academy of Sciences*, *117*(13), 7430–7436. https://doi.org/10.1073/pnas.1912064117

Alexopoulos, G. S. (2019). Mechanisms and treatment of late-life depression. *Translational Psychiatry*, *9*(1), 188. https://doi.org/10.1038/s41398-019-0514-6

Amico, E., & Goñi, J. (2018a). The quest for identifiability in human functional connectomes. *Scientific Reports*, *8*(1), Article 1. https://doi.org/10.1038/s41598-018-25089-1

Amico, E., & Goñi, J. (2018b). The quest for identifiability in human functional connectomes. *Scientific Reports*, *8*(1), 8254. https://doi.org/10.1038/s41598-018-25089-1

Andrews-Hanna, J. R., Snyder, A. Z., Vincent, J. L., Lustig, C., Head, D., Raichle, M. E., & Buckner, R. L. (2007). Disruption of Large-Scale Brain Systems in Advanced Aging. *Neuron*, *56*(5), 924–935. https://doi.org/10.1016/j.neuron.2007.10.038

Araujo, J. A., Studzinski, C. M., & Milgram, N. W. (2005). Further evidence for the cholinergic hypothesis of aging and dementia from the canine model of aging. *Progress in Neuro-Psychopharmacology and Biological Psychiatry*, *29*(3), 411–422. https://doi.org/10.1016/j.pnpbp.2004.12.008

Arnatkevičiūtė, A., Fulcher, B. D., & Fornito, A. (2019). A practical guide to linking brain-wide gene expression and neuroimaging data. *NeuroImage*, *189*, 353–367. https://doi.org/10.1016/j.neuroimage.2019.01.011

Babiloni, C., Binetti, G., Cassarino, A., Dal Forno, G., Del Percio, C., Ferreri, F., Ferri, R., Frisoni, G., Galderisi, S., Hirata, K., Lanuzza, B., Miniussi, C., Mucci, A., Nobili, F., Rodriguez, G., Luca Romani, G., & Rossini, P. M. (2006). Sources of cortical rhythms in adults during physiological aging: A multicentric EEG study. *Human Brain Mapping*, *27*(2), 162–172. https://doi.org/10.1002/hbm.20175

Baek, E. C., Hyon, R., López, K., Finn, E. S., Porter, M. A., & Parkinson, C. (2022). In-degree centrality in a social network is linked to coordinated neural activity. *Nature Communications*, *13*(1), Article 1. https://doi.org/10.1038/s41467-022-28432-3

Bagherzadeh, Y., Baldauf, D., Pantazis, D., & Desimone, R. (2020). Alpha Synchrony and the Neurofeedback Control of Spatial Attention. *Neuron*, *105*(3), 577-587.e5. https://doi.org/10.1016/j.neuron.2019.11.001

Baillet, S. (2017). Magnetoencephalography for brain electrophysiology and imaging. *Nature Neuroscience*, *20*(3), Article 3. https://doi.org/10.1038/nn.4504

Baillet, S., Mosher, J. C., & Leahy, R. M. (2001). Electromagnetic brain mapping. *IEEE Signal Processing Magazine*, *18*(6), 14–30. https://doi.org/10.1109/79.962275

Balestrieri, E., & Busch, N. A. (2022). Spontaneous Alpha-Band Oscillations Bias Subjective Contrast Perception. *Journal of Neuroscience*, *42*(25), 5058–5069. https://doi.org/10.1523/JNEUROSCI.1972-21.2022

Baracchini, G., Zhou, Y., Castanheira, J. D. S., Hansen, J. Y., Rieck, J., Turner, G. R., Grady, C. L., Misic, B., Nomi, J., Uddin, L. Q., & Spreng, R. N. (2023). *The biological role of local and global fMRI BOLD signal variability in human brain organization* [Preprint]. Neuroscience. https://doi.org/10.1101/2023.10.22.563476

Bari, S., Amico, E., Vike, N., Talavage, T. M., & Goñi, J. (2019). Uncovering multi-site identifiability based on resting-state functional connectomes. *NeuroImage*, *202*, 115967. https://doi.org/10.1016/j.neuroimage.2019.06.045

Başar, E. (1990). *Chaos in Brain Function: Containing Original Chapters by E. Basar and T. H. Bullock and Topical Articles Reprinted from the Springer Series in Brain Dynamics*. Springer Berlin Heidelberg.

Belova, E. M., Semenova, U., Gamaleya, A. A., Tomskiy, A. A., & Sedov, A. (2021). Voluntary movements cause beta oscillations increase and broadband slope decrease in the subthalamic nucleus of parkinsonian patients. *European Journal of Neuroscience*, *53*(7), 2205–2213. https://doi.org/10.1111/ejn.14715

Bethlehem, R. a. I., Seidlitz, J., White, S. R., Vogel, J. W., Anderson, K. M., Adamson, C., Adler, S., Alexopoulos, G. S., Anagnostou, E., Areces-Gonzalez, A., Astle, D. E., Auyeung, B., Ayub, M., Bae, J., Ball, G., Baron-Cohen, S., Beare, R., Bedford, S. A., Benegal, V., … Alexander-Bloch, A. F. (2022). Brain charts for the human lifespan. *Nature*, *604*(7906), Article 7906. https://doi.org/10.1038/s41586-022-04554-y

Betzel, R. F., Medaglia, J. D., Kahn, A. E., Soffer, J., Schonhaut, D. R., & Bassett, D. S. (2019). Structural, geometric and genetic factors predict interregional brain connectivity patterns

probed by electrocorticography. *Nature Biomedical Engineering*, *3*(11), Article 11. https://doi.org/10.1038/s41551-019-0404-5

Bodenmann, S., Rusterholz, T., Dürr, R., Stoll, C., Bachmann, V., Geissler, E., Jaggi-Schwarz, K., & Landolt, H.-P. (2009). The Functional Val158Met Polymorphism of COMT Predicts Interindividual Differences in Brain α Oscillations in Young Men. *Journal of Neuroscience*, *29*(35), 10855–10862. https://doi.org/10.1523/JNEUROSCI.1427-09.2009

Boon, L. I., Geraedts, V. J., Hillebrand, A., Tannemaat, M. R., Contarino, M. F., Stam, C. J., & Berendse, H. W. (2019). A systematic review of MEG-based studies in Parkinson's disease: The motor system and beyond. *Human Brain Mapping*, *40*(9), 2827–2848. https://doi.org/10.1002/hbm.24562

Borodovitsyna, O., Flamini, M., & Chandler, D. (2017). Noradrenergic Modulation of Cognition in Health and Disease. *Neural Plasticity*, *2017*, 6031478. https://doi.org/10.1155/2017/6031478

Bosboom, J. L. W., Stoffers, D., Stam, C. J., van Dijk, B. W., Verbunt, J., Berendse, H. W., & Wolters, E. Ch. (2006). Resting state oscillatory brain dynamics in Parkinson's disease: An MEG study. *Clinical Neurophysiology*, *117*(11), 2521–2531. https://doi.org/10.1016/j.clinph.2006.06.720

Boto, E., Holmes, N., Leggett, J., Roberts, G., Shah, V., Meyer, S. S., Muñoz, L. D., Mullinger, K. J., Tierney, T. M., Bestmann, S., Barnes, G. R., Bowtell, R., & Brookes, M. J. (2018). Moving magnetoencephalography towards real-world applications with a wearable system. *Nature*, *555*(7698), Article 7698. https://doi.org/10.1038/nature26147

Bouchard, T. J., & McGue, M. (2003). Genetic and environmental influences on human psychological differences. *Journal of Neurobiology*, *54*(1), 4–45. https://doi.org/10.1002/neu.10160

Bremner, J. D. (2006). Traumatic stress: Effects on the brain. *Dialogues in Clinical Neuroscience*, *8*(4), 445–461.

Briley, D. A., & Tucker-Drob, E. M. (2017). Comparing the Developmental Genetics of Cognition and Personality over the Lifespan. *Journal of Personality*, *85*(1), 51–64. https://doi.org/10.1111/jopy.12186

Brookes, M. J., Hale, J. R., Zumer, J. M., Stevenson, C. M., Francis, S. T., Barnes, G. R., Owen, J. P., Morris, P. G., & Nagarajan, S. S. (2011). Measuring functional connectivity using MEG: Methodology and comparison with fcMRI. *Neuroimage*, *56*(3), 1082–1104. https://doi.org/10.1016/j.neuroimage.2011.02.054

Brookes, M. J., Leggett, J., Rea, M., Hill, R. M., Holmes, N., Boto, E., & Bowtell, R. (2022). Magnetoencephalography with optically pumped magnetometers (OPM-MEG): The next generation of functional neuroimaging. *Trends in Neurosciences*, *45*(8), 621–634. https://doi.org/10.1016/j.tins.2022.05.008

Brookes, M. J., Woolrich, M., Luckhoo, H., Price, D., Hale, J. R., Stephenson, M. C., Barnes, G. R., Smith, S. M., & Morris, P. G. (2011). Investigating the electrophysiological basis of resting state networks using magnetoencephalography. *Proceedings of the National Academy of Sciences*, *108*(40), 16783–16788. https://doi.org/10.1073/pnas.1112685108

Brotchie, J. (2003). CB cannabinoid receptor signalling in Parkinson's disease. *Current Opinion in Pharmacology*, *3*(1), 54–61. https://doi.org/10.1016/S1471-4892(02)00011-5

Bruns, A., Eckhorn, R., Jokeit, H., & Ebner, A. (2000). Amplitude envelope correlation detects coupling among incoherent brain signals. *Neuroreport*, *11*(7), 1509–1514.

Bullmore, E., & Sporns, O. (2012). The economy of brain network organization. *Nature Reviews Neuroscience*, *13*(5), Article 5. https://doi.org/10.1038/nrn3214

Buolamwini, J., & Gebru, T. (2018). Gender Shades: Intersectional Accuracy Disparities in Commercial Gender Classification. *Proceedings of the 1st Conference on Fairness, Accountability and Transparency*, 77–91. https://proceedings.mlr.press/v81/buolamwini18a.html

Burt, J. B., Demirtaş, M., Eckner, W. J., Navejar, N. M., Ji, J. L., Martin, W. J., Bernacchia, A., Anticevic, A., & Murray, J. D. (2018). Hierarchy of transcriptomic specialization across human cortex captured by structural neuroimaging topography. *Nature Neuroscience*, *21*(9), 1251–1259. https://doi.org/10.1038/s41593-018-0195-0

Burton, C. L., Strauss, E., Hultsch, D. F., Moll, A., & Hunter, M. A. (2006a). Intraindividual Variability as a Marker of Neurological Dysfunction: A Comparison of Alzheimer's Disease and Parkinson's Disease. *Journal of Clinical and Experimental Neuropsychology*, *28*(1), 67–83. https://doi.org/10.1080/13803390490918318

Burton, C. L., Strauss, E., Hultsch, D. F., Moll, A., & Hunter, M. A. (2006b). Intraindividual Variability as a Marker of Neurological Dysfunction: A Comparison of Alzheimer's Disease and Parkinson's Disease. *Journal of Clinical and Experimental Neuropsychology*, *28*(1), Article 1. https://doi.org/10.1080/13803390490918318

Bush, G., Luu, P., & Posner, M. I. (2000). Cognitive and emotional influences in anterior cingulate cortex. *Trends in Cognitive Sciences*, *4*(6), 215–222. https://doi.org/10.1016/s1364-6613(00)01483-2

Button, K. S., Ioannidis, J. P. A., Mokrysz, C., Nosek, B. A., Flint, J., Robinson, E. S. J., & Munafò, M. R. (2013). Power failure: Why small sample size undermines the reliability of neuroscience. *Nature Reviews Neuroscience*, *14*(5), Article 5. https://doi.org/10.1038/nrn3475

Cabral, J., Kringelbach, M. L., & Deco, G. (2017). Functional connectivity dynamically evolves on multiple time-scales over a static structural connectome: Models and mechanisms. *NeuroImage*, *160*, 84–96. https://doi.org/10.1016/j.neuroimage.2017.03.045

Cai, H., Zhu, J., & Yu, Y. (2020). Robust prediction of individual personality from brain functional connectome. *Social Cognitive and Affective Neuroscience*, *15*(3), 359–369. https://doi.org/10.1093/scan/nsaa044

Cattell, R. B. (1963). Theory of fluid and crystallized intelligence: A critical experiment. *Journal of Educational Psychology*, *54*(1), 1–22. https://doi.org/10.1037/h0046743

Cattell, R. B. (1971). *Abilities: Their structure, growth, and action* (pp. xxii, 583). Houghton Mifflin.

Cavanagh, J. F., & Frank, M. J. (2014). Frontal theta as a mechanism for cognitive control. *Trends in Cognitive Sciences*, *18*(8), 414–421. https://doi.org/10.1016/j.tics.2014.04.012

Chalermpalanupap, T., Kinkead, B., Hu, W. T., Kummer, M. P., Hammerschmidt, T., Heneka, M. T., Weinshenker, D., & Levey, A. I. (2013). Targeting norepinephrine in mild cognitive impairment and Alzheimer's disease. *Alzheimer's Research & Therapy*, *5*(2), 21. https://doi.org/10.1186/alzrt175

Chase, H., Boudewyn, M., Carter, C., & Phillips, M. (2019). Transcranial direct current stimulation: A roadmap for research, from mechanism of action to clinical implementation. *Molecular Psychiatry*, *25*. https://doi.org/10.1038/s41380-019-0499-9

Chen, K.-H., Okerstrom, K. L., Kingyon, J. R., Anderson, S. W., Cavanagh, J. F., & Narayanan, N. S. (2016). Startle Habituation and Midfrontal Theta Activity in Parkinson Disease. *Journal of Cognitive Neuroscience*, *28*(12), 1923–1932. https://doi.org/10.1162/jocn_a_01012

Chini, M., Pfeffer, T., & Hanganu-Opatz, I. (2022). An increase of inhibition drives the developmental decorrelation of neural activity. *eLife*, *11*, e78811. https://doi.org/10.7554/eLife.78811

Chong, J. S. X., Ng, K. K., Tandi, J., Wang, C., Poh, J.-H., Lo, J. C., Chee, M. W. L., & Zhou, J. H. (2019). Longitudinal Changes in the Cerebral Cortex Functional Organization of Healthy Elderly. *Journal of Neuroscience*, *39*(28), 5534–5550. https://doi.org/10.1523/JNEUROSCI.1451-18.2019

Chou, Y., Hickey, P. T., Sundman, M., Song, A. W., & Chen, N. (2015). Effects of Repetitive Transcranial Magnetic Stimulation on Motor Symptoms in Parkinson Disease. *JAMA Neurology*, *72*(4), 432–440. https://doi.org/10.1001/jamaneurol.2014.4380

Chung, C. L., & Mak, M. K. Y. (2016). Effect of Repetitive Transcranial Magnetic Stimulation on Physical Function and Motor Signs in Parkinson's Disease: A Systematic Review and Meta-Analysis. *Brain Stimulation*, *9*(4), 475–487. https://doi.org/10.1016/j.brs.2016.03.017

Clark, D. L., Khalil, T., Kim, L. H., Noor, M. S., Luo, F., & Kiss, Z. HT. (2023). Aperiodic subthalamic activity predicts motor severity and stimulation response in Parkinson disease.

*Parkinsonism & Related Disorders*, *110*, 105397. https://doi.org/10.1016/j.parkreldis.2023.105397

Clayton, M. S., Yeung, N., & Cohen Kadosh, R. (2018). The many characters of visual alpha oscillations. *The European Journal of Neuroscience*, *48*(7), 2498–2508. https://doi.org/10.1111/ejn.13747

Cole, D. M., Smith, S. M., & Beckmann, C. F. (2010). Advances and pitfalls in the analysis and interpretation of resting-state FMRI data. *Frontiers in Systems Neuroscience*, *4*, 8. https://doi.org/10.3389/fnsys.2010.00008

Colombo, M. A., Napolitani, M., Boly, M., Gosseries, O., Casarotto, S., Rosanova, M., Brichant, J.-F., Boveroux, P., Rex, S., Laureys, S., Massimini, M., Chieregato, A., & Sarasso, S. (2019). The spectral exponent of the resting EEG indexes the presence of consciousness during unresponsiveness induced by propofol, xenon, and ketamine. *NeuroImage*, *189*, 631–644. https://doi.org/10.1016/j.neuroimage.2019.01.024

Costa, A. S., Dogan, I., Schulz, J. B., & Reetz, K. (2019a). Going beyond the mean: Intraindividual variability of cognitive performance in prodromal and early neurodegenerative disorders. *The Clinical Neuropsychologist*, *33*(2), Article 2. https://doi.org/10.1080/13854046.2018.1533587

Costa, A. S., Dogan, I., Schulz, J. B., & Reetz, K. (2019b). Going beyond the mean: Intraindividual variability of cognitive performance in prodromal and early neurodegenerative disorders. *The Clinical Neuropsychologist*, *33*(2), 369–389. https://doi.org/10.1080/13854046.2018.1533587

Cribbs, D. H., Berchtold, N. C., Perreau, V., Coleman, P. D., Rogers, J., Tenner, A. J., & Cotman, C. W. (2012). Extensive innate immune gene activation accompanies brain aging, increasing vulnerability to cognitive decline and neurodegeneration: A microarray study. *Journal of Neuroinflammation*, *9*(1), 179. https://doi.org/10.1186/1742-2094-9-179

da Silva Castanheira, J., Orozco Perez, H. D., Misic, B., & Baillet, S. (2021). Brief segments of neurophysiological activity enable individual differentiation. *Nature Communications*, *12*(1), Article 1. https://doi.org/10.1038/s41467-021-25895-8

da Silva Castanheira, J., Wiesman, A. I., Hansen, J. Y., Misic, B., Baillet, S., PREVENT-AD Research Group, & Quebec Parkinson Network. (2023). Neurophysiological brain-fingerprints of motor and cognitive decline in Parkinson's disease. *medRxiv: The Preprint Server for Health Sciences*, 2023.02.03.23285441. https://doi.org/10.1101/2023.02.03.23285441

Damoiseaux, J. S., Beckmann, C. F., Arigita, E. J. S., Barkhof, F., Scheltens, P., Stam, C. J., Smith, S. M., & Rombouts, S. a. R. B. (2008). Reduced resting-state brain activity in the "default network" in normal aging. *Cerebral Cortex (New York, N.Y.: 1991)*, *18*(8), 1856–1864. https://doi.org/10.1093/cercor/bhm207

Darmani, G., Drummond, N. M., Ramezanpour, H., Saha, U., Hoque, T., Udupa, K., Sarica, C., Zeng, K., Cortez Grippe, T., Nankoo, J.-F., Bergmann, T. O., Hodaie, M., Kalia, S. K., Lozano, A. M., Hutchison, W. D., Fasano, A., & Chen, R. (2023). Long-Term Recording of Subthalamic Aperiodic Activities and Beta Bursts in Parkinson's Disease. *Movement Disorders*, *38*(2), 232–243. https://doi.org/10.1002/mds.29276

Darmanis, S., Sloan, S. A., Zhang, Y., Enge, M., Caneda, C., Shuer, L. M., Hayden Gephart, M. G., Barres, B. A., & Quake, S. R. (2015). A survey of human brain transcriptome diversity at

the single cell level. *Proceedings of the National Academy of Sciences*, *112*(23), 7285–7290. https://doi.org/10.1073/pnas.1507125112

De Gennaro, L., Marzano, C., Fratello, F., Moroni, F., Pellicciari, M. C., Ferlazzo, F., Costa, S., Couyoumdjian, A., Curcio, G., Sforza, E., Malafosse, A., Finelli, L. A., Pasqualetti, P., Ferrara, M., Bertini, M., & Rossini, P. M. (2008). The electroencephalographic fingerprint of sleep is genetically determined: A twin study. *Annals of Neurology*, *64*(4), 455–460. https://doi.org/10.1002/ana.21434

de Souza Rodrigues, J., Ribeiro, F. L., Sato, J. R., Mesquita, R. C., & Júnior, C. E. B. (2019). Identifying individuals using fNIRS-based cortical connectomes. *Biomedical Optics Express*, *10*(6), 2889–2897. https://doi.org/10.1364/BOE.10.002889

Del Tredici, K., & Braak, H. (2013). Dysfunction of the locus coeruleus-norepinephrine system and related circuitry in Parkinson's disease-related dementia. *Journal of Neurology, Neurosurgery, and Psychiatry*, *84*(7), 774–783. https://doi.org/10.1136/jnnp-2011-301817

Delaveau, P., Salgado-Pineda, P., Fossati, P., Witjas, T., Azulay, J.-P., & Blin, O. (2010). Dopaminergic modulation of the default mode network in Parkinson's disease. *European Neuropsychopharmacology*, *20*(11), 784–792. https://doi.org/10.1016/j.euroneuro.2010.07.001

Desikan, R. S., Ségonne, F., Fischl, B., Quinn, B. T., Dickerson, B. C., Blacker, D., Buckner, R. L., Dale, A. M., Maguire, R. P., Hyman, B. T., Albert, M. S., & Killiany, R. J. (2006a). An automated labeling system for subdividing the human cerebral cortex on MRI scans into gyral based

regions of interest. *NeuroImage*, *31*(3), 968–980. https://doi.org/10.1016/j.neuroimage.2006.01.021

Desikan, R. S., Ségonne, F., Fischl, B., Quinn, B. T., Dickerson, B. C., Blacker, D., Buckner, R. L., Dale, A. M., Maguire, R. P., Hyman, B. T., Albert, M. S., & Killiany, R. J. (2006b). An automated labeling system for subdividing the human cerebral cortex on MRI scans into gyral based regions of interest. *NeuroImage*, *31*(3), 968–980. https://doi.org/10.1016/j.neuroimage.2006.01.021

Devilbiss, D. M., Page, M. E., & Waterhouse, B. D. (2006). Locus Ceruleus Regulates Sensory Encoding by Neurons and Networks in Waking Animals. *The Journal of Neuroscience*, *26*(39), 9860–9872. https://doi.org/10.1523/JNEUROSCI.1776-06.2006

Deza-Araujo, Y. I., Baez-Lugo, S., Vuilleumier, P., Chocat, A., Chételat, G., Poisnel, G., & Klimecki, O. M. (2021). Whole blood serotonin levels in healthy elderly are negatively associated with the functional activity of emotion-related brain regions. *Biological Psychology*, *160*, 108051. https://doi.org/10.1016/j.biopsycho.2021.108051

Díez-Cirarda, M., Strafella, A. P., Kim, J., Peña, J., Ojeda, N., Cabrera-Zubizarreta, A., & Ibarretxe-Bilbao, N. (2018). Dynamic functional connectivity in Parkinson's disease patients with mild cognitive impairment and normal cognition. *NeuroImage: Clinical*, *17*, 847–855. https://doi.org/10.1016/j.nicl.2017.12.013

Donoghue, T., Haller, M., Peterson, E. J., Varma, P., Sebastian, P., Gao, R., Noto, T., Lara, A. H., Wallis, J. D., Knight, R. T., Shestyuk, A., & Voytek, B. (2020a). Parameterizing neural power spectra into periodic and aperiodic components. *Nature Neuroscience*, *23*(12), Article 12. https://doi.org/10.1038/s41593-020-00744-x

Donoghue, T., Haller, M., Peterson, E. J., Varma, P., Sebastian, P., Gao, R., Noto, T., Lara, A. H., Wallis, J. D., Knight, R. T., Shestyuk, A., & Voytek, B. (2020b). Parameterizing neural power spectra into periodic and aperiodic components. *Nature Neuroscience*, *23*(12), Article 12. https://doi.org/10.1038/s41593-020-00744-x

Donoghue, T., Haller, M., Peterson, E. J., Varma, P., Sebastian, P., Gao, R., Noto, T., Lara, A. H., Wallis, J. D., Knight, R. T., Shestyuk, A., & Voytek, B. (2020c). Parameterizing neural power spectra into periodic and aperiodic components. *Nature Neuroscience*, *23*(12), 1655–1665. https://doi.org/10.1038/s41593-020-00744-x

Driessens, S. L. W., Galakhova, A. A., Heyer, D. B., Pieterse, I. J., Wilbers, R., Mertens, E. J., Waleboer, F., Heistek, T. S., Coenen, L., Meijer, J. R., Idema, S., De Witt Hamer, P. C., Noske, D. P., De Kock, C. P. J., Lee, B. R., Smith, K., Ting, J. T., Lein, E. S., Mansvelder, H. D., & Goriounova, N. A. (2023). Genes associated with cognitive ability and HAR show overlapping expression patterns in human cortical neuron types. *Nature Communications*, *14*(1), 4188. https://doi.org/10.1038/s41467-023-39946-9

Dubois, J., & Adolphs, R. (2016). Building a Science of Individual Differences from fMRI. *Trends in Cognitive Sciences*, *20*(6), 425–443. https://doi.org/10.1016/j.tics.2016.03.014

Dumas, J. A., & Newhouse, P. A. (2011). The Cholinergic Hypothesis of Cognitive Aging Revisited Again: Cholinergic Functional Compensation. *Pharmacology, Biochemistry, and Behavior*, *99*(2), 254–261. https://doi.org/10.1016/j.pbb.2011.02.022

Duncan, S., & Barrett, L. F. (2007). Affect is a form of cognition: A neurobiological analysis. *Cognition & Emotion*, *21*(6), 1184–1211. https://doi.org/10.1080/02699930701437931

*EEG Fingerprints: Phase Synchronization of EEG Signals as Biomarker for Subject Identification | IEEE Journals & Magazine | IEEE Xplore*. (n.d.). Retrieved June 30, 2023, from https://ieeexplore.ieee.org/document/8779640

Erraji-Benchekroun, L., Underwood, M. D., Arango, V., Galfalvy, H., Pavlidis, P., Smyrniotopoulos, P., Mann, J. J., & Sibille, E. (2005). Molecular aging in human prefrontal cortex is selective and continuous throughout adult life. *Biological Psychiatry*, *57*(5), 549–558. https://doi.org/10.1016/j.biopsych.2004.10.034

Falconer, D. S. (1965). The inheritance of liability to certain diseases, estimated from the incidence among relatives. *Annals of Human Genetics*, *29*(1), 51–76. https://doi.org/10.1111/j.1469-1809.1965.tb00500.x

Favaro, J., Colombo, M. A., Mikulan, E., Sartori, S., Nosadini, M., Pelizza, M. F., Rosanova, M., Sarasso, S., Massimini, M., & Toldo, I. (2023). The maturation of aperiodic EEG activity across development reveals a progressive differentiation of wakefulness from sleep. *NeuroImage*, *277*, 120264. https://doi.org/10.1016/j.neuroimage.2023.120264

Finn, E. S., Shen, X., Scheinost, D., Rosenberg, M. D., Huang, J., Chun, M. M., Papademetris, X., & Constable, R. T. (2015a). Functional connectome fingerprinting: Identifying individuals using patterns of brain connectivity. *Nature Neuroscience*, *18*(11), Article 11. https://doi.org/10.1038/nn.4135

Finn, E. S., Shen, X., Scheinost, D., Rosenberg, M. D., Huang, J., Chun, M. M., Papademetris, X., & Constable, R. T. (2015b). Functional connectome fingerprinting: Identifying individuals using patterns of brain connectivity. *Nature Neuroscience*, *18*(11), 1664–1671. https://doi.org/10.1038/nn.4135

Fiorenzato, E., Strafella, A. P., Kim, J., Schifano, R., Weis, L., Antonini, A., & Biundo, R. (2019). Dynamic functional connectivity changes associated with dementia in Parkinson's disease. *Brain*, *142*(9), 2860–2872. https://doi.org/10.1093/brain/awz192

Fischl, B. (2012). FreeSurfer. *NeuroImage*, *62*(2), 774–781. https://doi.org/10.1016/j.neuroimage.2012.01.021

Florin, E., & Baillet, S. (2015). The brain's resting-state activity is shaped by synchronized cross-frequency coupling of neural oscillations. *NeuroImage*, *111*, 26–35. https://doi.org/10.1016/j.neuroimage.2015.01.054

Forgas, J. P. (2008). Affect and Cognition. *Perspectives on Psychological Science*, *3*(2), 94–101.

Fornito, A., Zalesky, A., Bassett, D. S., Meunier, D., Ellison-Wright, I., Yucel, M., Wood, S. J., Shaw, K., O'Connor, J., Nertney, D., Mowry, B. J., Pantelis, C., & Bullmore, E. T. (2011). Genetic Influences on Cost-Efficient Organization of Human Cortical Functional Networks. *Journal of Neuroscience*, *31*(9), Article 9. https://doi.org/10.1523/JNEUROSCI.4858-10.2011

Foster, J. J., & Awh, E. (2019). The role of alpha oscillations in spatial attention: Limited evidence for a suppression account. *Current Opinion in Psychology*, *29*, 34–40. https://doi.org/10.1016/j.copsyc.2018.11.001

Fraschini, M., Hillebrand, A., Demuru, M., Didaci, L., & Marcialis, G. L. (2015). An EEG-Based Biometric System Using Eigenvector Centrality in Resting State Brain Networks. *IEEE Signal Processing Letters*, *22*(6), 666–670. https://doi.org/10.1109/LSP.2014.2367091

Fu, Y., Ma, Z., Hamilton, C., Liang, Z., Hou, X., Ma, X., Hu, X., He, Q., Deng, W., Wang, Y., Zhao, L., Meng, H., Li, T., & Zhang, N. (2015). Genetic influences on resting-state functional

networks: *A twin study*: Genetic Influences on Resting-State Functional Networks. *Human Brain Mapping*, *36*(10), Article 10. https://doi.org/10.1002/hbm.22890

Fulcher, B. D., & Fornito, A. (2016). A transcriptional signature of hub connectivity in the mouse connectome. *Proceedings of the National Academy of Sciences*, *113*(5), 1435–1440. https://doi.org/10.1073/pnas.1513302113

Fulcher, B. D., Little, M. A., & Jones, N. S. (2013). Highly comparative time-series analysis: The empirical structure of time series and their methods. *Journal of The Royal Society Interface*, *10*(83), 20130048. https://doi.org/10.1098/rsif.2013.0048

Fulcher, B. D., Murray, J. D., Zerbi, V., & Wang, X.-J. (2019). Multimodal gradients across mouse cortex. *Proceedings of the National Academy of Sciences*, *116*(10), 4689–4695. https://doi.org/10.1073/pnas.1814144116

Gan-Or, Z., Rao, T., Leveille, E., Degroot, C., Chouinard, S., Cicchetti, F., Dagher, A., Das, S., Desautels, A., Drouin-Ouellet, J., Durcan, T., Gagnon, J.-F., Genge, A., Karamchandani, J., Lafontaine, A.-L., Sun, S. L. W., Langlois, M., Levesque, M., Melmed, C., … Fon, E. A. (2020). The Quebec Parkinson Network: A Researcher-Patient Matching Platform and Multimodal Biorepository. *Journal of Parkinson's Disease*, *10*(1), 301–313. https://doi.org/10.3233/JPD-191775

Gao, M., Wong, C. H. Y., Huang, H., Shao, R., Huang, R., Chan, C. C. H., & Lee, T. M. C. (2020). Connectome-based models can predict processing speed in older adults. *NeuroImage*, *223*, 117290. https://doi.org/10.1016/j.neuroimage.2020.117290

Gao, R., Peterson, E. J., & Voytek, B. (2017). Inferring synaptic excitation/inhibition balance from field potentials. *NeuroImage*, *158*, 70–78. https://doi.org/10.1016/j.neuroimage.2017.06.078

Garrett, D. D., Kovacevic, N., McIntosh, A. R., & Grady, C. L. (2010). Blood Oxygen Level-Dependent Signal Variability Is More than Just Noise. *Journal of Neuroscience*, *30*(14), 4914–4921. https://doi.org/10.1523/JNEUROSCI.5166-09.2010

Garrett, D. D., Kovacevic, N., McIntosh, A. R., & Grady, C. L. (2011). The Importance of Being Variable. *Journal of Neuroscience*, *31*(12), 4496–4503. https://doi.org/10.1523/JNEUROSCI.5641-10.2011

Garrett, D. D., Kovacevic, N., McIntosh, A. R., & Grady, C. L. (2013). The modulation of BOLD variability between cognitive states varies by age and processing speed. *Cerebral Cortex (New York, N.Y.: 1991)*, *23*(3), 684–693. https://doi.org/10.1093/cercor/bhs055

Garrett, D. D., Samanez-Larkin, G. R., MacDonald, S. W. S., Lindenberger, U., McIntosh, A. R., & Grady, C. L. (2013). Moment-to-moment brain signal variability: A next frontier in human brain mapping? *Neuroscience and Biobehavioral Reviews*, *37*(4), 610–624. https://doi.org/10.1016/j.neubiorev.2013.02.015

Ge, S. X., Jung, D., & Yao, R. (2020). ShinyGO: A graphical gene-set enrichment tool for animals and plants. *Bioinformatics*, *36*(8), 2628–2629. https://doi.org/10.1093/bioinformatics/btz931

Geraedts, V. J., Boon, L. I., Marinus, J., Gouw, A. A., van Hilten, J. J., Stam, C. J., Tannemaat, M. R., & Contarino, M. F. (2018). Clinical correlates of quantitative EEG in Parkinson disease: A

systematic review. *Neurology*, *91*(19), 871–883. https://doi.org/10.1212/WNL.0000000000006473

Gerdeman, G. L., Ronesi, J., & Lovinger, D. M. (2002). Postsynaptic endocannabinoid release is critical to long-term depression in the striatum. *Nature Neuroscience*, *5*(5), 446–451. https://doi.org/10.1038/nn832

Girskis, K. M., Stergachis, A. B., DeGennaro, E. M., Doan, R. N., Qian, X., Johnson, M. B., Wang, P. P., Sejourne, G. M., Nagy, M. A., Pollina, E. A., Sousa, A. M. M., Shin, T., Kenny, C. J., Scotellaro, J. L., Debo, B. M., Gonzalez, D. M., Rento, L. M., Yeh, R. C., Song, J. H. T., … Walsh, C. A. (2021). Rewiring of human neurodevelopmental gene regulatory programs by human accelerated regions. *Neuron*, *109*(20), 3239-3251.e7. https://doi.org/10.1016/j.neuron.2021.08.005

Glahn, D. C., Winkler, A. M., Kochunov, P., Almasy, L., Duggirala, R., Carless, M. A., Curran, J. C., Olvera, R. L., Laird, A. R., Smith, S. M., Beckmann, C. F., Fox, P. T., & Blangero, J. (2010). Genetic control over the resting brain. *Proceedings of the National Academy of Sciences*, *107*(3), Article 3. https://doi.org/10.1073/pnas.0909969107

Gnambs, T. (2014). A meta-analysis of dependability coefficients (test–retest reliabilities) for measures of the Big Five. *Journal of Research in Personality*, *52*, 20–28. https://doi.org/10.1016/j.jrp.2014.06.003

Gnambs, T. (2016). Sociodemographic effects on the test-retest reliability of the Big Five Inventory. *European Journal of Psychological Assessment*, *32*(4), 307–311. https://doi.org/10.1027/1015-5759/a000259

Goetz, C. G., Poewe, W., Rascol, O., Sampaio, C., Stebbins, G. T., Counsell, C., Giladi, N., Holloway, R. G., Moore, C. G., Wenning, G. K., Yahr, M. D., & Seidl, L. (2004). *Movement* Disorder Society Task Force report on the Hoehn and Yahr staging scale: Status and recommendations The *Movement* Disorder Society Task Force on rating scales for Parkinson's disease. *Movement Disorders*, *19*(9), 1020–1028. https://doi.org/10.1002/mds.20213

Goh, J. O. S. (2011). Functional Dedifferentiation and Altered Connectivity in Older Adults: Neural Accounts of Cognitive Aging. *Aging and Disease*, *2*(1), 30–48.

Goodkind, M., Eickhoff, S. B., Oathes, D. J., Jiang, Y., Chang, A., Jones-Hagata, L. B., Ortega, B. N., Zaiko, Y. V., Roach, E. L., Korgaonkar, M. S., Grieve, S. M., Galatzer-Levy, I., Fox, P. T., & Etkin, A. (2015). Identification of a common neurobiological substrate for mental illness. *JAMA Psychiatry*, *72*(4), 305–315. https://doi.org/10.1001/jamapsychiatry.2014.2206

Greene, A. S., Gao, S., Scheinost, D., & Constable, R. T. (2018a). Task-induced brain state manipulation improves prediction of individual traits. *Nature Communications*, *9*(1), Article 1. https://doi.org/10.1038/s41467-018-04920-3

Greene, A. S., Gao, S., Scheinost, D., & Constable, R. T. (2018b). Task-induced brain state manipulation improves prediction of individual traits. *Nature Communications*, *9*(1), 2807. https://doi.org/10.1038/s41467-018-04920-3

Greene, A. S., Shen, X., Noble, S., Horien, C., Hahn, C. A., Arora, J., Tokoglu, F., Spann, M. N., Carrión, C. I., Barron, D. S., Sanacora, G., Srihari, V. H., Woods, S. W., Scheinost, D., & Constable, R. T. (2022). Brain–phenotype models fail for individuals who defy sample

stereotypes. *Nature*, *609*(7925), Article 7925. https://doi.org/10.1038/s41586-022-05118-w

Gross, J., Baillet, S., Barnes, G. R., Henson, R. N., Hillebrand, A., Jensen, O., Jerbi, K., Litvak, V., Maess, B., Oostenveld, R., Parkkonen, L., Taylor, J. R., van Wassenhove, V., Wibral, M., & Schoffelen, J.-M. (2013). Good practice for conducting and reporting MEG research. *NeuroImage*, *65*, 349–363. https://doi.org/10.1016/j.neuroimage.2012.10.001

Guardiola-Ripoll, M., & Fatjó-Vilas, M. (2023). A Systematic Review of the Human Accelerated Regions in Schizophrenia and Related Disorders: Where the Evolutionary and Neurodevelopmental Hypotheses Converge. *International Journal of Molecular Sciences*, *24*(4), 3597. https://doi.org/10.3390/ijms24043597

Guerra, A., Asci, F., D'Onofrio, V., Sveva, V., Bologna, M., Fabbrini, G., Berardelli, A., & Suppa, A. (2020). Enhancing Gamma Oscillations Restores Primary Motor Cortex Plasticity in Parkinson's Disease. *The Journal of Neuroscience*, *40*(24), 4788–4796. https://doi.org/10.1523/JNEUROSCI.0357-20.2020

Gurven, M., von Rueden, C., Massenkoff, M., Kaplan, H., & Vie, M. L. (2013). How Universal Is the Big Five? Testing the Five-Factor Model of Personality Variation Among Forager–Farmers in the Bolivian Amazon. *Journal of Personality and Social Psychology*, *104*(2), 354–370. https://doi.org/10.1037/a0030841

Habib, N., Avraham-Davidi, I., Basu, A., Burks, T., Shekhar, K., Hofree, M., Choudhury, S. R., Aguet, F., Gelfand, E., Ardlie, K., Weitz, D. A., Rozenblatt-Rosen, O., Zhang, F., & Regev, A. (2017). Massively parallel single-nucleus RNA-seq with DroNc-seq. *Nature Methods*, *14*(10), Article 10. https://doi.org/10.1038/nmeth.4407

Haegens, S., Cousijn, H., Wallis, G., Harrison, P. J., & Nobre, A. C. (2014). Inter- and intra-individual variability in alpha peak frequency. *NeuroImage*, *92*, 46–55. https://doi.org/10.1016/j.neuroimage.2014.01.049

Ham, S., & Lee, S.-J. V. (2020). Advances in transcriptome analysis of human brain aging. *Experimental & Molecular Medicine*, *52*(11), 1787–1797. https://doi.org/10.1038/s12276-020-00522-6

Hämäläinen, M., Hari, R., Ilmoniemi, R. J., Knuutila, J., & Lounasmaa, O. V. (1993). Magnetoencephalography—Theory, instrumentation, and applications to noninvasive studies of the working human brain. *Reviews of Modern Physics*, *65*(2), 413–497. https://doi.org/10.1103/RevModPhys.65.413

Hanganu, A., Bedetti, C., Degroot, C., Mejia-Constain, B., Lafontaine, A.-L., Soland, V., Chouinard, S., Bruneau, M.-A., Mellah, S., Belleville, S., & Monchi, O. (2014). Mild cognitive impairment is linked with faster rate of cortical thinning in patients with Parkinson's disease longitudinally. *Brain: A Journal of Neurology*, *137*(Pt 4), 1120–1129. https://doi.org/10.1093/brain/awu036

Hansen, J. Y., Markello, R. D., Vogel, J. W., Seidlitz, J., Bzdok, D., & Misic, B. (2021). Mapping gene transcription and neurocognition across human neocortex. *Nature Human Behaviour*, *5*(9), Article 9. https://doi.org/10.1038/s41562-021-01082-z

Hansen, J. Y., Shafiei, G., Markello, R. D., Smart, K., Cox, S. M. L., Nørgaard, M., Beliveau, V., Wu, Y., Gallezot, J.-D., Aumont, É., Servaes, S., Scala, S. G., DuBois, J. M., Wainstein, G., Bezgin, G., Funck, T., Schmitz, T. W., Spreng, R. N., Galovic, M., … Misic, B. (2022). Mapping neurotransmitter systems to the structural and functional organization of the human

neocortex. *Nature Neuroscience*, *25*(11), Article 11. https://doi.org/10.1038/s41593-022-01186-3

Harmelech, T., & Malach, R. (2013). Neurocognitive biases and the patterns of spontaneous correlations in the human cortex. *Trends in Cognitive Sciences*, *17*(12), 606–615. https://doi.org/10.1016/j.tics.2013.09.014

Harmsen, I. E., Rowland, N. C., Wennberg, R. A., & Lozano, A. M. (2018). Characterizing the effects of deep brain stimulation with magnetoencephalography: A review. *Brain Stimulation*, *11*(3), 481–491. https://doi.org/10.1016/j.brs.2017.12.016

Haufe, S., DeGuzman, P., Henin, S., Arcaro, M., Honey, C. J., Hasson, U., & Parra, L. C. (2018). Elucidating relations between fMRI, ECoG, and EEG through a common natural stimulus. *NeuroImage*, *179*, 79–91. https://doi.org/10.1016/j.neuroimage.2018.06.016

Haworth, C., Wright, M., Luciano, M., Martin, N., de Geus, E., van Beijsterveldt, C., Bartels, M., Posthuma, D., Boomsma, D., Davis, O., Kovas, Y., Corley, R., DeFries, J., Hewitt, J., Olson, R., Rhea, S.-A., Wadsworth, S., Iacono, W., McGue, M., … Plomin, R. (2010). The heritability of general cognitive ability increases linearly from childhood to young adulthood. *Molecular Psychiatry*, *15*(11), 1112–1120. https://doi.org/10.1038/mp.2009.55

Hawrylycz, M. J., Lein, E. S., Guillozet-Bongaarts, A. L., Shen, E. H., Ng, L., Miller, J. A., van de Lagemaat, L. N., Smith, K. A., Ebbert, A., Riley, Z. L., Abajian, C., Beckmann, C. F., Bernard, A., Bertagnolli, D., Boe, A. F., Cartagena, P. M., Chakravarty, M. M., Chapin, M., Chong, J., … Jones, A. R. (2012). An anatomically comprehensive atlas of the adult human brain transcriptome. *Nature*, *489*(7416), Article 7416. https://doi.org/10.1038/nature11405

Hawrylycz, M., Miller, J. A., Menon, V., Feng, D., Dolbeare, T., Guillozet-Bongaarts, A. L., Jegga, A. G., Aronow, B. J., Lee, C.-K., Bernard, A., Glasser, M. F., Dierker, D. L., Menche, J., Szafer, A., Collman, F., Grange, P., Berman, K. A., Mihalas, S., Yao, Z., … Lein, E. (2015). Canonical genetic signatures of the adult human brain. *Nature Neuroscience*, *18*(12), Article 12. https://doi.org/10.1038/nn.4171

Heinrichs-Graham, E., McDermott, T. J., Mills, M. S., Wiesman, A. I., Wang, Y.-P., Stephen, J. M., Calhoun, V. D., & Wilson, T. W. (2018). The lifespan trajectory of neural oscillatory activity in the motor system. *Developmental Cognitive Neuroscience*, *30*, 159–168. https://doi.org/10.1016/j.dcn.2018.02.013

Heinrichs-Graham, E., & Wilson, T. W. (2016). Is an absolute level of cortical beta suppression required for proper movement? Magnetoencephalographic evidence from healthy aging. *NeuroImage*, *134*, 514–521. https://doi.org/10.1016/j.neuroimage.2016.04.032

Herringa, R. J. (2017). Trauma, PTSD, and the Developing Brain. *Current Psychiatry Reports*, *19*(10), 69. https://doi.org/10.1007/s11920-017-0825-3

Hill, R. M., Boto, E., Rea, M., Holmes, N., Leggett, J., Coles, L. A., Papastavrou, M., Everton, S. K., Hunt, B. A. E., Sims, D., Osborne, J., Shah, V., Bowtell, R., & Brookes, M. J. (2020). Multi-channel whole-head OPM-MEG: Helmet design and a comparison with a conventional system. *NeuroImage*, *219*, 116995. https://doi.org/10.1016/j.neuroimage.2020.116995

Hodgkinson, C. A., Enoch, M.-A., Srivastava, V., Cummins-Oman, J. S., Ferrier, C., Iarikova, P., Sankararaman, S., Yamini, G., Yuan, Q., Zhou, Z., Albaugh, B., White, K. V., Shen, P.-H., & Goldman, D. (2010). Genome-wide association identifies candidate genes that influence the human electroencephalogram. *Proceedings of the National Academy of Sciences of*

*the United States of America*, *107*(19), 8695–8700. https://doi.org/10.1073/pnas.0908134107

Hoehn, M. M., & Yahr, M. D. (1967). Parkinsonism: Onset, progression, and mortality. *Neurology*, *17*(5), 427–427. https://doi.org/10.1212/WNL.17.5.427

Hohmann, A. G., & Herkenham, M. (2000). Localization of cannabinoid CB1 receptor mRNA in neuronal subpopulations of rat striatum: A double-label in situ hybridization study. *Synapse*, *37*(1), 71–80. https://doi.org/10.1002/(SICI)1098-2396(200007)37:1<71::AID-SYN8>3.0.CO;2-K

Holland, N., Robbins, T. W., & Rowe, J. B. (2021). The role of noradrenaline in cognition and cognitive disorders. *Brain*, *144*(8), 2243–2256. https://doi.org/10.1093/brain/awab111

Horien, C., Shen, X., Scheinost, D., & Constable, R. T. (2019). The individual functional connectome is unique and stable over months to years. *NeuroImage*, *189*, 676–687. https://doi.org/10.1016/j.neuroimage.2019.02.002

Horn, M. A., Gulberti, A., Gülke, E., Buhmann, C., Gerloff, C., Moll, C. K. E., Hamel, W., Volkmann, J., & Pötter-Nerger, M. (2020). A New Stimulation Mode for Deep Brain Stimulation in Parkinson's Disease: Theta Burst Stimulation. *Movement Disorders: Official Journal of the Movement Disorder Society*, *35*(8), 1471–1475. https://doi.org/10.1002/mds.28083

Hunt, B. A. E., Tewarie, P. K., Mougin, O. E., Geades, N., Jones, D. K., Singh, K. D., Morris, P. G., Gowland, P. A., & Brookes, M. J. (2016). Relationships between cortical myeloarchitecture and electrophysiological networks. *Proceedings of the National Academy of Sciences*, *113*(47), 13510–13515. https://doi.org/10.1073/pnas.1608587113

Iemi, L., Busch, N. A., Laudini, A., Haegens, S., Samaha, J., Villringer, A., & Nikulin, V. V. (2019). Multiple mechanisms link prestimulus neural oscillations to sensory responses. *eLife*, *8*, e43620. https://doi.org/10.7554/eLife.43620

Jones, D. T., Machulda, M. M., Vemuri, P., McDade, E. M., Zeng, G., Senjem, M. L., Gunter, J. L., Przybelski, S. A., Avula, R. T., Knopman, D. S., Boeve, B. F., Petersen, R. C., & Jack, C. R. (2011). Age-related changes in the default mode network are more advanced in Alzheimer disease. *Neurology*, *77*(16), 1524–1531. https://doi.org/10.1212/WNL.0b013e318233b33d

Jones, J. D., Valenzuela, Y. G., Uribe, C., Bunch, J., & Kuhn, T. P. (2022). Intraindividual variability in neuropsychological performance predicts longitudinal cortical volume loss in early Parkinson's disease. *Neuropsychology*, *36*, 513–519. https://doi.org/10.1037/neu0000809

Jubault, T., Gagnon, J.-F., Karama, S., Ptito, A., Lafontaine, A.-L., Evans, A. C., & Monchi, O. (2011). Patterns of cortical thickness and surface area in early Parkinson's disease. *NeuroImage*, *55*(2), 462–467. https://doi.org/10.1016/j.neuroimage.2010.12.043

Kanehisa, M., Furumichi, M., Tanabe, M., Sato, Y., & Morishima, K. (2017). KEGG: New perspectives on genomes, pathways, diseases and drugs. *Nucleic Acids Research*, *45*(D1), D353–D361. https://doi.org/10.1093/nar/gkw1092

Karl, A., Schaefer, M., Malta, L. S., Dörfel, D., Rohleder, N., & Werner, A. (2006). A meta-analysis of structural brain abnormalities in PTSD. *Neuroscience & Biobehavioral Reviews*, *30*(7), 1004–1031. https://doi.org/10.1016/j.neubiorev.2006.03.004

Karrer, T. M., McLaughlin, C. L., Guaglianone, C. P., & Samanez-Larkin, G. R. (2019). Reduced serotonin receptors and transporters in normal aging adults: A meta-analysis of PET and

SPECT imaging studies. *Neurobiology of Aging*, *80*, 1–10. https://doi.org/10.1016/j.neurobiolaging.2019.03.021

Kaufmann, T., Alnæs, D., Brandt, C. L., Bettella, F., Djurovic, S., Andreassen, O. A., & Westlye, L. T. (2018a). Stability of the Brain Functional Connectome Fingerprint in Individuals With Schizophrenia. *JAMA Psychiatry*, *75*(7), 749–751. https://doi.org/10.1001/jamapsychiatry.2018.0844

Kaufmann, T., Alnæs, D., Brandt, C. L., Bettella, F., Djurovic, S., Andreassen, O. A., & Westlye, L. T. (2018b). Stability of the Brain Functional Connectome Fingerprint in Individuals With Schizophrenia. *JAMA Psychiatry*, *75*(7), 749. https://doi.org/10.1001/jamapsychiatry.2018.0844

Kaufmann, T., Alnæs, D., Doan, N. T., Brandt, C. L., Andreassen, O. A., & Westlye, L. T. (2017a). Delayed stabilization and individualization in connectome development are related to psychiatric disorders. *Nature Neuroscience*, *20*(4), Article 4. https://doi.org/10.1038/nn.4511

Kaufmann, T., Alnæs, D., Doan, N. T., Brandt, C. L., Andreassen, O. A., & Westlye, L. T. (2017b). Delayed stabilization and individualization in connectome development are related to psychiatric disorders. *Nature Neuroscience*, *20*(4), 513–515. https://doi.org/10.1038/nn.4511

Kennis, M., Rademaker, A. R., & Geuze, E. (2013). Neural correlates of personality: An integrative review. *Neuroscience & Biobehavioral Reviews*, *37*(1), 73–95. https://doi.org/10.1016/j.neubiorev.2012.10.012

Kim, J., Criaud, M., Cho, S. S., Díez-Cirarda, M., Mihaescu, A., Coakeley, S., Ghadery, C., Valli, M., Jacobs, M. F., Houle, S., & Strafella, A. P. (2017). Abnormal intrinsic brain functional network dynamics in Parkinson's disease. *Brain*, *140*(11), 2955–2967. https://doi.org/10.1093/brain/awx233

Kim, J., Lee, J., Kim, E., Choi, J. H., Rah, J.-C., & Choi, J.-W. (2022). Dopamine depletion can be predicted by the aperiodic component of subthalamic local field potentials. *Neurobiology of Disease*, *168*, 105692. https://doi.org/10.1016/j.nbd.2022.105692

Kim, Y.-C., Han, S.-W., Alberico, S. L., Ruggiero, R. N., De Corte, B., Chen, K.-H., & Narayanan, N. S. (2017). Optogenetic Stimulation of Frontal D1 Neurons Compensates for Impaired Temporal Control of Action in Dopamine-Depleted Mice. *Current Biology*, *27*(1), 39–47. https://doi.org/10.1016/j.cub.2016.11.029

Koen, J. D., & Rugg, M. D. (2019). Neural Dedifferentiation in the Aging Brain. *Trends in Cognitive Sciences*, *23*(7), 547–559. https://doi.org/10.1016/j.tics.2019.04.012

Kong, R., Tan, Y. R., Wulan, N., Ooi, L. Q. R., Farahibozorg, S.-R., Harrison, S., Bijsterbosch, J. D., Bernhardt, B. C., Eickhoff, S., & Thomas Yeo, B. T. (2023). Comparison between gradients and parcellations for functional connectivity prediction of behavior. *NeuroImage*, *273*, 120044. https://doi.org/10.1016/j.neuroimage.2023.120044

Korgaonkar, M. S., Ram, K., Williams, L. M., Gatt, J. M., & Grieve, S. M. (2014). Establishing the resting state default mode network derived from functional magnetic resonance imaging tasks as an endophenotype: A twins study. *Human Brain Mapping*, *35*(8), 3893–3902. https://doi.org/10.1002/hbm.22446

Krajcovicova, L., Mikl, M., Marecek, R., & Rektorova, I. (2012). The default mode network integrity in patients with Parkinson's disease is levodopa equivalent dose-dependent. *Journal of Neural Transmission*, *119*(4), 443–454. https://doi.org/10.1007/s00702-011-0723-5

Krienen, F. M., Yeo, B. T. T., Ge, T., Buckner, R. L., & Sherwood, C. C. (2016). Transcriptional profiles of supragranular-enriched genes associate with corticocortical network architecture in the human brain. *Proceedings of the National Academy of Sciences*, *113*(4), E469–E478. https://doi.org/10.1073/pnas.1510903113

Krishnan, A., Williams, L. J., McIntosh, A. R., & Abdi, H. (2011). Partial Least Squares (PLS) methods for neuroimaging: A tutorial and review. *NeuroImage*, *56*(2), 455–475. https://doi.org/10.1016/j.neuroimage.2010.07.034

Kuntsi, J., & Klein, C. (2011a). Intraindividual Variability in ADHD and Its Implications for Research of Causal Links. In C. Stanford & R. Tannock (Eds.), *Behavioral Neuroscience of Attention Deficit Hyperactivity Disorder and Its Treatment* (Vol. 9, pp. 67–91). Springer Berlin Heidelberg. https://doi.org/10.1007/7854_2011_145

Kuntsi, J., & Klein, C. (2011b). Intraindividual Variability in ADHD and Its Implications for Research of Causal Links. In C. Stanford & R. Tannock (Eds.), *Behavioral Neuroscience of Attention Deficit Hyperactivity Disorder and Its Treatment* (Vol. 9, pp. 67–91). Springer Berlin Heidelberg. https://doi.org/10.1007/7854_2011_145

Lai, H., Wang, S., Zhao, Y., Zhang, L., Yang, C., & Gong, Q. (2019). Brain gray matter correlates of extraversion: A systematic review and meta-analysis of voxel-based morphometry studies. *Human Brain Mapping*, *40*(14), 4038–4057. https://doi.org/10.1002/hbm.24684

Lake, B. B., Chen, S., Sos, B. C., Fan, J., Kaeser, G. E., Yung, Y. C., Duong, T. E., Gao, D., Chun, J., Kharchenko, P. V., & Zhang, K. (2018). Integrative single-cell analysis of transcriptional and epigenetic states in the human adult brain. *Nature Biotechnology*, *36*(1), Article 1. https://doi.org/10.1038/nbt.4038

Lee, P. H., Baker, J. T., Holmes, A. J., Jahanshad, N., Ge, T., Jung, J.-Y., Cruz, Y., Manoach, D. S., Hibar, D. P., Faskowitz, J., McMahon, K. L., de Zubicaray, G. I., Martin, N. H., Wright, M. J., Öngür, D., Buckner, R., Roffman, J., Thompson, P. M., & Smoller, J. W. (2016). Partitioning heritability analysis reveals a shared genetic basis of brain anatomy and schizophrenia. *Molecular Psychiatry*, *21*(12), Article 12. https://doi.org/10.1038/mp.2016.164

Lendner, J. D., Helfrich, R. F., Mander, B. A., Romundstad, L., Lin, J. J., Walker, M. P., Larsson, P. G., & Knight, R. T. (2020). An electrophysiological marker of arousal level in humans. *eLife*, *9*, e55092. https://doi.org/10.7554/eLife.55092

Lennert, T., Samiee, S., & Baillet, S. (2021). Coupled oscillations enable rapid temporal recalibration to audiovisual asynchrony. *Communications Biology*, *4*(1), Article 1. https://doi.org/10.1038/s42003-021-02087-0

Leppäaho, E., Renvall, H., Salmela, E., Kere, J., Salmelin, R., & Kaski, S. (2019). Discovering heritable modes of MEG spectral power. *Human Brain Mapping*, *40*(5), 1391–1402. https://doi.org/10.1002/hbm.24454

Li, J., Bzdok, D., Chen, J., Tam, A., Ooi, L. Q. R., Holmes, A. J., Ge, T., Patil, K. R., Jabbi, M., Eickhoff, S. B., Yeo, B. T. T., & Genon, S. (2022). Cross-ethnicity/race generalization failure of behavioral prediction from resting-state functional connectivity. *Science Advances*, *8*(11), eabj1812. https://doi.org/10.1126/sciadv.abj1812

Li, L., Wei, Y., Zhang, J., Ma, J., Yi, Y., Gu, Y., Li, L. M. W., Lin, Y., & Dai, Z. (2021). Gene expression associated with individual variability in intrinsic functional connectivity. *NeuroImage*, *245*, 118743. https://doi.org/10.1016/j.neuroimage.2021.118743

Li, M., Santpere, G., Imamura Kawasawa, Y., Evgrafov, O. V., Gulden, F. O., Pochareddy, S., Sunkin, S. M., Li, Z., Shin, Y., Zhu, Y., Sousa, A. M. M., Werling, D. M., Kitchen, R. R., Kang, H. J., Pletikos, M., Choi, J., Muchnik, S., Xu, X., Wang, D., … Sestan, N. (2018). Integrative functional genomic analysis of human brain development and neuropsychiatric risks. *Science*, *362*(6420), eaat7615. https://doi.org/10.1126/science.aat7615

Litvak, V., Florin, E., Tamás, G., Groppa, S., & Muthuraman, M. (2021). EEG and MEG primers for tracking DBS network effects. *NeuroImage*, *224*, 117447. https://doi.org/10.1016/j.neuroimage.2020.117447

Logothetis, N. K., Pauls, J., Augath, M., Trinath, T., & Oeltermann, A. (2001). Neurophysiological investigation of the basis of the fMRI signal. *Nature*, *412*(6843), 150–157. https://doi.org/10.1038/35084005

Lucas-Jiménez, O., Ojeda, N., Peña, J., Díez-Cirarda, M., Cabrera-Zubizarreta, A., Gómez-Esteban, J. C., Gómez-Beldarrain, M. Á., & Ibarretxe-Bilbao, N. (2016). Altered functional connectivity in the default mode network is associated with cognitive impairment and brain anatomical changes in Parkinson's disease. *Parkinsonism & Related Disorders*, *33*, 58–64. https://doi.org/10.1016/j.parkreldis.2016.09.012

MacDonald, S. W. S., Nyberg, L., & Bäckman, L. (2006). Intra-individual variability in behavior: Links to brain structure, neurotransmission and neuronal activity. *Trends in Neurosciences*, *29*(8), 474–480. https://doi.org/10.1016/j.tins.2006.06.011

Madsen, T. M., Treschow, A., Bengzon, J., Bolwig, T. G., Lindvall, O., & Tingström, A. (2000). Increased neurogenesis in a model of electroconvulsive therapy. *Biological Psychiatry*, *47*(12), 1043–1049. https://doi.org/10.1016/S0006-3223(00)00228-6

Maidan, I., Hacham, R., Galperin, I., Giladi, N., Holtzer, R., Hausdorff, J. M., & Mirelman, A. (2022). Neural Variability in the Prefrontal Cortex as a Reflection of Neural Flexibility and Stability in Patients With Parkinson Disease. *Neurology*, *98*(8), e839–e847. https://doi.org/10.1212/WNL.0000000000013217

Malone, S. M., Burwell, S. J., Vaidyanathan, U., Miller, M. B., McGue, M., & Iacono, W. G. (2014). Heritability and Molecular-Genetic Basis of Resting EEG Activity: A Genome-Wide Association Study. *Psychophysiology*, *51*(12), 1225–1245. https://doi.org/10.1111/psyp.12344

Malva, J. O., Moreira, R., Martins, B., Novo, J., Pereira, F. C., Raposo, R., Oriá, R. B., & Ribeiro, C. F. (2021). Chapter 13—Neuroinflammation and aging. In C. R. Martin, V. R. Preedy, & R. Rajendram (Eds.), *Assessments, Treatments and Modeling in Aging and Neurological Disease* (pp. 139–151). Academic Press. https://doi.org/10.1016/B978-0-12-818000-6.00013-5

Marcus, D. S., Harwell, J., Olsen, T., Hodge, M., Glasser, M. F., Prior, F., Jenkinson, M., Laumann, T., Curtiss, S. W., & Van Essen, D. C. (2011). Informatics and data mining tools and strategies for the human connectome project. *Frontiers in Neuroinformatics*, *5*, 4. https://doi.org/10.3389/fninf.2011.00004

Marek, S., Tervo-Clemmens, B., Calabro, F. J., Montez, D. F., Kay, B. P., Hatoum, A. S., Donohue, M. R., Foran, W., Miller, R. L., Hendrickson, T. J., Malone, S. M., Kandala, S., Feczko, E.,

Miranda-Dominguez, O., Graham, A. M., Earl, E. A., Perrone, A. J., Cordova, M., Doyle, O., … Dosenbach, N. U. F. (2022). Reproducible brain-wide association studies require thousands of individuals. *Nature*, *603*(7902), Article 7902. https://doi.org/10.1038/s41586-022-04492-9

Margulies, D. S., Ghosh, S. S., Goulas, A., Falkiewicz, M., Huntenburg, J. M., Langs, G., Bezgin, G., Eickhoff, S. B., Castellanos, F. X., Petrides, M., Jefferies, E., & Smallwood, J. (2016). Situating the default-mode network along a principal gradient of macroscale cortical organization. *Proceedings of the National Academy of Sciences*, *113*(44), 12574–12579. https://doi.org/10.1073/pnas.1608282113

Markello, R. D., Arnatkeviciute, A., Poline, J.-B., Fulcher, B. D., Fornito, A., & Misic, B. (2021). Standardizing workflows in imaging transcriptomics with the abagen toolbox. *eLife*, *10*, e72129. https://doi.org/10.7554/eLife.72129

Markello, R. D., Hansen, J. Y., Liu, Z.-Q., Bazinet, V., Shafiei, G., Suárez, L. E., Blostein, N., Seidlitz, J., Baillet, S., Satterthwaite, T. D., Chakravarty, M. M., Raznahan, A., & Misic, B. (2022a). neuromaps: Structural and functional interpretation of brain maps. *Nature Methods*, *19*(11), Article 11. https://doi.org/10.1038/s41592-022-01625-w

Markello, R. D., Hansen, J. Y., Liu, Z.-Q., Bazinet, V., Shafiei, G., Suárez, L. E., Blostein, N., Seidlitz, J., Baillet, S., Satterthwaite, T. D., Chakravarty, M. M., Raznahan, A., & Misic, B. (2022b). *neuromaps: Structural and functional interpretation of brain maps* [Preprint]. Neuroscience. https://doi.org/10.1101/2022.01.06.475081

Markello, R. D., & Misic, B. (2021). Comparing spatial null models for brain maps. *NeuroImage*, *236*, 118052. https://doi.org/10.1016/j.neuroimage.2021.118052

Markovic, A., Achermann, P., Rusterholz, T., & Tarokh, L. (2018). Heritability of Sleep EEG Topography in Adolescence: Results from a Longitudinal Twin Study. *Scientific Reports*, *8*(1), Article 1. https://doi.org/10.1038/s41598-018-25590-7

Mars, R. B., Passingham, R. E., & Jbabdi, S. (2018). Connectivity Fingerprints: From Areal Descriptions to Abstract Spaces. *Trends in Cognitive Sciences*, *22*(11), 1026–1037. https://doi.org/10.1016/j.tics.2018.08.009

Maschke, C., Duclos, C., Owen, A. M., Jerbi, K., & Blain-Moraes, S. (2023). Aperiodic brain activity and response to anesthesia vary in disorders of consciousness. *NeuroImage*, *275*, 120154. https://doi.org/10.1016/j.neuroimage.2023.120154

Mattys, S. L., Baddeley, A., & Trenkic, D. (2018). Is the superior verbal memory span of Mandarin speakers due to faster rehearsal? *Memory & Cognition*, *46*(3), 361–369. https://doi.org/10.3758/s13421-017-0770-8

Mayhew, A. J., & Meyre, D. (2017). Assessing the Heritability of Complex Traits in Humans: Methodological Challenges and Opportunities. *Current Genomics*, *18*(4), 332–340. https://doi.org/10.2174/1389202918666170307161450

McCrae, R. R., & Costa Jr., P. T. (1997). Personality trait structure as a human universal. *American Psychologist*, *52*(5), 509–516. https://doi.org/10.1037/0003-066X.52.5.509

McGinnis, S. M., Brickhouse, M., Pascual, B., & Dickerson, B. C. (2011). Age-Related Changes in the Thickness of Cortical Zones in Humans. *Brain Topography*, *24*(3–4), 279–291. https://doi.org/10.1007/s10548-011-0198-6

McIntosh, A. R., Bookstein, F. L., Haxby, J. V., & Grady, C. L. (1996). Spatial pattern analysis of functional brain images using partial least squares. *NeuroImage*, *3*(3 Pt 1), 143–157. https://doi.org/10.1006/nimg.1996.0016

McIntosh, A. R., & Lobaugh, N. J. (2004). Partial least squares analysis of neuroimaging data: Applications and advances. *NeuroImage*, *23*, S250–S263. https://doi.org/10.1016/j.neuroimage.2004.07.020

McIntosh, A. R., & Mišić, B. (2013). Multivariate statistical analyses for neuroimaging data. *Annual Review of Psychology*, *64*, 499–525. https://doi.org/10.1146/annurev-psych-113011-143804

McKenzie, A. T., Wang, M., Hauberg, M. E., Fullard, J. F., Kozlenkov, A., Keenan, A., Hurd, Y. L., Dracheva, S., Casaccia, P., Roussos, P., & Zhang, B. (2018). Brain Cell Type Specific Gene Expression and Co-expression Network Architectures. *Scientific Reports*, *8*(1), Article 1. https://doi.org/10.1038/s41598-018-27293-5

*MEG, myself, and I: individual identification from neurophysiological brain activity*. (n.d.). Retrieved October 23, 2023, from https://zenodo.org/records/5181836

Meltzer, C. C., Smith, G., DeKosky, S. T., Pollock, B. G., Mathis, C. A., Moore, R. Y., Kupfer, D. J., & Reynolds, C. F. (1998). Serotonin in Aging, Late-Life Depression, and Alzheimer's Disease: The Emerging Role of Functional Imaging. *Neuropsychopharmacology*, *18*(6), Article 6. https://doi.org/10.1016/S0893-133X(97)00194-2

Merkin, A., Sghirripa, S., Graetz, L., Smith, A. E., Hordacre, B., Harris, R., Pitcher, J., Semmler, J., Rogasch, N. C., & Goldsworthy, M. (2022). Do age-related differences in aperiodic neural

activity explain differences in resting EEG alpha? *Neurobiology of Aging*. https://doi.org/10.1016/j.neurobiolaging.2022.09.003

Merkin, A., Sghirripa, S., Graetz, L., Smith, A. E., Hordacre, B., Harris, R., Pitcher, J., Semmler, J., Rogasch, N. C., & Goldsworthy, M. (2023). Do age-related differences in aperiodic neural activity explain differences in resting EEG alpha? *Neurobiology of Aging*, *121*, 78–87. https://doi.org/10.1016/j.neurobiolaging.2022.09.003

Michalareas, G., Vezoli, J., van Pelt, S., Schoffelen, J.-M., Kennedy, H., & Fries, P. (2016). Alpha-Beta and Gamma Rhythms Subserve Feedback and Feedforward Influences among Human Visual Cortical Areas. *Neuron*, *89*(2), 384–397. https://doi.org/10.1016/j.neuron.2015.12.018

Mikulincer, M., Shaver, P. R., Cooper, M. L., & Larsen, R. J. (Eds.). (2015). *APA handbook of personality and social psychology, Volume 4: Personality processes and individual differences* (pp. xxviii, 727). American Psychological Association. https://doi.org/10.1037/14343-000

Miller, J. A., Ding, S.-L., Sunkin, S. M., Smith, K. A., Ng, L., Szafer, A., Ebbert, A., Riley, Z. L., Royall, J. J., Aiona, K., Arnold, J. M., Bennet, C., Bertagnolli, D., Brouner, K., Butler, S., Caldejon, S., Carey, A., Cuhaciyan, C., Dalley, R. A., … Lein, E. S. (2014). Transcriptional landscape of the prenatal human brain. *Nature*, *508*(7495), Article 7495. https://doi.org/10.1038/nature13185

Miller, M. B., & Van Horn, J. D. (2007). Individual variability in brain activations associated with episodic retrieval: A role for large-scale databases. *International Journal of*

*Psychophysiology: Official Journal of the International Organization of Psychophysiology*, *63*(2), 205–213. https://doi.org/10.1016/j.ijpsycho.2006.03.019

Miranda-Dominguez, O., Feczko, E., Grayson, D. S., Walum, H., Nigg, J. T., & Fair, D. A. (2018). Heritability of the human connectome: A connectotyping study. *Network Neuroscience*, *02*(02), 175–199. https://doi.org/10.1162/netn_a_00029

Miranda-Dominguez, O., Mills, B. D., Carpenter, S. D., Grant, K. A., Kroenke, C. D., Nigg, J. T., & Fair, D. A. (2014). Connectotyping: Model Based Fingerprinting of the Functional Connectome. *PLoS ONE*, *9*(11), e111048. https://doi.org/10.1371/journal.pone.0111048

Mišić, B., & Sporns, O. (2016). From regions to connections and networks: New bridges between brain and behavior. *Current Opinion in Neurobiology*, *40*, 1–7. https://doi.org/10.1016/j.conb.2016.05.003

Mollon, J., Knowles, E. E. M., Mathias, S. R., Gur, R., Peralta, J. M., Weiner, D. J., Robinson, E. B., Gur, R. E., Blangero, J., Almasy, L., & Glahn, D. C. (2021). Genetic influence on cognitive development between childhood and adulthood. *Molecular Psychiatry*, *26*(2), Article 2. https://doi.org/10.1038/s41380-018-0277-0

Moretti, D. V., Paternicò, D., Binetti, G., Zanetti, O., & Frisoni, G. B. (2013). EEG upper/low alpha frequency power ratio relates to temporo-parietal brain atrophy and memory performances in mild cognitive impairment. *Frontiers in Aging Neuroscience*, *5*, 63. https://doi.org/10.3389/fnagi.2013.00063

Morillon, B., & Baillet, S. (2017). Motor origin of temporal predictions in auditory attention. *Proceedings of the National Academy of Sciences*, *114*(42), E8913–E8921. https://doi.org/10.1073/pnas.1705373114

Mosher, J. C., Baillet, S., & Leahy, R. M. (2003). Equivalence of linear approaches in bioelectromagnetic inverse solutions. *IEEE Workshop on Statistical Signal Processing, 2003*, 294–297. https://doi.org/10.1109/SSP.2003.1289402

Mowinckel, A. M., & Vidal-Piñeiro, D. (2022). *ggseg: Plotting Tool for Brain Atlases* (1.6.5) [Computer software]. https://cran.r-project.org/web/packages/ggseg/index.html

Myers, B. L., & Badia, P. (1995). Changes in circadian rhythms and sleep quality with aging: Mechanisms and interventions. *Neuroscience & Biobehavioral Reviews*, *19*(4), 553–571. https://doi.org/10.1016/0149-7634(95)00018-6

Narayanan, N. S., Rodnitzky, R. L., & Uc, E. Y. (2013). Prefrontal dopamine signaling and cognitive symptoms of Parkinson's disease. *Reviews in the Neurosciences*, *24*(3). https://doi.org/10.1515/revneuro-2013-0004

Nemy, M., Cedres, N., Grothe, M. J., Muehlboeck, J.-S., Lindberg, O., Nedelska, Z., Stepankova, O., Vyslouzilova, L., Eriksdotter, M., Barroso, J., Teipel, S., Westman, E., & Ferreira, D. (2020). Cholinergic white matter pathways make a stronger contribution to attention and memory in normal aging than cerebrovascular health and nucleus basalis of Meynert. *NeuroImage*, *211*, 116607. https://doi.org/10.1016/j.neuroimage.2020.116607

Nentwich, M., Ai, L., Madsen, J., Telesford, Q. K., Haufe, S., Milham, M. P., & Parra, L. C. (2020). Functional connectivity of EEG is subject-specific, associated with phenotype, and different from fMRI. *NeuroImage*, *218*, 117001. https://doi.org/10.1016/j.neuroimage.2020.117001

Niso, G., Rogers, C., Moreau, J. T., Chen, L.-Y., Madjar, C., Das, S., Bock, E., Tadel, F., Evans, A. C., Jolicoeur, P., & Baillet, S. (2016a). OMEGA: The Open MEG Archive. *NeuroImage*, *124*, 1182–1187. https://doi.org/10.1016/j.neuroimage.2015.04.028

Niso, G., Rogers, C., Moreau, J. T., Chen, L.-Y., Madjar, C., Das, S., Bock, E., Tadel, F., Evans, A. C., Jolicoeur, P., & Baillet, S. (2016b). OMEGA: The Open MEG Archive. *NeuroImage*, *124*, 1182–1187. https://doi.org/10.1016/j.neuroimage.2015.04.028

Noble, S., Spann, M. N., Tokoglu, F., Shen, X., Constable, R. T., & Scheinost, D. (2017). Influences on the Test-Retest Reliability of Functional Connectivity MRI and its Relationship with Behavioral Utility. *Cerebral Cortex (New York, N.Y.: 1991)*, *27*(11), 5415–5429. https://doi.org/10.1093/cercor/bhx230

Nomi, J. S., Bolt, T. S., Ezie, C. E. C., Uddin, L. Q., & Heller, A. S. (2017). Moment-to-Moment BOLD Signal Variability Reflects Regional Changes in Neural Flexibility across the Lifespan. *Journal of Neuroscience*, *37*(22), 5539–5548. https://doi.org/10.1523/JNEUROSCI.3408-16.2017

*Noradrenergic modulation of rhythmic neural activity shapes selective attention—ScienceDirect*. (n.d.). Retrieved May 8, 2023, from https://www.sciencedirect.com/science/article/pii/S1364661321002643?via%3Dihub

Norden, D. M., & Godbout, J. P. (2013). Review: Microglia of the aged brain: primed to be activated and resistant to regulation. *Neuropathology and Applied Neurobiology*, *39*(1), 19–34. https://doi.org/10.1111/j.1365-2990.2012.01306.x

Nottage, J. F., & Horder, J. (2015). State-of-the-Art Analysis of High-Frequency (Gamma Range) Electroencephalography in Humans. *Neuropsychobiology*, *72*(3–4), 219–228. https://doi.org/10.1159/000382023

Obermeyer, Z., Powers, B., Vogeli, C., & Mullainathan, S. (2019). Dissecting racial bias in an algorithm used to manage the health of populations. *Science (New York, N.Y.)*, *366*(6464), 447–453. https://doi.org/10.1126/science.aax2342

Ochsner, K. N., & Gross, J. J. (2005). The cognitive control of emotion. *Trends in Cognitive Sciences*, *9*(5), 242–249. https://doi.org/10.1016/j.tics.2005.03.010

Olde Dubbelink, K. T. E., Stoffers, D., Deijen, J. B., Twisk, J. W. R., Stam, C. J., & Berendse, H. W. (2013). Cognitive decline in Parkinson's disease is associated with slowing of resting-state brain activity: A longitudinal study. *Neurobiology of Aging*, *34*(2), Article 2. https://doi.org/10.1016/j.neurobiolaging.2012.02.029

Oswal, A., Brown, P., & Litvak, V. (2013). Synchronized neural oscillations and the pathophysiology of Parkinson's disease: *Current Opinion in Neurology*, *26*(6), 662–670. https://doi.org/10.1097/WCO.0000000000000034

Pang, J. C., Aquino, K. M., Oldehinkel, M., Robinson, P. A., Fulcher, B. D., Breakspear, M., & Fornito, A. (2023). Geometric constraints on human brain function. *Nature*, *618*(7965), Article 7965. https://doi.org/10.1038/s41586-023-06098-1

Park, D. C., Polk, T. A., Park, R., Minear, M., Savage, A., & Smith, M. R. (2004). Aging reduces neural specialization in ventral visual cortex. *Proceedings of the National Academy of Sciences*, *101*(35), 13091–13095. https://doi.org/10.1073/pnas.0405148101

Parker, K. L., Chen, K.-H., Kingyon, J. R., Cavanagh, J. F., & Narayanan, N. S. (2014). D1-Dependent 4 Hz Oscillations and Ramping Activity in Rodent Medial Frontal Cortex during Interval Timing. *The Journal of Neuroscience*, *34*(50), 16774–16783. https://doi.org/10.1523/JNEUROSCI.2772-14.2014

Parker, K. L., Chen, K.-H., Kingyon, J. R., Cavanagh, J. F., & Narayanan, N. S. (2015). Medial frontal ∼4-Hz activity in humans and rodents is attenuated in PD patients and in rodents with cortical dopamine depletion. *Journal of Neurophysiology*, *114*(2), 1310–1320. https://doi.org/10.1152/jn.00412.2015

Parkinson, C., Kleinbaum, A. M., & Wheatley, T. (2018). Similar neural responses predict friendship. *Nature Communications*, *9*(1), Article 1. https://doi.org/10.1038/s41467-017-02722-7

Pereira, J. B., Svenningsson, P., Weintraub, D., Brønnick, K., Lebedev, A., Westman, E., & Aarsland, D. (2014). Initial cognitive decline is associated with cortical thinning in early Parkinson disease. *Neurology*, *82*(22), 2017–2025. https://doi.org/10.1212/WNL.0000000000000483

Peters, R. (2006). Ageing and the brain: This article is part of a series on ageing edited by Professor Chris Bulpitt. *Postgraduate Medical Journal*, *82*(964), 84–88. https://doi.org/10.1136/pgmj.2005.036665

Pizzagalli, F., Auzias, G., Yang, Q., Mathias, S. R., Faskowitz, J., Boyd, J. D., Amini, A., Rivière, D., McMahon, K. L., de Zubicaray, G. I., Martin, N. G., Mangin, J.-F., Glahn, D. C., Blangero, J., Wright, M. J., Thompson, P. M., Kochunov, P., & Jahanshad, N. (2020). The reliability and

heritability of cortical folds and their genetic correlations across hemispheres. *Communications Biology*, *3*(1), Article 1. https://doi.org/10.1038/s42003-020-01163-1

Poewe, W., Seppi, K., Tanner, C. M., Halliday, G. M., Brundin, P., Volkmann, J., Schrag, A.-E., & Lang, A. E. (2017). Parkinson disease. *Nature Reviews Disease Primers*, *3*(1), Article 1. https://doi.org/10.1038/nrdp.2017.13

Poldrack, R. A., & Gorgolewski, K. J. (2014). Making big data open: Data sharing in neuroimaging. *Nature Neuroscience*, *17*(11), Article 11. https://doi.org/10.1038/nn.3818

Poldrack, R. A., Kittur, A., Kalar, D., Miller, E., Seppa, C., Gil, Y., Parker, D. S., Sabb, F. W., & Bilder, R. M. (2011). The Cognitive Atlas: Toward a Knowledge Foundation for Cognitive Neuroscience. *Frontiers in Neuroinformatics*, *5*, 17. https://doi.org/10.3389/fninf.2011.00017

Posthuma, D., de Geus, E. J. C., Mulder, E. J. C. M., Smit, D. J. A., Boomsma, D. I., & Stam, C. J. (2005). Genetic components of functional connectivity in the brain: The heritability of synchronization likelihood. *Human Brain Mapping*, *26*(3), Article 3. https://doi.org/10.1002/hbm.20156

Power, J. D., Mitra, A., Laumann, T. O., Snyder, A. Z., Schlaggar, B. L., & Petersen, S. E. (2014). Methods to detect, characterize, and remove motion artifact in resting state fMRI. *NeuroImage*, *84*, 320–341. https://doi.org/10.1016/j.neuroimage.2013.08.048

Power, R. A., & Pluess, M. (2015). Heritability estimates of the Big Five personality traits based on common genetic variants. *Translational Psychiatry*, *5*(7), e604. https://doi.org/10.1038/tp.2015.96

Provencher, D., Hennebelle, M., Cunnane, S. C., Bérubé-Lauzière, Y., & Whittingstall, K. (2016). Cortical Thinning in Healthy Aging Correlates with Larger Motor-Evoked EEG Desynchronization. *Frontiers in Aging Neuroscience*, *8*. https://www.frontiersin.org/articles/10.3389/fnagi.2016.00063

R Core Team. (2022). *R: A Language and Environment for Statistical Computing*. R Foundation for Statistical Computing. https://www.R-project.org/

Raz, N., & Rodrigue, K. M. (2006). Differential aging of the brain: Patterns, cognitive correlates and modifiers. *Neuroscience and Biobehavioral Reviews*, *30*(6), 730–748. https://doi.org/10.1016/j.neubiorev.2006.07.001

Rempe, M. P., Lew, B. J., Embury, C. M., Christopher-Hayes, N. J., Schantell, M., & Wilson, T. W. (2022). Spontaneous sensorimotor beta power and cortical thickness uniquely predict motor function in healthy aging. *NeuroImage*, *263*, 119651. https://doi.org/10.1016/j.neuroimage.2022.119651

Rempe, M. P., Ott, L. R., Picci, G., Penhale, S. H., Christopher-Hayes, N. J., Lew, B. J., Petro, N. M., Embury, C. M., Schantell, M., Johnson, H. J., Okelberry, H. J., Losh, K. L., Willett, M. P., Losh, R. A., Wang, Y.-P., Calhoun, V. D., Stephen, J. M., Heinrichs-Graham, E., Kurz, M. J., & Wilson, T. W. (2023). Spontaneous cortical dynamics from the first years to the golden years. *Proceedings of the National Academy of Sciences*, *120*(4), e2212776120. https://doi.org/10.1073/pnas.2212776120

Rétey, J. V., Adam, M., Honegger, E., Khatami, R., Luhmann, U. F. O., Jung, H. H., Berger, W., & Landolt, H.-P. (2005). A functional genetic variation of adenosine deaminase affects the

duration and intensity of deep sleep in humans. *Proceedings of the National Academy of Sciences*, *102*(43), 15676–15681. https://doi.org/10.1073/pnas.0505414102

Ricard, J. A., Parker, T. C., Dhamala, E., Kwasa, J., Allsop, A., & Holmes, A. J. (2023). Confronting racially exclusionary practices in the acquisition and analyses of neuroimaging data. *Nature Neuroscience*, *26*(1), Article 1. https://doi.org/10.1038/s41593-022-01218-y

Richard Clark, C., Veltmeyer, M. D., Hamilton, R. J., Simms, E., Paul, R., Hermens, D., & Gordon, E. (2004). Spontaneous alpha peak frequency predicts working memory performance across the age span. *International Journal of Psychophysiology: Official Journal of the International Organization of Psychophysiology*, *53*(1), 1–9. https://doi.org/10.1016/j.ijpsycho.2003.12.011

Richiardi, J., Altmann, A., Milazzo, A.-C., Chang, C., Chakravarty, M. M., Banaschewski, T., Barker, G. J., Bokde, A. L. W., Bromberg, U., Büchel, C., Conrod, P., Fauth-Bühler, M., Flor, H., Frouin, V., Gallinat, J., Garavan, H., Gowland, P., Heinz, A., Lemaître, H., … IMAGEN CONSORTIUM. (2015). Correlated gene expression supports synchronous activity in brain networks. *Science*, *348*(6240), 1241–1244. https://doi.org/10.1126/science.1255905

Rieck, J. R., DeSouza, B., Baracchini, G., & Grady, C. L. (2022). Reduced modulation of BOLD variability as a function of cognitive load in healthy aging. *Neurobiology of Aging*, *112*, 215–230. https://doi.org/10.1016/j.neurobiolaging.2022.01.010

Robertson, I. H. (2013). A noradrenergic theory of cognitive reserve: Implications for Alzheimer's disease. *Neurobiology of Aging*, *34*(1), 298–308. https://doi.org/10.1016/j.neurobiolaging.2012.05.019

Rocca, D. L., Campisi, P., Vegso, B., Cserti, P., Kozmann, G., Babiloni, F., & Fallani, F. D. V. (2014). Human brain distinctiveness based on EEG spectral coherence connectivity. *IEEE Transactions on Bio-Medical Engineering*, *61*(9), 2406–2412. https://doi.org/10.1109/TBME.2014.2317881

Rodríguez, J. J., Noristani, H. N., & Verkhratsky, A. (2012). The serotonergic system in ageing and Alzheimer's disease. *Progress in Neurobiology*, *99*(1), 15–41. https://doi.org/10.1016/j.pneurobio.2012.06.010

Romano, A., Trosi Lopez, E., Liparoti, M., Polverino, A., Minino, R., Trojsi, F., Bonavita, S., Mandolesi, L., Granata, C., Amico, E., Sorrentino, G., & Sorrentino, P. (2022). The progressive loss of brain network fingerprints in Amyotrophic Lateral Sclerosis predicts clinical impairment. *NeuroImage: Clinical*, *35*, 103095. https://doi.org/10.1016/j.nicl.2022.103095

Rosenberg, M. D., Finn, E. S., Scheinost, D., Constable, R. T., & Chun, M. M. (2017a). Characterizing Attention with Predictive Network Models. *Trends in Cognitive Sciences*, *21*(4), Article 4. https://doi.org/10.1016/j.tics.2017.01.011

Rosenberg, M. D., Finn, E. S., Scheinost, D., Constable, R. T., & Chun, M. M. (2017b). Characterizing Attention with Predictive Network Models. *Trends in Cognitive Sciences*, *21*(4), 290–302. https://doi.org/10.1016/j.tics.2017.01.011

Rosenberg, M. D., Finn, E. S., Scheinost, D., Papademetris, X., Shen, X., Constable, R. T., & Chun, M. M. (2016). A neuromarker of sustained attention from whole-brain functional connectivity. *Nature Neuroscience*, *19*(1), Article 1. https://doi.org/10.1038/nn.4179

Rosenberg, M. D., Martinez, S. A., Rapuano, K. M., Conley, M. I., Cohen, A. O., Cornejo, M. D., Hagler, D. J., Meredith, W. J., Anderson, K. M., Wager, T. D., Feczko, E., Earl, E., Fair, D. A., Barch, D. M., Watts, R., & Casey, B. J. (2020). Behavioral and Neural Signatures of Working Memory in Childhood. *Journal of Neuroscience*, *40*(26), 5090–5104. https://doi.org/10.1523/JNEUROSCI.2841-19.2020

Rosenberg, M. D., Scheinost, D., Greene, A. S., Avery, E. W., Kwon, Y. H., Finn, E. S., Ramani, R., Qiu, M., Constable, R. T., & Chun, M. M. (2020). Functional connectivity predicts changes in attention observed across minutes, days, and months. *Proceedings of the National Academy of Sciences*, *117*(7), 3797–3807. https://doi.org/10.1073/pnas.1912226117

Rossiter, H. E., Davis, E. M., Clark, E. V., Boudrias, M.-H., & Ward, N. S. (2014). Beta oscillations reflect changes in motor cortex inhibition in healthy ageing. *NeuroImage*, *91*, 360–365. https://doi.org/10.1016/j.neuroimage.2014.01.012

Ruppert, M. C., Greuel, A., Freigang, J., Tahmasian, M., Maier, F., Hammes, J., van Eimeren, T., Timmermann, L., Tittgemeyer, M., Drzezga, A., & Eggers, C. (2021). The default mode network and cognition in Parkinson's disease: A multimodal resting-state network approach. *Human Brain Mapping*, *42*(8), 2623–2641. https://doi.org/10.1002/hbm.25393

Sadaghiani, S., Brookes, M. J., & Baillet, S. (2022). Connectomics of human electrophysiology. *NeuroImage*, *247*, 118788. https://doi.org/10.1016/j.neuroimage.2021.118788

Sahay, A., & Hen, R. (2007). Adult hippocampal neurogenesis in depression. *Nature Neuroscience*, *10*(9), Article 9. https://doi.org/10.1038/nn1969

Salat, D. H., Buckner, R. L., Snyder, A. Z., Greve, D. N., Desikan, R. S. R., Busa, E., Morris, J. C., Dale, A. M., & Fischl, B. (2004). Thinning of the Cerebral Cortex in Aging. *Cerebral Cortex*, *14*(7), 721–730. https://doi.org/10.1093/cercor/bhh032

Salmela, E., Renvall, H., Kujala, J., Hakosalo, O., Illman, M., Vihla, M., Leinonen, E., Salmelin, R., & Kere, J. (2016). Evidence for genetic regulation of the human parieto-occipital 10-Hz rhythmic activity. *The European Journal of Neuroscience*, *44*(3), 1963–1971. https://doi.org/10.1111/ejn.13300

Salter, M. W., & Stevens, B. (2017). Microglia emerge as central players in brain disease. *Nature Medicine*, *23*(9), Article 9. https://doi.org/10.1038/nm.4397

Samaha, J., Iemi, L., Haegens, S., & Busch, N. A. (2020). Spontaneous Brain Oscillations and Perceptual Decision-Making. *Trends in Cognitive Sciences*, *24*(8), 639–653. https://doi.org/10.1016/j.tics.2020.05.004

Sareen, E., Zahar, S., Ville, D. V. D., Gupta, A., Griffa, A., & Amico, E. (2021a). Exploring MEG brain fingerprints: Evaluation, pitfalls, and interpretations. *NeuroImage*, *240*, 118331. https://doi.org/10.1016/j.neuroimage.2021.118331

Sareen, E., Zahar, S., Ville, D. V. D., Gupta, A., Griffa, A., & Amico, E. (2021b). Exploring MEG brain fingerprints: Evaluation, pitfalls, and interpretations. *NeuroImage*, *240*, 118331. https://doi.org/10.1016/j.neuroimage.2021.118331

Sareen, E., Zahar, S., Ville, D. V. D., Gupta, A., Griffa, A., & Amico, E. (2021c). Exploring MEG brain fingerprints: Evaluation, pitfalls, and interpretations. *NeuroImage*, *240*, 118331. https://doi.org/10.1016/j.neuroimage.2021.118331

Scally, B., Burke, M. R., Bunce, D., & Delvenne, J.-F. (2018). Resting-state EEG power and connectivity are associated with alpha peak frequency slowing in healthy aging. *Neurobiology of Aging*, *71*, 149–155. https://doi.org/10.1016/j.neurobiolaging.2018.07.004

Schaefer, A., Kong, R., Gordon, E. M., Laumann, T. O., Zuo, X.-N., Holmes, A. J., Eickhoff, S. B., & Yeo, B. T. T. (2018). Local-Global Parcellation of the Human Cerebral Cortex from Intrinsic Functional Connectivity MRI. *Cerebral Cortex*, *28*(9), 3095–3114. https://doi.org/10.1093/cercor/bhx179

Schliebs, R., & Arendt, T. (2011). The cholinergic system in aging and neuronal degeneration. *Behavioural Brain Research*, *221*(2), 555–563. https://doi.org/10.1016/j.bbr.2010.11.058

Schmitt, J. E., Raznahan, A., Liu, S., & Neale, M. C. (2020). The Heritability of Cortical Folding: Evidence from the Human Connectome Project. *Cerebral Cortex (New York, NY)*, *31*(1), 702–715. https://doi.org/10.1093/cercor/bhaa254

Schoenfeld, T. J., & Cameron, H. A. (2015). Adult Neurogenesis and Mental Illness. *Neuropsychopharmacology*, *40*(1), 113–128. https://doi.org/10.1038/npp.2014.230

Seidlitz, J., Nadig, A., Liu, S., Bethlehem, R. A. I., Vértes, P. E., Morgan, S. E., Váša, F., Romero-Garcia, R., Lalonde, F. M., Clasen, L. S., Blumenthal, J. D., Paquola, C., Bernhardt, B., Wagstyl, K., Polioudakis, D., de la Torre-Ubieta, L., Geschwind, D. H., Han, J. C., Lee, N. R., … Raznahan, A. (2020). Transcriptomic and cellular decoding of regional brain vulnerability to neurogenetic disorders. *Nature Communications*, *11*(1), Article 1. https://doi.org/10.1038/s41467-020-17051-5

Shafiei, G., Baillet, S., & Misic, B. (2022). Human electromagnetic and haemodynamic networks systematically converge in unimodal cortex and diverge in transmodal cortex. *PLoS Biology*, *20*(8), e3001735. https://doi.org/10.1371/journal.pbio.3001735

Shafiei, G., Markello, R. D., Makowski, C., Talpalaru, A., Kirschner, M., Devenyi, G. A., Guma, E., Hagmann, P., Cashman, N. R., Lepage, M., Chakravarty, M. M., Dagher, A., & Mišić, B. (2020). Spatial Patterning of Tissue Volume Loss in Schizophrenia Reflects Brain Network Architecture. *Biological Psychiatry*, *87*(8), 727–735. https://doi.org/10.1016/j.biopsych.2019.09.031

Shields, G. S., Sazma, M. A., & Yonelinas, A. P. (2016). The Effects of Acute Stress on Core Executive Functions: A Meta-Analysis and Comparison with Cortisol. *Neuroscience and Biobehavioral Reviews*, *68*, 651–668. https://doi.org/10.1016/j.neubiorev.2016.06.038

Shrout, P. E., & Fleiss, J. L. (1979a). Intraclass correlations: Uses in assessing rater reliability. *Psychological Bulletin*, *86*(2), 420–428. https://doi.org/10.1037/0033-2909.86.2.420

Shrout, P. E., & Fleiss, J. L. (1979b). Intraclass correlations: Uses in assessing rater reliability. *Psychological Bulletin*, *86*(2), 420–428. https://doi.org/10.1037/0033-2909.86.2.420

Singh, A., Cole, R. C., Espinoza, A. I., Evans, A., Cao, S., Cavanagh, J. F., & Narayanan, N. S. (2021a). Timing variability and midfrontal ~4 Hz rhythms correlate with cognition in Parkinson's disease. *Npj Parkinson's Disease*, *7*(1), 14. https://doi.org/10.1038/s41531-021-00158-x

Singh, A., Cole, R. C., Espinoza, A. I., Evans, A., Cao, S., Cavanagh, J. F., & Narayanan, N. S. (2021b). Timing variability and midfrontal ~4 Hz rhythms correlate with cognition in Parkinson's disease. *Npj Parkinson's Disease*, *7*(1), Article 1. https://doi.org/10.1038/s41531-021-00158-x

Singh, A., Richardson, S. P., Narayanan, N., & Cavanagh, J. F. (2018a). Mid-frontal theta activity is diminished during cognitive control in Parkinson's disease. *Neuropsychologia*, *117*, 113–122. https://doi.org/10.1016/j.neuropsychologia.2018.05.020

Singh, A., Richardson, S. P., Narayanan, N., & Cavanagh, J. F. (2018b). Mid-frontal theta activity is diminished during cognitive control in Parkinson's disease. *Neuropsychologia*, *117*, 113–122. https://doi.org/10.1016/j.neuropsychologia.2018.05.020

Smit, C. M., Wright, M. J., Hansell, N. K., Geffen, G. M., & Martin, N. G. (2006). Genetic variation of individual alpha frequency (IAF) and alpha power in a large adolescent twin sample. *International Journal of Psychophysiology: Official Journal of the International Organization of Psychophysiology*, *61*(2), 235–243. https://doi.org/10.1016/j.ijpsycho.2005.10.004

Smit, D. J. A., Posthuma, D., Boomsma, D. I., & Geus, E. J. C. (2005). Heritability of background EEG across the power spectrum. *Psychophysiology*, *42*(6), Article 6. https://doi.org/10.1111/j.1469-8986.2005.00352.x

Smith, S. M., Vidaurre, D., Beckmann, C. F., Glasser, M. F., Jenkinson, M., Miller, K. L., Nichols, T. E., Robinson, E. C., Salimi-Khorshidi, G., Woolrich, M. W., Barch, D. M., Uğurbil, K., & Van Essen, D. C. (2013). Functional connectomics from resting-state fMRI. *Trends in Cognitive Sciences*, *17*(12), 666–682. https://doi.org/10.1016/j.tics.2013.09.016

Soreq, L., UK Brain Expression Consortium, North American Brain Expression Consortium, Rose, J., Soreq, E., Hardy, J., Trabzuni, D., Cookson, M. R., Smith, C., Ryten, M., Patani, R., & Ule, J. (2017). Major Shifts in Glial Regional Identity Are a Transcriptional Hallmark of Human Brain Aging. *Cell Reports*, *18*(2), 557–570. https://doi.org/10.1016/j.celrep.2016.12.011

Sorrentino, P., Rucco, R., Lardone, A., Liparoti, M., Troisi Lopez, E., Cavaliere, C., Soricelli, A., Jirsa, V., Sorrentino, G., & Amico, E. (2021a). Clinical connectome fingerprints of cognitive decline. *NeuroImage*, *238*, 118253. https://doi.org/10.1016/j.neuroimage.2021.118253

Sorrentino, P., Rucco, R., Lardone, A., Liparoti, M., Troisi Lopez, E., Cavaliere, C., Soricelli, A., Jirsa, V., Sorrentino, G., & Amico, E. (2021b). Clinical connectome fingerprints of cognitive decline. *NeuroImage*, *238*, 118253. https://doi.org/10.1016/j.neuroimage.2021.118253

Sorrentino, P., Rucco, R., Lardone, A., Liparoti, M., Troisi Lopez, E., Cavaliere, C., Soricelli, A., Jirsa, V., Sorrentino, G., & Amico, E. (2021c). Clinical connectome fingerprints of cognitive decline. *NeuroImage*, *238*, 118253. https://doi.org/10.1016/j.neuroimage.2021.118253

Spisak, T., Bingel, U., & Wager, T. D. (2023). Multivariate BWAS can be replicable with moderate sample sizes. *Nature*, *615*(7951), Article 7951. https://doi.org/10.1038/s41586-023-05745-x

Stampacchia, S., Asadi, S., Ribaldi, F., Tomczyk, S., Altomare, D., Pievani, M., Frisoni, G., Amico, E., & Garibotto, V. (2021). Towards fingerprinting and identifiability within the Alzheimer's continuum using resting-state functional connectivity. *Alzheimer's & Dementia*, *17*(S4), e057724. https://doi.org/10.1002/alz.057724

Stein, R. B., Gossen, E. R., & Jones, K. E. (2005). Neuronal variability: Noise or part of the signal? *Nature Reviews Neuroscience*, *6*(5), Article 5. https://doi.org/10.1038/nrn1668

Stoffers, D., Bosboom, J. L. W., Deijen, J. B., Wolters, E. C., Berendse, H. W., & Stam, C. J. (2007). Slowing of oscillatory brain activity is a stable characteristic of Parkinson's disease without dementia. *Brain*, *130*(7), 1847–1860. https://doi.org/10.1093/brain/awm034

Stoffers, D., Bosboom, J. L. W., Wolters, E. Ch., Stam, C. J., & Berendse, H. W. (2008a). Dopaminergic modulation of cortico-cortical functional connectivity in Parkinson's disease: An MEG study. *Experimental Neurology*, *213*(1), Article 1. https://doi.org/10.1016/j.expneurol.2008.05.021

Stoffers, D., Bosboom, J. L. W., Wolters, E. Ch., Stam, C. J., & Berendse, H. W. (2008b). Dopaminergic modulation of cortico-cortical functional connectivity in Parkinson's disease: An MEG study. *Experimental Neurology*, *213*(1), 191–195. https://doi.org/10.1016/j.expneurol.2008.05.021

Stothart, G., & Kazanina, N. (2016). Auditory perception in the aging brain: The role of inhibition and facilitation in early processing. *Neurobiology of Aging*, *47*, 23–34. https://doi.org/10.1016/j.neurobiolaging.2016.06.022

Strömmer, J. M., Põldver, N., Waselius, T., Kirjavainen, V., Järveläinen, S., Björksten, S., Tarkka, I. M., & Astikainen, P. (2017). Automatic auditory and somatosensory brain responses in relation to cognitive abilities and physical fitness in older adults. *Scientific Reports*, *7*(1), Article 1. https://doi.org/10.1038/s41598-017-14139-9

Sudlow, C., Gallacher, J., Allen, N., Beral, V., Burton, P., Danesh, J., Downey, P., Elliott, P., Green, J., Landray, M., Liu, B., Matthews, P., Ong, G., Pell, J., Silman, A., Young, A., Sprosen, T., Peakman, T., & Collins, R. (2015). UK Biobank: An Open Access Resource for Identifying the Causes of a Wide Range of Complex Diseases of Middle and Old Age. *PLOS Medicine*, *12*(3), e1001779. https://doi.org/10.1371/journal.pmed.1001779

Sultzer, D. L., Lim, A. C., Gordon, H. L., Yarns, B. C., & Melrose, R. J. (2022). Cholinergic receptor binding in unimpaired older adults, mild cognitive impairment, and Alzheimer's disease

dementia. *Alzheimer's Research & Therapy*, *14*(1), 25. https://doi.org/10.1186/s13195-021-00954-w

Tadel, F., Baillet, S., Mosher, J. C., Pantazis, D., & Leahy, R. M. (2011). Brainstorm: A User-Friendly Application for MEG/EEG Analysis. *Computational Intelligence and Neuroscience*, *2011*, 1–13. https://doi.org/10.1155/2011/879716

Takahashi, T., Cho, R. Y., Murata, T., Mizuno, T., Kikuchi, M., Mizukami, K., Kosaka, H., Takahashi, K., & Wada, Y. (2009). Age-related variation in EEG complexity to photic stimulation: A multiscale entropy analysis. *Clinical Neurophysiology : Official Journal of the International Federation of Clinical Neurophysiology*, *120*(3), 476–483. https://doi.org/10.1016/j.clinph.2008.12.043

Tanti, A., Belliveau, C., Nagy, C., Maitra, M., Denux, F., Perlman, K., Chen, F., Mpai, R., Canonne, C., Théberge, S., McFarquhar, A., Davoli, M. A., Belzung, C., Turecki, G., & Mechawar, N. (2022). Child abuse associates with increased recruitment of perineuronal nets in the ventromedial prefrontal cortex: A possible implication of oligodendrocyte progenitor cells. *Molecular Psychiatry*, *27*(3), Article 3. https://doi.org/10.1038/s41380-021-01372-y

Tay, T. L., Béchade, C., D'Andrea, I., St-Pierre, M.-K., Henry, M. S., Roumier, A., & Tremblay, M.-E. (2017). Microglia Gone Rogue: Impacts on Psychiatric Disorders across the Lifespan. *Frontiers in Molecular Neuroscience*, *10*, 421. https://doi.org/10.3389/fnmol.2017.00421

Taylor, J. R., Williams, N., Cusack, R., Auer, T., Shafto, M. A., Dixon, M., Tyler, L. K., Cam-CAN, & Henson, R. N. (2017). The Cambridge Centre for Ageing and Neuroscience (Cam-CAN) data repository: Structural and functional MRI, MEG, and cognitive data from a cross-

sectional adult lifespan sample. *NeuroImage*, *144*, 262–269. https://doi.org/10.1016/j.neuroimage.2015.09.018

Tessitore, A., Esposito, F., Vitale, C., Santangelo, G., Amboni, M., Russo, A., Corbo, D., Cirillo, G., Barone, P., & Tedeschi, G. (2012). Default-mode network connectivity in cognitively unimpaired patients with Parkinson disease. *Neurology*, *79*(23), 2226–2232. https://doi.org/10.1212/WNL.0b013e31827689d6

Thalmann, M., Souza, A. S., & Oberauer, K. (2019). How does chunking help working memory? *Journal of Experimental Psychology. Learning, Memory, and Cognition*, *45*(1), 37–55. https://doi.org/10.1037/xlm0000578

*The Cholinergic Hypothesis of Geriatric Memory Dysfunction | Science*. (n.d.). Retrieved August 15, 2023, from https://www.science.org/doi/abs/10.1126/science.7046051

Thomas, P. D. (2017). The Gene Ontology and the meaning of biological function. *Methods in Molecular Biology (Clifton, N.J.)*, *1446*, 15. https://doi.org/10.1007/978-1-4939-3743-1_2

Thut, G., & Pascual-Leone, A. (2010). A review of combined TMS-EEG studies to characterize lasting effects of repetitive TMS and assess their usefulness in cognitive and clinical neuroscience. *Brain Topography*, *22*(4), 219–232. https://doi.org/10.1007/s10548-009-0115-4

Thuwal, K., Banerjee, A., & Roy, D. (2021). Aperiodic and Periodic Components of Ongoing Oscillatory Brain Dynamics Link Distinct Functional Aspects of Cognition across Adult Lifespan. *eNeuro*, *8*(5), ENEURO.0224-21.2021. https://doi.org/10.1523/ENEURO.0224-21.2021

Tinkhauser, G., Pogosyan, A., Tan, H., Herz, D. M., Kühn, A. A., & Brown, P. (2017). Beta burst dynamics in Parkinson's disease OFF and ON dopaminergic medication. *Brain: A Journal of Neurology*, *140*(11), 2968–2981. https://doi.org/10.1093/brain/awx252

Torrecillos, F., Tinkhauser, G., Fischer, P., Green, A. L., Aziz, T. Z., Foltynie, T., Limousin, P., Zrinzo, L., Ashkan, K., Brown, P., & Tan, H. (2018). Modulation of Beta Bursts in the Subthalamic Nucleus Predicts Motor Performance. *The Journal of Neuroscience: The Official Journal of the Society for Neuroscience*, *38*(41), 8905–8917. https://doi.org/10.1523/JNEUROSCI.1314-18.2018

Tremblay-Mercier, J., Madjar, C., Das, S., Pichet Binette, A., Dyke, S. O. M., Étienne, P., Lafaille-Magnan, M.-E., Remz, J., Bellec, P., Louis Collins, D., Natasha Rajah, M., Bohbot, V., Leoutsakos, J.-M., Iturria-Medina, Y., Kat, J., Hoge, R. D., Gauthier, S., Tardif, C. L., Mallar Chakravarty, M., … Breitner, J. C. S. (2021). Open science datasets from PREVENT-AD, a longitudinal cohort of pre-symptomatic Alzheimer's disease. *NeuroImage: Clinical*, *31*, 102733. https://doi.org/10.1016/j.nicl.2021.102733

Troisi Lopez, E., Minino, R., Liparoti, M., Polverino, A., Romano, A., De Micco, R., Lucidi, F., Tessitore, A., Amico, E., Sorrentino, G., Jirsa, V., & Sorrentino, P. (2023). Fading of brain network fingerprint in Parkinson's disease predicts motor clinical impairment. *Human Brain Mapping*, *44*(3), 1239–1250. https://doi.org/10.1002/hbm.26156

Uddin, L. Q. (2020). Bring the Noise: Reconceptualizing Spontaneous Neural Activity. *Trends in Cognitive Sciences*, *24*(9), 734–746. https://doi.org/10.1016/j.tics.2020.06.003

Uddin, L. Q. (2021). Cognitive and behavioural flexibility: Neural mechanisms and clinical considerations. *Nature Reviews Neuroscience*, *22*(3), Article 3. https://doi.org/10.1038/s41583-021-00428-w

Underwood, C. F., & Parr-Brownlie, L. C. (2021). Primary motor cortex in Parkinson's disease: Functional changes and opportunities for neurostimulation. *Neurobiology of Disease*, *147*, 105159. https://doi.org/10.1016/j.nbd.2020.105159

Valizadeh, S. A., Liem, F., Mérillat, S., Hänggi, J., & Jäncke, L. (2018). Identification of individual subjects on the basis of their brain anatomical features. *Scientific Reports*, *8*(1), Article 1. https://doi.org/10.1038/s41598-018-23696-6

van Eimeren, T., Monchi, O., Ballanger, B., & Strafella, A. P. (2009). Dysfunction of the Default Mode Network in Parkinson Disease: A Functional Magnetic Resonance Imaging Study. *Archives of Neurology*, *66*(7), 877–883. https://doi.org/10.1001/archneurol.2009.97

Van Essen, D. C., Ugurbil, K., Auerbach, E., Barch, D., Behrens, T. E. J., Bucholz, R., Chang, A., Chen, L., Corbetta, M., Curtiss, S. W., Della Penna, S., Feinberg, D., Glasser, M. F., Harel, N., Heath, A. C., Larson-Prior, L., Marcus, D., Michalareas, G., Moeller, S., … Yacoub, E. (2012). The Human Connectome Project: A data acquisition perspective. *NeuroImage*, *62*(4), Article 4. https://doi.org/10.1016/j.neuroimage.2012.02.018

Van Horn, J. D., Grafton, S. T., & Miller, M. B. (2008). Individual Variability in Brain Activity: A Nuisance or an Opportunity? *Brain Imaging and Behavior*, *2*(4), 327–334. https://doi.org/10.1007/s11682-008-9049-9

Váša, F., & Mišić, B. (2022). Null models in network neuroscience. *Nature Reviews Neuroscience*, *23*(8), 493–504. https://doi.org/10.1038/s41583-022-00601-9

Vazey, E. M., & Aston-Jones, G. (2014). Designer receptor manipulations reveal a role of the locus coeruleus noradrenergic system in isoflurane general anesthesia. *Proceedings of the National Academy of Sciences of the United States of America*, *111*(10), 3859–3864. https://doi.org/10.1073/pnas.1310025111

Veerapa, E., Grandgenevre, P., El Fayoumi, M., Vinnac, B., Haelewyn, O., Szaffarczyk, S., Vaiva, G., & D'Hondt, F. (2020). Attentional bias towards negative stimuli in healthy individuals and the effects of trait anxiety. *Scientific Reports*, *10*(1), Article 1. https://doi.org/10.1038/s41598-020-68490-5

Voytek, B., & Knight, R. T. (2015). Dynamic Network Communication as a Unifying Neural Basis for Cognition, Development, Aging, and Disease. *Biological Psychiatry*, *77*(12), 1089–1097. https://doi.org/10.1016/j.biopsych.2015.04.016

Voytek, B., Kramer, M. A., Case, J., Lepage, K. Q., Tempesta, Z. R., Knight, R. T., & Gazzaley, A. (2015a). Age-Related Changes in 1/f Neural Electrophysiological Noise. *Journal of Neuroscience*, *35*(38), 13257–13265. https://doi.org/10.1523/JNEUROSCI.2332-14.2015

Voytek, B., Kramer, M. A., Case, J., Lepage, K. Q., Tempesta, Z. R., Knight, R. T., & Gazzaley, A. (2015b). Age-Related Changes in 1/f Neural Electrophysiological Noise. *Journal of Neuroscience*, *35*(38), 13257–13265. https://doi.org/10.1523/JNEUROSCI.2332-14.2015

Wachinger, C., Golland, P., Kremen, W., Fischl, B., & Reuter, M. (2015). BrainPrint: A Discriminative Characterization of Brain Morphology. *NeuroImage*, *109*, 232–248. https://doi.org/10.1016/j.neuroimage.2015.01.032

Wang, H., He, Y., Sun, Z., Ren, S., Liu, M., Wang, G., & Yang, J. (2022). Microglia in depression: An overview of microglia in the pathogenesis and treatment of depression. *Journal of Neuroinflammation*, *19*(1), 132. https://doi.org/10.1186/s12974-022-02492-0

Waschke, L., Donoghue, T., Fiedler, L., Smith, S., Garrett, D. D., Voytek, B., & Obleser, J. (2021). Modality-specific tracking of attention and sensory statistics in the human electrophysiological spectral exponent. *eLife*, *10*, e70068. https://doi.org/10.7554/eLife.70068

Waschke, L., Kloosterman, N. A., Obleser, J., & Garrett, D. D. (2021). Behavior needs neural variability. *Neuron*, *109*(5), 751–766. https://doi.org/10.1016/j.neuron.2021.01.023

Wei, Y., de Lange, S. C., Scholtens, L. H., Watanabe, K., Ardesch, D. J., Jansen, P. R., Savage, J. E., Li, L., Preuss, T. M., Rilling, J. K., Posthuma, D., & van den Heuvel, M. P. (2019). Genetic mapping and evolutionary analysis of human-expanded cognitive networks. *Nature Communications*, *10*(1), Article 1. https://doi.org/10.1038/s41467-019-12764-8

Welch, P. (1967). The use of fast Fourier transform for the estimation of power spectra: A method based on time averaging over short, modified periodograms. *IEEE Transactions on Audio and Electroacoustics*, *15*(2), 70–73. https://doi.org/10.1109/TAU.1967.1161901

Werling, D. M., Pochareddy, S., Choi, J., An, J.-Y., Sheppard, B., Peng, M., Li, Z., Dastmalchi, C., Santpere, G., Sousa, A. M. M., Tebbenkamp, A. T. N., Kaur, N., Gulden, F. O., Breen, M. S., Liang, L., Gilson, M. C., Zhao, X., Dong, S., Klei, L., … Sestan, N. (2020). Whole-Genome and RNA Sequencing Reveal Variation and Transcriptomic Coordination in the Developing Human Prefrontal Cortex. *Cell Reports*, *31*(1), 107489. https://doi.org/10.1016/j.celrep.2020.03.053

Whitaker, K. J., Vértes, P. E., Romero-Garcia, R., Váša, F., Moutoussis, M., Prabhu, G., Weiskopf, N., Callaghan, M. F., Wagstyl, K., Rittman, T., Tait, R., Ooi, C., Suckling, J., Inkster, B., Fonagy, P., Dolan, R. J., Jones, P. B., Goodyer, I. M., the NSPN Consortium, & Bullmore, E. T. (2016). Adolescence is associated with genomically patterned consolidation of the hubs of the human brain connectome. *Proceedings of the National Academy of Sciences*, *113*(32), 9105–9110. https://doi.org/10.1073/pnas.1601745113

Whitham, E. M., Pope, K. J., Fitzgibbon, S. P., Lewis, T., Clark, C. R., Loveless, S., Broberg, M., Wallace, A., DeLosAngeles, D., Lillie, P., Hardy, A., Fronsko, R., Pulbrook, A., & Willoughby, J. O. (2007). Scalp electrical recording during paralysis: Quantitative evidence that EEG frequencies above 20 Hz are contaminated by EMG. *Clinical Neurophysiology: Official Journal of the International Federation of Clinical Neurophysiology*, *118*(8), 1877–1888. https://doi.org/10.1016/j.clinph.2007.04.027

Wiesman, A. I., Castanheira, J. da S., Degroot, C., Fon, E. A., Baillet, S., Group, P.-A. R., & Network, Q. P. (2022). *A sagittal gradient of pathological and compensatory effects of neurophysiological slowing in Parkinson's disease* (p. 2022.08.05.22278436). medRxiv. https://doi.org/10.1101/2022.08.05.22278436

Wiesman, A. I., da Silva Castanheira, J., & Baillet, S. (2022a). Stability of spectral estimates in resting-state magnetoencephalography: Recommendations for minimal data duration with neuroanatomical specificity. *NeuroImage*, *247*, 118823. https://doi.org/10.1016/j.neuroimage.2021.118823

Wiesman, A. I., da Silva Castanheira, J., & Baillet, S. (2022b). Stability of spectral estimates in resting-state magnetoencephalography: Recommendations for minimal data duration

with neuroanatomical specificity. *NeuroImage*, *247*, 118823. https://doi.org/10.1016/j.neuroimage.2021.118823

Wiesman, A. I., da Silva Castanheira, J., & Baillet, S. (2022c). Stability of spectral estimates in resting-state magnetoencephalography: Recommendations for minimal data duration with neuroanatomical specificity. *NeuroImage*, *247*, 118823. https://doi.org/10.1016/j.neuroimage.2021.118823

Wiesman, A. I., da Silva Castanheira, J., Degroot, C., Fon, E. A., Baillet, S., & Network, Q. P. (2023). Adverse and compensatory neurophysiological slowing in Parkinson's disease. *Progress in Neurobiology*, *231*, 102538. https://doi.org/10.1016/j.pneurobio.2023.102538

Wiesman, A. I., Donhauser, P. W., Degroot, C., Diab, S., Kousaie, S., Fon, E. A., Klein, D., & Baillet, S. (2023). Aberrant neurophysiological signaling associated with speech impairments in Parkinson's disease. *Npj Parkinson's Disease*, *9*(1), Article 1. https://doi.org/10.1038/s41531-023-00495-z

Wilson, H., Niccolini, F., Pellicano, C., & Politis, M. (2019). Cortical thinning across Parkinson's disease stages and clinical correlates. *Journal of the Neurological Sciences*, *398*, 31–38. https://doi.org/10.1016/j.jns.2019.01.020

Wilson, L. E., da Silva Castanheira, J., & Baillet, S. (2022). Time-resolved parameterization of aperiodic and periodic brain activity. *eLife*, *11*, e77348. https://doi.org/10.7554/eLife.77348

Winterer, G., Mahlberg, R., Smolka, M. N., Samochowiec, J., Ziller, M., Rommelspacher, H.-P., Herrmann, W. M., Schmidt, L. G., & Sander, T. (2003). Association Analysis of Exonic Variants of the GABAB-Receptor Gene and Alpha Electroencephalogram Voltage in

Normal Subjects and Alcohol-Dependent Patients. *Behavior Genetics*, *33*(1), 7–15. https://doi.org/10.1023/A:1021043315012

Wohleb, E. S., & Delpech, J.-C. (2017). Dynamic cross-talk between microglia and peripheral monocytes underlies stress-induced neuroinflammation and behavioral consequences. *Progress in Neuro-Psychopharmacology & Biological Psychiatry*, *79*(Pt A), 40–48. https://doi.org/10.1016/j.pnpbp.2016.04.013

Woo, C.-W., Chang, L. J., Lindquist, M. A., & Wager, T. D. (2017). Building better biomarkers: Brain models in translational neuroimaging. *Nature Neuroscience*, *20*(3), Article 3. https://doi.org/10.1038/nn.4478

Yamashita, M., Yoshihara, Y., Hashimoto, R., Yahata, N., Ichikawa, N., Sakai, Y., Yamada, T., Matsukawa, N., Okada, G., Tanaka, S. C., Kasai, K., Kato, N., Okamoto, Y., Seymour, B., Takahashi, H., Kawato, M., & Imamizu, H. (2018). A prediction model of working memory across health and psychiatric disease using whole-brain functional connectivity. *eLife*, *7*, e38844. https://doi.org/10.7554/eLife.38844

Yarkoni, T. (2015). Neurobiological substrates of personality: A critical overview. In *APA handbook of personality and social psychology, Volume 4: Personality processes and individual differences* (pp. 61–83). American Psychological Association. https://doi.org/10.1037/14343-003

Yarkoni, T., Poldrack, R. A., Nichols, T. E., Van Essen, D. C., & Wager, T. D. (2011). Large-scale automated synthesis of human functional neuroimaging data. *Nature Methods*, *8*(8), 665–670. https://doi.org/10.1038/nmeth.1635

Yeo, B. T. T., Krienen, F. M., Sepulcre, J., Sabuncu, M. R., Lashkari, D., Hollinshead, M., Roffman, J. L., Smoller, J. W., Zöllei, L., Polimeni, J. R., Fischl, B., Liu, H., & Buckner, R. L. (2011). The organization of the human cerebral cortex estimated by intrinsic functional connectivity. *Journal of Neurophysiology*, *106*(3), 1125–1165. https://doi.org/10.1152/jn.00338.2011

Yoo, K., Rosenberg, M. D., Hsu, W.-T., Zhang, S., Li, C.-S. R., Scheinost, D., Constable, R. T., & Chun, M. M. (2018). Connectome-based predictive modeling of attention: Comparing different functional connectivity features and prediction methods across datasets. *NeuroImage*, *167*, 11–22. https://doi.org/10.1016/j.neuroimage.2017.11.010

Yu, J., & Fischer, N. L. (2022). Age-specificity and generalization of behavior-associated structural and functional networks and their relevance to behavioral domains. *Human Brain Mapping*, *43*(8), 2405–2418. https://doi.org/10.1002/hbm.25759

Yu, Y., Escobar Sanabria, D., Wang, J., Hendrix, C. M., Zhang, J., Nebeck, S. D., Amundson, A. M., Busby, Z. B., Bauer, D. L., Johnson, M. D., Johnson, L. A., & Vitek, J. L. (2021). Parkinsonism Alters Beta Burst Dynamics across the Basal Ganglia-Motor Cortical Network. *The Journal of Neuroscience: The Official Journal of the Society for Neuroscience*, *41*(10), 2274–2286. https://doi.org/10.1523/JNEUROSCI.1591-20.2021

Yuval-Greenberg, S., Tomer, O., Keren, A. S., Nelken, I., & Deouell, L. Y. (2008). Transient induced gamma-band response in EEG as a manifestation of miniature saccades. *Neuron*, *58*(3), 429–441. https://doi.org/10.1016/j.neuron.2008.03.027

Zhang, Y., Sloan, S. A., Clarke, L. E., Caneda, C., Plaza, C. A., Blumenthal, P. D., Vogel, H., Steinberg, G. K., Edwards, M. S. B., Li, G., Duncan, J. A., Cheshier, S. H., Shuer, L. M., Chang, E. F., Grant, G. A., Gephart, M. G. H., & Barres, B. A. (2016). Purification and Characterization of

Progenitor and Mature Human Astrocytes Reveals Transcriptional and Functional Differences with Mouse. *Neuron*, *89*(1), 37–53. https://doi.org/10.1016/j.neuron.2015.11.013

Zhu, H., Huang, J., Deng, L., He, N., Cheng, L., Shu, P., Yan, F., Tong, S., Sun, J., & Ling, H. (2019). Abnormal Dynamic Functional Connectivity Associated With Subcortical Networks in Parkinson's Disease: A Temporal Variability Perspective. *Frontiers in Neuroscience*, *13*. https://www.frontiersin.org/articles/10.3389/fnins.2019.00080

Zietsch, B. P., Hansen, J. L., Hansell, N. K., Geffen, G. M., Martin, N. G., & Wright, M. J. (2007). Common and specific genetic influences on EEG power bands delta, theta, alpha, and beta. *Biological Psychology*, *75*(2), 154–164. https://doi.org/10.1016/j.biopsycho.2007.01.004

Zwir, I., Arnedo, J., Del-Val, C., Pulkki-Råback, L., Konte, B., Yang, S. S., Romero-Zaliz, R., Hintsanen, M., Cloninger, K. M., Garcia, D., Svrakic, D. M., Rozsa, S., Martinez, M., Lyytikäinen, L.-P., Giegling, I., Kähönen, M., Hernandez-Cuervo, H., Seppälä, I., Raitoharju, E., … Cloninger, C. R. (2020). Uncovering the complex genetics of human character. *Molecular Psychiatry*, *25*(10), Article 10. https://doi.org/10.1038/s41380-018-0263-6

# Appendix A: Supplemental Information chapter 2

## MEG fingerprinting is robust against sample demographics

The OMEGA data repository contains 158 participants, with a subset (N=47) scanned at multiple occasions several days apart. OMEGA consists essentially of data from healthy controls with a 18-73-year age span (SD=14.7 years; Supplementary Table 1).

One potential confound that could have inflated our ability to fingerprint individuals is the heterogeneity introduced by both healthy and clinical populations in the OMEGA cohort. To address this concern, we ran a secondary analysis where we performed the fingerprinting procedures described in the manuscript with only healthy controls (N=130). The results, reported in Supplementary table 2, demonstrated that fingerprinting performances were not biased by the patients/controls heterogeneity of the OMEGA sample. We observed a decrease of less than 1% in performance relative to fingerprinting from the entire cohort. Further, there was no clear relationship between differentiability** and demographics (Supplementary Figure 1)., using connectome (age: r= 0.08, p = 0.2; gender: t=-0.27, p = 0.7; handedness: t=-0.51, p = 0.6; clinical status: t=-0.87, p = 0.3; two-tailed) and spectral fingerprinting (age: r= 0.10, p = 0.1; gender: t= 0.62, p = 0.5; handedness: t= 0.13, p = 0.8; clinical status: t= 0.84, p = 0.3; two-tailed).

** Please note that differentiability may also be referred to as self-identifiability (Iself) in our analysis scripts.

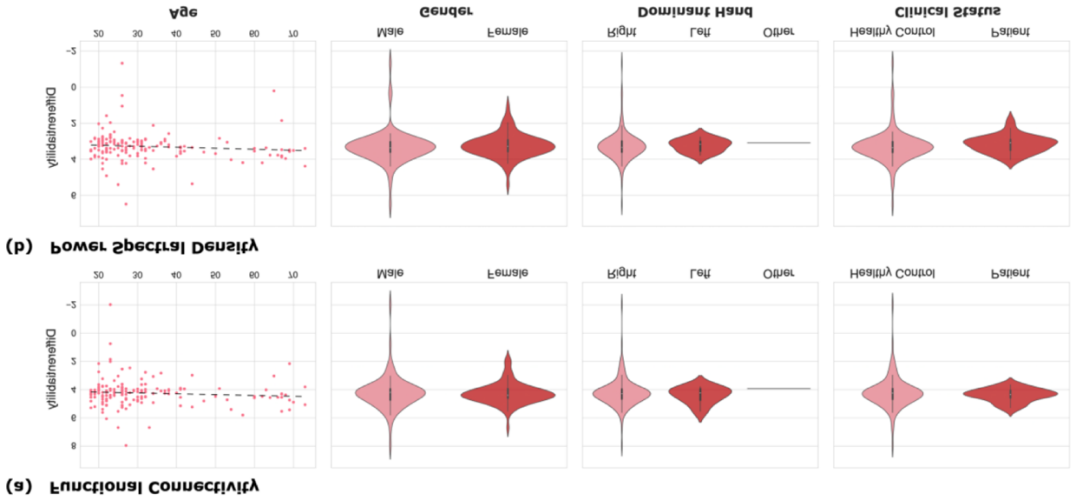


## Supplementary Figure 1: Differentiability is not associated with demographics

The plots depict demographic variables and corresponding differentiability scores across both (a) connectome and (b) spectral broadband within-session fingerprinting (n = 158). Demographic variables included age, biological sex, dominant hand, and healthy vs. patient categories. (a) There was no clear relationship between age, biological sex, dominant hand, and

healthy vs. patient categories and differentiability for broadband within-session connectome fingerprinting. (b) There was no clear relationship between age, biological sex, dominant hand, and healthy vs. patient categories and differentiability for broadband within-session connectome fingerprinting. Differences in demographics did not drive differentiability. The center of the boxplot depicts the median (Q2), the box extends from the Q1 to Q3 quartile values of the data, and the whiskers extend to show the range of the data (i.e., the farthest datapoint within the 1.5 * IQR (IQR = Q3 -Q1) interval). Source data are provided as Source Data File.

Acquisition parameters did not affect both fingerprinting performances (Supplementary Figure 2). Participants with longer recordings (i.e., more data) were not more differentiable (connectome: r=-0.02, p = 0.7; spectral: r= 0.02, p = 0.8). This observation is consistent with the shortened fingerprinting results, which demonstrate individuals were differentiable from shorter 30-second recordings (see below).

Taken together, these supplemental results demonstrate that MEG fingerprinting is robust against data artifacts, heterogeneous sample demographics, and acquisition parameters.

| | Within-session data | Between-session data |
|---|---|---|
| Age | 31.9 ± 14.7 | 26.7 ± 11.6 |
| Gender | 77 Females | 24 Females |
| Dominant Hand | 147 Right, 8 Left, 1 Other | 44 Right, 3 Left |
| Clinical Status | 130 Healthy Controls<br>22 ADHD<br>6 Chronic Pain | 25 Healthy Controls<br>22 ADHD |

Supplementary table 1: OMEGA participant demographics. Demographic variables summarized for both subsets of the OMEGA data repository.

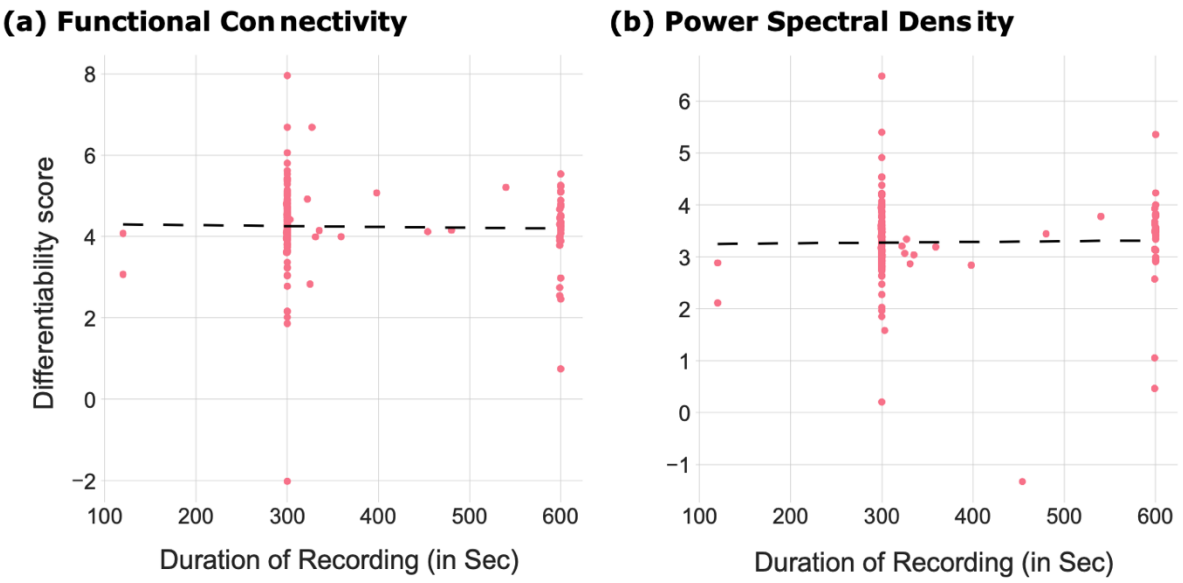


Supplementary Figure 2: Recording duration did not affect differentiability. Scatter plots of differentiability vs. duration of data collections, for the broadband within-session challenge. There was no clear relationship between differentiability and the duration of the MEG recordings across participants. Source data are provided as Source Data file.

| | All Participants | | Only Healthy Controls | |
|---|---|---|---|---|
| | Dataset 1 to Dataset 2 | Dataset 2 to Dataset 1 | Dataset 1 to Dataset 2 | Dataset 2 to Dataset 1 |
| Connectome | 94.9% | 94.3% | 93.8% | 93.0% |
| Spectral | 96.2% | 96.2% | 95.3% | 95.3% |

Supplementary table 2. Fingerprinting performances of healthy controls

Differentiation performances of connectome and spectral broadband within-session fingerprinting obtained from for the entire repository (healthy controls and patients), and from healthy participants only. Each column reports fingerprinting performances from dataset 1 to dataset 2 and vice-versa (see Figure 1 and Methods for details). Overall, differentiation accuracy decreased slightly by ~0.9% when comprising healthy participants only. Consistent with our findings reported in Supplementary Figure 2, clinical status did not play a major role in the differentiation of individuals.

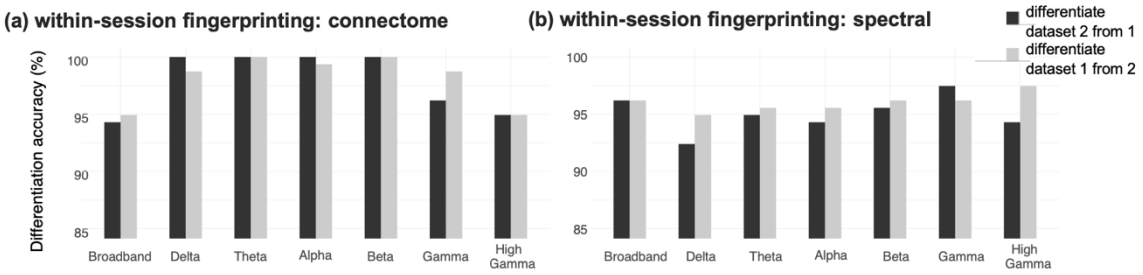


Supplementary Figure 3: Differentiation accuracy from within-session datasets

Results from MEG within-session fingerprinting. Differentiation accuracy for (a) connectome and (b) spectral fingerprinting (broadband and narrowband data). The accuracy scores are reported for differentiation from dataset 1 to dataset 2 and vice-versa, as explained in Methods. Source data are provided as a Source Data file.

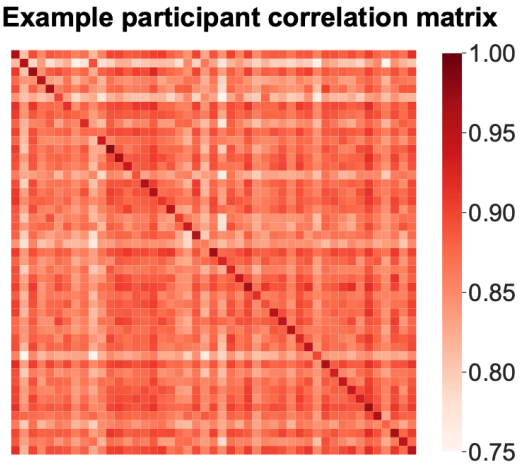


Supplementary Figure 4: Example participant correlation matrix for fingerprinting

Exemplar participant correlation matrix derived from between-session data used for fingerprinting. The study-identity of participants was determined by the highest correlation statistics taken across rows (e.g., to differentiate dataset-2 from dataset-1) or columns (to differentiate dataset-1 from dataset-2).

## Data reduction from principal component analysis does not improve MEG fingerprinting substantially

Amico and Goñi (1) previously reported improvements to participant differentiation when using data reduction techniques prior to fingerprinting, using e.g., principal component analysis (PCA). We reproduced their approach, using PCA to reduce the dimensionality of the connectome and spectral feature spaces prior to fingerprinting. Our results provided little support to PCA reconstruction improving differentiation accuracy, as shown Supplementary Figure 5 and in Supplementary table 3. PCA increased differentiability by less than 1.5%. Data reduction had limited beneficial impact possibly because of high fingerprinting performances at

baseline (without data reduction). We also emphasize that we conducted MEG source time series extraction via a PCA of all local time series within each parcel. It is therefore likely that this dimension reduction procedure contributed to improve signal-to-noise ratio and limited the impact of subsequent PCA of features.

| | Original (un-reconstructed) | | PCA Reconstructed | |
|---|---|---|---|---|
| | Dataset 1 to Dataset 2 | Dataset 2 to Dataset 1 | Dataset 1 to Dataset 2 | Dataset 2 to Dataset 1 |
| Connectome | 94.9% | 94.3% | 96.2% | 96.2% |
| Spectral | 96.2% | 96.2% | 96.2% | 96.2% |

Supplementary table 3: Limited contribution of data reduction from principal component analysis to MEG fingerprinting. Performances in differentiation accuracy for connectome and spectral broadband within-session fingerprinting, for both original and PCA-reconstructed data (1). PCA data reduction improved connectome fingerprinting performances only slightly (about 2%). It had virtually no effect on spectral fingerprinting performances.

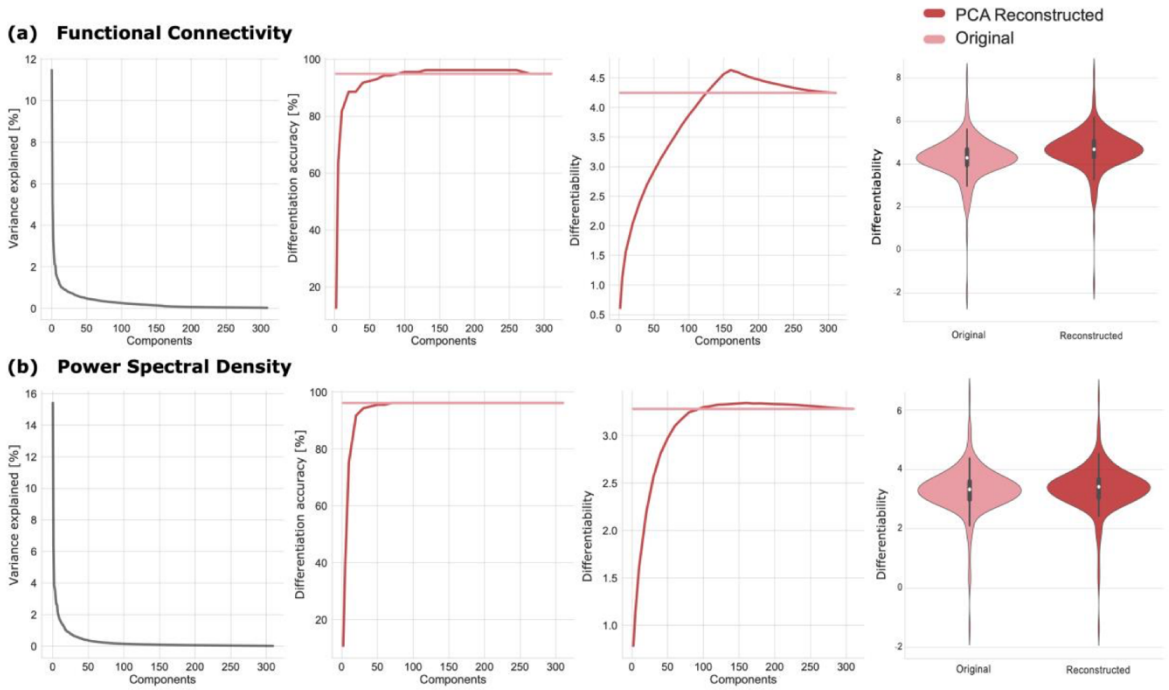


Supplementary Figure 5: Limited benefit of PCA reconstruction to differentiation accuracy

PCA reconstruction as proposed by Amico and Goñi (2018) had limited effect on (a) connectome 105 and (b) spectral within-session fingerprinting (n= 158). The original results (Figure 2) are plotted against PCA-reconstructed results. From left to right, plots show i) PCA components plotted vs. their respective fractions of signal variance explained, ii) differentiation accuracy across PCA components, iii) average differentiability scores across PCA components, and iv) violin plots of differentiability scores before and after PCA reconstruction for both (a) connectome and (b) spectral fingerprinting. Overall, PCA reconstruction did not substantially improve differentiation accuracy. The center of the boxplot depicts the median (Q2), the box extends from the Q1 to Q3 quartile values of the data, and the whiskers extend to show the range of the data (i.e., the farthest datapoint within the 1.5 * IQR (IQR = Q3 - Q1) interval). Source data are provided as a Source Data file.

### Fingerprinting with 30-second data segments

We challenged MEG fingerprinting using short 30-second data segments (i.e., shortened within-session fingerprinting). We epoched participants' MEG recordings into three datasets of 30 second, where the first dataset was the first 30 seconds of the recording after having removed the initial five seconds, the second dataset was the 30 seconds immediately following the first dataset, and the last dataset was the last 30-second segment of the recording after having removed the last ten seconds (see Figure 1). Cropping the initial and last few seconds from recordings excluded edge, filtering, and other session artifacts. The lengths of the short datasets and epochs were determined from the participant with the shortest available recording. This procedure yielded three data segments for fingerprinting purposes via 6 possible dataset pairs (i.e., dataset 1 and 2; dataset 2 and 3; and dataset 1 and 3 and vice-versa). Results for all possible combinations of datasets are reported in Supplementary Figure 6.

Connectome fingerprinting successfully differentiated individuals across all possible combinations of datasets (Supplementary Figure 6). Fingerprinting from recordings collected closer in time (e.g., dataset-1 and dataset-2) outperformed differentiation from datasets collected further apart in time (e.g., between dataset-1 and dataset-3). Overall, spectral fingerprinting yielded lower differentiation accuracy than connectome fingerprinting, in particular from datasets further apart in time.

In a similar fashion, we challenged MEG fingerprinting using short 30-second data segments from different sessions (i.e., between-session fingerprinting). This yielded 6 epochs of data for fingerprinting (i.e., three from both the first and second recording, see Figure 1a). Fingerprinting results averaged across all possible data pairs are reported Figure 3c. Connectome fingerprinting performances were greater than those from spectral fingerprinting. Differentiation from slower frequency data components performed worse in comparison to higher bands – see main article body for a discussion.

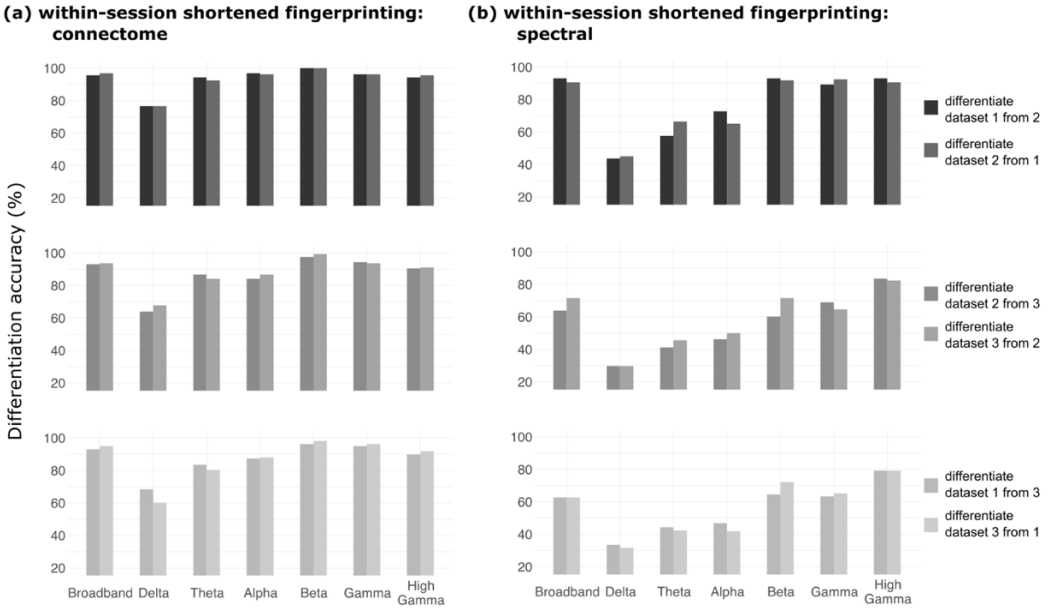


Supplementary Figure 6: Differentiation accuracy from shortened within-session datasets
Differentiation results from shortened within-session datasets (30 seconds) for (a) connectome and (b) spectral broadband and narrowband fingerprinting. The accuracy scores are reported for differentiation from all possible combinations of datasets, (i.e., dataset 1 to predict dataset 2, dataset 3 to predict dataset 2, etc.; see Methods for details). Differentiation accuracy increased as datasets were proximal in time (i.e., fingerprinting accuracy for dataset 1 to dataset 2 was greater than for dataset 1 to dataset 3). Source data are provided as a Source Data file.

## Fingerprinting across recording sessions

We also report fingerprinting accuracy performances from all possible pairs of datasets for the between-session fingerprinting challenge in Supplementary Figure 7. Overall, spectral fingerprinting outperformed connectome fingerprinting, as discussed in the main text.

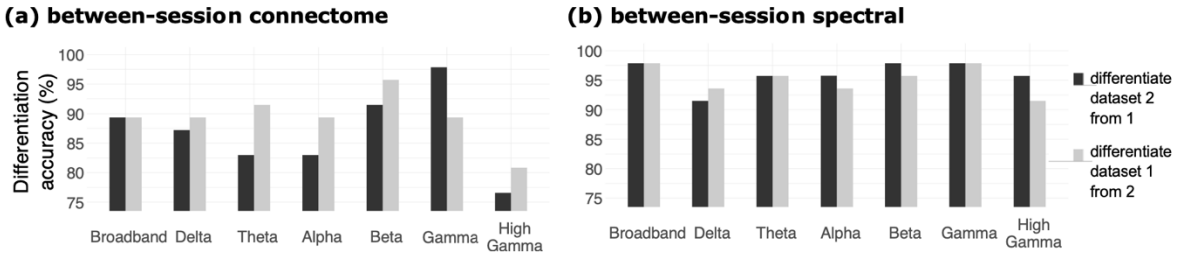


Supplementary Figure 7: Between-session differentiation accuracy. Results from MEG between-session fingerprinting. Differentiation accuracy for both (a) connectome and (b) spectral broadband and narrowband fingerprinting. The accuracy scores are reported for fingerprinting from dataset 1 to dataset 2 and vice-versa (see Methods). Source data are provided as a Source Data file.

### Individuals cannot be differentiated from their respective imaging kernels

We verified that the within-session fingerprinting of individuals was not possible from empty-room
166 data (i.e., with no participant under the MEG sensor array) processed through their respective imaging kernel of beamformer weights. Indeed, these latter are defined from individual anatomy and head position under the MEG sensor array, which may have been sufficient information to drive differentiation. We therefore ran the same fingerprinting pipeline on each session's empty-room data transformed through the corresponding individual's beamformer imaging kernel, which was identical for each of the within-session data segments used. Note that for the between-session challenges, the imaging kernels were adjusted to the respective individual head positions measured during each session. These analyses demonstrated that the imaging kernel information did not contribute substantially to MEG fingerprinting (overall performance was below 20% on average).

We also ran the MEG fingerprinting pipeline directly from the sensor data of the empty-room recordings, without transformation through individual imaging kernels, to assess the floor level of differentiation performances from non-brain data only. The data confirmed substantially lower levels of fingerprinting (<5% accuracy on average; see Supplementary Figure 8).

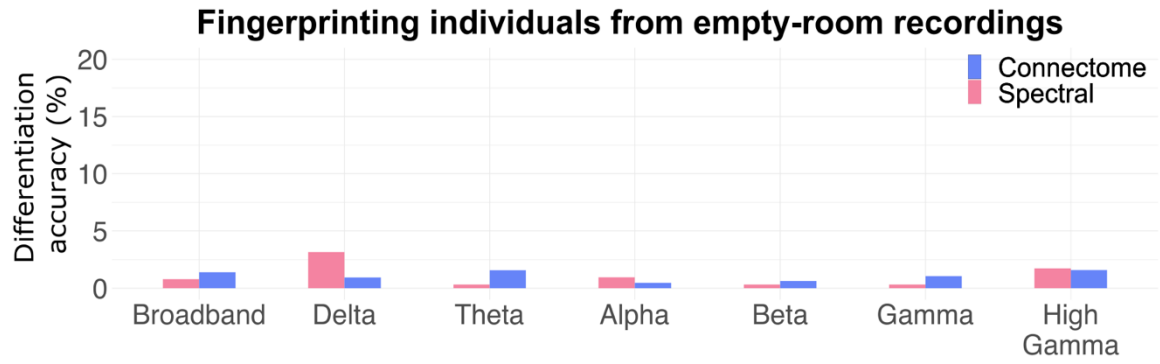


Supplementary Figure 8: Verification of failed fingerprinting from non-brain data (empty-room recordings). Results for the empty-room sensor fingerprinting challenge. As expected, differentiation accuracies of connectome and spectral broadband and narrowband fingerprinting were substantially lower than from actual MEG data with individuals present. Source data are provided as a Source Data file.

### Fingerprinting from scalp data only

We also performed MEG fingerprinting from individual sensor data, with no MEG source reconstruction to assess the added value of source modeling. We replicated the above MEG fingerprinting pipelines from the within-, within-shortened, and between- session analyses. Differentiation performances were less than with source modeling, especially from signal components in higher frequency bands and for the shortened challenges (see Supplementary Figure 9, 10, & 11). Yet for other signal components and longer durations, individuals remain

differentiable from sensor-level data collected between sessions (>60% accuracy from broadband data), albeit with lower accuracy than when using MEG source transformations, which explicitly account for different head positions between sessions.
Taken together with the empty-room fingerprinting tests above, these results provide evidence that brain signals, not environmental conditions, were crucial for individual differentiation.

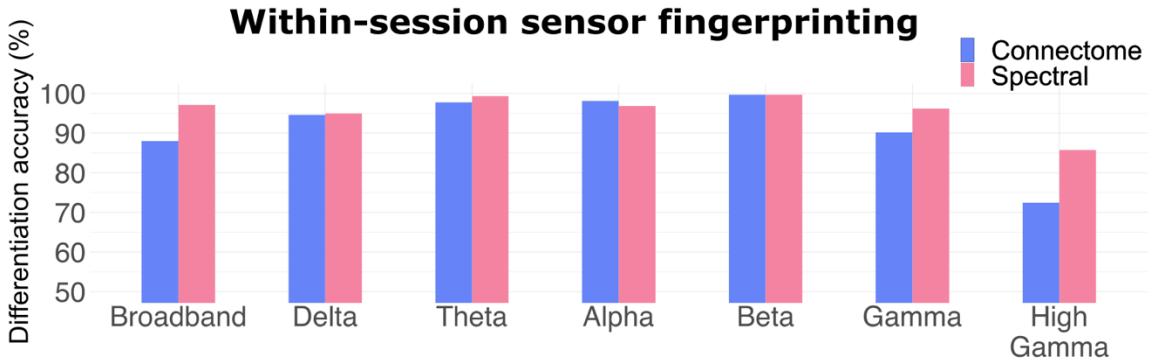


Supplementary Figure 9: Within-session differentiation from MEG sensor data (no source modeling). Results from MEG sensor data in the within-session fingerprinting challenge. The differentiation accuracy statistics are shown for both connectome and spectral broadband and narrowband fingerprinting. The average accuracy scores are reported across differentiation from dataset-1 to dataset-2 and vice-versa (see Methods). Source data are provided as a Source Data file.

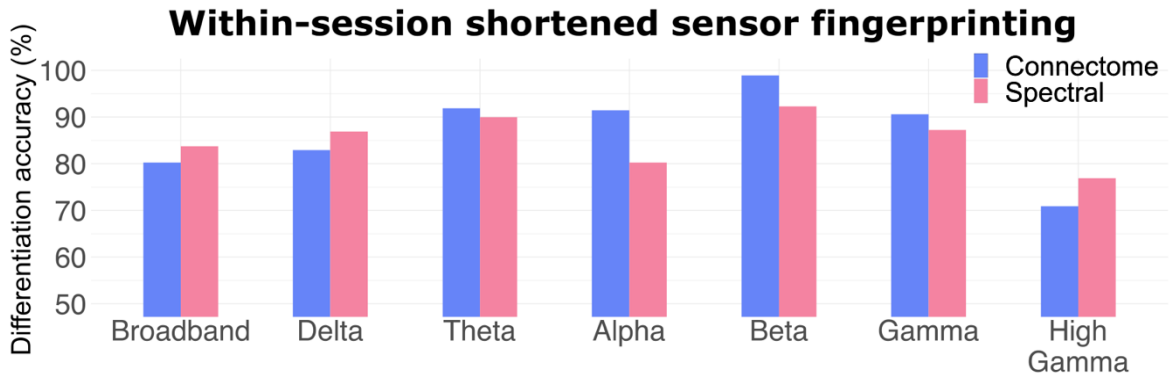


Supplementary Figure 10 Within-session differentiation from shortened (30-s) MEG sensor data (no source modeling). Results from MEG sensor data in the within-session shortened fingerprinting challenge. The differentiation accuracy statistics are shown for both connectome and spectral broadband and narrowband fingerprinting. The average accuracy scores are reported across differentiation from all possible pairs of datasets (see Methods). Source data are provided as a Source Data file.

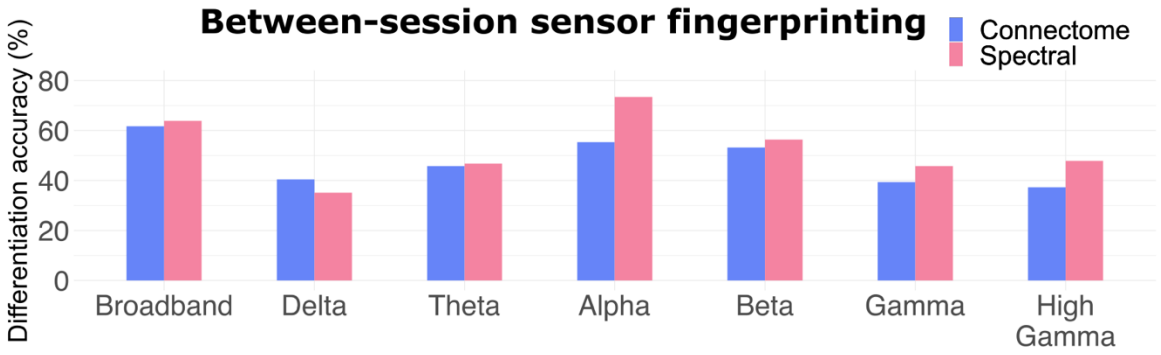


Supplementary Figure 11: Between-session differentiation from MEG sensor data (no source modeling). Results from MEG sensor data in the between-session fingerprinting challenge. The differentiation accuracy statistics are shown for both connectome and spectral broadband and narrowband fingerprinting. The average accuracy scores are reported across differentiation from dataset-1 to dataset-2 and vice-versa (see Methods). Source data are provided as a Source Data file.

## Salient neurophysiological features for fingerprinting

We reported in the main manuscript intraclass correlations (ICC) to determine which features contributed to individual differentiation the most. We also performed two additional analyses, deriving group consistency and differential power. These two metrics were proposed by Finn and colleagues (2) to identify the features which were the most consistent across their cohort, and the features which were the most consistent within individuals but different across participants, respectively (2). Differential power measures the empirical probability that a given feature is more likely to have a higher edgewise product vector across individuals than within the same individual. Taking the sum of the natural log of this probability across subjects yields differential power (2). The higher the differential power, the better a feature discriminates between individuals. Results for differential power are plotted in Figures S7 and S9. We found that the most discriminant connectome features were the visual and limbic networks across frequency bands, while the most discriminant spectral features remained along midline structures for fast oscillatory signal components. Overall, these results confirmed the ICC analysis results, with the addition of the contributions of spectral power in the beta and gamma band along the supplementary motor, motor, and somatosensory cortices.

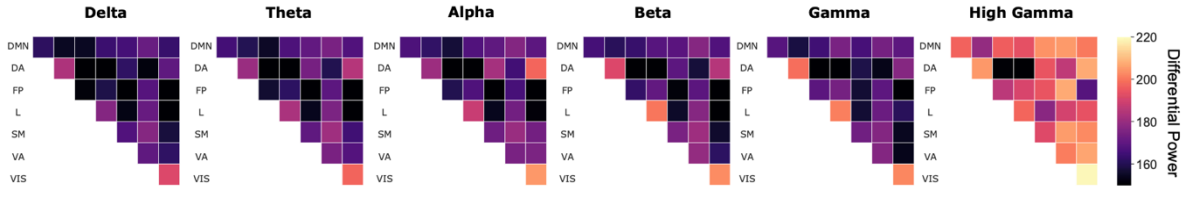


Supplementary Figure 12: Differential power connectome fingerprinting

Differential Power (DP) analysis for broadband connectome fingerprinting of the within-session dataset (see Figure 1). Mean DP plotted within frequency bands and per resting-state network as
defined by (3): Default Mode Network (DMN), Dorsal Attention (DA), Frontal-Parietal (FP), Limbic
(L), Somato-Motor (SM), Ventral Attention (VA), and Visual (VIS). The higher the DP, the more the corresponding functional connection was essential for fingerprinting. The outstanding connections determined by DP for fingerprinting were the Visual network across all frequency bands, and the Limbic network in the beta and gamma bands.

Group consistency reflects edges that are consistent across individuals. Group consistency was computed from the mean edgewise product vector across all subjects (2). Large values of group consistency highlight features that are consistent both within participants and across the cohort. Our analyses are shown Figures S8 and S10. The resulting most consistent connectome features remained along the diagonal of the FC matrix (i.e., connections within the same networks) specifically in the Dorsal Attention and Fronto-Parietal networks. The most consistent features for spectral fingerprinting were in the lower frequency bands, specifically in the lateral frontal cortices. This outcome was consistent with our ICC results (see Manuscript).

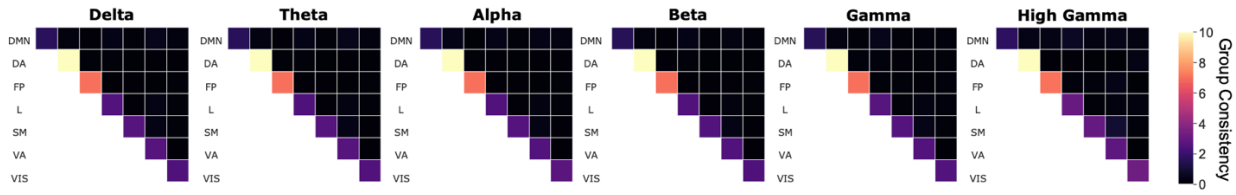


Supplementary Figure 13: Group consistency connectome fingerprinting
Group Consistency (GC) analysis for broadband connectome fingerprinting of the within-session dataset (see Figure 1). Mean GC plotted within frequency bands according to the labels from Default Mode Network (DMN), Dorsal Attention (DA), Frontal-Parietal (FP), Limbic (L), Somato-Motor (SM), Ventral Attention (VA), and Visual (VIS). The higher the GC, the more consistent was a functional connection within an individual and across the cohort. The most consistent connections were those along the diagonal, specifically for the Dorsal Attention and Frontal-Parietal networks across all frequency bands.

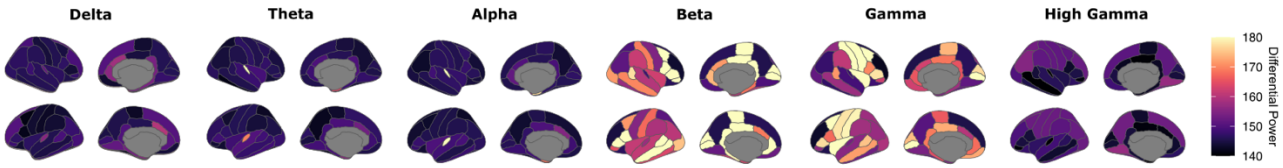


## Supplementary Figure 14: Differential power spectral fingerprinting

Differential Power (DP) analysis for broadband spectral fingerprinting of the within-session dataset (see Figure 1). Mean DP plotted within frequency bands according to the Desikan-Killiany atlas (4). The higher the DP, the more a given frequency band and ROI distinguished between individuals. The most characteristic regions and frequencies were medial structures for the beta band, and temporal and central regions for gamma band signals.

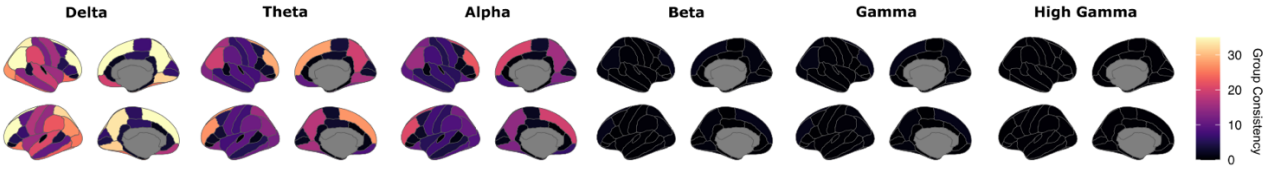


## Supplementary Figure 15: Group consistency spectral fingerprinting

Group Consistency (GC) analyses for broadband spectral fingerprinting of the within-session dataset (see Figure 1). Mean GC plotted within frequency bands according to the Desikan-Killiany. The higher the GC, the more a given frequency band and ROI remained consistent within individuals and across the cohort. The most stable frequencies were the lower bands (delta and theta) and the most consistent regions across individuals were lateral frontal areas.

## Partial Least Squares (PLS) analysis

293 We tested whether differences in resting-state neurophysiological signals related to
294 meaningful demographic features using an exploratory Partial Least Squares (PLS) analysis. PLS is a multivariate statistical method that relates two data matrices based on latent variables (LV) that explain the highest covariance between the two datasets. Here, our two datasets consist of a demographic matrix (i.e., age, gender, handedness, and clinical status) and a neurophysiological data matrix (i.e., spectral power or functional connectome). Latent variables (which explain the most covariance between both matrices), and their corresponding variance explained are plotted Figure 16. Significance of each latent variable was assessed via permutation tests. Permuting the rows of the data allowed us to compute an associate p-value for each latent variable (see Manuscript). We chose to explore the first significant latent variable which explained the most variance for each neurophysiological signal feature (i.e., the first component for connectomes and spectral data). The resulting weights associated to the latent neural and demographic components are depicted Figure 5 along with their bootstrapped ratios. These results corroborate how neurophysiological signals at rest, in addition to differentiating individuals, carry meaningful information about participant demographics.

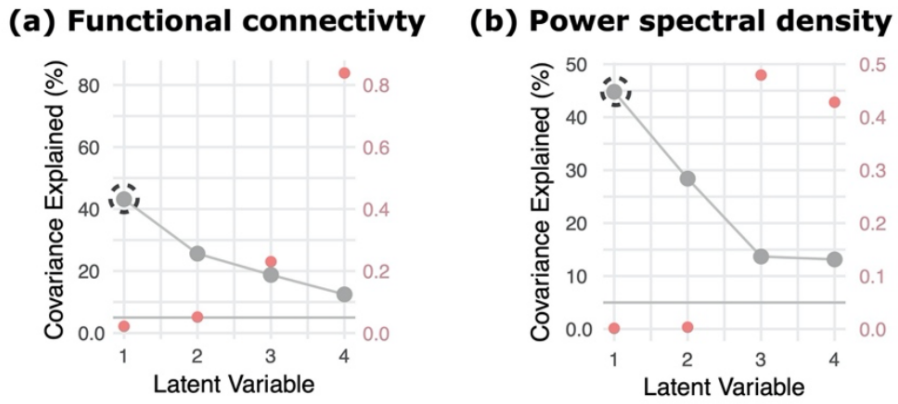


Supplementary Figure 16: PLS latent variables

Results for the PLS analysis conducted for both (a) connectome and (b) spectral fingerprinting features. Each plot depicts the latent components obtained for each of the PLS analyses, their corresponding variance explained, and permuted p-value (right axis). P-values were determined based on permutations of the data to obtain a null distribution. One significant latent variable explained 43.1% of the variance for connectome fingerprinting (p = 0.021) and two latent variables explained 44.7% (p = 0.001) and 28.3% (p = 0.003) of the variance for spectral fingerprinting, respectively. We explored in the main Manuscript only the first significant component for each method (i.e., the circled component). Source data are provided as a Source Data file.

## Supplementary References


1. E. Amico, J. Goñi, The quest for identifiability in human functional connectomes. Sci. Rep. 8, 8254 (2018).
2. E. S. Finn, X. Shen, D. Scheinost, M. D. Rosenberg, J. Huang, M. M. Chun, X. Papademetris, R. T. Constable, Functional connectome fingerprinting: identifying individuals using patterns of brain connectivity. Nat. Neurosci. 18, 1664–1671 (2015).
3. B. T. Yeo, Thomas, F. M. Krienen, J. Sepulcre, M. R. Sabuncu, D. Lashkari, M. Hollinshead, J. L. Roffman, J. W. Smoller, L. Zöllei, J. R. Polimeni, B. Fischl, H. Liu, R. L. Buckner, The organization of the human cerebral cortex estimated by intrinsic functional connectivity. J. Neurophysiol. 106, 1125–1165 (2011).
4. R. S. Desikan, F. Ségonne, B. Fischl, B. T. Quinn, B. C. Dickerson, D. Blacker, R. L. Buckner, A. M. Dale, R. P. Maguire, B. T. Hyman, M. S. Albert, R. J. Killiany, An automated labeling system for subdividing the human cerebral cortex on MRI scans into gyral based regions of interest. NeuroImage. 31, 968–980 (2006).

# Appendix B: Supplemental Information chapter 3

## Demographic characteristics of the participant cohort

We used the 606 individuals with both resting state scans and sensorimotor task MEG recordings. This consisted of individuals spanning the entire adult lifespan from 18 years old to 89 years old (mean age= 54.69; sd= 18.28). The demographic characteristics of all participants are presented in Table S1.

| | Sex (f) | Handedness | Mmse (sd) | Catell Intelligence performance |
|---|---|---|---|---|
| All participants N=606 | 299 | 78.9 (49.2) | 28.95 (1.25) | 31.9 (6.76) |
| Young adults (18-45) N=204 | 103 | 75.3 (52.5) | 29.3 (1.05) | 36.7 (4.33) |
| Adults (45-65) N=194 | 100 | 76.6 (53.3) | 29.1 (1.07) | 32.8 (4.96) |
| Older adults (65+) N=208 | 96 | 84.9 (40.8) | 28.4 (1.38) | 26.2 (6.03) |

Table S1. Demographics of participants.

## Individuals are differentiable regardless of age group

We found that individuals' broadband brain-fingerprints derived from task-free brain activity remain differentiable across age groups. To further investigate this finding, we tested whether the self-similarity of brain-fingerprints of individuals differed across age. We observed that the self-similarity of brain-fingerprints does not linearly relate with age (β=-4.62, SE= 2.45, 95% CI [-9.43, 0.20], p=0.06, $BF_{01}$= 1.96, see Table S2). In addition, we tested whether older adults were easier to differentiate from the entire cohort. Here, we defined differentiability (da Silva Castanheira et al., 2021), a score that represents an individual who shows a greater self-similarity of their brain-fingerprint features than other-similarity and is therefore easy to differentiate from the cohort. We observed a weakly linear relationship between differentiability and age (β= 6.14, SE= 1.12, 95% CI [3.94, 8.34], p< 0.001, $BF_{01}$= 6.38 $10^{-6}$, see Table S3 & Figure S1), which explains only 4.6% of variance.

| | Age | | |
|---|---|---|---|
| *Predictors* | *Estimates* | *CI* | *p* |
| (Intercept) | 64.67 | 54.16 – 75.18 | **<0.001** |
| artanh (self-similairty) | -4.62 | -9.43 – 0.20 | 0.060 |
| Observations | 606 | | |
| $R^2$ / $R^2$ adjusted | 0.006 / 0.004 | | |

Supplemental Table 2. The autocorrelation of task-free broadband brain-fingerprints do not linearly relate to age.

| | Age | | |
|---|---|---|---|
| *Predictors* | *Estimates* | *CI* | *p* |
| Intercept | 39.77 | 34.23 – 45.30 | **<0.001** |
| differentiability | 6.14 | 3.94 – 8.34 | **<0.001** |
| Observations | 606 | | |
| $R^2$ / $R^2$ adjusted | 0.047 / 0.046 | | |

Supplemental Table 3. We report a weak linear relationship between the easy in which we can differentiate an individual from the entire cohort and their age.

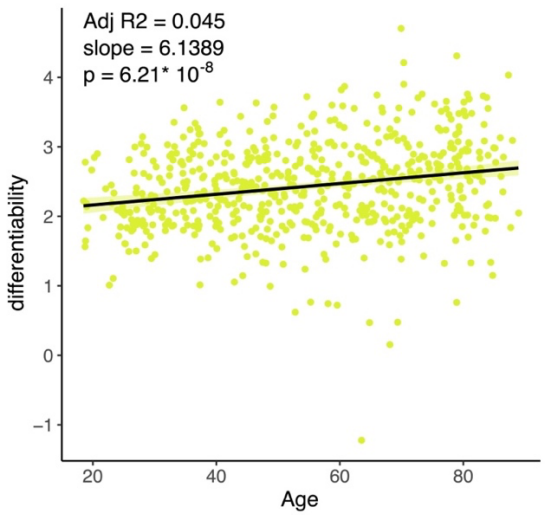


Figure S1: Individual differentiability is weakly linearly related to age.

We preformed the fingerprinting analysis using neurophysiological signals restricted to the conventional frequency bands of electrophysiology: delta (1-4Hz), theta (4-8Hz), alpha (8-13Hz), beta (13-30Hz), gamma (30-50Hz) and high gamma (50-150Hz). Across all challenges except for the adult cohort (45-65 years old), the highest differentiation accuracy was achieved by the beta band: 96.6% ([96.0, 97.7] CI) young adults, 95.3% ([93.7, 97.1] CI) older adults, and 95.3% ([94.4, 96.3] CI) across all participants. This result is consistent with our previous work(da Silva Castanheira et al., 2021). The band with the highest differentiation accuracy for the adult cohort was the gamma band (96.7% [92.0, 97.7] CI; see Figure 2a). The band exhibiting the worst differentiation accuracy across all challenges, except for the young adult cohort (18-45 years old), was delta: 82.3% ([79.4, 85.7] CI) adults, 80.3% ([77.7, 82.9] CI) older adults, and 79.2% ([76.7, 81.9] CI) across all participants (See Figure S2).

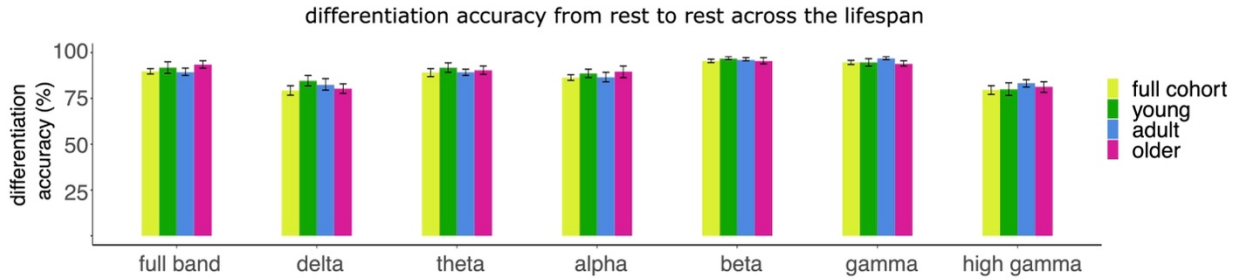


Figure S2: Individuals are differentiable from band-limited brain-fingerprints across age groups. Differentiation accuracy using broadband and band-limited spectral brain-fingerprints derived from ~4-min data lengths. The error bars show bootstrapped 95% confidence intervals.

We then tested the relevance of arrhythmic signal components of brain activity to differentiation accuracy (Donoghue et al., 2020b). We parametrized the regional MEG-source power spectra and assessed differentiation accuracy from the resulting arrhythmic brain-fingerprints (see Methods). We found that inter-individual differentiation performance for the entire cohort was lower when using arrhythmic brain-fingerprints in comparison to the broadband brain-fingerprints 47.1% (CI [46.0, 48.0]), but remained well above chance. Similarly, we observed lower inter-individual differentiation accuracies for arrhythmic brain-fingerprints across the age-cohorts: differentiation accuracy for young adults was 81.1% ([77.7, 84.6] CI), 77.4% ([75.4, 80.0] CI) for adults, and 82.2% ([79.4, 85.1] CI) for older adults. These differentiation accuracies were qualitatively similar to those from using the entire spectral brain-fingerprints (see Figure S3).

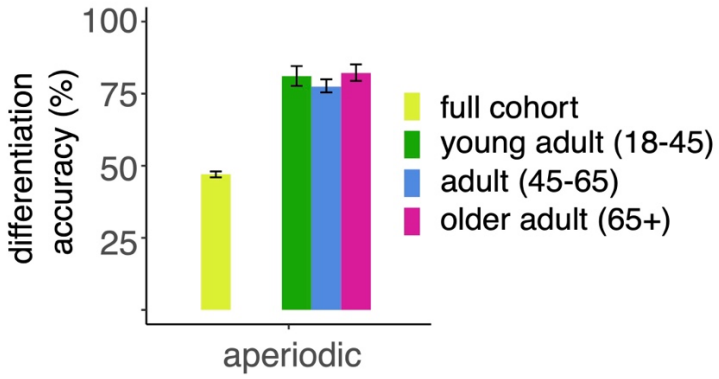


Figure S3: Participants are differentiable from arrhythmic spectral brain-fingerprints. Differentiation accuracy using brain-fingerprints derived from the arrhythmic features of brain activity as parametrized by specparam(Donoghue et al., 2020b). The error bars show bootstrapped 95% confidence intervals.

To verify the stability of brain fingerprints across the adult lifespan we relied on approximately 8 minutes of MEG recordings of a sensorimotor task. Here, we replicated our fingerprinting approach (see Figure 1) to test if brain-fingerprints derived from resting-state recordings differentiate individuals based on brain-fingerprints derived from task recordings in MEG. The brain-fingerprint differentiation accuracy for all participants using broadband neurophysiological signals was 77.0% ([72.4, 81.4] CI). Broadband differentiation accuracy did not substantially vary across age-cohorts: differentiation accuracy for young adults was 77.0% ([70.9, 82.9] CI), 81.1% ([76.6, 85.7] CI) for adults, and 80.6% ([75.4, 86.3] CI) for older adults (Figure S4). This replicates our resting-state findings (see Figure 1a).

We repeated the above analyses (i.e., task to rest brain-fingerprinting) for band-limited brain-fingerprints. Across all challenges except for the young adults, the highest differentiation accuracy was achieved by the beta band: 96.3% ([93.1, 99.4] CI) adults, 96.6% ([94.3, 98.9] CI) older adults, and 93.6% ([90.7, 96.3] CI) across the entire cohort. The band with the highest differentiation accuracy for the young adult cohort was the gamma band (94.1% [92.6, 95.4] CI; see Figure S4). The band exhibiting the worst differentiation accuracy across all challenges, except for the adult cohort, was alpha: 58.0% ([53.1, 62.9] CI) young adults, 63.1% ([60.6, 65.7] CI) older adults, and 59.3% ([56.6, 62.1] CI) across the entire cohort (see Figure S4).

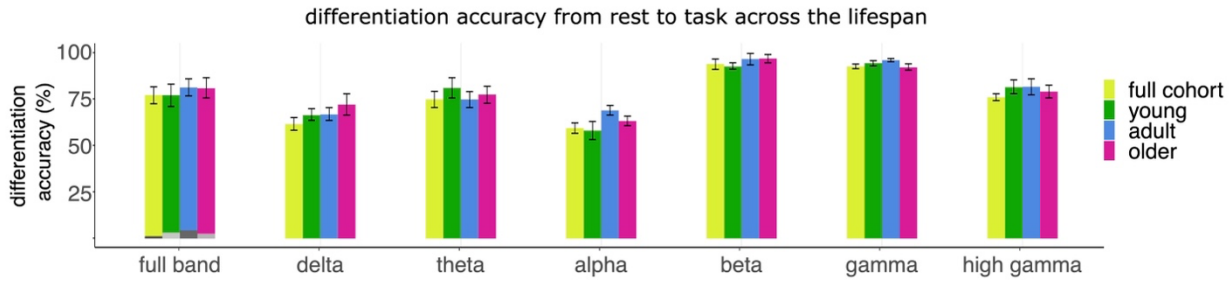


Figure S4: Participants can be differentiated from task-based brain-fingerprints.
We differentiated participants based on spectral brain-fingerprints derived from i) task-free brain activity and ii) a sensorimotor task to verify the robustness of the spectral brain-fingerprint. We plot the differentiation accuracies from this fingerprinting challenge based on broadband and band-limited spectral brain-fingerprints. The error bars show bootstrapped 95% confidence intervals.

### Brief 30-second recording can differentiate individuals

Our previous work demonstrated that individuals can be differentiated from brain-fingerprints derived from brief recordings(da Silva Castanheira et al., 2021). In line with these results, we aimed to differentiate the largest cohort of individuals (N= 606) to date using short 30-second recordings of data and tested whether brain-fingerprints become increasingly variable with age. We find that brain-fingerprinting from brief recordings generalizes to a much wider age range than our previous work, achieving 67.0% differentiation accuracy (computed 95% CI [64.9, 69.0]) (presented in Figure 1a points).

### Brain-fingerprints are robust against data recording artefacts

We verified the robustness of spectral brain-fingerprints against environmental and physiological artefacts.

First, we found that individuals are not differentiable on the basis of environmental factors specific to the respective days of the MEG recording. We pre-processed the empty-room recordings of each participant similarly to their resting-state data. Using the same imaging projectors as those for their original MEG data, we mapped each session's empty-room data onto the respective participant's cortical surfaces. The accuracy of empty-room individual differentiation was considerably lower than that of the spectral brain-fingerprints (<5%; Figures 1a & S4).

Second, we tested the robustness of brain-fingerprinting against typical physiological artefacts, including head motion, heart-rate variability, and eye blinks. Individual differentiability was not correlated to head motion (r=0.08, p> .05, $BF_{01}$= 1.60), cardiac (r=-0.03, p= .39, $BF_{01}$= 7.30) or ocular (r=0.00, p= .97, $BF_{01}$= 10.51) artefacts.

Third, we then regressed out the variance associated with physiological artefacts from the spectral features of brain-fingerprints and replicated the fingerprinting analysis pipeline. The resulting differentiation accuracy was qualitatively similar to our broadband analysis: 89.3% accuracy ([87.2, 91.1] CI) for all participants, 91.8% ([88.0, 94.9] CI) for young adults, 88.5% ([85.7, 91.4] CI) for adults, and 92.2% ([89.7, 94.3] CI) for older adults (see Figure 1a). Taken together, these results indicate that brain-fingerprinting is robust against environmental and physiological artifacts akin to our previous results(da Silva Castanheira et al., 2021).

### Salient neurophysiological features for brain-fingerprinting

We quantified the most salient neurophysiological brain-fingerprint features for differentiating all individuals using intra-class correlations (Amico & Goñi, 2018a; da Silva Castanheira et al., 2021). We found that medial brain regions were the most salient for differentiating all individuals (Figure S5): the bilateral caudal anterior cingulate showed the highest ICC for differentiating individuals (ICC= 0.88), while the right superior temporal cortex the lowest (ICC= 0.75; see Figure S5).

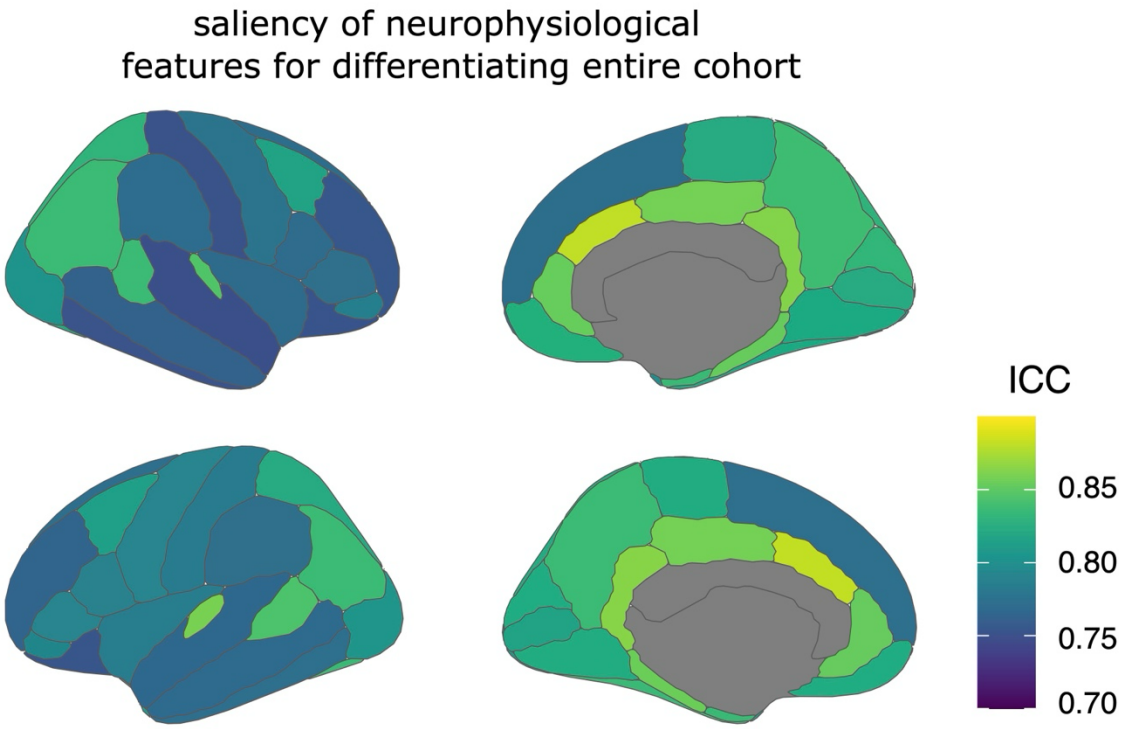


Figure S5: Salient neurophysiological brain-fingerprint features for differentiating individuals across the entire cohort.

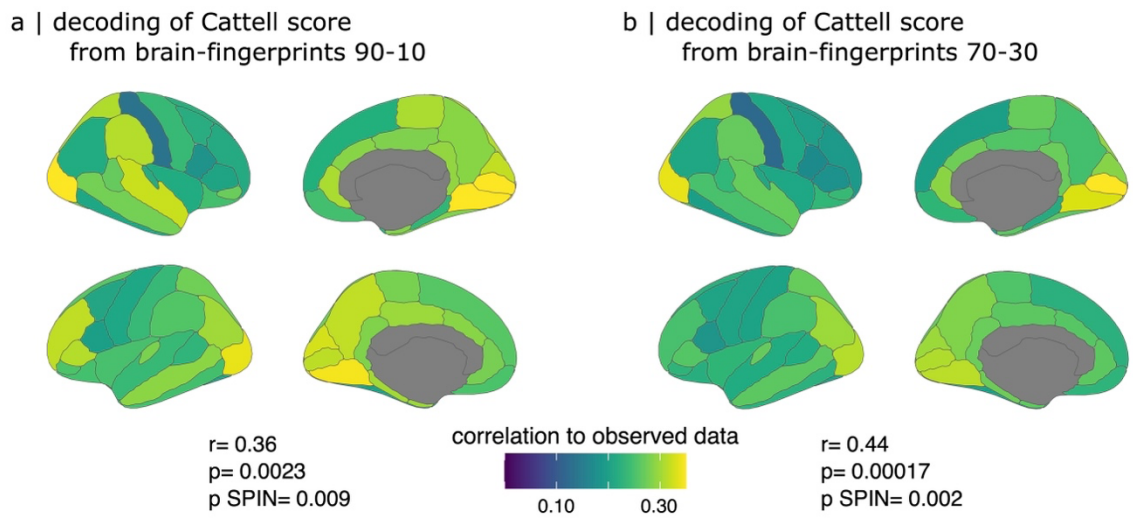


Figure S6: Decoding of Fluid intelligence test performance does not depend on cross-validation strategy. Topography of decoding performance (correlation between observed and decoded fluid intelligence scores) from the spectral brain-fingerprint features of each cortical parcel of the Desikan-Killiani atlas (Desikan et al., 2006a). The observed topography of decoding performance remains similar regardless of the cross-validation method (left: 90-10% cross-validation split, right: 70-30% cross-validation split). The topographies of decoding performance remain correlated to the salient features for differentiating individuals (i.e., Figure S5) regardless of the cross-validation method.

## References

1. da Silva Castanheira, J., Orozco Perez, H. D., Misic, B. & Baillet, S. Brief segments of neurophysiological activity enable individual differentiation. Nat. Commun. 12, 5713 (2021).
2. Donoghue, T. et al. Parameterizing neural power spectra into periodic and aperiodic components. Nat. Neurosci. 23, 1655–1665 (2020).
3. Amico, E. & Goñi, J. The quest for identifiability in human functional connectomes. Sci. Rep. 8, 8254 (2018).
4. Desikan, R. S. et al. An automated labeling system for subdividing the human cerebral cortex on MRI scans into gyral based regions of interest. NeuroImage 31, 968–980 (2006).

# Appendix C: Supplemental Information chapter 4

## Participants

The study participants were patients with Parkinson's disease from the QPN data repository and age-matched healthy controls from the Prevent-AD data repositories (Gan-Or et al., 2020; Niso et al., 2016a; Tremblay-Mercier et al., 2021). Table S1 provides their demographics, which we tested for sample differences in terms of age and education, using an unpaired t-test and gender and handedness with a Chi-square test. No significant differences were found. We replicated our analyses with a second sample of healthy controls obtained from the Cambridge enter for Aging Neuroscience (CamCAN) dataset (see Methods for demographics details).

Table S1: Participant demographics.

| | *Patients* | *Controls (Prevent-AD)* | *Uncorrected p-values* |
|---|---|---|---|
| *age* | 64.63 (8.66) | 61.98 (8.89) | 0.09 |
| *gender (female)* | 23 | 24 | 0.13 |
| *handedness (right)* | 67 | 48 | 1.0 |
| *education* | 15.11 (3.11) | 15.54 (3.58) | 0.48 |
| *Hoehn & Yahr score* | 1.97 (0.71) | NA | |
| *UPDRS III* | 32.55 (14.74) | NA | |
| *MoCA* | 24.43 (4.03) | NA | |

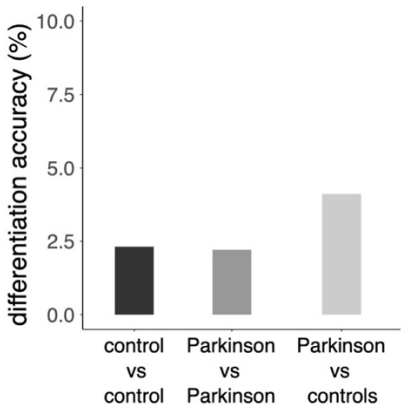


Figure S1: Differentiation accuracy from empty-room data.

Differentiation accuracies from brain-fingerprints derived from empty-room recordings performed around the MEG visit of each participant.

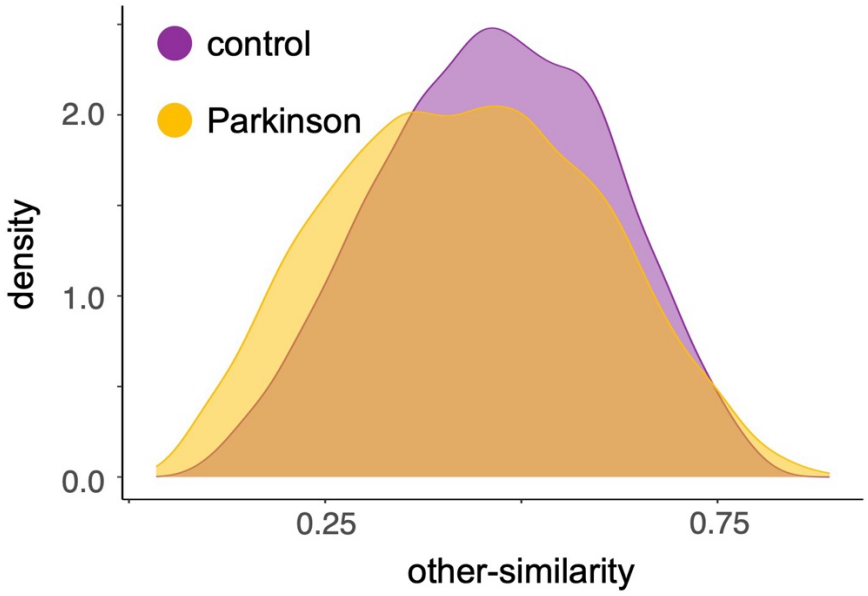


Figure S2: Empirical densities of other-similarity brain-fingerprint statistics.
The empirical densities of inter-individual *other-similarity* brain-fingerprints statistics are similar between patients with Parkinson's disease and healthy age-matched controls. See **Moment-to-moment arrhythmic fluctuations are increased in Parkinson's disease** for a detailed description of the *self-similarity* statistics.

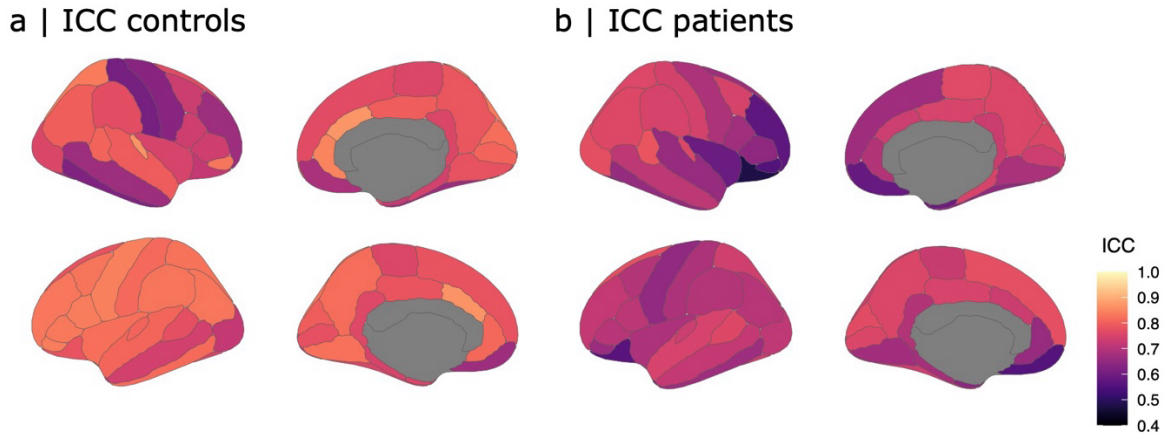


Figure S3: Relative contribution of rhythmic features for fingerprinting.
Cortical maps of intra-class correlation coefficients (ICCs) for (a) controls (Prevent-AD), and (b) PD patients.

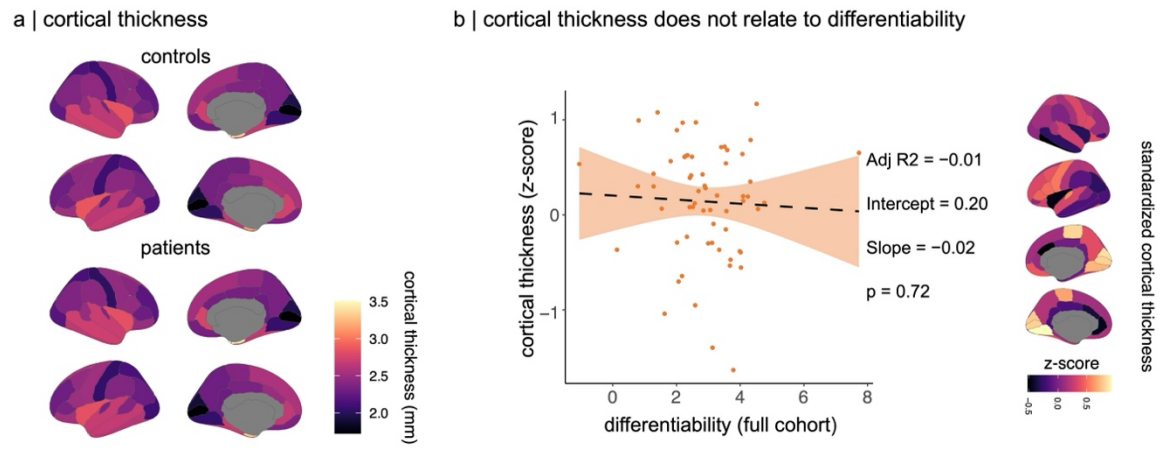


Figure S4: Cortical thickness alterations not related to patient differentiation.
(a) Average cortical thickness measured in control participants and patients with PD. (b) left panel: linear regression analysis showing no relationship between individual differentiability and the average standardized cortical thickness of each patient (averaged across ROIs) (see Methods). Right panel: brain maps of average standardized cortical thickness of patients with PD.

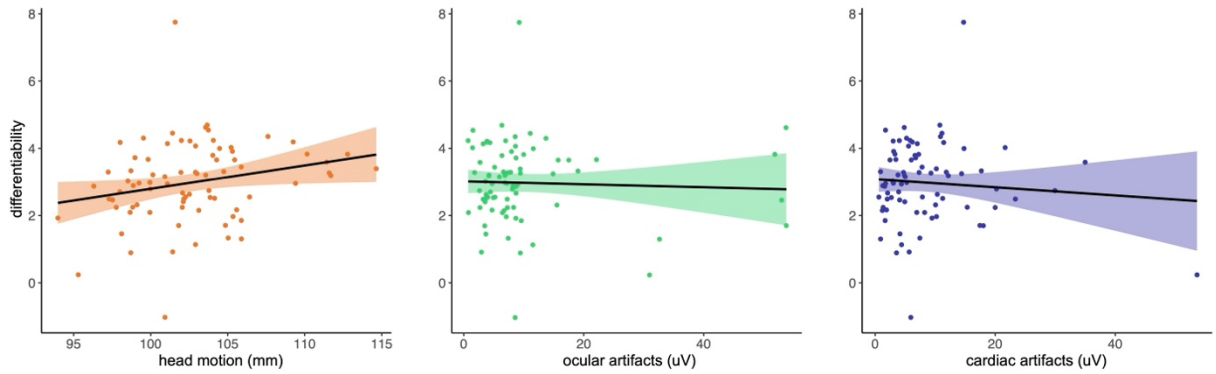


Figure S5: Individual differentiability does not relate to cardiac or ocular artifacts (middle and right panels). A moderate linear relationship exists between individual differentiability and head motion in the patient group.

Differentiability between patients with PD was correlated to head motion (r= 0.23, *p*= 0.04), but not to cardiac or ocular artifacts (r=-0.04, *p*= 0.71; r=-0.08, *p*= 0.46 respectively). There was, however, little evidence in favour of the relationship between head motion and differentiability (BF= 2.04; Figure S5).

## Robustness and Replicability of Disease-Stage Decoding Using Spectral Brain-Fingerprints

The decoding of disease stages is related to the key features of the brain's spectral fingerprint. Specifically, the ability to distinguish disease stages based on regional brain-fingerprint characteristics correlates with changes in interclass correlation (ICC) between patients and control groups, as shown in Figure 3a.

To ensure that our findings were robust and not biased by our initial 80-20 cross-validation strategy, we conducted additional tests using 90-10 and 70-30 cross-validation ratios (i.e., training the decoder with 90% and 70% of the data respectively, and testing it with the remaining 10% and 30%). These tests yielded results consistent with our initial findings, as detailed in Figure S6.

Further, we replicated this analysis using the control sample from the Cambridge Center for Aging Neuroscience (CamCAN). The results confirmed that, similar to the Prevent-AD sample of healthy controls, the pattern of disease-stage decoding aligns with the cortical map of ICC difference scores. This was true for both 90-10 (correlation coefficient r= 0.46, p< 0.01, $p_{spin}$< 0.001) and 70-30 cross-validation ratios (r= 0.54, p< 0.01, $p_{spin}$< 0.001).

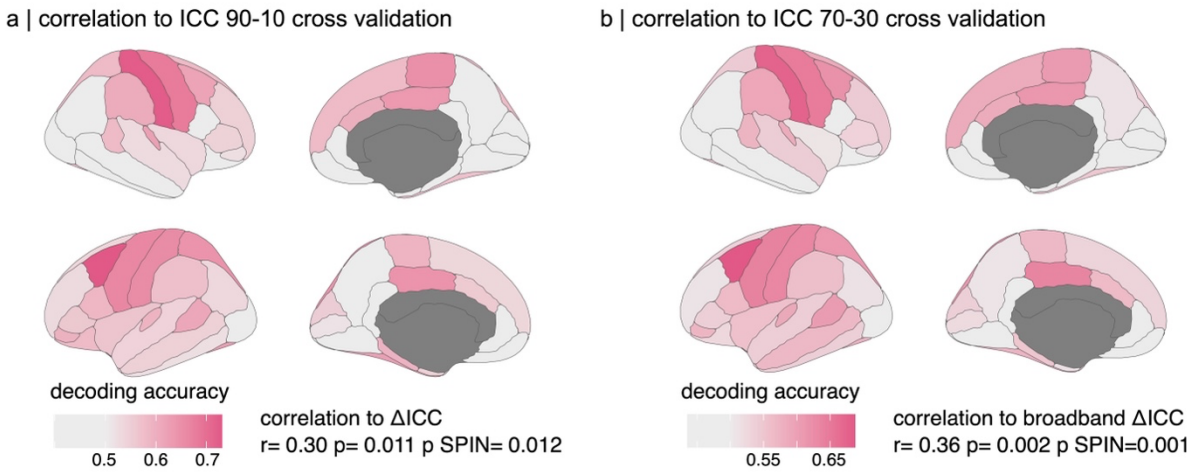


Figure S6: Stability of Disease Stage Decoding Across Various Cross-Validation Schemes.
Decoding accuracies for Parkinson's disease stages (Hoehn & Yahr stages, binarized) derived from the rhythmic brain-fingerprint features from each cortical parcels of the Desikan-Killiany atlas using a) 90-10 and b) 70-30 cross-validation ratios. The cortical maps show consistency in the topographical distribution of decoding accuracies, irrespective of the cross-validation protocol employed. Moreover, a correlation persists between the decoding accuracy for Parkinson's disease stages at each cortical parcel and the prominence of the respective brain-fingerprint features within those parcels (Δ ICC; see Figure 3a), across different cross-validation strategies. These phenomena are further validated in the CamCAN cohort, as detailed in the preceding text.

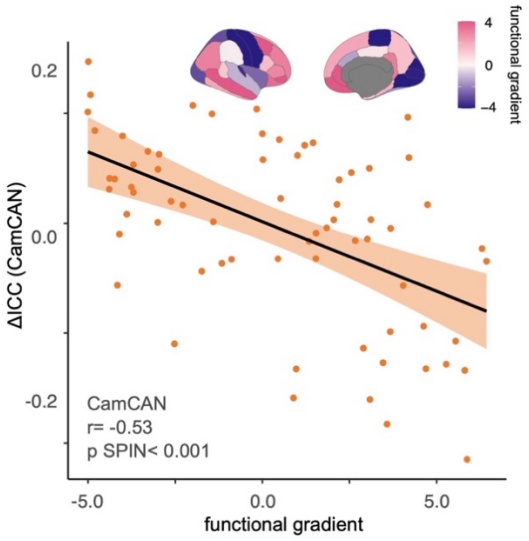


Figure S7: Topographical alignment of spectral brain-fingerprints with the functional hierarchy: CamCAN sample. Top: Cortical map illustrating the first unimodal-to-transmodal functional gradient, sourced from *neuromaps* (Markello et al., 2022a). Bottom: Linear association between the weights of cortical regions in this functional gradient (as per *neuromaps*) and their prominence in the PD brain-fingerprint (Figure 3a, bottom; CamCAN sample).

Table S2: Short-Term Variability in Self-Similarity of Brain-Fingerprints from 30-Second Datasets in Patients.

| | atanh(self-similarity) | | |
|---|---|---|---|
| *Predictors* | *Estimates* | *CI* | *p* |
| (Intercept) | 1.19 | 1.13 – 1.25 | **<0.001** |
| Head motion | -0.03 | -0.06 – 0.01 | 0.149 |
| Group [Parkinson] | -0.02 | -0.10 – 0.05 | 0.546 |
| gap duration [ploy 1st degree] | -9.95 | -12.56 – -7.34 | **<0.001** |
| gap duration [ploy 2nd degree] | 2.76 | 1.68 – 3.83 | **<0.001** |
| Group [Parkinson] × gap duration [ploy 1st degree] | -3.77 | -7.16 – -0.38 | **0.029** |
| Group [Parkinson] × gap duration [ploy 2nd degree] | -0.03 | -1.43 – 1.36 | 0.961 |
| **Random Effects** | | | |
| $\sigma^2$ | 0.07 | | |
| $\tau_{00\ SubjId}$ | 0.05 | | |
| $\tau_{11\ SubjId.poly(gap\ duration,\ 2)1}$ | 86.88 | | |
| $\tau_{11\ SubjId.poly(gap\ duration,\ 2)2}$ | 7.32 | | |
| $\rho_{01}$ | 0.27 | | |
| | -0.40 | | |
| ICC | 0.46 | | |
| $N_{SubjId}$ | 133 | | |
| Observations | 10374 | | |
| Marginal $R^2$ / Conditional $R^2$ | 0.115 / 0.521 | | |

Table S3: Short-Term Variability in Self-Similarity of arrhythmic Brain-Fingerprints from 30-Second Datasets in Patients.

| | atanh(arrhythmic self-similarity) | | |
|---|---|---|---|
| *Predictors* | *Estimates* | *CI* | *p* |
| (Intercept) | 1.63 | 1.57 – 1.70 | **<0.001** |
| Head motion | 0.02 | -0.02 – 0.05 | 0.359 |
| Group [Parkinson] | -0.02 | -0.11 – 0.06 | 0.608 |
| gap duration [ploy 1st degree] | -15.19 | -18.72 – -11.66 | **<0.001** |
| gap duration [ploy 2nd degree] | 4.82 | 3.29 – 6.36 | **<0.001** |
| Group [Parkinson] × gap duration [ploy 1st degree] | -3.67 | -8.25 – 0.92 | 0.117 |
| Group [Parkinson] × gap duration [ploy 2nd degree] | -0.47 | -2.47 – 1.52 | 0.641 |
| **Random Effects** | | | |
| $\sigma^2$ | 0.10 | | |
| $\tau_{00\ SubjId}$ | 0.06 | | |
| $\tau_{11\ SubjId.poly(gap\ duration,\ 2)1}$ | 161.32 | | |
| $\tau_{11\ SubjId.poly(gap\ duration,\ 2)2}$ | 19.28 | | |
| $\rho_{01}$ | 0.34 | | |
| | -0.46 | | |
| ICC | 0.42 | | |
| $N_{SubjId}$ | 133 | | |
| Observations | 10374 | | |
| Marginal $R^2$ / Conditional $R^2$ | 0.151 / 0.504 | | |

Table S4: Short-Term Variability in Self-Similarity of rhythmic Brain-Fingerprints from 30-Second Datasets in Patients.

| | atanh(rhythmic self-similarity) | | |
|---|---|---|---|
| *Predictors* | *Estimates* | *CI* | *p* |
| (Intercept) | 0.98 | 0.92 – 1.05 | **<0.001** |
| Head motion | -0.03 | -0.07 – 0.01 | 0.147 |
| Group [Parkinson] | 0.02 | -0.07 – 0.11 | 0.646 |
| gap duration [ploy 1st degree] | -8.67 | -11.23 – -6.12 | **<0.001** |
| gap duration [ploy 2nd degree] | 2.08 | 1.02 – 3.14 | **<0.001** |
| Group [Parkinson] × gap duration [ploy 1st degree] | -3.33 | -6.65 – -0.02 | **0.049** |
| Group [Parkinson] × gap duration [ploy 2nd degree] | 1.17 | -0.20 – 2.55 | 0.095 |
| **Random Effects** | | | |
| $\sigma^2$ | 0.05 | | |
| $\tau_{00\ SubjId}$ | 0.06 | | |
| $\tau_{11\ SubjId.poly(gap\ duration,\ 2)1}$ | 85.02 | | |
| $\tau_{11\ SubjId.poly(gap\ duration,\ 2)2}$ | 9.14 | | |
| $\rho_{01}$ | 0.22 | | |
| | -0.29 | | |
| ICC | 0.58 | | |
| $N_{SubjId}$ | 133 | | |
| Observations | 10374 | | |
| Marginal $R^2$ / Conditional $R^2$ | 0.097 / 0.623 | | |

## References


1. Niso, G. et al. OMEGA: The Open MEG Archive. NeuroImage 124, 1182–1187 (2016).
2. Tremblay-Mercier, J. et al. Open science datasets from PREVENT-AD, a longitudinal cohort of pre-symptomatic Alzheimer's disease. NeuroImage Clin. 31, 102733 (2021).
3. Gan-Or, Z. et al. The Quebec Parkinson Network: A Researcher-Patient Matching Platform and Multimodal Biorepository. J. Park. Dis. 10, 301–313 (2020).
4. Markello, R. D. et al. neuromaps: structural and functional interpretation of brain maps. Nat. Methods 19, 1472–1479 (2022).

# Appendix D: Supplemental Information chapter 5

## Sensitivity analyses

We verified the robustness of spectral brain-fingerprints against environmental and physiological artefacts.

First, we computed our ability to differentiate individuals on the basis of environmental factors respective to the day of the MEG recording using empty-room recordings. We pre-processed the empty-room recordings of each participant similar to their resting-state data and used the same imaging projectors as the resting-state data to derive empty-room noise brain-fingerprints for each individual. The accuracy of empty-room individual differentiation was considerably lower than that of the spectral brain-fingerprints (<1.7% for broadband brain-fingerprints; Figures 2a grey bars & Figure S1, see Methods for details).

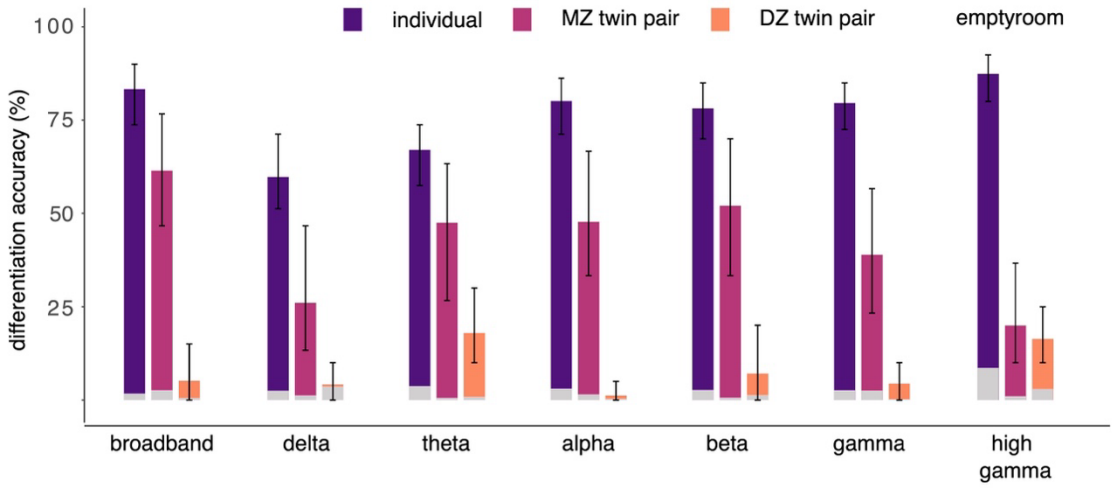


Figure S1: Spectral brain-fingerprints differentiate individuals and MZ twin pairs.
**Differentiation accuracy using broadband and narrow-band spectral brain-fingerprints derived from ~5-min data lengths. The error bars show bootstrapped 95% confidence intervals, while the grey segments at the foot of each bar plot indicate the null differentiation accuracy obtained from empty-room MEG recordings.**

Second, we regressed out the variance associated with physiological artefacts from the spectral features of brain-fingerprints and replicated the fingerprinting analysis pipeline (see Methods). The resulting differentiation accuracy was qualitatively similar to Figure 2a: The differentiation accuracy for all participants was 82.7% ([75.0, 88.8] 95% CI ), 59.8% ([46.7, 76.7] 95% CI) for matching MZ twin pairs, and 7.0% ([0.0, 20.0] 95% CI) for matching DZ twin pairs using

broadband brain-phenotype features (see Figure S2). Taken together, these results suggest that our ability to differentiate individuals and match twin pairs is not driven by idiosyncratic physiology unrelated to brain activity.

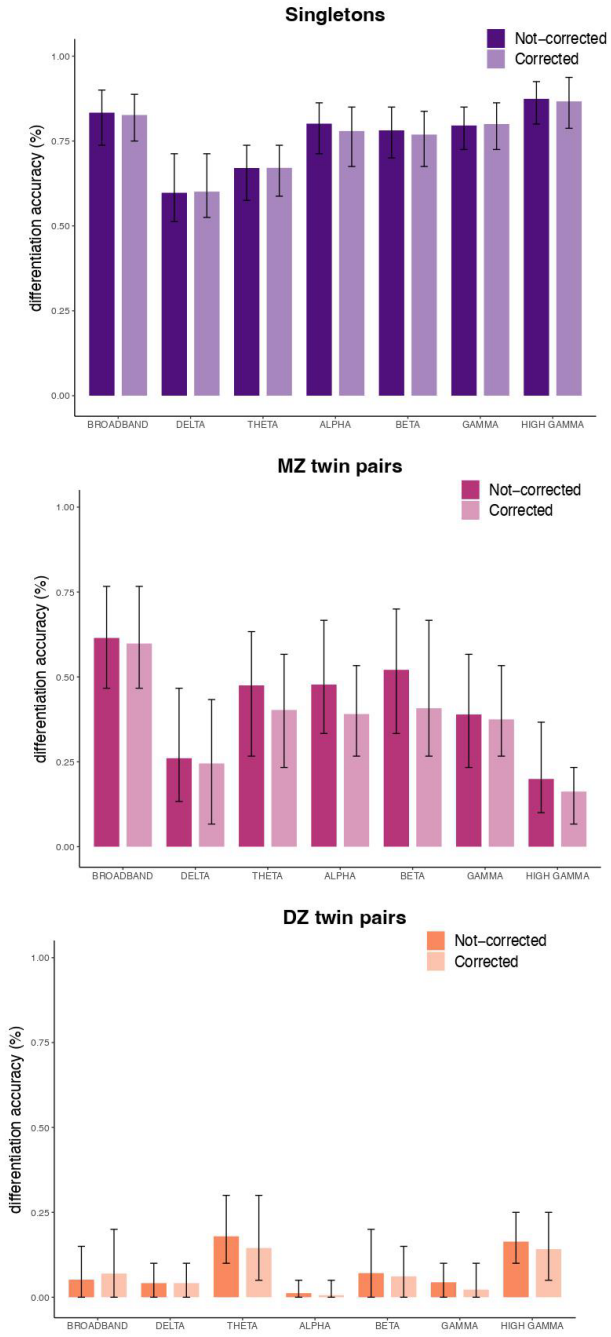


Figure S2: Physiological artifacts do not impact differentiation accuracy.
Comparison of the differentiation accuracy scores before and after regressing out the effects of artifacts on PSDs, for singletons (top panel), MZ twin pairs (middle panel) and DZ twin pairs (bottom panel).

Lastly, we tested whether our ability to differentiate MZ twin pairs based on their spectral brain-fingerprints was driven by anatomical similarity (See Monozygotic twin differentiation not driven by anatomy).

### Robustness of salient features for participant differentiation

We computed the ICC by averaging the results calculated with bootstrapped cohorts of the original dataset, including each time only one randomly chosen twin per pair (see Methods) to remove any effects due to the presence of twins. We evaluated the influence of including twins by calculating the ICC for the full dataset. The two ICCs are 98.6% similar when looking at all features.

We also verified the spatial similarity for each frequency band, to ensure the global correlation was not an effect on only one band. We computed the similarity by averaging the ICC values per frequency band for every region of the Schaefer atlas. We additionally averaged all the frequency bands to get a broadband heritability. The broadband spatial correlation is 99.4% (p-value < 1e-4). The similarity is above 98.1% for every band (p-value < 1e-4).

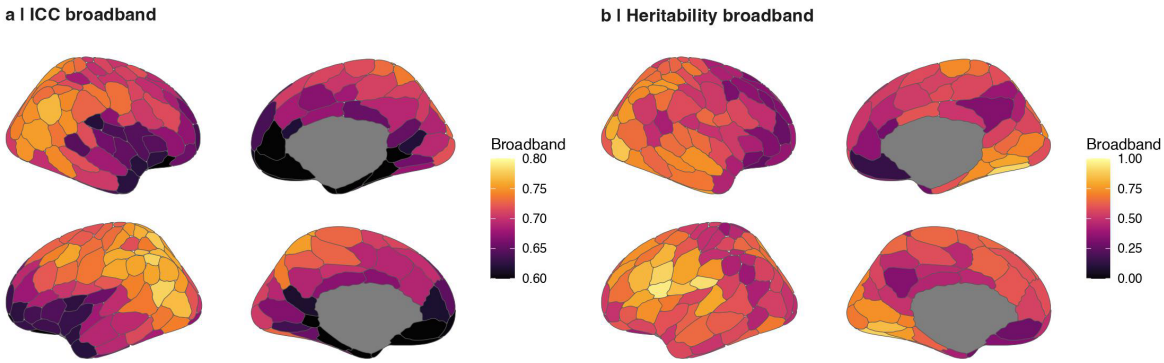


Figure S3: Broadband brain maps of salient features for fingerprinting and heritable brain phenotypes.

## Gene ontology analyses using KEGG database

We reproduced our gene ontology analyses using the ShinyGO[1] tool (http://bioinformatics.sdstate.edu/go/) and the Kyoto Encyclopedia of Genes and Genomes (KEGG) database. The result of this analysis is presented in Figure S4, and in the Supplemental Data.

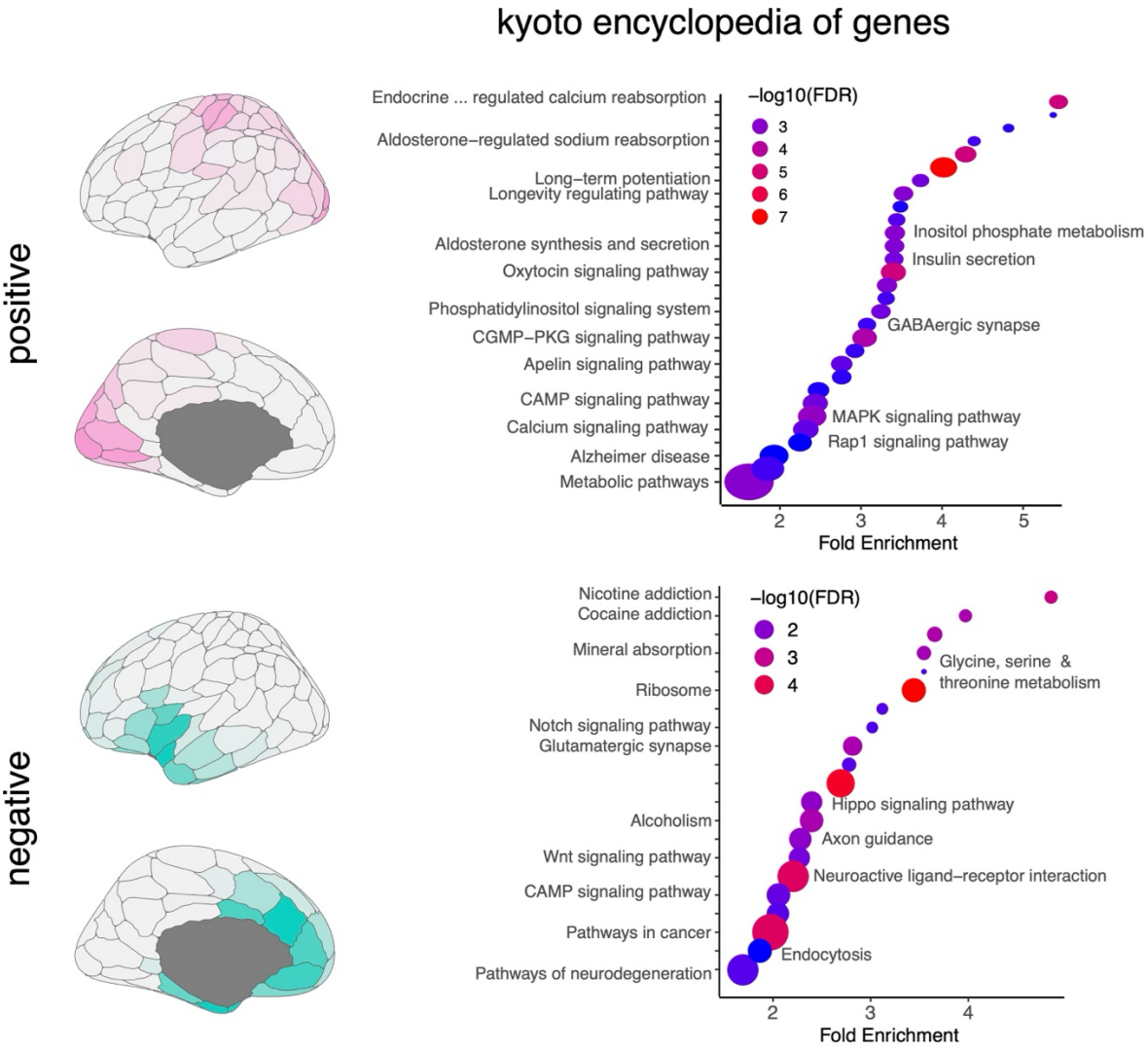


Figure S4: Genes that contribute to the reported PLS latent component was assessed by computing loadings. Left panel: gene brain score pattern for positive and negative loadings. Molecular processes were inferred from the genes with the top 50% of positive (pink) and negative (blue) loadings using a gene enrichment analysis (see Methods). Right panel: KEGG gene ontology analysis for the positive and negative gene loadings. The size of each dot represents the number of genes associated with the biological process; their colour represents the FDR-corrected p values.

### Psychological activations and differentiation PLS analysis

We further tested whether the identified psychological-processes pattern from our PLS analysis (see Manuscript) would equally covary with participant differentiation. We anticipate that this relationship should hold as both psychological-processes and differentiation covary with similar gene expression signatures (see Manuscript). As expected, the psychological-processes differentiation PLS had a single significant latent variable (p= 0.002) explaining 87.0% of the covariance between psychological-processes activations and differentiable brain activity (85.2% covariance explained, $P_{SPIN}$= 0.002, 95% CI = [54.24., 87.37]; Figure 4b left panel). The ICC loadings and term loadings were significantly linearly related to the loadings obtained from the previously reported PLS analysis (ICC loadings similarity, r=0.78; term loading similarity, r= 0.92).

### Monozygotic twin differentiation not driven by anatomy

We tested whether our ability to differentiate MZ twin pairs based on their spectral brain-fingerprints was driven by anatomical similarity. We first verified that MZ twins were more similar in terms of their anatomical features extracted from Freesurfer[2] than DZ twins, and unrelated subjects (see Methods). Indeed, we observed that the average correlation of anatomical features between MZ twin pairs was (r= 0.99), whereas it was significantly lower for DZ twin pairs (r= 0.93; see Figure 3a left). We investigated which anatomical features were the most heritable and observed that measures of Gaussian brain curvature (h= 1.75) and thickness (h= 1.75) were the most heritable across the entire cortex. These results corroborate previous literature reporting the heritability of anatomical brain features. We, therefore, assessed the extent to which anatomy contributes to heritable brain fingerprints.

To do so, we computed the linear relationship between the similarity of spectral brain-fingerprints between MZ twin pairs and their anatomical features (see Figure 3b, and Methods for details). We did not observe any significant linear relationship between spectral broadband similarity and anatomy for both MZ (r= 0.32, p= 0.06) and DZ (r=-0.22, p= 0.32; see Figure 3b right) twin pairs. We repeated the above analysis for alpha-band similarity (MZ: r= 0.31, p= 0.08; DZ: r=-0.17, p= 0.45) and beta band similarity (MZ: r= 0.32, p= 0.07; DZ: r=-0.15, p= 0.51). Bayes factor analyses corroborate this interpretation with minimal evidence for the alternative hypothesis (see Supplemental Table S1). Taken together, these results indicate that while brain curvature and cortical thickness are highly heritable brain-phenotypes, they do not appear to influence our ability to differentiate individuals.

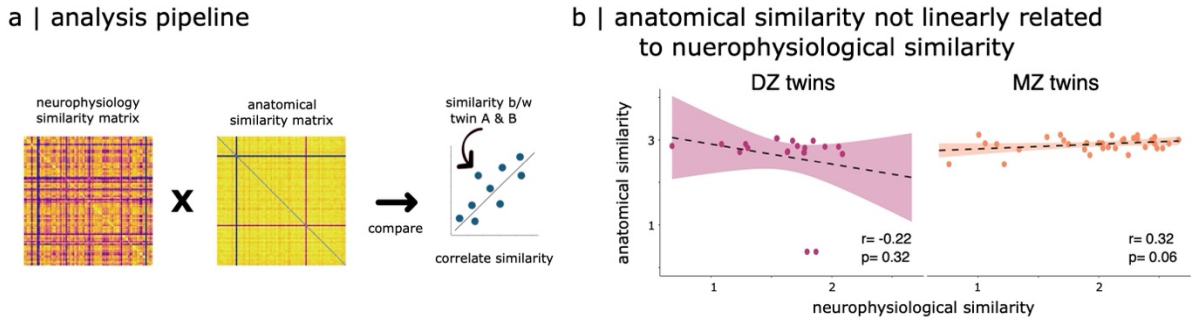


Figure S5: MZ twin differentiation not influenced by anatomical similarity.
(a) Analysis pipeline for the relationship between anatomical similarity and neurophysiological (aka brain fingerprint similarity). We first compute the two participant similarity matrixes, Fisher transform the similarity, and compute the linear relationship between anatomical and brain-fingerprint similarity for i) DZ twin pairs and ii) MZ twin pairs. (b) Scatter plot of the linear relationship between the neurophysiological similarity between (aka brain-fingerprints) and anatomical similarity for DZ (right panel) and MZ (left panel) twin pairs.

| | Pearson's r | | $BF_{10}$ | |
|---|---|---|---|---|
| | MZ | DZ | MZ | DZ |
| Relationship between anatomy and broadband spectral similarity | 0.32 | -0.22 | 1.65 | 0.68 |
| Relationship between anatomy and alpha spectral similarity | 0.31 | -0.17 | 1.46 | 0.57 |
| Relationship between anatomy and beta spectral similarity | 0.31 | -0.15 | 1.60 | 0.54 |

Table S1: Pearson's correlation between anatomical similarity and brain-fingerprint similarity.
We computed the linear relationship between anatomical similarity and i) broadband, ii) alpha band, and iii) beta band similarity among twin pairs. Bayes factor evidence for the linear relationship between spectral and anatomical similarity between twin pairs was in favour of the null hypothesis. A Bayes factor greater than 3 (or less than 1/3) is considered moderate evidence.

## References

1. Ge, S. X., Jung, D. & Yao, R. ShinyGO: a graphical gene-set enrichment tool for animals and plants. Bioinformatics 36, 2628–2629 (2020).
2. Fischl, B. FreeSurfer. NeuroImage 62, 774–781 (2012).